Author/s:
Marshall, Jessica Peta Suan

Title:
Genetic and pharmacological targeting of Heat shock protein 72 (Hsp72) in the 5xFAD*Tg30 mouse model of Alzheimer's disease

Date:
2020

Persistent Link:
https://hdl.handle.net/11343/268070

Genetic and pharmacological targeting of Heat shock protein 72 (Hsp72) in the *5xFAD*Tg30* mouse model of Alzheimer's disease

Jessica Peta Suan Marshall (818005)

ORCID ID: 0000-0002-0209-0068

November 2020

Doctor of Philosophy

Faculty of Medicine, Dentistry and Health Sciences

Florey Department

Submitted in total fulfilment for the degree of *Doctor of Philosophy*

In affiliation with the Florey Institute of Neuroscience and Mental Health and the Baker Heart and Diabetes Institute

Abstract

The impact of Alzheimer's disease (AD) is profound. In Australia, around 460,000 patients have dementia, AD being the most common form. An estimated 1.2 million people are involved in their care and it is the second leading cause of death. It is difficult to provide statistics purely on AD due to the difficulty in diagnosis, but an estimated 70% of dementia cases are AD (322,000 patients) (Dementia Australia 2018). Overexpression of the cytoprotective Heat Shock Protein 72 (Hsp72) is currently under investigation as a potential therapeutic option for prevention and treatment of AD due to its many protective mechanisms. The series of projects in this thesis aim to better understand the effects of upregulating Hsp72 in relation to behaviour, cognition and metabolism in a mouse model of AD.

The aim of the first study was to replicate and extend on the characterisation of a recently developed mouse model of AD. The mutant *5xFAD* (overexpressing human APP and Presenilin-1) was crossed with *Tg30* (overexpressing tau) to produce *5xFAD*Tg30* mice and investigate the effects of tau accumulation in the presence of amyloid pathology, which closely resembles human AD. A comprehensive battery of behavioural and physiological tests were performed to observe cognitive and physical decline over time, between 3-8 months of age. In agreement with one previous report (Heraud *et.al* 2014), we observed a decline in Rotarod performance from 6 months onwards compared with wildtype control (WT). While we noted a decrease in spatial awareness and memory (Morris water maze) and significant genotype differences in anxiety-like behaviour (large open field) by 8 months, memory function (Y-maze) and novel object recognition were not significantly affected. The *5xFAD*Tg30* mice had a 40% decrease in survival by 10 months of age. Additionally, *5xFAD*Tg30* mice were smaller, with a significant difference in body weight, tibialis anterior skeletal muscle weight and tibia length. Our results successfully reproduced aspects of the previously published description of

this model (Heraud *et.al* 2014), while adding further additional characterisation of the model. This initial characterisation study demonstrated that the model develops many aspects associated with AD including frailty, early death and initiation of cognitive decline to complement the previously described AD-like brain pathology, specifically the presence of amyloid-beta (Aβ) pathology with tau accumulation and neurofibrillary tangle (NFT) development, found in this model (Heraud *et.al* 2014).

Hsp72 has been shown to play a cytoprotective role in AD- related research by inhibiting Aβ oligomerization, enhancing its clearance, restoring tau homeostasis and inhibiting neuronal apoptosis. Hence, the aim of the second study was to genetically overexpress Hsp72 and study its effects on the *5xFAD*Tg30* mouse model of AD. As in the first study, we crossed *5xFAD* and *Tg30* mice, to create the double transgenic, *5xFAD*Tg30*, then crossed the double transgenic mice with Hsp72 overexpressing transgenic mice (*Hsp72 Tg*) to create the triple transgenic, *5xFAD*Tg30*Hsp72Tg*.

BGP -15 is a compound described to be a co-inducer of Hsp72, and therefore, our third study hypothesized that pharmacologically activating Hsp72 with this compound may be advantageous in preventing or delaying AD progression and associated pathology. *5xFAD*Tg30* mice were treated with BGP-15 or vehicle in their drinking water in a randomised and blinded study in both male and female mice from the ages of 2-10months. A comprehensive battery of behavioural and metabolic tests was conducted for both the second and third studies, and results compared to littermate WT mice.

We observed significant declines in Rotarod, Y-Maze and Novel Object performance and increased seizure activity in the 5xFAD*Tg30 mice compared to wildtype, however neither

Hsp72 overexpression (study 2) nor BGP-15 treatment (study 3) rescued this decline. Hsp72 overexpression was partially effective in maintaining lean mass in male mice and improved performance on the elevated plus maze. In males there was a 38% decrease in survival rates by 10months of age in the *5xFAD*Tg30* mice, which was improved by BGP-15 treatment to only a 14% loss ($p=0.07$). In conclusion, BGP-15 may improve survival rates in a gender specific manner (male), while overexpression of Hsp72 leads to maintenance of lean mass in male 5xFAD*Tg30 mice. Both avenues used to target Hsp72 were insufficient, however, to protect against the observed cognitive deficits in the model.

Declaration

This is to certify that:

1) The thesis comprises only my original work towards the PhD except where indicated

2) Due acknowledgement has been made in the text to all other material used; and

3) The thesis is fewer than 100,000 words in length, exclusive of tables,

bibliographies and appendices

Signed:

Jessica Marshall

27/11/2020

Acknowledgments

This research was conducted on the lands of the Boon wurrung and Wurundjeri people and I wish to acknowledge them as the Traditional Owners of the land. I would also like to pay my respects to their Elders, past and present, and Aboriginal Elders of other communities. Always was, always will be, Aboriginal land.

This research was supported by the Yulgibar Foundation, the Shine On Foundation, the Calvert-Jones Foundation, the Dementia Australia Research Foundation Scientia Professor Henry Brodaty PhD Scholarship, and the Baker Institute Bright Sparks and Florey Institute scholarships. With thanks to N-Gene for supplying our drug of interest, BGP-15.

"*It always seems impossible until it's done*"

-Nelson Mandela

This quote hung above my desk during the entire duration of my PhD and was my candidature mantra over the past several years. I am thankful to everyone who made the seemingly impossible, possible.

"*Nevertheless, she persisted*"

-2018 Women's History Month rally cry

They say it takes a village to raise a child, and it has certainly taken a large metropolis city to raise and support this PhD candidate.

Dr. Darren Henstridge. Firstly, thank you for everything. There are few words to describe the enormous impact you have made to my life both as a scientist and as a person. You have been with me on this crazy journey the last 5 years of my life, taught me with patience, mentored me with kindness, encouraged me with enthusiasm and cared for me as a friend. I am very grateful for the time you have spent supporting and looking after my project- even remotely after you left. You have taught me to be independent, resilient, and I want to acknowledge and thank you for everything you have done. Doctor Daz the Super Supervisor.

Prof. Mark Febbraio. Thank you sincerely for taking me on as an Honours student in your lab all those years ago and having the trust in me to take on a PhD project. While it has been a completely remote supervision, thank you for supervising me and providing an unlimited wealth of knowledge. It has been an honour to work under your name.

Prof. Paul Adlard. You have shown so much care and support over the years, to a student who randomly asked you to supervise her and I am forever grateful that we picked you as a supervisor. You are as kind as you are intelligent (which is a lot) and you never seemed to mind when I popped in for help. You have been monumental in getting everything done, from all the mundane paperwork we palmed off to you, to letting me infiltrate your lab- I always felt like I had your unwavering support. I also knew you were cool from the first moment I met you- I knew someone with multiple gum ball machines full of treats in their office would be someone I could get along with!

Prof. Nigel Jones. You were a lifesaver- thank you for taking me under your wing and for the enormous amount of help and resources you shared with me. I am forever grateful for yourself, Elysia and Anna for the support and work you all did. You became my adopted-supervisor and I thank you so much.

To everyone in the Febbraio, Adlard, Drew, Calkin, Jones, Medcalf and Petratos labs, the scientists in these labs are outstanding and I literally could not have gotten half the work I did, done, without you all. From sharing resources, knowledge, a helping hand or training- I am not the scientist today, nor would I have been able to present the data in this thesis, without your help. Science is truly a collaborative effort and I am thankful that each of you were willing to collaborate with me. Thank you especially to Casey, Lydia, Mirjana, Travis, Sarah, Aowen, Bridgette, Anna, Elysia, Fiona, Steve and Erica. To my Advisory Panel; Claire, Blair, Peter and Scott, thank you for your time, wise words of advice and helping to advance me through each milestone.

To my friends at Baker and Florey. Our PhD's and jobs may have been the most isolating times we have been through, but I truly have found some of my best friends at work. Kwanie Kwan, Adam, Emily, Ishant, Michael, Big Wheels, Nicola, Hamdi, Camila, Gerard, Kim, thank you guys especially, for the chats, shoulders to cry on, discos to dance with and loose times we've shared. You guys are literally the best part of my PhD and I love you the most.

To my friends. Thank you for always asking how my PhD is going and then hugging me when I self-combust into tears. I have some fierce friendships and loyal girls in my life, and I love you all so much. Ella, Carmela, Amanda, Kayla, Courtney, Alex, Rach, Kae-Lin- we have

watched each other grow into strong, intelligent, successful women and I am constantly inspired by you all. Thank you for always showing me love.

To my mum. I love you more than words can describe. We have both been through so much, especially you, and I am the luckiest person in the world to call you family. You were never disappointed when I needed time off- giving me the courage to put my health first. Your love and care have gotten me through. Even though you will probably never understand a word of this thesis, I hope it has made you proud. I live to make you proud.

To my Nick. Without this sounding like wedding vows, I never really understood what it meant when people said "My partner brings out the best in me" until I met you. You literally make me the best version of me. You challenge me, you encourage me, you give me the space to let my light shine and you never attempt to dull who I am. I am obsessed with you. I love you. Thank you for instilling confidence in me- only you know how much my confident exterior is sometimes a façade and you help build me up every single day. I am grateful that I got to go through this journey with you by my side.

And finally, to my future self. One day, when you are old and grey, you may look back at this and struggle to remember this chapter of your life. So, I wanted to include a small section so you would never forget how strong, resilient and bad ass of a woman you were/still are. You completed a PhD against so many personal, physical and mental struggles, and you completed the last quarter of it during a global pandemic #missRona. During your time completing your PhD, you cut yourself off from toxic family, you had a failing organ removed, you ended a relationship and found the true love of your life, you went through trauma and lost friends who didn't believe you, you started a business and launched your own line of science merchandise,

you performed in 8 full scale theatre shows and you were locked in your house for over 8 straight months (and still counting). If you ever, ever, start to doubt yourself, wherever you end up in life or career- look at this document right here and remember what it represents. You worked bloody hard on these experiments, spent 3 bouts of 5-8month periods isolated in a dark silent room with your animals, shed so many tears and had so many bouts of anxiety and imposter-like feelings. But you got through it- not many people in the world can say that they have completed a PhD, and yet here you are. 2020 has been a challenging year, but it has also been a great year. You took a little while longer to complete this PhD than you originally thought, but you are about to embark on an exciting, new and truly worthwhile career, moving interstate with your soon to be fiancé. It is all so wonderful on the other side and it is a time I hope you never forget. And if no-one has told you in a while; well done. I am proud of you.

Table of Contents

List of Abbreviations-

Aβ- Amyloid beta

AD- Alzheimer's disease

AED- anti-epileptic drugs

APP- Amyloid precursor protein

APOE- Apolipoprotein E

ATP- Adenosine triphosphate

β-HAD- β-hydroxyacyl-CoA dehydrogenase

BMI- body mass index

CD33- sialic acid binding Ig-like lectin 3

CLAMS- comprehensive laboratory animal monitoring system

CNS- Central nervous system

DMD- Duschenne muscular dystrophy

DRP-1 Dynamin related protein-1

ECAR- Extracellular acidification rate

ETC- Electron transport chain

fAD- Familial Alzheimer's disease

FTD- Frontotemporal dementia

GM3- monosialodihexosylganglioside 3

GSK3- glycogen synthase kinase-3

HDAC- Histone deacetylases

HSE- Heat Shock Element

HSF- Heat Shock Factor

HSP-Heat Shock Protein

Hsp72- Heat Shock Protein 72

WT- Wildtype control

IDE- Insulin degrading enzyme

IGF-1- Insulin-like Growth Factor 1

JNK- c-jun amino terminal kinase

NAD- nicotinamide-adenine dinucleotide

NC- normal chow diet

NFT- Neurofibrillary tangles

Nrf1- Nuclear Respiratory Factor 1

OBX- olfactory bulbectomy

oGTT- oral gavage glucose tolerance test

OCR- Oxygen consumption rate

PARP 1- Poly ADP Ribose Polymerase 1

PS1- Presenilin-1

PS2- Presenilin-2

QC- quality control

RER- respiratory exchange ratio

T2D- Type 2 Diabetes

TFAM- transcription factor A, mitochondrial

TLR- Toll-like receptor

TNFα- Tumor necrosis factor alpha

TREM2- Triggering receptor expressed on myeloid cells 2

2-[2-[4-(trifluoromethoxy)phenyl]hydrazinylidene]-propanedinitrile - FCCP

1 Literature Review

Preface

Figures in this chapter are original but adapted from cited sources, unless specified. Components of figures were created using Servier Medical ART.

1.1 Introduction

Alzheimer's disease (AD) is a condition characterised by the progressive loss of cognitive function and is the most common form of dementia. It is associated with several comorbidities such as Type 2 Diabetes (T2D), hypertension and chronic kidney and obstructive pulmonary diseases (Chatterjee *et al*., 2017). In recent years, the incidence and prevalence of AD have been increasing both worldwide and nationally; currently in Australia over 460,000 patients are affected with dementia, with AD accounting for up to 70% of cases (Dementia Australia 2018). There is no cure for AD; current and past available drugs can help to mask symptoms, but do not treat the underlying disease or delay its progression. Hence, identifying new targets for the treatment of AD are required.

Heat Shock Protein's, specifically Heat Shock Protein 72 (Hsp72), is currently an attractive therapeutic target to treat and potentially slow the progression of AD. HSP's are molecular chaperones which can help prevent protein aggregation and denaturation as well as remove damaged and misfolded proteins (Meriin and Sherman, 2005). A number of studies have suggested that HSPs are regulators of neurodegenerative processes which correlated to protein misfolding in patients with AD (Meriin and Sherman, 2005, Franklin *et al*., 2005, Magrane *et* al., 2004*)*. Together, evidence has been accumulating that targeting Hsp72 in the brain could be a therapy for AD. AD is a complex neurodegenerative disease, where currently, no drug has been identified to treat the myriad of dysfunctional processes as a collective. Hence, new

pharmacological approaches and the importance of studying potential cellular mechanisms are warranted. This thesis and literature review will examine the role of Hsp72 as a potential therapeutic treatment to delay the progression of AD.

1.2 Alzheimer's Disease

1.2.1 Background

AD is a devastating neurodegenerative disorder, characterised by the aggregation of two proteins, extracellular amyloid-beta (Aβ) and intracellular tau into plaques and neurofibrillary tangles (NFT's) respectively. AD disrupts the process of neurons connecting at synapses, damaging the brain's communication network. It is the most common form of dementia, which, in Australia, is the second leading cause of death (ABS 2018). The word dementia is used as an umbrella term for neurological disorders with the core symptom being a decline in brain function. Other types/causes of dementia include vascular dementia, Lewy Body disease and frontotemporal dementia.

AD was first identified in 1907 by German psychiatrist Alois Alzheimer after a patient, Auguste Deter died after experiencing years of strange behaviour and dementia (Hippius 2003). From 1901, Alzheimer observed this behaviour, including delusions, trouble sleeping and paranoia until her death in 1906, when he could then examine her brain post-mortem. Alzheimer noted the shrinkage of the outer layer of the brain, the cortex, as well as the identification of two deposits- now referred to as amyloid plaques and tau tangles. Since then, scientists have been researching the mechanisms behind the development of these aggregates as well as the downstream effects they can cause. There are two classes of AD, sporadic and familial, sporadic being the most common. Sporadic AD generally occurs after the age of 65 years and can include symptoms beginning with short term memory loss, loss of sense of direction and erratic emotions, to loss of gross motor control and strength and even epileptic seizures (Bature *et al*., 2017). Familial Alzheimer's disease (FAD) is characterised by clinical onset prior to the age of 60, as well as Mendelian inheritance. It represents less than 1% of all AD cases and is caused by mutations in three different genes encoding Aβ precursor protein

(APP) on chromosome 21, presenilin-1 (*PSEN1*) on chromosome 14, and presenilin-2 (*PSEN2*) on chromosome 1 (Johnson *et.al* 2017).

While the average clinical duration of AD is 10 years, the disease manifests pre-symptomatically for up to 20 years in its preclinical phase (Bachman *et al*., 1993, Hebert *et al.*, 1995, Evans *et al*., 2003, Kawas *et al*., 2000). Although AD has been recognised as a disease for over 100 years, scientists still do not have a clear understanding of the disease process. From mild cognitive impairment to severe AD, symptoms include short term memory loss, poor object recognition, poor judgement/thinking/understanding and loss of gross motor control and strength. However, accurate epidemiology is difficult to obtain due to the confounding variable of co-morbidities such as cerebrovascular disease (Masters *et al*., 2015) and incorrect reporting. Caution must be taken when looking at data from dementia studies as opposed to specifically AD studies, which can lead to a misrepresentation of the disorder.

Despite numerous modifiable risk factors being identified as associated with the onset of AD such as T2D, hypertension, obesity and physical inactivity, there are no current interventions that have addressed the primary disease mechanisms (Norton *et al*., 2014). Debate also remains as to whether AD is indeed modifiable or preventable or if it is undeniably a normal part of aging. It is evident that researchers remain unclear on the relationship between amyloid, tau and their relative contribution to the cellular process underlying AD pathology and symptoms.

1.2.2 Evolution of Alzheimer's disease

While the molecular and signalling pathways leading to disease pathology remaining unclear, the pathological evolution of AD is quite well mapped **(Figure 1.1)**. Aβ generally begins to deposit in the frontal and temporal lobes, moving to the hippocampus and limbic system. This process, according to the amyloid cascade hypothesis is thought to precede NFT aggregation, which starts in the medial temporal lobes and hippocampus, before progressively spreading to the rest of the neocortex.

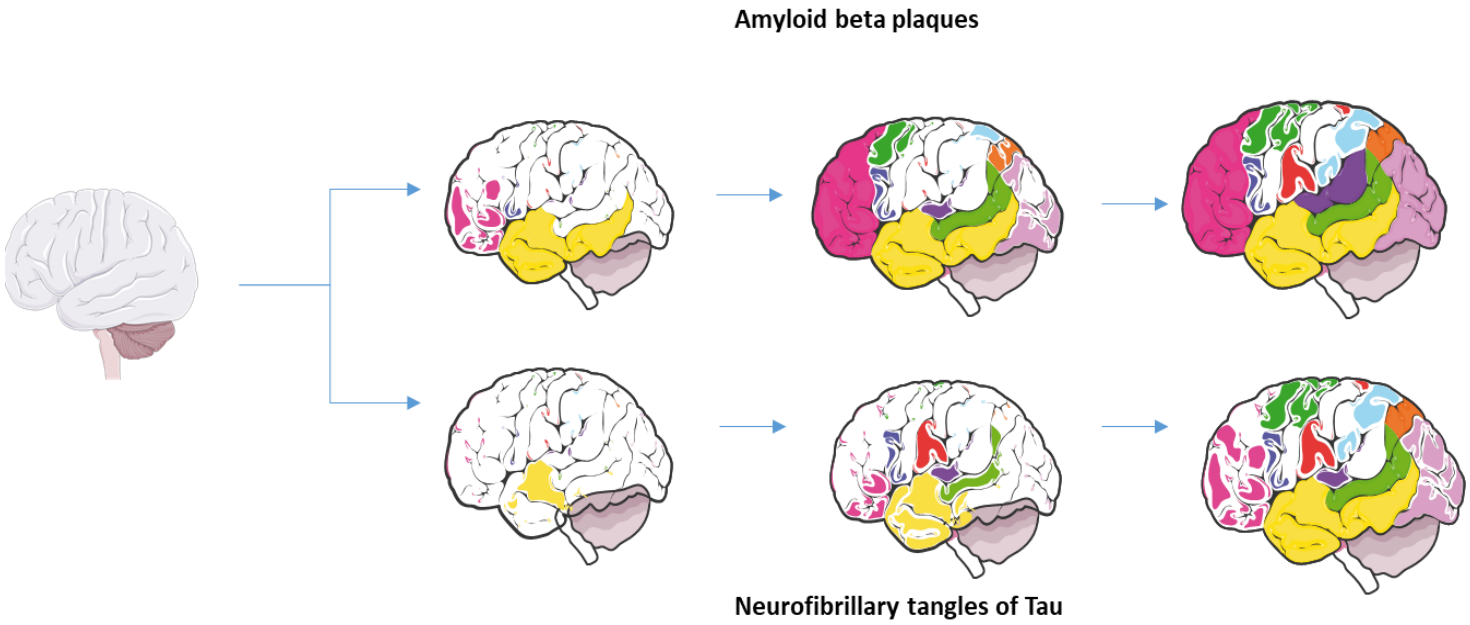

Figure 1.1 Evolution of Alzheimer's disease pathology over time. *Aβ aggregates begin to deposit in the frontal and temporal lobes of the brain before progressing to the hippocampus and limbic system. Tau aggregation begin in the medial temporal lobes and hippocampus before progressing to the rest of the neocortex. Different colours indicate different regions of the brain. Adapted from Masters et.al 2015.*

1.2.3 Amyloid beta (Aβ)

Aβ, being the main component of plaques found in AD patients, has been at the forefront of research endeavours. While Aβ is a normal product of the metabolism of APP, its accumulation due to decreased clearance creates toxic effects within the brain. The normal function of APP remains unknown to researchers, although it is believed to play a role in synaptic plasticity and synaptogenesis (Selkoe, 2008, Turner *et al*., 2003). Aβ is created when APP is cut by the cleaving enzymes β- and γ- secretase, of which the protein presenilin is a subcomponent. Mutations in any of the two presenilin genes, PSEN1 and PSEN2, modify the ratio of Aβ42 and Aβ40 (overproduction of both Aβ40 and Aβ42) in the plasma, two of the many isoforms of Aβ (Potter, 2011, Scheuner *et al.*, 1996), as do mutations in APP (Hecimovic *et al*., 2004). Most importantly, it appears to be that any three of these mutations can result in the overproduction of the Aβ40 isoform which is highly prone to aggregation (Golde *et al*., 2000), central to AD pathogenesis. Conversely, studies have shown in mild sporadic AD, there is indeed no significant difference in the average production of Aβ, however a decrease of its clearance (Mawuenyega *et al*., 2010). It could be, that there is no increase in the production of Aβ, but rather an increase in the isoform Aβ40 over Aβ42, along with the decreased clearance of overall Aβ. The mechanisms underlying the decreased clearance remain unknown, with further research needed, however researchers believe it could involve the protein Apolipoprotein E (APOE).

In 1991, APOE was first linked to AD and the defective clearance of Aβ through its immunoreactivity in Aβ deposits, as well as polymorphisms during transcription that have been associated to the disease (Namba *et al*., 1991, Artiga *et al*., 1998). One of the four alleles of APOE, APOE4, has been shown to increase the risk of developing AD (Farrer *et al*., 1997) as well as creating an earlier age of onset (Corder *et al*., 1993, Khachaturian *et al*., 2004) because of its potential role as a pathogenic chaperone for Aβ (Holtzman *et al*., 2000). APOE4 does not

alter Aβ synthesis (Holtzman, 2001) but increases its deposition, as seen in a mouse model of AD (Holtzman *et al*., 2000). Additionally, an APOE knockout in a mouse model resulted in animals with inhibited Aβ clearance (Deane *et al*., 2008).

It is important to note that the evidence of the involvement of Aβ and the amyloid cascade hypothesis (stating tau accumulation and neurodegeneration is a downstream event) is based on data with patients with FAD, therefore the relevance for sporadic AD, which accounts for 99% of cases, is questionable (Castellani 2011). Mutations in the APP gene, for example, only account for a small proportion of AD cases, so there may be other more complex genetic factors at play. If the amyloid cascade hypothesis held true, it would be expected that an Aβ-targeting drug candidate successfully slowed down the progression of AD in a clinical trial. This of course, has not been the case, however common considerations for this usually include treatment being administered too late, drug candidates not being strong enough or that the cascade hypothesis is oversimplified.

Ultimately, however, the molecular relationship between Aβ, and the secondary compromised protein, tau is extremely complex and early diagnosis is still not possible. This is evidenced via research showing it is possible tau accumulation can occur without initial increases in Aβ. Additionally, tauopathy can be seen in many conditions but Aβ is specific to AD.

1.2.4 Tau

While significant research has focussed on plaques and their associated toxicity, much less is known about the impact of the second pathological landmark discovered by Alois Alzheimer over a century ago; NFT. In a healthy neuron, molecules are carried on a series of tracts of microtubules which are stabilised by the protein, tau (Goedert and Spillantini, 2006). In AD, tau, through a process only partially known, becomes modified and dissociates from microtubules. During this process, the protein adopts an abnormal shape and moves from the axon to the cell body. Tau can appear in either soluble or insoluble forms and it is the insoluble forms which can aggregate together as tangles. Research is unclear on the impact of the different isoforms of tau, although it is known that both total tau levels and phosphorylated tau levels are moderately increased in the cerebral spinal fluid of AD patients (Ryman *et al*., 2014). It is, however, known that modified tau can indeed spread across synapses, somehow making healthy tau, toxic. It is thought that tau aggregation is induced by Aβ oligomers that dissociate from plaques, as well as being formed on the pathway to making plaques, and are toxic to adjacent synapses. Further, NFT's strongly correlates with neuronal loss and cognitive decline (Arriagada *et al*., 1992, Duyckaerts *et al*., 1998, Giannakopoulos *et al*., 2003, Gomez-Isla *et al*., 1997).

While the molecular relationship between Aβ and tau is poorly understood, evidence is growing that the two work together to play a role in neuronal dysfunction (Ittner and Gotz, 2011). Further, the depletion of tau prevented Aβ toxicity in AD models (Rapoport *et al*., 2002, Ittner *et al*., 2010). Interestingly, Ittner and colleagues showed in a recent study that phosphorylation of tau is part of an Aβ toxicity-inhibiting response, challenging the dogma that tau phosphorylation mediates toxic processes (Ittner *et al*., 2016). This provided evidence that tau may have a protective role in early AD through the, one of many tau sites, T205 phosphorylation site, a finding contrary to past and many current beliefs. It is increasingly clear

that to understand the disease as a whole, tau must be considered as much as Aβ, as does their interaction. AD models where both are present are, therefore, warranted.

1.2.5 AD and Neuroinflammation

A link between chronic inflammation and age-related diseases, including AD, have been well documented (Fuller *et.al* 2020; Zhang *et.al* 2013). The long-lasting dysregulation of inflammatory responses is currently under investigation for its impact on brain function and facilitating the onset and progression of neurodegeneration in AD (Newcombe, 2018).

Inflammation leads to the secretion or upregulation of inflammatory cytokines such as tumour necrosis factor alpha (TNFα), c-jun amino terminal kinase (JNK) and p38 MAP kinase. These markers of inflammation are all known to contribute to cell death and inflammatory reactions, which are of course, important in the progression of AD. In 2013, scientists claimed that neuroinflammation contributes to disease pathogenesis as much, if not more than Aβ plaques and tangles (Zhang *et.al* 2013). This was supported by recent findings at the time, showing genes for immune receptors such as Triggering receptor expressed on myeloid cells 2 (TREM2) (Guerreiro *et.al* 2013) and Sialic Acid-Binding Immunoglobulin-Like Lectin 3 (CD33) (Bradshaw *et.al* 2013; Griciuc *et.al* 2013) were associated with AD.

1.2.5a Microglia

Microglia, being the resident phagocytes within the central nervous system (CNS) play a role in engulfing Aβ fibrils. In AD, microglia bind to Aβ oligomers and fibrils via receptors such as class A scavenger receptor A1, CD36, CD14, α6β1 integrin, CD47 and toll like receptors (TLR) (TLR2, TLR4, TLR6 and TLR9) (Bamberger *et al* 2003; Paresce *et.al* 1996; Stewart *et.al* 2010; Liu *et.al* 2005) and can mediate an inflammatory response. Inefficient clearance of Aβ is thought to be the result from increased cytokine activity, downregulating phagocytosis receptors, leading to insufficient microglial phagocytic capacity (Hickman *et.al* 2008).

1.2.5b Astroglia

Astrocytes are central for maintaining synaptic transmission, which in animal models of AD have been shown to go through atrophy and thought to contribute to cognitive deficits (Olabarria *et.* Al 2010; Olabarria *et.al* 2011; Yeh *et.al* 2011; Kulijewicz-Nawrot 2012; Beauquis *et.al* 2013). Like microglia, astroglia release cytokines, interleukins, nitric oxide, and other potentially cytotoxic molecules when exposed to Aβ, potentially exacerbating the inflammatory response. Astrocytes have the potential to degrade Aβ, via astrocyte-dependent lipidation of ApoE which in turn, increases the ability of microglia to clear Aβ (Jiang *et.al* 2008; Terwel 2011). Additionally, astrocytes can up-regulate the expression of extracellular Aβ-degrading proteases such as Insulin degrading enzyme (IDE). Impaired function and atrophy of astrocytes can therefore negatively contribute to the clearance of Aβ.

While the pathological accumulation of Aβ is a key factor that drives neuroinflammatory responses in AD, understanding a clear "why" and "how" these responses occur have yet to be elucidated. It is understood that there is a microglial response, however this simplicity ignores the complex nature of the release of inflammatory mediators. Other factors, such as chronic inflammation seen in metabolic disorders like T2D and obesity must also be taken into consideration when looking at AD and lifetime risk.

1.2.5 AD as a metabolic disease

In more recent years, there has been an increasing amount of research focussing on the relationship between dementia, AD and metabolic diseases such as T2D, obesity and dyslipidaemia. While associations between these diseases are numerous, so too are the resulting pathways that are continuing to be discovered that could play important roles in the development and progression of AD. Here, we discuss three prominent areas of metabolic dysfunction and their links to AD.

1.2.5a Mitochondrial structure and function

Mitochondrial structure and function abnormalities have been recognised in AD for quite some time (Saraiva *et al*., 1985). These abnormalities include a decrease in mitochondrial respiration, alterations in morphology and the downregulation of mitochondrial oxidative phosphorylation in hippocampus and cortex of AD patients (Zhang *et.al* 2015; Minjarez *et.al* 2016). The activity of several mitochondrial specific enzymes is also reduced in AD and has therefore encouraged the hypothesis that AD is a disease of perturbed brain energy metabolism (Blass *et al*., 2002, Gibson *et al*., 1998, Sorbi *et al*., 1983). Biogenesis and mitophagy in respect to mitochondria involves the process of the production of new mitochondria and the process of programmed organelle death, respectively. Fusion (the joining of mitochondria) and fission (separation of mitochondria) involve the alteration of mitochondria to form constantly changing tubular networks. The regulations of these dynamics are crucial for the health of the cell (Hales, 2010). Healthy metabolic function is a balance between biogenesis, fusion, fission and mitophagy. When there is an increase in healthy mitochondria and the removal of damaged mitochondria, enhanced metabolic function is achieved. When this fails to occur, an increase in neuronal cell death can result. It has been shown that oxidative damage and poor metabolic function of the mitochondria occurs before Aβ plaque formation supporting the causative role of

mitochondrial dysfunction and oxidative stress in AD (Zhao *et.al* 2013). In various neurodegenerative diseases, such as AD, misfolded proteins accumulate in the mitochondria and cause the functional decline of these organelles through bioenergetics deficits, apoptosis and autophagy. The role that damaged mitochondria play in the pathogenesis of AD is now a therapeutic target for interventions in AD pathophysiology.

One such pathway that can affect this is the Poly ADP Ribose Polymerase 1 (PARP-1) pathway. PARP-1 increases during times of oxidative stress, which increases nicotinamide-adenine dinucleotide (NAD) depletion, causing an energy crisis and leading to cell death. PARP-1 has also been shown at higher levels in AD human brains during post mortem analysis, and animal models crossing an Aβ mutant with a PARP-1 knockout attenuated brain dysfunction as seen in the Aβ mutant controls (Martire *et al*., 2015).

1.2.5b Obesity and Type 2 Diabetes

Considering the recent link between obesity, T2D and an increased risk of cognitive impairment and AD (Profenno *et al*., 2010), some researchers have even gone so far to suggest AD may be described as 'Type 3 Diabetes' (de la Monte and Wands, 2008). There are still, however, conflicting research showing no association of BMI (Stewart *et al*., 2005), an inverse association (Nourhashemi *et al.*, 2003) or a U-shaped association (Luchsinger *et al*., 2007), with both high and low BMI to an increased risk of AD. It must be noted that BMI is only a bio marker of obesity and not necessarily the gold standard indicator of metabolic disease or diabetes.

However, growing evidence supports the hypothesis that there is some sort of association. From an insulin signalling perspective, evidence has shown that transfection of cells with dysfunctional insulin receptors is associated with increased accumulation of Aβ oligomers (Zhao *et al*., 2009), as well as these oligomers further causing insulin receptor dysfunction

(Townsend *et al*., 2007). Additionally, impaired insulin signalling is thought to be an upstream impairment leading to tau hyperphosphorylation (Maccioni *et al.*, 2010) as obesity and T2D increase glycogen synthase kinase-3 (GSK-3) expression, a key protein that phosphorylates tau.

Insulin is readily transported across the blood-brain barrier and receptors are highly concentrated in areas of the brain such as hippocampus, cerebral cortex, hypothalamus and olfactory bulb. Due to their localisation, it can be said that Insulin plays an important role in influencing memory through modulation of synaptic structures and potentiation of neurotransmitters such as acetylcholine which are important in cognitive function (Zhao and Townsend, 2009).

It is also interesting to note that the development of insulin resistance and diabetes is preceded by changes in levels of insulin-like growth factor-1 (IGF-1). IGF-1 is a hormone that promotes cell survival, prevents apoptosis, and stimulates neurogenesis in the hippocampus- all areas affected in early AD. IGF also appears to inhibit abnormal tau phosphorylation and Aβ deposition in cell cultures and in transgenic mouse models of AD (Qiu *et al*., 1997). Wild-type mice with low IGF-1, as well as IGF1–deficient mice, show reduced adult hippocampal neurogenesis and impaired spatial learning. In clinical studies, lower IGF-1 levels were associated with greater brain Aβ burden within families that have an APP mutation, and lower levels were also associated with poorer baseline cognition and accelerated cognitive decline in healthy adults (Westwood *et al.*, 2014)

In regards to obesity, Knight and colleagues investigated the effects of high fat feeding in triple transgenic (3xTgAD) AD mice containing both amyloid and tau pathology (Knight *et al*., 2014). A high fat diet exacerbated impaired memory in AD mice as well as impaired the memory of healthy control animals after 16 months. Interestingly, this was independent of an increased amyloid plaque burden or tau pathology after post-mortem analysis.

Together, current evidence suggests that obesity and T2D may contribute to, but may not be sufficient to cause AD. Further research into the effects of a high fat diet/obesity on the progression of AD is warranted.

1.2.5c Lipid metabolomics

Lipid-mediated signalling and the dysregulation of certain lipid pathways has been implicated in several neuro-degenerative diseases, such as AD, because of their critical aspects in brain function. In 1901, when Alois Alzheimer first described the hallmarks of the disease, there was indeed a third landmark he described- alongside the well-known Aβ plaques and NFT's of tau, the third landmark included "adipose inclusions", suggesting abnormal lipid metabolism (Foley, 2010). Additionally, post-mortem biochemical analyses of patients with AD have shown alterations in lipid composition (Chan *et.al* 2012). Despite this, the detailed link between AD and lipid metabolism was only formally recognised almost a century later with the identification of the ε4 allele of APOE (Corder, 1993). The *ε*4 allele of the APOE gene is the strongest genetic risk factor for the sporadic form of AD (Corder 1993). APOE is a prominent regulator of cholesterol metabolism in the brain and mediates the uptake of other lipoproteins in the brain. It has been shown to bind to Aβ to modulate its aggregation and clearance and a number of studies have linked its role with cholesterol to the pathogenesis of AD (Bu, 2009; Kim, 2009).

Lipids can be simplified and broken down into three major families: Glycerophospholipids (such as Phosphatidylglycerol and Phosphatidylserine), Sphingolipids (such as Syphingomyelin and Hexosylceramine) and Neutrolipids (including triglycerides and cholesterols). It is now well accepted that many, if not all these different classes of lipids are implicated in the pathogenesis of AD as they modulate the pathogenic potential of both Aβ and tau by affecting their ability to aggregate. The lipid composition of cell membranes can also

have significant impacts on the trafficking activities of important membrane-bound proteins that are involved in AD pathogenesis such as β- and γ-secretases (Hartmann, 2007). This in turn, directly regulates γ-secretase-mediated production of Aβ (Simons, 1998; Fassbender, 2001; Wahrle, 2002). Conversely, increasing cholesterol or sphingolipids increased γ-secretase activity and the amyloidogenic processing of APP (Osenkowski, 2008; Osawa, 2008).

Additional families implicated in the production of Aβ include sphingolipids and phospholipids, with early studies showing that during the earliest clinically recognisable stage of AD, ceramide (a sphingolipid) levels are elevated (He, 2010). Sphingolipids are directly involved in APP metabolism and Grimm and colleagues (Grimm, 2005) found the inhibition of the enzyme mediator of sphyingomyelin to ceramide reduced Aβ secretion. This was found to be due to the inhibition of γ-secretase activity. Additionally, several phospholipids, including phosphoinositides have been reported to have had altered composition and metabolism in early AD brain tissue (Stokes, 1987; Oliveira, 2010). Inhibition of this pathway was further shown to reduce levels of Aβ both *in vitro* and *in vivo* (Petanceska, 1999; Haugabook, 2001).

Gangliosides are another membrane glycosphingolipid that are shown to be modulators of Aβ aggregation (Ariga, 2017; Matsuzaki, 2010). Genetic evidence also suggests that gangliosides are a key modifier and modulator of Aβ deposition. The loss of GM2 synthase in a mouse model of AD leads to an accumulation of GM3 and a loss of GM1. In turn, this results in the accumulation of Aβ in the brain and suggests the affinity of Aβ for GM3 (Yanagisawa, 2007). Conversely, injections of GM1 into a mouse model of AD decreased Aβ burden (Matsuoka, 2003).

Unlike the membrane bound APP and secretases, tau lies within the cytoplasm and its relationship with lipids is not as direct. There are many downstream effects from lipid metabolism effected Aβ pathways, which in effect, affect tau phosphorylation. Additionally, cholesterol levels affecting Aβ in turn can induce tau proteolysis by calpain and proteolytic

cleavage of tau, which has been shown to be an early step leading to tau pathology (Johnson 2006; de Calignon 2010).

There is now significant evidence to suggest the role of lipid metabolism and its effects on neurodegenerative diseases such as AD. A recent review identified 65 articles referring to cholesterols and AD, 35 to fatty acids and 40 to phospholipids, all as biomarkers to this disease (Zarrouk, 2018). A recent study conducted plasma lipidomic profiling to investigate the relationship of plasma lipid species with gender, age and AD (Lim *et al* 2020). This study identified 108 lipid species associated with increasing age and AD diagnosis. From those 108, 47 lipid species were negatively associated with AD (decrease with increasing age) and the other 61 lipid species were positively associated (increased with increasing age). Further, when examining associations with lipid species and APOE ε4 allele status, there were 18 lipid species associations with both AD and APOE ε4. There were 13 lipid species associated with aging, *APOE* ε4, and AD and 53 lipid species associated with gender, aging, and AD. Interestingly, *APOE* ε4 was only weakly associated with the plasma lipidome as a whole, and the study showed stronger associations with APOE *ε2,* suggesting a protective effect that may be more tightly linked to lipid metabolism than the risk associated with the *APOE* ε4 allele (Lim *et al* 2020). Lipid biomarkers may be a new wave of diagnostic tools for identification of those at risk of AD and present as therapeutic targets in the future.

1.3 Models of Alzheimer's Disease

1.3.1 Background

Genetically altered mouse models allow scientists to study key pathological hallmarks of disease, as well as trial therapeutics pre-clinically. As previously eluded to, AD is a complex disease, and it is likely previous research into therapies and treatments have been hampered due to the lack of an appropriate and physiologically accurate mouse model of AD. As evidence continues to grow around the relationship between Aβ and tau, scientists are becoming increasingly aware that a pre-clinical model should mimic the disease pathologically more accurately. In general, brains with AD have both amyloid plaques and tau tangles as part of their pathology, therefore, pre-clinical models should also. As a result, this would involve a model that allows researchers to investigate the effects of tau accumulation in the presence of amyloid pathology. To date, there are several mouse models that display both amyloid and tau pathology, including the Tg2576/JNPL3 cross, hAPP (Swe)/wildtype human Tau and the 3xTg-AD mouse. The 3xTg-AD model also contains mutations in PS1. Interestingly, previous animal models expressing mutated APP and/or PS1 genes do not form NFT's, even while expressing the human tau protein (Boutajangout *et al*., 2004).

Using dual genetically altered mice can aid scientists in the understanding of Aβ interaction with tau and how it causes cellular, behavioural and even whole-body metabolic damage. This interaction has been hypothesized as essential in the development of AD by numerous groups (Gotz, 2001 Lewis 2001; Hurtado 2010) and therefore has become a focus of this thesis.

1.3.2 The 5xFAD*Tg30 model of Alzheimer's disease

As mentioned, there are numerous models that have modelled Aβ and tau pathology. At the time of commencing this project, preparations were in place to obtain the 3xTg-AD mouse model for use. However, the commercial supplier noted a potentially significant phenotype drift in the colony, and so rather than take that risk, an alternate novel mouse model that had recently been published by Heraud and colleagues (Heraud *et.al* 2014), named the *5xFAD*Tg30* model was utilised. The data presented on this model demonstrated brain pathology consistent with human AD pathology. Specifically, and importantly, the generation of this model led to the production of NFT's, tau misprocessing and Aβ pathology, hallmarks of human AD and meeting the criteria for a valid mouse model of AD.

The *5xFAD*Tg30* model crosses the *5xFAD* model with the *Tg30* model creating a double transgenic. *5xFAD* is a model that develops Aβ pathology and Tg30 is a model that transgenically overexpresses mutant human tau.

5xFAD mice overexpresses mutant human APP (695) with Swedish (K670N, M671L), Florida (1716V) and London (V7171) FAD mutations. It also expresses human PS1 with two FAD mutations M146L and L286V. Both transgenes are driven by the mouse Thy1 promotor to cause overexpression in the brain. This model generates Aβ-42 almost exclusively, inducing neurodegeneration and amyloid plaque formation (Oakley *et al*., 2006).

Tg30 mice express a mutated tau transgene (IN4R human tau isoform with G272V and P301S mutations) under transcriptional control of the Thy1 promotor. This model develops age-dependant brain and hippocampal atrophy, progressive motor impairment with neurogenic muscle atrophy and a decreased survival rate (Leroy *et al*., 2007). Together the *5xFAD*Tg30* model was shown to be overall smaller in size, have a decreased survival and a decreased motor phenotype.

1.3.2a Pathology

As previously mentioned, the *5xFAD*Tg30* model is a rapidly progressing model expressing both human mutant tau and Aβ. It was found that tau pathology was significantly more severe in brains of *5xFAD*Tg30* mice compared to the single *Tg30* mice, which also occurred in similar models expressing tau and APP (Bolmont 2007; Hurtado 2010; Lewis 2001; Paulson 2008). This severity increased with age, as well as phosphorylation, misfolding and truncation of tau. In addition to this, at 9-months of age, higher levels of insoluble endogenous murine tau were detected, which was recruited from murine tau into paired helical filaments.

Aβ pathology on the other hand, despite increasing with age, was lower in *5xFAD*Tg30* mice compared to single *5xFAD* mice. This decrease was consistent with both soluble and insoluble isoforms and correlated to the trend in reduced expression of human mutant APP and PS1. Despite this reduction seen in *5xFAD*Tg30* mice, significant neuronal loss in the hippocampus was still observed, suggesting this loss could be related to the tau pathology (Heraud *et.al* 2014). Previously, evidence has shown that targeting the reduction of tau levels can mediate Aβ toxicity, through mediating premature lethality, memory deficits, and seizure susceptibility of APP23 mice (Ittner *et.al* 2010). Together, evidence is growing that targeting tau as well as Aβ is a suitable strategy in the treatment of AD.

1.3.2b Behaviour

While Heraud and colleagues maintained a pathological focus during their characterisation of this novel model, they did conduct some minor assessments of motor function and spatial memory at both 3 and 6 months of age. Using the rotarod, severe motor impairments were observed at 6 months, but not 3 months, with higher impairment in the *5xFAD*Tg30* mice

compared to either *5xFAD* or *Tg30* animals. A Y-maze test was carried out only at 3 months of age and there were no significant differences between genotypes and this early age point. Thus, the precise whole-body phenotype that the *5xFAD*Tg30* brain pathology produces is yet to be determined.

1.3.2 Conclusions

Utilising a more advanced and pathologically accurate mouse model of AD could be beneficial in translating pre-clinical therapeutic treatment results to human treatment. Here, we have briefly described the first characterisations of a recently developed mouse model with mutations in APP, PS1 and mutant human tau, expressing both Aβ and tau pathologies. At the time of this project's commencement, from the review of the literature of various mouse models of both Aβ and tau overexpression it was agreed upon that this model was the most similar to the brain pathology seen in human AD. Despite this, reproducibility needed to be examined, as well as an in-depth behavioural analysis and characterisation of other facets such as the models metabolic and lipidomic profile which are yet to be described. Heraud and colleagues focused primarily on the brain pathology of the *5xFAD*Tg30* model, hence, this thesis looks to further extend this characterisation with a battery of behavioural tests to track cognition over their lifetime. Other characterisations which could be implicated in the human disease, such as metabolism were also investigated. These aspects will serve as *Chapter 2* of this thesis.

.

1.4 Heat Shock Protein 72

1.4.1 Introduction

In 1962, Italian Scientist Ferruccio Ritossa unexpectedly discovered the application of 'heat shock' during a *Drosophila melanogaster* experiment after incubator settings were accidentally adjusted. Subsequently, the observation of new Hsp RNA synthesis induced by environmental conditions demonstrated its importance in gene expression (Ritossa, 1962, Ritossa, 1996). Since then, the inducible isoform of the HSP70 family, Hsp72, has been extensively studied. Given the abundance and highly conserved nature of Hsp72, it is no wonder that it is of great importance to cellular homeostasis. Hsp72 functions at the cellular level to protect cells against many stressful conditions by repairing and refolding damaged or denatured proteins. As a molecular chaperone, Hsp72 can help prevent protein aggregation and denaturation as well as remove damaged and misfolded proteins (Meriin and Sherman, 2005). Located on chromosome 6, the inducible form of Hsp72 is transcribed from the *hspa1a* and *hspa1b* gene. These genes are located in the major histocompatibility complex class III region, in a cluster of genes which encode for similar proteins.

1.4.2 Regulation

Hsp72 is the main inducible form of the HSP70kDa family and its synthesis is increased by a broad array of physiological stressors (Kregel, 2002). There are multiple different family classes of heat shock proteins, which are characterised by their molecular weight, including but not limited to HSP100, HSP90, HSP70 and HSP60. Temperature stress was the initial stimulus known to increase expression pathway; however, it is now known that multiple signals can activate expression. In addition to temperature stress, hypoxia (Iwaki *et al*., 1993), acidosis (Weitzel *et al*., 1985), ischemia reperfusion (Cairo *et al*., 1985) and reactive oxygen species (Wallen *et al*., 1997) are all known to induce Hsp72 transcription. Once the stressor is sensed by the cell, an inactive heat shock factor separates from an inactive HSP within the cytosol and becomes phosphorylated by protein kinases. After the trimerization of the phosphorylated heat shock factor, it enters the nucleus and binds to the heat shock element in the promotor region of the HSP gene to promote transcription. The resultant mRNA is transcribed and leaves the nucleus where the functional protein is synthesised in the cytosol (**Figure 1.2).**

The understanding of the precise regulation of HSP's (particularly HSP70) has shifted over time. Earlier studies indicate both transcriptional and post transcriptional regulatory steps are required for HSP production (Mizzen 1988; Petersen 1989; Wu 1986). Conversely, other studies demonstrated a HSP mRNA increase independent of HSP protein expression (Bruce 1993; Hensold 1990). It is now known that there are indeed various levels of pre-/post-transcriptional and translational regulations for the expression of HSP70 family members. Pre-transcriptional regulation has greatest influence, as HSP70 mRNA is associated with functional protein production (Silver 2012). Hsp72 is a cytosolic protein and it is well known that large molecules such as proteins are incapable of crossing the cell membrane. However, there is some evidence of pathway sequences encoding Hsp72 release (Gastpar 2005; Mambula 2006), suggesting that under certain conditions, Hsp72 can be released from the cell.

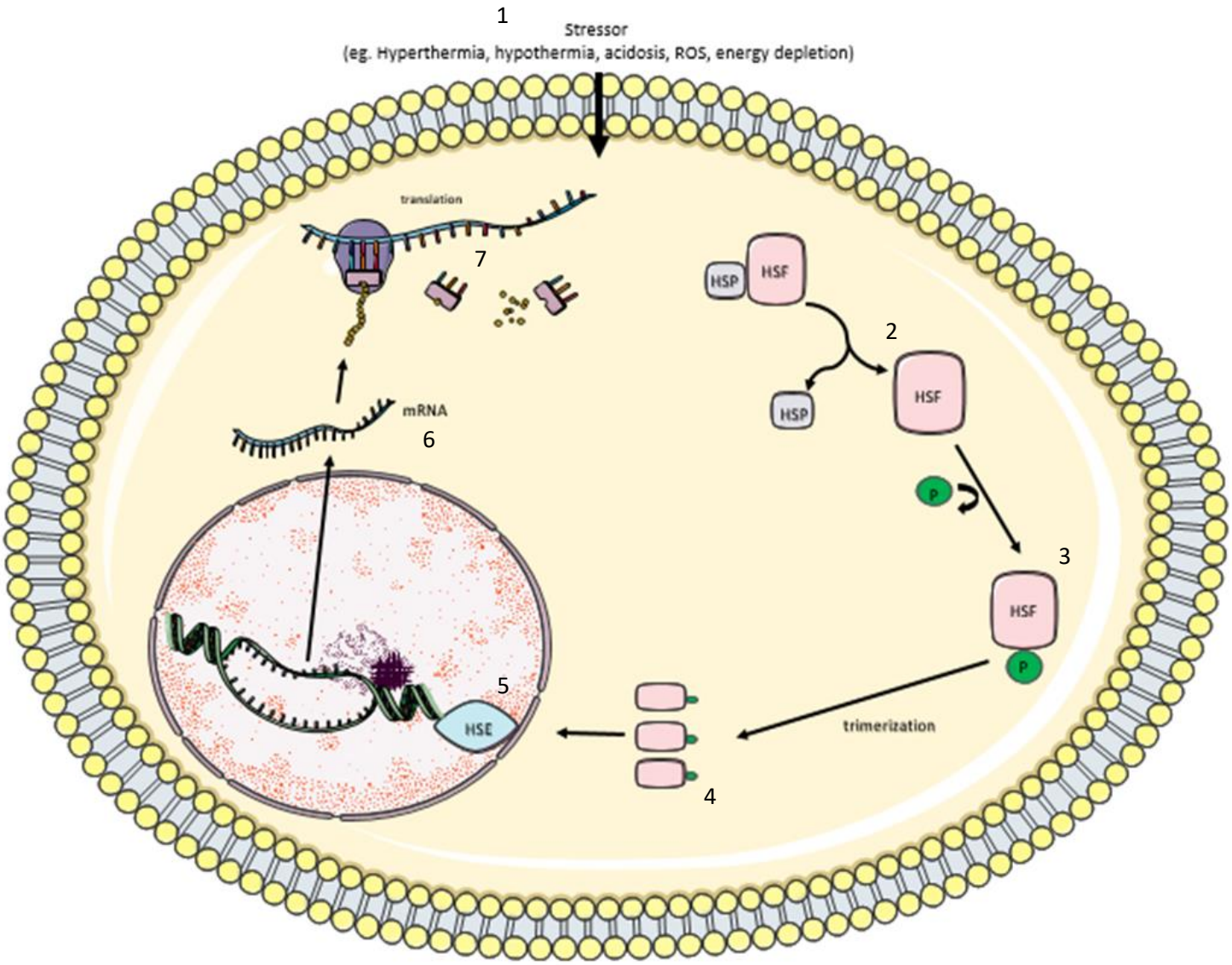

Figure 1.2 Schematic diagram of the mechanism for increased expression of HSP70/72 within a cell. (1) *Once a stressor is sensed by the cell, the Heat Shock Factor complex (consisting of inactive Heat Shock Factor (HSF) and Heat Shock Protein) separates (2), before HSF becomes phosphorylated (3). After the trimerization of phosphorylated HSF (4), this product enters the nucleus to bind to the Heat Shock Element (HSE) on the promoter region of the HSP gene, promoting transcription (5). The resultant mRNA leaves the nucleus (6) to get translated into protein within the cytosol (7). Adapted from Kregel 2002.*

1.4.3 Structure

The Hsp70 multigene family performs functions on non-native polypeptides using ATP binding and hydrolysis. HSP binds to protein substrates to assist with folding, degradation, transport, regulation and aggregation prevention. It consists of two highly conserved domain structures: a 45kDa N-terminal ATPase binding domain and a 25kDa C-terminal substrate binding domain **(Figure 1.3).** This C-terminal is further split into a β-sandwich domain and a α-helical domain (Mayer 2005). The N-terminus domain is formed of two lobes, forming a cleft that binds ATP with a nucleotide binding cassette (Bork 1992). The two main domains are connected by a small linker (Bork 1992).

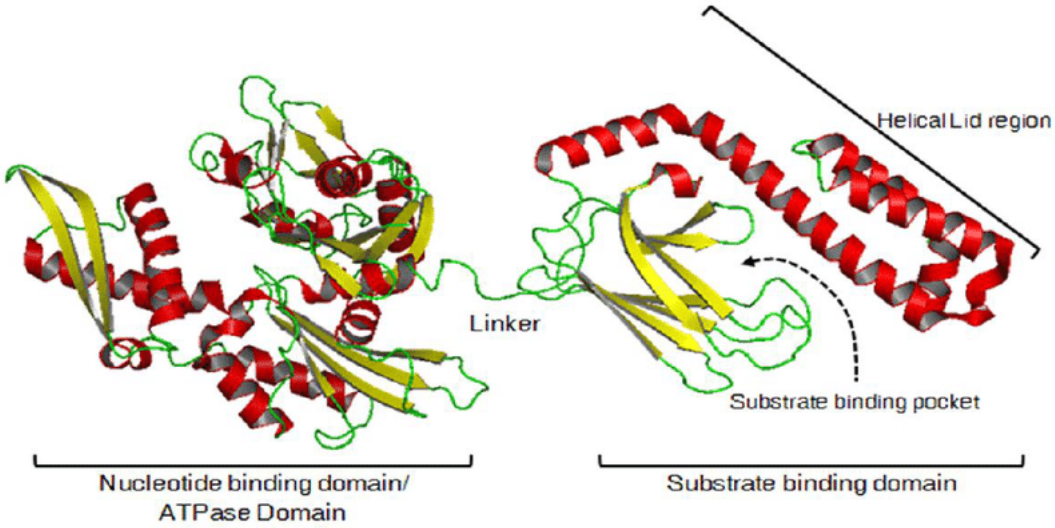

Figure 1.3 Protein structure of HSP70. *The HSP70 structure consists of two subdomains; the Nucleotide binding domain or ATPase domain and the Substrate binding domain. Sourced from Sharma et.al 2001*

1.4.4 Function

Many of the functions of HSP70 rely on the cross talk between the two sub domains of its structure, influenced by ATP (Turturici 2011). As previously eluded to, HSP70 is a protein naturally found in the body responsible for multiple tasks, and its function is vital for the health and growth of proteins and cells. It assists in folding new proteins (Turturici 2011; Bork 1992; Schaffitzel) during their conformational stage, transporting proteins and vesicles (Pratt 2003) as well as the degradation of damaged or unwanted proteins (Bercovich 1997). The folding and assembling of proteins are achieved via a rapid but controlled process of binding and releasing substrates, and this in turn, helps to prevent aggregation (Broadley 2009). The binding occurs to a non-native substrate with an exposed hydrophobic area and an accessible polypeptide backbone, which attaches to the substrate binding domain of HSP70. Consequently, ATP on the nucleotide binding domain hydrolyses, closing the substrate binding domain and stabilising the product (Hartl, 2002). HSP's can also unfold misfolded proteins, by binding and releasing hydrophobic amino acid chains, triggering ATP-driven conformational change (Murphy, 2013).

1.4.5 Hsp72 and inflammation

The long-lasting dysregulation of inflammatory responses is currently under investigation for its impact on brain function and facilitating the onset and progression of neurodegeneration in AD (Newcombe, 2018). Therefore, it is imperative to understand inflammation and the linkage of inflammation to Hsp72.

Due to its cytoprotective nature, Hsp72 has been utilised in experiments to protect against inflammatory stress. HSP's inhibit inflammatory kinases and have been associated with the inhibition of JNK1 activation (Gabai *et al.* 1997). A study performed by Chung et.al (Chung *et al*. 2008) involved mice undergoing heat therapy once a week for 16 weeks, increasing the core temperature to 41˚ C for 15 minutes. Mice exposed to this therapy were found to be protected against insulin resistance which was associated with an increase in Hsp72 levels and a decrease of JNK1 phosphorylation in muscle. This treatment observation has also been confirmed by Morino *et.al* and Gupte *et.al* (Morino *et al*. 2008; Gupte *et al.* 2009;), with Morino and colleagues using mild electrical stimulation to increase Hsp72 for 12 weeks and was associated with the decreased phosphorylation of JNK1. Due to the role of inflammatory kinases in the role of insulin signalling, Hsp72 Tg mice were assessed for JNK1 phosphorylation, with JNK1 phosphorylation being completely prevented in Hsp72 Tg mice (Chung *et al.* 2008). Collectively, the data suggests that over-expression of Hsp72 inhibits the JNK1 pathway of inflammation. Although these studies were in the context of obesity and insulin resistance, the role of Hsp72 in the reduction of JNK1 is apparent and gives rise to its potential in protective effects against other damaging inflammatory responses.

1.4.6 Role of Hsp72 in mitochondrial biogenesis and metabolic function

In respect to mitochondria, biogenesis and mitophagy involve the process producing new mitochondria and the process of programmed mitochondrial break down, respectively. The regulations of these dynamic processes are crucial for the health of the cell (Hales 2010). As mentioned previously, healthy metabolic function is a balance between biogenesis, fusion, fission and mitophagy. The link between AD and metabolic disorders, which can stem from disordered mitochondrial and metabolic function, is becoming increasingly apparent, so too is the role of Hsp72 and its associations with these disorders.

Previous studies have shown an increase in biogenesis markers such as Nuclear Respiratory Factor 1 (Nrf1) and transcription factor A, mitochondrial (TFAM) in Hsp72 Tg mice, in comparison to WT, which suggests a key role in the biogenesis process (Henstridge *et al*. 2014). Electron micrograph of skeletal muscle in mice fed a normal chow diet found a significantly increased number of mitochondria in the Hsp72 Tg mice compared to the WT, which coincides with previous work suggesting that heat stress-induced Hsp72 expressions stimulates mitochondrial biogenesis (Liu & Brooks 2012). Functional capacity, however, per unit mitochondria remained the same between genotypes and it is important to note that increased mitochondrial density may not necessarily equate to increased mitochondrial function. Currently, the overexpression of Hsp72 is a pathway of interest as it has been previously linked to oxidative potential.

Henstridge and colleagues additionally demonstrated that Hsp72 plays an important role in skeletal muscle mitochondria and oxidative metabolism (Henstridge *et al*. 2014). When assessed for whole body oxygen consumption via metabolic caging, Hsp72 Tg mice were also found to have a significant increase in VO_2 (volume of oxygen consumed), which coincided with an increase in activity and mitochondria number. These data were consistent with previous studies from Chung, Liu and Gupte; all showing markers of oxidative metabolism in skeletal

muscle are increased in Hsp72 Tg mice (Chung *et al*. 2008), C2C12 (immortalized mouse myoblast) muscle cells (Liu & Brooks 2012) and rats using heat treatment to induce expression (Gupte *et al.* 2009). Collectively, it is now thought that Hsp72 regulates energy balance via improved oxidative metabolism in skeletal muscle. Hsp72 Tg mice were found to have increased oxidative enzymes; citrate-synthase and β-hydroxyacyl-CoA dehydrogenase (β-HAD), decreased intramuscular lipid accumulation and increased mitochondria number. Consequently, knock out models of Hsp72 were found to have decreased oxidative enzymes and an increase number of enlarged, dysmorphic mitochondria (Drew *et al*. 2014).

Recently, it was identified that this Hsp72 Tg model not only over-expresses Hsp72 in the muscle but also the brain (Marshall *et.al* 2018). While the above data focussed on skeletal muscle, the knowledge that the Hsp72 Tg mouse model also had overexpression of Hsp72 within the brain, makes it a viable tool to cross this model with an AD mouse model for further research.

1.4.7 Pharmacological targets

Taking into consideration the significance of Hsp72 as understood through existent findings, it is now a potential therapeutic treatment for numerous diseases and ways in which the protein can be further induced are currently being investigated. By manipulating Heat Shock Factor-1 (HSF-1) which is the central regulator of Hsp72 (Dokladny *et al.* 2013), Hsp72 protein expression can be up-regulated.

There have been several compounds now identified that can induce Hsp72 expression. Geldanamycin is a naturally occurring antibiotic that has been shown to be an effective HSP70 inducer, with anti-cancer properties (Auluck *et.al* 2002). Its use has also shown benefits in mouse models of Huntington's disorder (Hay *et.al* 2004), supporting the theory of its therapeutic effects in protein misfolding disorders. However, despite these promising results, Geldanamycin is unfortunately water insoluble and at high levels, has shown hepatic toxicity, deeming it unsuitable for clinical use (Powers *et.al* 2007).

Dexamethasone is a glucocorticoid used primarily as an anti-inflammatory and immunosuppressant, which has been proposed to directly activate heat shock factor 1.
(Sun 2000). However, later studies showed that while an optimum cocktail of drug had a robust effect on HSP70, it had no effect on the inducible Hsp72 (Zhang 2014).

Geranylgeranylacetone (GGA) is predominantly used as an antiulcer medication which also has potential therapeutic effects for conditions such as colitis, ischemia, and retinal detachment. GGA is thought to prolong HSF1 activation and has been found to increase circulating HSP70 by 24% (Kavanagh *et.al* 2011), improving glucose tolerance in diabetic monkeys.

An additional compound called BGP-15 was discovered while investigating HSP's and is now considered a known co-inducer of Hsp72 (Literati-Nagy 2009). It is a nicotinic amidoxime derivative and is water soluble. Unlike other compounds, it has been found to be safe and well

tolerated in clinical trials with no adverse effects. BGP-15 is currently in Phase 2 clinical trials for insulin resistance/ T2D. This compound will be the focus of *Chapter 4* of this thesis.

The number of disorders triggered by misfolded proteins are significant, therefore it is crucial to find a way to manipulate targets such as Hsp72 that work to repair and degrade damaged/aggregated proteins. Despite this promising target, the translation of Hsp72-activating drugs to the clinic has been a challenge, due to high toxicity and low solubility of trialled drugs. The compound BGP-15, initially used for its protective effects in insulin resistance is now a potential focus, due its solubility, efficacy and safety. From personal communication with the manufacturers of the compound (N-Gene Inc), ~20-80ng/ml of BGP-15 was found to accumulate in the brain when administered at a dose of 100mg/kg/day. This means that via unknown transportation mechanisms, the compound can pass through the blood brain barrier. BGP-15 will be the compound of focus moving forward in this thesis and will be further discussed later in this review.

1.5 Hsp72 in Alzheimer's disease

1.5.1 Overview

Considering the accumulation of Aβ and tau in the brain, AD is considered a disease where proteins are misfolded and aggregate, which may suggest the importance of molecular chaperones in the manifestation of these protein-aggregate diseases. In the cellular environment, proteins are extremely vulnerable to abnormal folding and aggregation, which may lead to toxic species.

The HSP proteins, known for their chaperoning ability, have now been associated with AD pathogenesis and its potential as a pharmacologically modulated target in AD treatment. A number of studies have suggested that HSPs are regulators of neurodegenerative processes which correlated to protein misfolding in patients with AD (Meriin and Sherman, 2005, Franklin *et al*., 2005, Magrane *et al.*, 2004). Similarly, in cellular models of AD, HSP70 overexpression showed therapeutic effects (Evans *et al*., 2006). Together, evidence suggests that targeting Hsp72 in the brain could potentially be utilised as a therapy for AD. As mentioned, currently that are no available drugs that effectively treat, prevent or slow the progression of AD. Hence, new pharmacological approaches and the importance of studying potential cellular mechanisms are warranted.

1.5.2 Hsp72 in patients with AD

The Hsp72 pathway is of great interest due to previous research showing that Hsp72 is increased in brain tissue of AD patients when compared to control brains. A human study by Hamos and colleagues found anti-Hsp72 antibodies 'intensely stained neuritic plaques and neurofibrillary tangles' (Hamos *et al*., 1991) in post mortem AD brains **(Figure 1.4)**. Healthy control subjects, in comparison, showed Hsp72 immuno-reactivity at very low levels which was further supported by Western Blot analysis. Importantly, areas of the brain that contained the highest concentrations of plaques and tangles had a direct relationship with Hsp72 immunoreactivity.

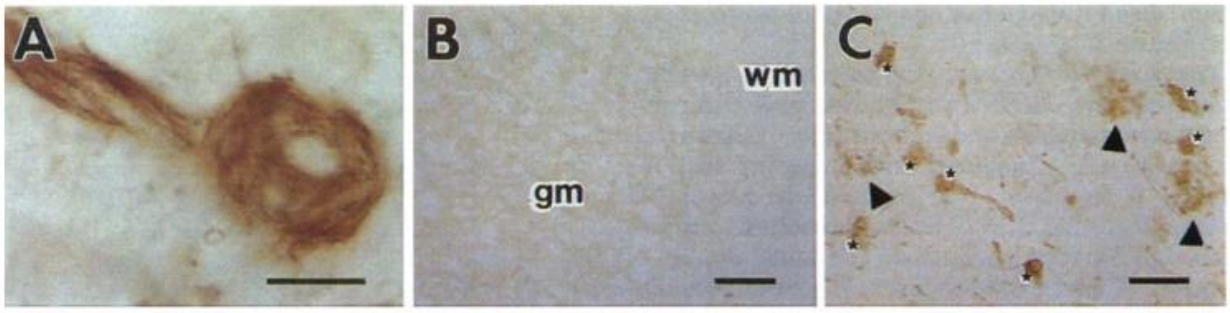

Figure 1.4. **Post-mortem images of stained brain tissue from an AD patient.** *(A) Hsp72 immunoreactivity in a neurofibrillary tangle from hippocampus tissue in AD patient. (B) Hsp72 staining in the entorhinal cortex of cognitive control patient gm= grey matter, wm=white matter. (C) Hsp72 staining of plaques (triangles) and tangles (stars) in subiculum of AD patient. A = 10 µm, B-C = 50 µm. Source: (Hamos et al., 1991)*

Importantly, this study was confirmed by Perez and colleagues whom reported that there was increased synthesis of Hsp72 in AD brains, observing mature Hsp72 on immunoblots and newly synthesized Hsp72 via 2D electrophoretic separation and immunoprecipitation (Perez *et al.*, 1991). Immunoblot results determined increased levels of mature Hsp72 in AD homogenates were from the temporal cortex and not the cerebellum, suggesting the increase is specifically associated with the disease as AD pathology does not show disease in the cerebellum. Furthermore, this study provided evidence of increased synthesis which was measured by *in vitro* translation products of polysomes. After quantitation, Hsp72 was found at levels 2-3-fold higher than control, however when mRNA was analysed, increases in AD samples were not evident. Previous cell work has shown that HSP genes can undergo translational regulation to increase protein synthesis in the absence of increased HSP mRNA (Scott and Pardue, 1981, Storti *et al*., 1980), which may explain these results.

While both studies agree that a relationship between Hsp72 and AD exists, neither is clear on the relationship type. It is thought that HSP's bind to abnormal proteins to disrupt or prevent their aggregation (Lewis and Pelham, 1985) or induce proteolysis by targeting abnormal proteins (Chiang *et al*., 1989). Together, this might indicate that Hsp72 expression is activated by unknown mechanisms during the development of plaques and tangles as a defence mechanism. However, finding high level staining only in pathological tissue could indicate that the body produces an ineffective amount to be a protective mechanism for each neuron. At the very least, it is clear that the stress response is an important relationship in the pathology of AD. Perez and colleagues suggest that an interaction of the stress response with the initial events of AD actually exacerbate the pathology, hence the high Hsp72 levels in AD post mortem tissues (Perez *et al*., 1991).

More recently, several reviews have identified the upregulation of HSPs, through heat therapy, as therapeutic targets for the treatment of neurodegenerative diseases including AD (Carman

et al., 2013; Kalmar *et al*., 2014; Schapira *et al*., 2014; Ciechanover and Kwon, 2017; Webster *et al*., 2017; Klaips *et al.,* 2018). Exceptionally interestingly, a study in 2017 found the incidence of AD was reduced in people who undertook moderate to frequent sauna bathing (Laukkanen *et al*., 2017). While the mechanisms of action require further investigation, this review will continue to explore Hsp72 as a strategy for the treatment of AD.

1.5.3 Hsp72 inhibits Aβ oligomerisation

The assembly of Aβ produces multiple structures including dimers and oligomers, the latter which is believed to be the most neurotoxic and important in AD development (Shankar *et al.*, 2008, Honjo *et al.*, 2012). The 'amyloid cascade hypothesis' describes how the aggregation of Aβ triggers the series of downstream events seen in AD progression such as tau hyper-phosphorylation, synaptic loss of function, neuronal death, inflammation and plaque deposition.

Recent research has found evidence that activation of Hsp72 can protect against both Aβ aggregates and tau formation (Evans *et al*., 2006, Magrane *et al.*, 2004, Patterson *et al.*, 2011), with *in vitro* studies suggesting the expression of heat shock proteins suppress the progression of the disease (Magrane *et al*., 2004, Muchowski and Wacker, 2005). Excitingly, in the first *in vivo* study, Hoshino and colleagues (Hoshino *et al.*, 2011) investigated the effect of over expressing Hsp70/Hsp72 on a mutant model of AD (the model APPsw). Results demonstrated that overexpression of Hsp70 suppressed the pathological phenotypes of the disease as well as its resultant cognitive deficits. It was further found that Hsp70 had positive effects on anti-aggregation, neuroprotection and stimulation of amyloid clearance. APPsw/Hsp70 animals showed a significant decrease in soluble beta amyloid in both the hippocampus and cerebral cortex compared to APPsw/WT animals

Currently, it is suggested that Hsp72 can recognise Aβ oligomers via their hydrophobic regions and modify their conformation to prevent aggregation (Evans *et al*., 2006). Other neurodegenerative diseases that display aggregation of proteins have similarly shown a reduction of protein aggregation and symptoms attenuated with the overexpression of Hsp's including polyglutamine diseases and Parkinson's disease (Adachi *et al*., 2003, Katsuno *et al*., 2005, Muchowski and Wacker, 2005, Lo Bianco *et al.*, 2008)

1.5.4 Hsp72 enhances Aβ clearance

Further in Hoshino's 2011 study, using a mutant APP AD model, they found that an overexpression of Hsp72 upregulated the expression of IDE. IDE is a gene involved in the clearance of Aβ, and this was the proposed mechanism of action for the suppressed pathology results seen earlier. IDE was interestingly upregulated in both the AD model and in WT animals crossed with Hsp72 Tg animals. Conversely, *neprilysin* or *ece-2,* other genes involved in the clearance of Aβ did not have higher mRNA expression in the Hsp72 Tg animals.

The enhancement of Aβ clearance through Hsp72 can also be attributed to the upregulation of TGF-β1 expression. This is a key cytokine regulating the response of the brain to injury and inflammation, which has also been suggested to suppress the progression of AD. In addition to this, it stimulates the clearance of Aβ through activation of phagocytic microglia.

Hoshino's study, while promising, used a model of AD expressing mutant APP and did not include a tau model. Experiments *in vivo* with tau overexpressing mice, or both tau and Aβ expressing, are yet to be studied. Aβ and tau are both important in the progression of AD and no one is yet to have studied the overexpression of Hsp72 in a model of AD that has both features.

1.5.5 Hsp72 promotes tau binding to microtubules

Tau homeostasis is regulated by its expression, phosphorylation and turnover. When its homeostasis is disrupted, it leads to the dissociation of tau from microtubules, the hyperphosphorylation of this dissociated tau, eventuating in the toxic aggregates of NFT's. There are now numerous studies suggesting that HSP70 might help to promote tau binding to microtubules, thereby preventing tauopathies (Dou 2003; Petrucelli 2004; Miyata 2011). The pathogenic effect of tau is hypothesized to come from the inability of hyperphosphorylated tau to bind to microtubules, so by increasing the stability, studies have seen a decrease in tau aggregates as a result.

1.5.6 Hsp72 inhibits tau aggregation

HSP70 has also been linked to tau aggregates with protective benefits. *In vitro* studies have found HSP70 to be potent inhibitors of tau aggregation, preventing the formation of fibrils (Patterson *et al*., 2011). Patterson and colleagues showed that HSP70 bound directly to soluble monomeric tau and saw a dose-dependent reduction in the level of tau aggregation with increasing HSP concentrations.

As previously mentioned, HSP has been found to stabilise tau to microtubules, however in the case of already dissociated tau, HSP70 has been found to interact with pre-existing tau aggregates, preferentially binding to oligomeric over filamentous tau (Patterson *et al*., 2011). This prevented any further aggregation from occurring. Furthermore, treatment with HSP70 on tau aggregates prevented the toxic effects that they have on axonal transport, which plays a critical role in neuronal function and promoted tau degradation (Shimura *et al*., 2004, Petrucelli *et al*., 2004, Jinwal *et al.*, 2010, Miyata *et al*., 2011, Wang *et al.*, 2010) (Summary in Fig.6).

As mentioned, although *in vitro* results are promising, experiments *in vivo* in tau over-expressing mice are yet to be studied.

1.5.7 Hsp72 and protection in the brain

Evidence from post-mortem AD brains show extensive tissue degeneration. *In vitro* and *in vivo* studies have shown that the accumulation of Aβ has led to neuronal loss (Viana *et al*., 2011) largely due to DNA damage, leading to apoptosis. Oxidative insults and thermal stress are also known to induce apoptosis in the development of AD. In 1994, Mailhos and colleagues discovered that overexpression of Hsp70 attenuated thermal stress induced neuronal death (Mailhos *et al*., 1994). This mechanism was elucidated in 2012, when Sabirzhanov and colleagues demonstrated that Hsp70 inhibits neuronal cell death by modulating Apaf-1 caspase-dependent and AIF caspase-independent pathways (Sabirzhanov *et al.*, 2012).

Therapeutic effects of Hsp72 are already being researched with promising results. In 2013, Bobkova and colleagues found protective effects of endogenous, inducible Hsp70 in animals post olfactory bulbectomy (OBX) (Bobkova *et al.*, 2013). OBX animals are known to develop several pathologies including Aβ accumulation, and with the results demonstrating a high level of inducible Hsp70 synthesis with treatment and the recovery of spatial memory, Bobkova supported the idea of Hsp72 as a therapeutic target. With this knowledge, they extended the Hsp72 theory and began treating animals with intranasal-administered recombinant human Hsp72. This treatment was found to enter the afflicted areas of the brain and reduce Aβ plaque formation in OBX and 5XFAD AD models of mice (Bobkova *et al.*, 2014). Remarkably, the therapeutic effect was induced by a single course treatment, with long term effects. Together, considering the growing evidence of the effects of over expression of Hsp72 in *in vitro* and *in vivo* studies, as well as the exogenous Hsp72 effects, further studies into Hsp72's potential as a therapeutic treatment for a more closely related human AD model are warranted. Investigating Hsp72 in a model with both Aβ and tau pathology would be an attractive option.

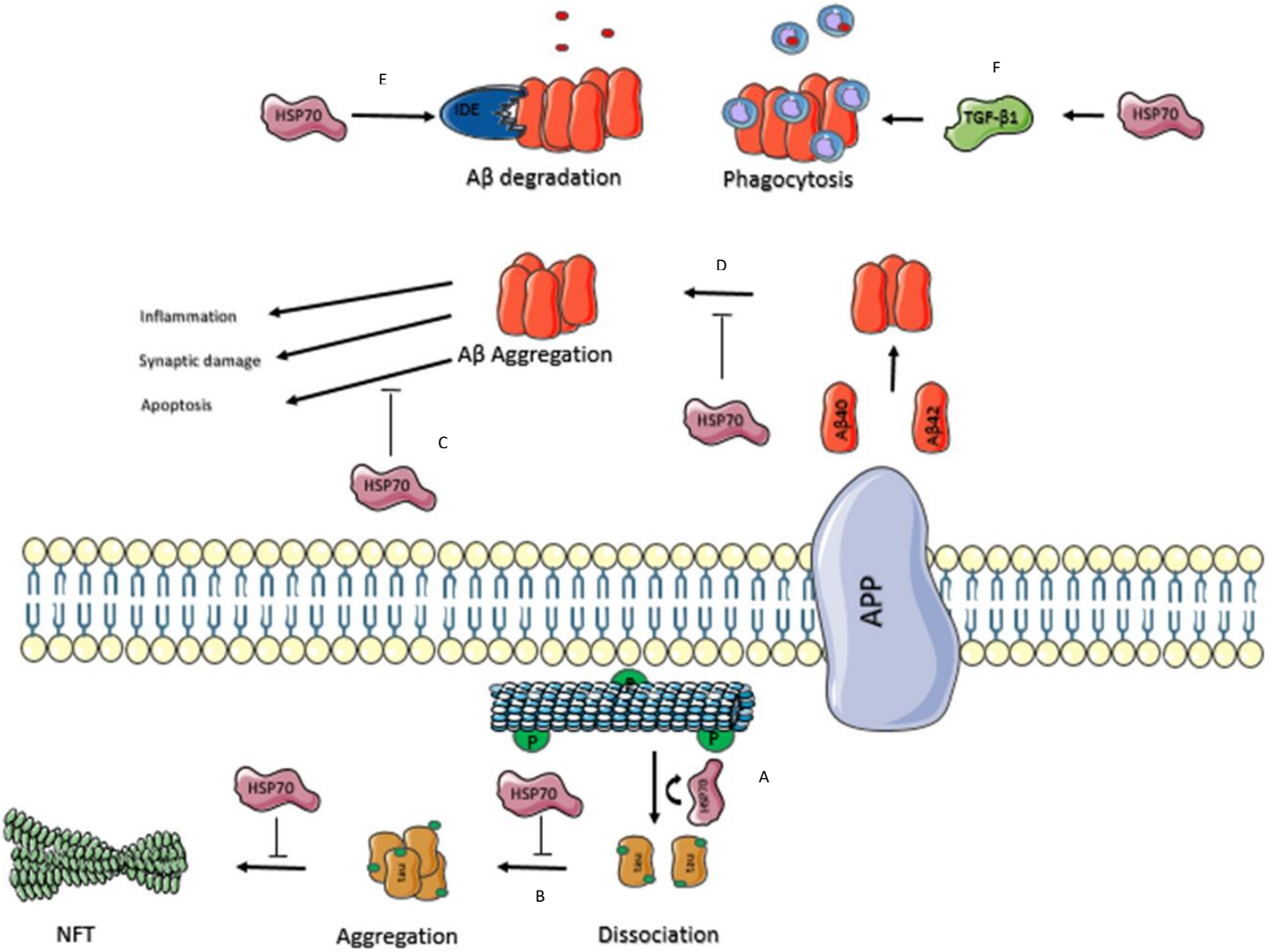

Figure 1.5 ***Summary of HSP70 in the pathogenesis of Alzheimer's disease.*** *HSP70 has numerous effects on the pathology of AD. A) HSP70 promotes tau binding to microtubules. B) HSP70 directly inhibits tau aggregation at multiple stages, preventing NFT formation. C) HSP70 prevents apoptosis. D) HSP70 inhibits Aβ aggregation. E) HSP70 promotes Aβ degradation by promoting insulin degrading enzyme, promoting Aβ clearance. F) HSP70 promotes phagocytosis of Aβ by inducing TGF-β1.* Image adapted from Lu et.al 2014

1.5.8 Heat therapy, metabolic dysfunction and Alzheimer's disease

It is becoming apparent that the complex etiology of AD requires new, multifactorial approaches to its therapeutics. As previously mentioned, metabolic dysfunction, such as reduced insulin sensitivity has been demonstrated to be impaired in those with AD compared to healthy individuals (Morris *et.al* 2016). This increased risk may be mechanistically driven by insulin's effects on several cellular processes within the brain, such as Aβ trafficking and tau phosphorylation (de la Monte *et.al* 2012; Morris *et.al* 2012) Chronic heat therapy, such as water immersion or sauna use, is a non-pharmacological way to induce the Hsp72 response and has demonstrated positive effects on cardiovascular and metabolic adaptations in both healthy (Brunt *et.al* 2016) and obese (Ely *et.al* 2019) individuals. Alongside this, heat therapy has had remarkable results *in vivo*, on vascular health, metabolism and mitochondrial health (Chung *et.al* 2008; Drew *et.al* 2014; Geiger *et.al* 2011; Gupte *et.al* 2009; Rogers *et.al* 2016). Due to heat therapies effects on inducing HSP's, it has recently been speculated that in the context of brain health, it may be a beneficial modality for dementia and AD (Von Schulze *et.al* 2020). The potential now exists to treat these dysfunctions through HSP induction with chronic heat therapy, therefore lowering the risk of dementia and AD.

Additionally, there is the potential of heat therapy directly protecting the brain, through facilitating the delivery of molecular mediators within extracellular vesicles. Extracellular vesicles can carry protein throughout circulation and have been shown to play a role in the regulation of nerve regeneration and synaptic function (DeLeo *et.al* 2018; Yuyama *et.al* 2014). Exceptionally, when directly injected into the brain, they have been shown to eliminate protein aggregates (Yuyama *et.al* 2014). While heat therapy in human trials have shown significant increases in skeletal muscle Hsp72 (Hafen *et.al* 2018) brain Hsp72 has not yet been investigated. As a result, extracellular vesicles are now being utilised as they are known to be able to carry HSP's (Whitham *et.al* 2018) and can cross the blood-brain barrier.

Together, research has shown that heat therapy and the induction of HSP's have protective benefits against dysfunctions that pose as high-risk factors for AD and could therefore be another potential area of interest for AD therapy. Moreover, this type of therapeutic intervention could hold a higher compliance in at-risk groups, compared to other interventions such as exercise or medication (Akerman *et.al* 2019). Additionally, with the potential to increase inter-organ crosstalk, through extracellular vesicles, this type of therapy that targets whole-body metabolic and chaperoning systems could be a viable solution.

1.6 BGP-15

1.6.1 Overview and structure

BGP-15 (chemical formula C14H22N4O2·2HCl) is a nicotinic amidoxime derivative and was first developed to improve insulin sensitivity (Literati-Nagy 2009), however many pharmaceutical effects have now been identified. The compound was developed from older generation compounds designed to activate HSP's and is now known as a Hsp72 co-inducing compound. BGP-15 increases HSP induction via inhibiting the acetylation of heat shock factor 1, prolonging the duration of it binding to heat shock elements activating Hsp72 (Gombos *et al*. 2011). It is a small molecule that is water soluble, which makes it an attractive option pharmaceutically.

In addition to inducing HSP, BGP is now a drug of interest for many disorders, due to its versatility. It has been reported as well tolerated and safe (Literati-Nagy 2009) and is now in Phase 2 clinical trials for treatment against insulin resistance (Literati-Nagy, 2013). Its versatility has meant it has been shown to have benefits for a multitude of other diseases including Duchenne muscular dystrophy (Gehrig 2012), heart failure and atrial fibrillation (Sapra, 2014) and traumatic brain injury (Eroglu, 2014). It is clear that BGP-15 has a wide range of effects for a suite of disease types, which could be put down to its multiple mechanisms of effects other than Hsp72 induction. These include inhibiting Poly(ADP-ribose) polymerase-1 (PARP-1), inhibiting Histone deacetylases (HDAC), suppressing inflammatory markers and increasing IGF-1 receptor (summarised below), which are also reported to be important players in the progression of AD. Together, these targets of BGP-15 warrant further investigation into its potential as a pharmacological therapy against AD.

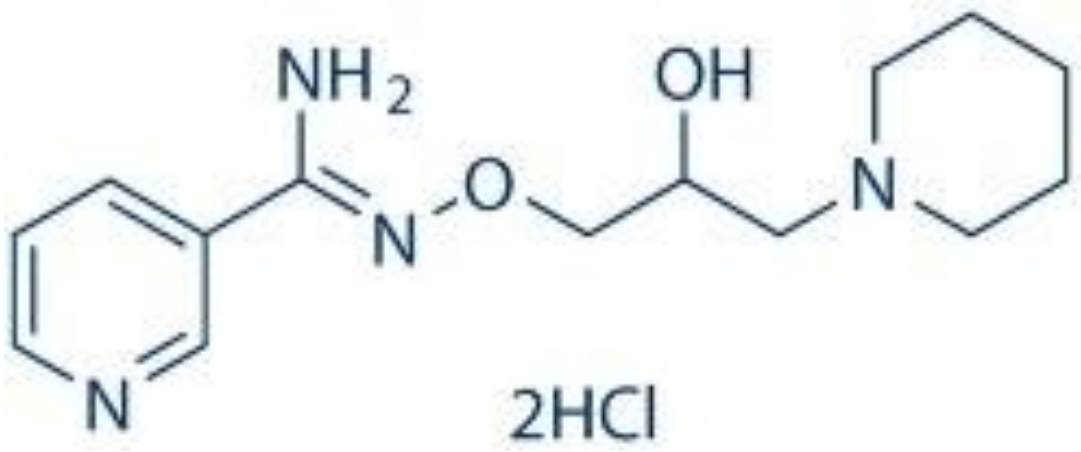

Figure 1.6 ***Chemical structure of Hsp72 co-inducing compound, BGP-15.*** *(O-(2-hydroxy-3-piperidinepropyl)-pyridine-carbonic acid-amidoxime dihydrochloride). Source: Peto 2020*

1.6.2 BGP-15 increases IGF-1 receptor

Insulin-like growth factor-1 (IGF-1) is a hormone normally induced by physical activity, promoting survival, preventing apoptosis and stimulating neurogenesis in the hippocampus (Westwood 2014). While generally mentioned in the context of T2D and growth, IGF-1 has also been shown to be implicated in AD. Abnormal tau phosphorylation and Aβ deposition in both cell culture and AD mouse models were inhibited with IGF-1 (Hong 1997). Additionally, animals with low IGF-1 showed reduced hippocampal neurogenesis and impaired spatial learning (Llorens-Martin 2010), suggesting an important role in brain development and function. Clinically, in patients who had an APP mutation, low IGF-1 levels were associated with greater Aβ burden, as well as poorer baseline cognition, and increased rate of cognitive decline over time (Mustafa 1999; Dik 2003; Al-Delaimy 2009; Kalmijn 2000). An epidemiological study additionally found that lower serum IGF-1 levels increased the risk of AD in older and middle-age people. Conversely, among cognitively healthy participants, higher serum IGF-1 levels were associated with greater total brain volume (Westwood 2014).
Since IGF-1 has been shown to be a key hormone beneficial to cell survival, preventing apoptosis, researchers have been investigating ways to stimulate its production. It has since been discovered that BGP-15 increases IGF-1 expression by increasing its phosphorylation, which resulted in protections against heart failure and atrial fibrillation (Sapra 2014). Interestingly, this was independent of HSP70. The suggested mechanism of action for this was alterations of membrane-localized receptor proteins via enhancing membrane fluidity and monosialodihexosylganglioside 3 (GM3) (Gombos 2011).

1.6.3 BGP-15 inhibits Histone deacetylases

HDAC's, regulate the level of histone acetylation and further affect downstream gene expression. Abnormal acetylation of histone is involved in the pathology of AD. Previously, it's been shown that the activity of HDAC's regulate the duration and magnitude of HSF1 binding to DNA, the promotor region to ultimately express HSP (Westerheide 2009; Zelin, 2015). Other HDAC inhibitors have been shown to improve memory and learning, as well as affecting the activities of the Aβ and tau, via decreasing production and phosphorylation.

With this in mind, a recent study found that cells treated with BGP-15 had a decreased activity of HDAC's, which was associated with increased chromatin accessibility, lowering the threshold for heat shock response activation (Budzynski 2017). By increasing chromatin accessibility for transcription machinery at gene loci *HSPA1A,* it showed that BGP-15 can accelerate the activation and attenuation of the HSF1 cycle. Despite this, it is important to note at this time, that the inhibition of HDAC's using BGP-15 was not as effective as other currently known inhibitors, and BGP-15 could not inhibit the activity of purified HDAC (Budzynski 2017).

1.6.4 BGP-15 inhibits PARP-1

PARP-1 is an enzyme responsible for genome stability, transcriptional regulation, and long-term potentiation in neurons. PARP-1 increases during times of oxidative stress and DNA damage, which leads to NAD depletion, causing an energy crisis and cell death. The excessive activation of PARP-1 leads to the accumulation of poly(ADP-ribose) (PAR), a molecule that signals programmed cell death. Consequently, PARP-1 has been associated with the pathogenesis of many CNS disorders such as neuro-inflammation and neurodegenerative diseases. PARP-1 has also been shown at higher levels in AD human brains during post-mortem analysis (Love 1999). Interestingly, animal models crossing an Aβ mutant with a PARP knockout attenuated brain dysfunction as seen in the Aβ mutant controls (Kauppinen 2002). Aβ has also been found to activate PARP-1 in both cellular and animal models of AD (Martire, 2013; Abeti, 2011).

The Hsp72 co-inducer, BGP-15, is a multi-target compound that fluidises yet stabilises membranes. Interestingly, one of the additional targets that BGP-15 has been found to modulate is the PARP-1 pathway. During an ischemia-reperfusion insult, it was found that BGP-15 protected the heart via direct inhibition of the PARP-1 pathway (Szabados 2000).

PARP-1 inhibition via the use of BGP-15 has also been shown to protect the mitochondria from oxidative damage which plays a crucial role in AD pathophysiology. As previously mentioned, the role and health of mitochondria play a crucial factor in the pathogenesis of AD. It has been shown that PARP-1 plays a regulatory role in mitochondrial dysfunctions as the resultant NAD depletion from PAR accumulation ultimately depletes ATP, leading to energy failure and cell death (Bai 2012; Bai 2015).

1.6.5 BGP-15 and the mitochondria and inflammation

Through inhibiting PARP-1, BGP-15 has the potential to inhibit crucial pathways responsible for the progression of AD via decreasing mitochondrial dysfunction and neuronal cell death. Additional processes that contribute to cell death, apart from the PARP-1 pathway, are markers of inflammation such as c-jun amino terminal kinase (JNK), p38 MAP Kinase and tumor necrosis factor-α (TNFα). As previously discussed, inflammation is a key factor in the pathogenesis of AD, hence targeting these markers could be beneficial. Inflammation results in the secretion of inflammatory cytokines, including TNFα which activates JNK and p38 (Wellen 2005; (Raingeaud 1995). Hsp72 was previously found to markedly suppress JNK in vitro (Gabai 1997; Park 2001) as well as TNFα gene expression (Meldrum 2003). Consequently, research moved on to focus on the effects of BGP-15 and identified that BGP-15 activation of Hsp72 prevented JNK phosphorylation via enhanced phosphorylation and expression of HSF-1 (Chung 2008). The hypothesis that BGP-15 can suppress inflammatory markers was further supported when another group found BGP-15 prevented cardiotoxicity via suppressing JNK and p38 MAP kinase (Sarszegi 2012).

In addition to this, Wu and colleagues (Wu *et.al* 2015) showed that treatment of obese females with BGP-15 increased the amount of TFAM and Dynamin related protein-1 (DRP1), which are mitochondrial replication factors, as well as mtDNA content in oocytes. This indicated an amplified mitochondrial fission as a possible mechanism of action to improve resultant oocyte developmental potential, supporting the notion that BGP-15) is able to reverse mitochondrial dysfunction.

BGP-15 is an interesting compound to test in the setting of AD not only for its Hsp72 activating capabilities but also other targets such as those previously mentioned; the HDAC pathway, PARP-1 pathway, JNK and IGF-1. Many pathways that have been shown to be altered via

BGP-15 are implicated in AD progression, therefore the potential for BGP-15 to play a protective role in AD via the Hsp72 pathway or its various other mechanisms of action is of great interest.

1.7 Challenges in AD Modelling, Treatment Strategies and Gaps in Knowledge

Due to species differences in physiology and drug responses, translation of observations in rodent models to application in humans is a major challenge. As previously mentioned, current research in pre-clinical AD models primarily focusses on either an Aβ expressing model, or a tau expressing model. The expression of both Aβ and tau pathology in a mouse model would be advantageous to not only elucidating the pathological progression of disease, but to also trial therapeutic targets. Animal models are useful in understanding fundamental biological and disease processes, particularly where human experimentation is not feasible. This would include the use of a mouse model to study a potential new drug, appropriate enough to accurately mimic human physiology.

While an array of *in vitro* studies has been performed to show promising results when treating Aβ and tau aggregates with potential targets, such as Hsp72, less work has been conducted *in vivo.* Additionally, *in vivo* work has primarily been performed on mouse models expressing mutations resulting in either Aβ or tau. Regardless of *in vitro* success, in absence of suitable animal models, the conduct of animal experiments that accurately mimic human experiments are needed, in order to increase the likelihood of successful translation.

Additionally, limitations arise when research is restricted to therapeutics that only treat one facet of the disease. AD has been shown to be a complex disease, so therapeutic targets that treat one particular pathway may never gain clinical relevance. Targets, just like the disease, need to become multi-faceted, treating multiple areas. Again, this would be most beneficial to apply to a model expressing both Aβ and tau. As mentioned, activating HSP has multiple modes of action that can improve the pathology and behaviour as seen in AD- these now need to be trialled in an advanced mouse model. Moreover, the issue of delivery and efficacy of a pharmacological treatment targeting the brain is a major challenge.

The importance in increasing the translatability and clinical relevance of basic research should not be underestimated. The potential to activate Hsp72 remains a promising therapeutic strategy to treat and slow the progression of AD, with a well-mimicked pre-clinical model.

It is also important to note at this time, that previous research into the therapeutic benefits of BGP-15 as mentioned, have primarily been conducted in models of insulin resistance, obesity or a variety of cardiovascular assaults. It is difficult to ascertain if these benefits will translate across disease models as little has been investigated with BGP-15 in the space of AD. Currently, just one paper can be found on BGP-15 and its protective benefits on neuronal death in a model of familial dysautonomia (Ohlen 2017). Further research on BGP-15 in the space of neuroscience is warranted.

1.8 Conclusions

Pursuing therapeutic targets to increase Aβ clearance and prevent Aβ and tau aggregation is an active area of research with regards to prevention of disease, treatment of symptoms and toxic pathology in individuals with AD. Discovery of novel mechanisms that enhance clearance and prevent aggregation have aided in the development of potential strategies to treat individuals with, or at the risk of, AD. One such target is the activation of HSPs, more specifically, the inducible form of HSP70, Hsp72.

This project will increase our understanding of the pathology of AD and the potential of Hsp72 as a therapy. This project will aim to investigate the role of Hsp72 in the brain in a pre-clinical mouse model of AD, using transgenic overexpression and BGP-15 treatment. This is a novel design, using a model expressing both Aβ and tau in order to study the effects of Hsp72 in a pre-clinical model that most closely resembles the human condition. Together these studies will determine whether brain Hsp72 induction is efficacious in delaying AD progression.

It is hypothesised that overexpression of Hsp72 in the brain will help to prevent the accumulation of amyloid plaques and tau tangles within the brain. It is anticipated that this project has high clinical relevance, by treating AD mice with BGP-15, to determine if drug induced Hsp72 can prevent the protein accumulation. If successful, clinical trials can be fast-tracked as BGP-15 has previously been tested safely and without adverse side effects in humans for T2D.

1.9 Experimental rationale

Targeting Hsp72 in the brain is a potential therapeutic option to prevent or delay the progression of cognitive decline and pathology as seen in AD. Investigation of strategies aimed to improve AD pathology, performed in mouse models expressing both amyloid and tau pathology will inform a better understanding of results that more accurately mimic human pathology. Collectively, the studies presented in this thesis have the potential to inform future therapeutic approaches using appropriate pre-clinical models and targeting Hsp72 for the treatment and/or the prevention of AD and its complications.

1.10 Aims

1) To replicate and extensively further characterise the *5xFAD*Tg30* mouse model of AD.

2) To investigate the effects of overexpression of Hsp72 in the brain of *5xFAD*Tg30* mice via genetic overexpression.

3) To investigate the effects of long-term administration of the Hsp72 co-inducing compound, BGP-15, in the *5xFAD*Tg30* mice.

2 Characterisation of the *5xFAD*Tg30* mouse model of Alzheimer's disease

Preface

Current evidence suggests that the onset and progression of AD is characterised by the accumulation of two proteins, namely amyloid and tau. It is suggested that research into therapies and treatments have been hampered by the unavailability of an appropriate and physiologically accurate mouse model of this disease. Therefore, to directly study further treatment therapies, it is important to conduct these in a pre-clinical model which represents the human disease as closely as possible.

The aim of this study was to investigate a recently developed mouse model of AD expressing human amyloid and tau in the brain and characterise its metabolic and behavioural phenotype. This study was performed on two separate cohorts of animals, one for behavioural phenotyping and the other for metabolic phenotyping. At the time of project initiation, the paper from Heraud and colleagues on the generation and description of a new mouse model, *5xFAD*Tg30*, was only recently published. Data from this paper suggested this was an appropriate model based on the brain pathology, however, a more in-depth characterisation of whole-body physiology was required to understand the complete phenotype associated with the model.

2.1 Introduction

As outlined in *Chapter 1*, development of a robust pre-clinical model of AD is important not only as good representation to study mechanisms of disease, but also an important step for future therapeutic development.

According to the amyloid cascade hypothesis, the hyperphosphorylation of tau and its aggregation occurs post APP cleavage (giving rise to Aβ), yet transgenic animals expressing mutated APP and/or PS1 gene(s) do not develop NFT (Boutajangout *et al*., 2004). Additionally, APP models bred with a Frontotemporal dementia (FTD) mutant tau, saw an increase in tau pathology (Hurtado *et al*., 2010, Lewis *et al.,* 2001, Paulson *et al.,* 2008, Perez *et al*., 2005, Stover *et al*., 2015, Seino *et al*., 2010, Terwel *et al*., 2008). This knowledge suggests that indeed there is interplay between amyloid and tau in playing a role in neuronal dysfunction and that disregarding one over the other in preclinical trials could be detrimental. Past APP/tau models have been described as slow developing and relatively modest (Paulson *et al.,* 2008, Perez *et al.,* 2005, Seino *et al*., 2010, Terwel *et al*., 2008) and does not include a mutant PS1 gene. The involvement of PS1 in tau pathology has not been as extensively researched as the APP/tau model, therefore, a new model expressing APP/PS1/tau could be warranted.

In 2014, Heraud and colleagues (Heraud *et al*., 2014) developed a new APP/PS1/tau mouse model of AD, crossing the *5xFAD* and *Tg30* models to generate *5xFAD*Tg30* and extensively characterised the brain pathology, compared to the respective single transgenes and wildtype (WT) controls. Pathological findings of this study showed *5xFAD*Tg30* transgenic animals developed NFT's, phosphorylated tau and Aβ pathology. Prior APP/tau models do not develop NFT's despite expressing tau proteins, hence the novelty of this model.

At present, Heraud's publication is the only study describing the *5xFAD*Tg30* model. Whilst some minimal behavioural tests were conducted, experiments were not comprehensive or long term, nor was there any metabolic testing completed. As AD is a progressive disease, we expect

the behavioural phenotype to continue to change over time. Additionally, as described in *Chapter 1*, AD is also linked to an array of metabolic conditions. Hence, to address these issues, the purpose of this study, was to generate the *5xFAD*Tg30* animals to determine if we could further extend the characterisation of this model.

2.2 Materials and methods

2.2.1 Generation of 5xFAD*Tg30 mice

All activities involving the use of animals for research were approved by the Alfred Medical Research Education Precinct Animal Ethics Committee (AMREP AEC) and conducted according to the guidelines of the National Health and Medical Research Council of Australia for animal experimentation. Heterozygous *5xFAD* and *Tg30* animals were crossed to produce the double transgenic, *5xFAD*Tg30* as described in Heraud *et.al* 2014. Mice were genotyped from tail clip samples performed by Transnetyx (TN, USA) using real-time PCR. WT animals were littermate controls **(See Supp 1-2 for animal flow charts)**. All transgenes are under a *Thy-1* brain specific promoter. The mice were on a C57/Bl6 genetic background. Mice were fed a normal chow diet (NC) (14.0MJ/kg, 75.2% kJ from carbohydrate, 4.8% from fat, 20% from protein; Specialty Feeds, Glen Forrest, Western Australia, Australia) during their lifespan. During the experiment, mice had free access to food and water (except for in fasting periods before a glucose tolerance test) and were housed at 22±1°C on a 12 h light/dark cycle. A cohort of animals was relocated to Florey Institute of Neuroscience and Mental Health (Melbourne, Australia) at two months of age for behavioural tests, with a one-month familiarisation period, while a separate cohort remained at Baker Heart and Diabetes Institute for metabolic analyses. All animals were culled at 10months age, via Lethabarb injection. Animals were perfused with PBS and brain excised and cut into hemispheres.

2.2.2 Behavioural Characterisation

An extensive battery of behavioural tests was performed monthly to track cognitive performance over time.

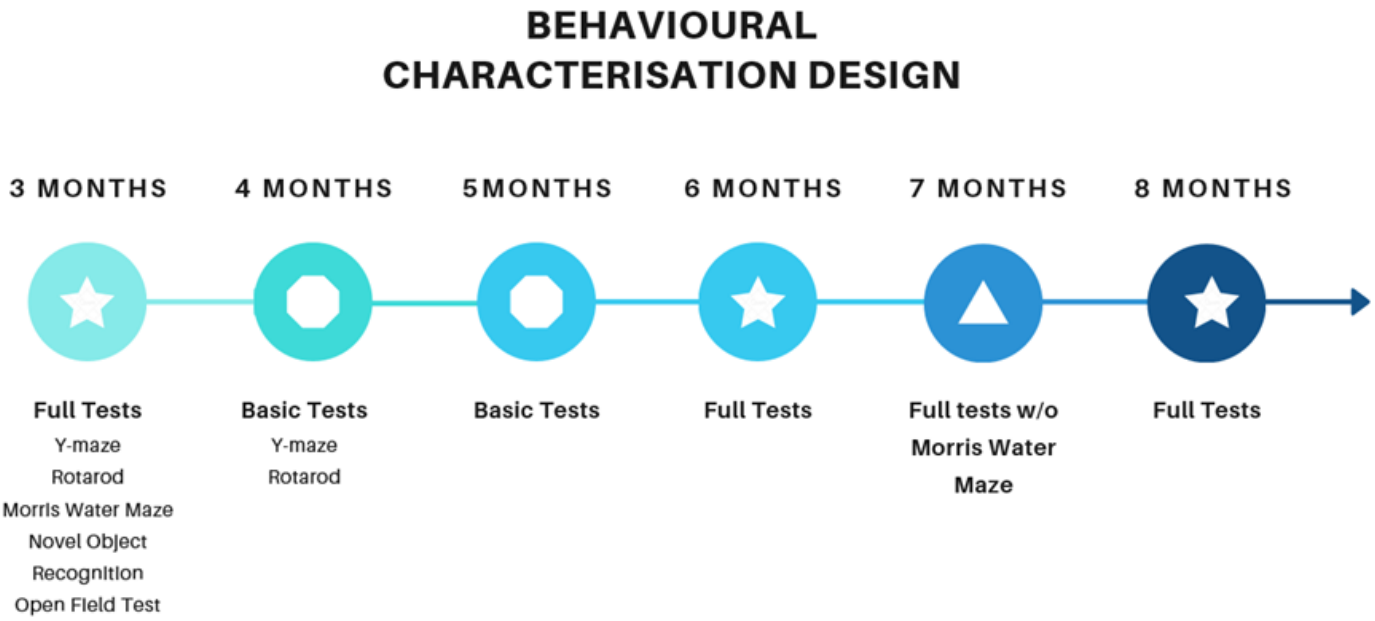

Figure 2.i ***Behavioural characterisation timeline.*** *A comprehensive battery of behavioural tests was performed at 3, 6 and 8 months of age. Basic tests were performed at 4 and 5 months of age. At 7 months of age, a comprehensive battery was performed, without (w/o) the Morris Water Maze. Animals were transported from the Baker Institute to the Florey Institute of Neuroscience and Mental Health at 2 months of age.*

Gross motor strength and control: Rotarod

To evaluate gross motor control, agility and muscular strength and endurance, animals were placed in individual lanes where they attempted to stay balanced on an incrementally accelerating spinning rod, for up to five minutes. Mice were pre-trained on the Rotarod (Ugo Basile, Gemonio Italy) for a 5-minute trial at a constant speed of 4rpm. The next day, the testing phase was carried out with the Rotarod set at an accelerating speed ranging from 4 - 40 rpm over the 5 min. The time the animal fell off the rotating rod was recorded. The testing phase included 3 trials where the average was taken as the final result.

Memory Function: Y-maze

To assess memory function, and tendency to explore new environments, a Y-Maze was set up with 3 identical arms, 30cm in length, which were symmetrical to each other. For the first trial, each individual mouse was placed at the end of the home arm of the Y-Maze, facing away from the centre and was allowed to explore 2 of the 3 Y-Maze arms for 10 minutes. A partition blocking off the novel arm of the maze was in place during this initial trial. Each of the three arms were marked by a unique cue attached to the end to differentiate it from the others. The cues used in the present study were 2-dimentional pictures of black and white symbols including a circle, stripes and triangles. After a two-hour interval, the test was repeated with the partition removed so that all arms, including the novel arm, were available to explore. The time spent in each of the 3 accessible arms was recorded during a 5-minute test via video. Data, including arm entries and time spent in each arm, were recorded and analysed using CleverSysTM (VA, USA) rodent tracking software.

Anxiety-like behaviour: Open Field

To assess anxiety-like behaviour, animals were placed inside the centre of a large open field arena (60cm high x 1 meter in diameter) under bright flood lights which were used to illuminate the arena to 1000 lux. The animal was placed in the arena, exposing it to the brightly lit open field area and during this time movement were recorded using automated Topscan tracking software (CleverSys, VA, USA). Each trial ran for 10 minutes before the mouse returned to its home cage. Time spent in the centre compared with the parameter was recorded and quantified using CleverSys Topscan tracking software.

Memory and novel object recognition

To assess short term memory and novel object recognition, animals were evaluated by the differences in the exploration time of novel and familiar objects.

During *Trial 1 habituation phase*: Mice were placed in a plastic chamber (35cm x 35cm x 35cm) and allowed to explore the empty chamber for 10 minutes. Next, during *Trial 2 acquisition phase*, animals were placed in the same chamber with two of objects, being the same, to explore. The objects were positioned 10cm from each other and 8cm from the nearest wall. Animals could explore the objects for 10 minutes. Finally, during *Trail 3 retention phase*, immediately one of the objects from *Trial 2* was placed in the chamber along with a different, novel object. Animals could explore for 10 minutes. The amount of time the animals explored each object was recorded using automated Topscan tracking software (Cleversys, VA, USA). 'Exploration' was recorded by number of bouts the animals' nose came within an approximately 5cm radius from each object.

Learning, spatial memory and recognition

To assess learning, spatial memory and spatial recognition, a Morris Water Maze test was conducted over a 7-day training period, as described in (Gladding *et al*., 2018). A 1.5 m pool was filled with water and mixed with white paint to make opaque with a smaller diameter platform (10cm) placed in a set position. Over the course of up to 10 days, mice were trained to find the hidden platform using visual cues around the room.

Training trials: The mouse is placed in the pool facing a wall such that its heading is not biased when it starts to swim. It is given 120sec to swim around the pool and find the hidden platform. If it does not find the platform within that time it is placed on the platform and kept there for 10secs to understand that there is a way out of the water. The starting position is randomised across trials so that the mouse must rely on spatial cues, and not on static sequences of movement, to find the platform. Animals perform 4 trials per day, placed in different areas of the pool. Within a block of trials, a mouse is given 10-minutes between trials to rest and to dry off.

Probe trial: performed after the last training trial (up to day 10). The hidden platform is removed from the pool and the mouse swims for 1 min. The path that the mouse swims is tracked and analysed for the proportion of swim time and/or path length spent in each quadrant of the pool, swim speed, and the number of times the path crosses the former location of the hidden platform.

2.2.3 Metabolic Characterisation

An extensive battery of metabolic tests was performed monthly and periodically to track metabolic phenotype over time in an additional cohort.

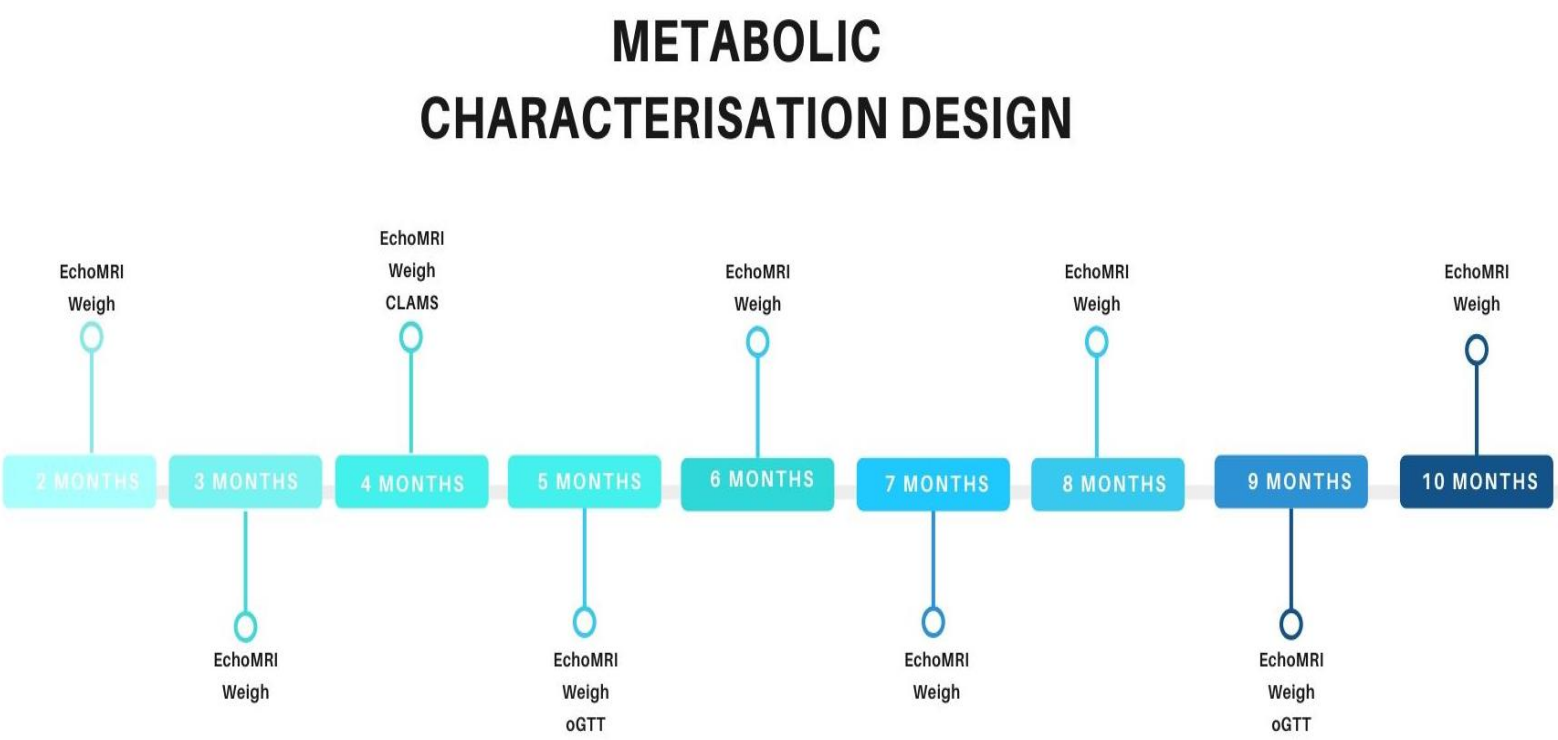

Figure 2.ii Metabolic characterisation timeline. *A comprehensive battery of metabolic tests were performed each month from 2-10 months of age. Animals were put into a Comprehensive Laboratory Animal Monitoring System (CLAMS) machine at 5 months and an oGTT was performed at both 5 and 9 months of age.*

Body Composition Analysis

Fat mass and lean mass were measured using a 4-in-1 EchoMRI (EchoMRI^{TM}, Houston, TX, USA) and standard laboratory scales were used for body mass (Mettler Toledo, Greifensee, Switzerland). EchoMRI was performed monthly, from 2months of age to 10 months of age, and animals were weighed weekly.

Oral glucose tolerance test

Oral glucose tolerance tests (oGTT) were performed on fasted (6hr) mice at 5 months and 9 months. At 5 months, mice received an oral gavage of 2g glucose/kg lean body mass (25% w/v glucose solution), and blood glucose levels were measured via a glucometer (AccuCheck, Roche Diabetes Care, NSW, Australia) at the indicated times on the blood that was collected from the tail. At 9 months, mice received a set dose of glucose at 50mg/mouse in an attempt to elucidate potential biases due to the large discrepancies in lean mass between the genotypes.

Metabolic caging analyses

A Comprehensive Laboratory Animal Monitoring System (CLAMS, Columbus Instruments, Columbus, OH, USA) was utilized to measure various metabolic parameters as previously described (Lancaster and Henstridge, JOVE, 2018). Mice were placed into individually housed chambers and oxygen consumption (VO_2), respiratory exchange ratio (RER), Energy expenditure (heat) and total movement (beam breaks) were recorded over 48hr. The first 24hr served as an acclimatisation period and the 24-48hr period served as the period we analysed.

2.2.4 Lipidomics

Lipid Extraction

10µL of plasma was aliquoted into a 1.5mL eppendorf tube and 100µL of 1-butanol/methanol (1:1, v/v) with 5 mM ammonium formate containing international standards (ISTDs) was added. The mixture was vortexed for 10sec, sonicated for 60min in a sonic water bath at 20°C and then centrifuged (16,000 × g, 10min, 20°C). The supernatant was transferred into a 0.2mL glass insert with Teflon insert cap for analysis.

Liquid Chromatography Mass Spectrometry

Mass spectrometry was performed by colleagues in the Lipidomics Laboratory at the Baker Heart and Diabetes Institute, methods were as follows. Analysis of extracts was performed on an Agilent 6490 QQQ mass spectrometer with an Agilent 1290 series HPLC system and a ZORBAX eclipse plus C18 column set at 60˚C. Mass spectrometry analysis was performed in positive ion mode with dynamic scheduled multiple reaction monitoring.

The solvent system consisted of solvent A) 50% H_2O; 30% acetonitrile; 20% isopropanol (v/v/v) containing 10mM ammonium formate and solvent B) 1% H_2O; 9% acetonitrile; 90% isopropanol (v/v/v) containing 10mM ammonium formate. A stepped linear gradient with a 15-minute cycle time per sample was performed with a 1mL sample injection.

The gradient was as follows; starting with a flow rate of 0.4ml/minute at 10% B and increasing to 45% B over 2.7 minutes, then to 53% over 0.1 minutes, to 65% over 6.2 minutes, to 89% over 0.1 minute, to 92% over 1.9 minutes and finally to 100% over 0.1 minute. The solvent was then held at 100% B for 0.8 minutes (total 11.9 minutes). Equilibration was as follows, solvent was decreased from 100% B to 10% B over 0.1 minute and held for an additional 0.9 minutes.

Flow rate was then switched to 0.6 ml/minute for 1 minute before returning to 0.4 ml/minute over 0.1 minutes. Solvent B was held at 10% B for a further 0.9 minutes at 0.4ml/minutes for a total cycle time of 15 minutes.

The following mass spectrometer conditions were used; gas temperature, 150˚C, gas flow rate 17L/min, nebulizer 20psi, Sheath gas temperature 200˚C, capillary voltage 3500V and sheath gas flow 10L/min.

Quantification and Statistical Analysis

Chromatographic peaks were integrated using the Mass Hunter (B.07.00, Agilent Technologies) software and assigned to a specific lipid species based on MRM (precursor/product) ion pairs and retention time. Quantification was achieved by using the ratio of each analyte peak with the corresponding internal standard as seen in (Huynh *et.al* 2019).

Statistical analysis was carried out on Matlab 2013a or R (3.4.0). Plasma lipidomic data was log10 transformed prior to statistical analysis. Data expressed as pmol/ul plasma, significance determined by two-tailed t-test and corrected for multiple comparisons using the Benjamini-Hochberg false discovery rate correction set to 0.05. Lipids were significant if the FDR-corrected p-value< 0.05

2.2.5 Tissue Collection and Survival

Endpoint was determined at 10 months, and animals were culled using IP injection of Lethabarb (diluted in saline). Brains were harvested and weighed, then dissected into hemispheres for histology and western blotting.

2.2.6 Western Blotting

Tissue samples were homogenised in protein lysis buffer (50mM HEPES, 2mM EDTA, 50mM β-glycerophosphate, 1mM DL-Dithiothreitol (DTT), 1mM Na3VO4, 1.0% Triton X-100, 10% glycerol), 1mM NaF, 1mM PMSF, 0.05% protease inhibitor cocktail (P8340; Sigma, St.Louis, MO, USA), 0.05% phosphatase inhibitor cocktail (P5726; Sigma, St. Louis, MO, USA). The protein concentration was determined using the Pierce BCA Protein Assay Kit (Life Technologies, Carlsbad, CA, USA). Absorbance was read at 560nm. Equal amounts of protein were solubilised in 4X Laemmeli's buffer (40% glycerol, 8.2% SDS, 50% 0.5M Tris-HCl (pH 6.8), 0.5mL 1% Bromophenol blue, 10% H_2O and 20mM DTT). Proteins were denatured at 85˚C for 5-10 minutes.

Samples were then run on a sodium dodecyl sulfate polyacrilamide gel electrophoresis (SDS-PAGE). Proteins were transferred onto a nitrocellulose membrane (Bio-Rad Laboratories, Hercules, CA, USA, Cat #162-0112) at 4˚C at 100˚V for 2hr or 25V overnight. Membranes were washed in TBST (137mM NaCl, 20mM Tris with 0.1% Tween), blocked in TBST with 5% skim milk powder, washed again and incubated with the appropriate primary antibody (22C11, gifted by Ashley Bush [made in house], 1:2000 in TBST; anti-human tau, 1:2000 in TBST, Dako, CA USA) overnight at 4C. After washing, membranes were incubated again at 4C for 2 hours with the appropriate secondary antibody (Anti-mouse IgG HRP linked antibody from sheep GE Healthcare, Buckinghamshire, UK; Goat anti-rabbit IgG, Sigma) (dilution 1:2000 in TBST, 2.5% BSA). Membranes were washed again in TBST and visualized using

Super Signal chemiluminescent substrate (Thermo Scientific, Waltham, MA, USA. Cat#34080 and #34095) and pictures taken using Chemidoc XRS (Biorad, Hercules, CA, USA). Quantification was performed using Quantity One 1-D Analysis Software.

2.3 Results

2.3.1 Gross motor strength and control

In order to replicate and further extend Heraud's characterisation of the *5xFAD*Tg30* animals, rotarod experiments were performed monthly, as an indicator to gross motor strength and control over time. Motor abilities were not different between genotypes at 3, 4 or 5 months of age. Consistent with the Heraud study, motor loss was not seen until 6 months of age, with a steady decline until end point, compared with WT ($p<0.01$) **(Figure 2.1).** Females displayed a significant motor phenotype from 6 months of age (**Figure 2.1C,** $p<0.05$), and males from 7 months of age **(Figure 2.1B)** suggesting a slower developing motor phenotype in males compared with females.

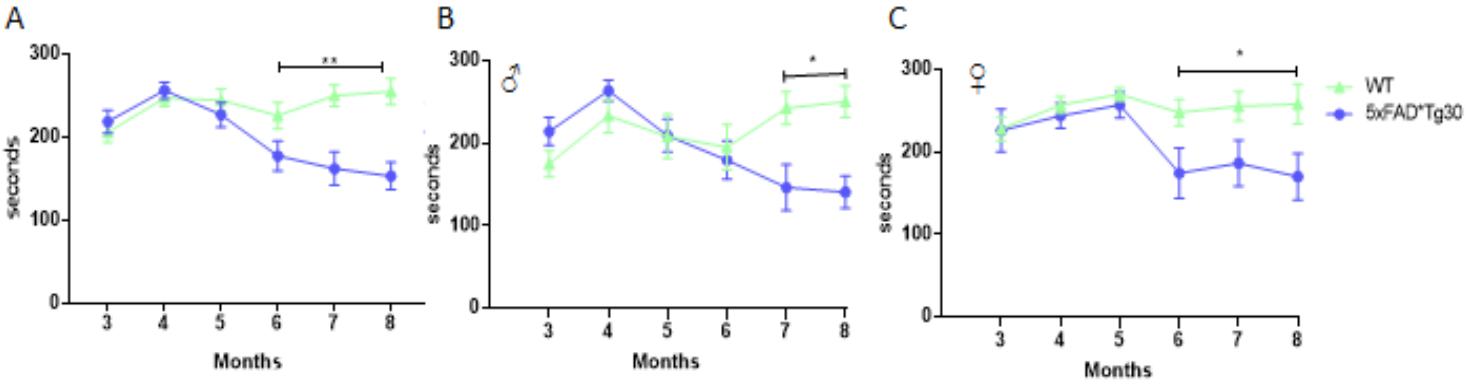

Figure 2.1 ***Latency to fall off rotarod, displayed between 3-8months of age.*** *5xFAD*Tg30 animals displayed a significant motor phenotype from 6 months onwards, compared to WT. Male 5xFAD*Tg30 displayed significant motor phenotype at from 7months onwards. Average of three trials per month. (A) Total cohort, n=15-17 per group (B) Male animals only, n=7-9 per group (C) Female animals only, n=6-10 per group. Two-way repeated measures ANOVA with Holm-Sidak post-hoc analysis. *p<0.05 **p<0.01 genotype effect Graph represents Mean ± SEM*

2.3.2 Memory function

To extend the previous characterisation on memory function, we assessed Y-Maze performance monthly, as an indication of memory function/decline over time. Analysis of memory function with the Y-Maze test carried out at 3, 4 and 5 months, before the appearance of motor deficits, did not show any significant differences between genotypes **(Figure 2.2).** Animals displayed normal memory, as seen in the significant differences between *familiar* and *novel* arms ($p<0.05$).

At 6, 7 and 8 months of age, once motor deficits had appeared, there remained no significant differences between genotypes in memory function **(Figure 2.3)**. Significant differentiation between *familiar* and *novel* arms were seen in both genotypes ($p<0.05$). Thus, *5xFAD*Tg30* mice did not show alterations of memory function in the Y-Maze test by 8 months of age. There was, however, the potential initiation of cognitive deficits at 8 months, as seen by the trended decrease in time spent in the *novel arm* for *5xFAD*Tg30* animals, compared to WT performance. This did not reach significance.

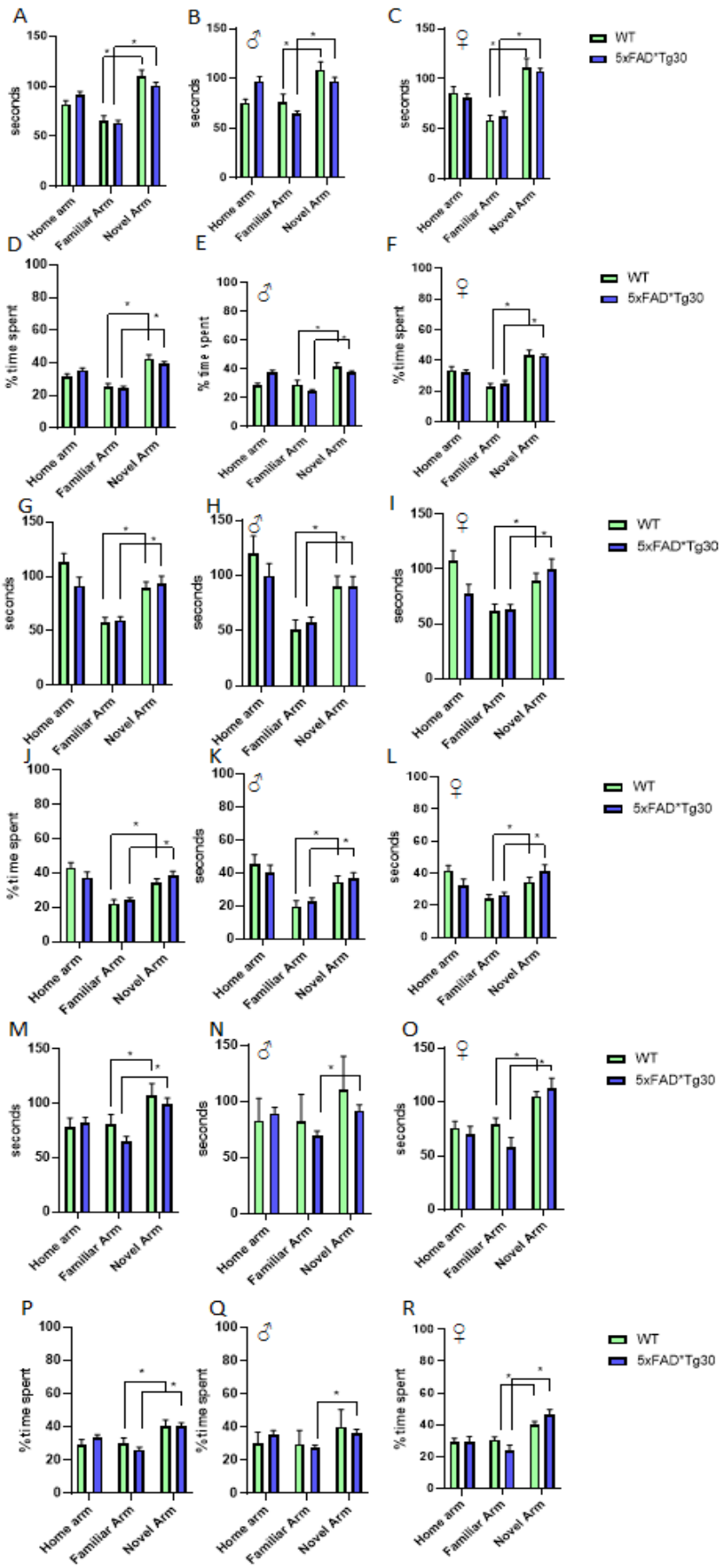

Figure 2.2 ***Duration and percentage of time spent in each arm of the Y-maze between 3-5 months of age*** *(A-C) seconds spent and (D-F) % of time spent at 3 months. (G-I) seconds spent and (J-L) % time spent at 4 months (M-O) seconds spent and (P-R) % of time spent at 5 months. Animals had 10 minutes familiarisation, before a 5-minute trial, 2 hours later. No significant differences between genotypes at 3-5 months. (A,D,G,J,M,P) Total cohort, n=16-17 per group (B,E,H,K,N,Q) Male animals only, n=7-10 per group (C,F,I,L,O,R) Female animals only, n=6-10 per group. 2tailed, type 2 students t-test performed *p<0.05 familiar vs. novel, representing the test was successful. Graph represents Mean ± SEM*

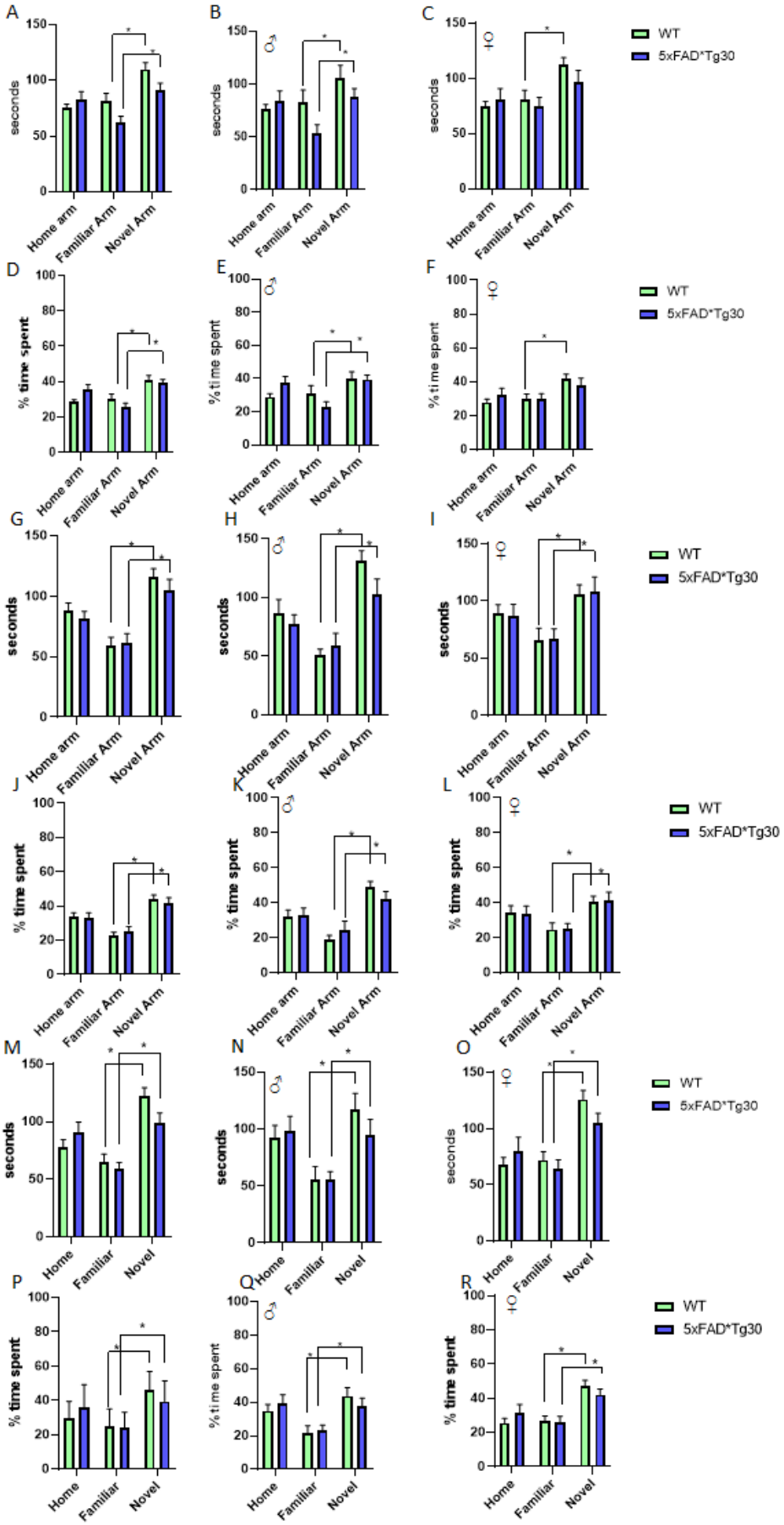

Figure 2.3 ***Duration and percentage of time spent in each arm of the Y-maze between 6-8 months of age*** *(A-C) seconds spent and (D-F) % of time spent at 6 months. (G-I) seconds spent and (J-L) % time spent at 7 months (M-O) seconds spent and (P-R) % of time spent at 8 months. Animals had 10 minutes familiarisation, before a 5-minute trial, 2 hours later. No significant differences between genotypes at 6-8 months. (A,D,G,J,M,P) Total cohort, n=15-17 per group (B,E,H,K,N,Q) Male animals only, n=7-9 per group (C,F,I,L,O,R) Female animals only, n=6-10 per group. 2tailed, type 2 students t-test performed *p<0.05 familiar vs. novel, representing the test was successful. Graph represents Mean ± SEM*

2.3.3 Anxiety-like behaviour

Anxiety-like behaviour was next assessed over time, using the large open field maze. At 3 and 6 months, *5xFAD*Tg30* animals spent significantly more time in the centre of the maze and significantly less time in the corner areas of the maze compared to WT control ($p<0.05$) **(Figure 2.4)**. This preference was retained between both genders. At 7 months of age, there were no genotype effects between maze locations. At 8 months of age, *5xFAD*Tg30* animals again spent significantly more time in the centre of the maze and less time in the corner areas of the maze compared to WT control. Male animals did not show this genotype difference. Thus, *5xFAD*Tg30* animals appear to display less anxiety-like behaviour compared to WT control and could indicate higher risk-taking behaviour. This could indicate an inability to recognise danger or vulnerability, as indicated by their increased time spent in the middle of the arena. The deficit in identifying a potentially hazardous situation (exposure in a brightly lit arena) could further suggest misprocessing in the areas of thinking and reasoning.

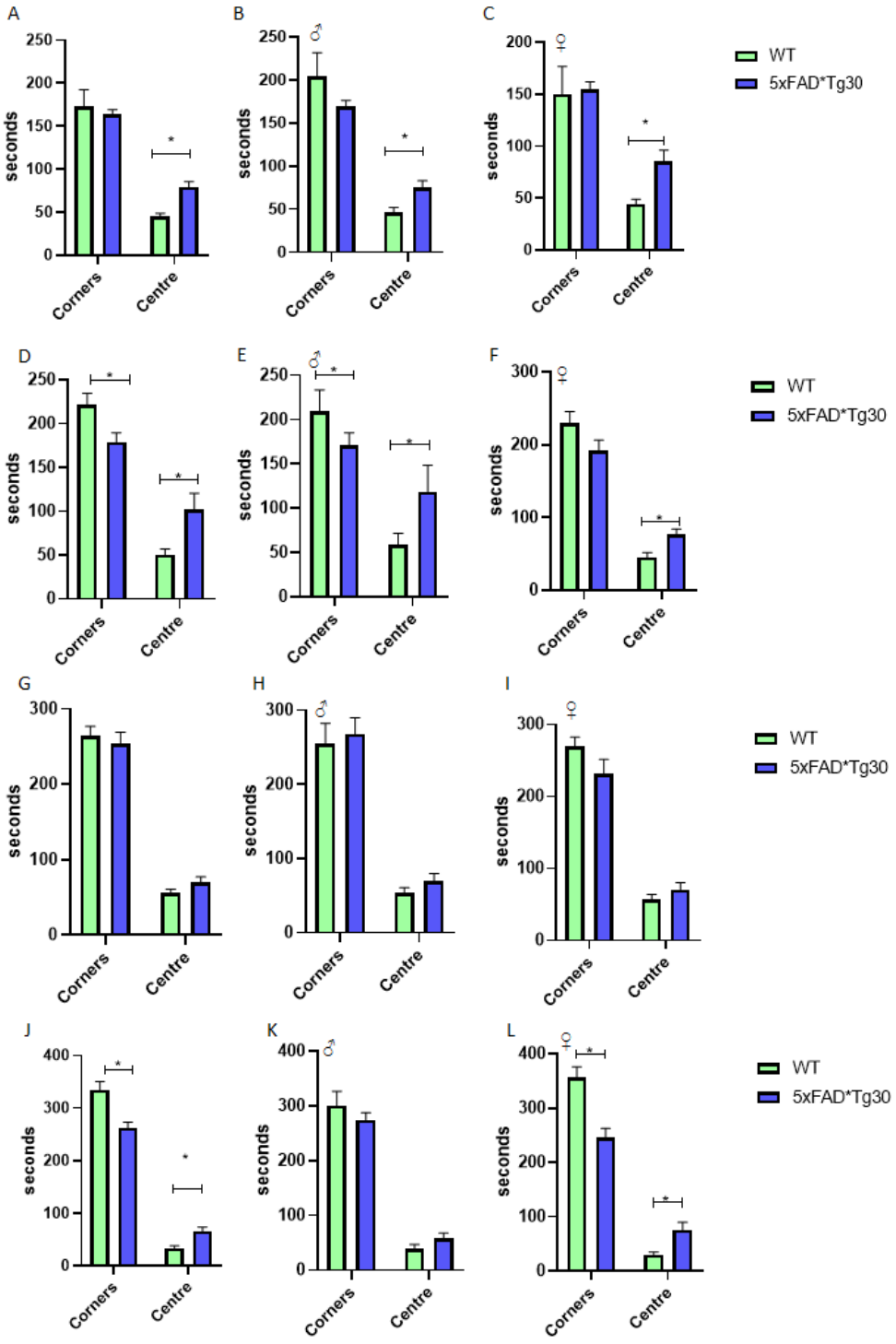

Figure 2.4 ***Duration time spent in areas of a large open field arena at 3-8 months of age***. *(A-C) 3months (D-F) 6 months (G-I) 7months (J-L) 8months. Animals had 10 minutes in the arena lit with bright lights, corners and centre of arena tracked. (A,D,G,J) Total cohort, n=16-17 per group (B,E,H,K) Male animals only, n=7-10 per group (C,F,I,L) Female animals only, n=6-10 per group. 2tailed, type 2 students t-test performed *p<0.05 genotype effect in duration spent in area of the field. Graph represents Mean ± SEM*

2.3.4 Memory and novel object recognition

To assess cognitive decline regarding object recognition, a novel object maze was performed at 3, 6, 7 and 8 months of age **(Figure 2.5)**. At 3 months of age, before the appearance of motor deficits, there was no object recognition apparent between either genotype, suggesting further familiarisation was needed. *5xFAD*Tg30* animals explored both objects significantly more than WT control, which appeared to be attributable to the male animals **(Figure 2.5 A-B)**

At 6 months, both genotypes displayed novel object recognition ($p<0.05$), but there were no genotype effects. Female *5xFAD*Tg30* animals did not explore the *novel object* significantly more than the *familiar*.

At 7 months, there was a genotype effect on novel object recognition, as WT animals displayed a greater number of exploratory bouts towards the *novel object*, but this did not occur in the *5xFAD*Tg30* animals.

Interestingly, at 8 months, this novel object recognition returned, and both genotypes displayed significantly more bouts of exploratory behaviour towards the *novel object* compared to the *familiar*, however, there were no genotype effects.

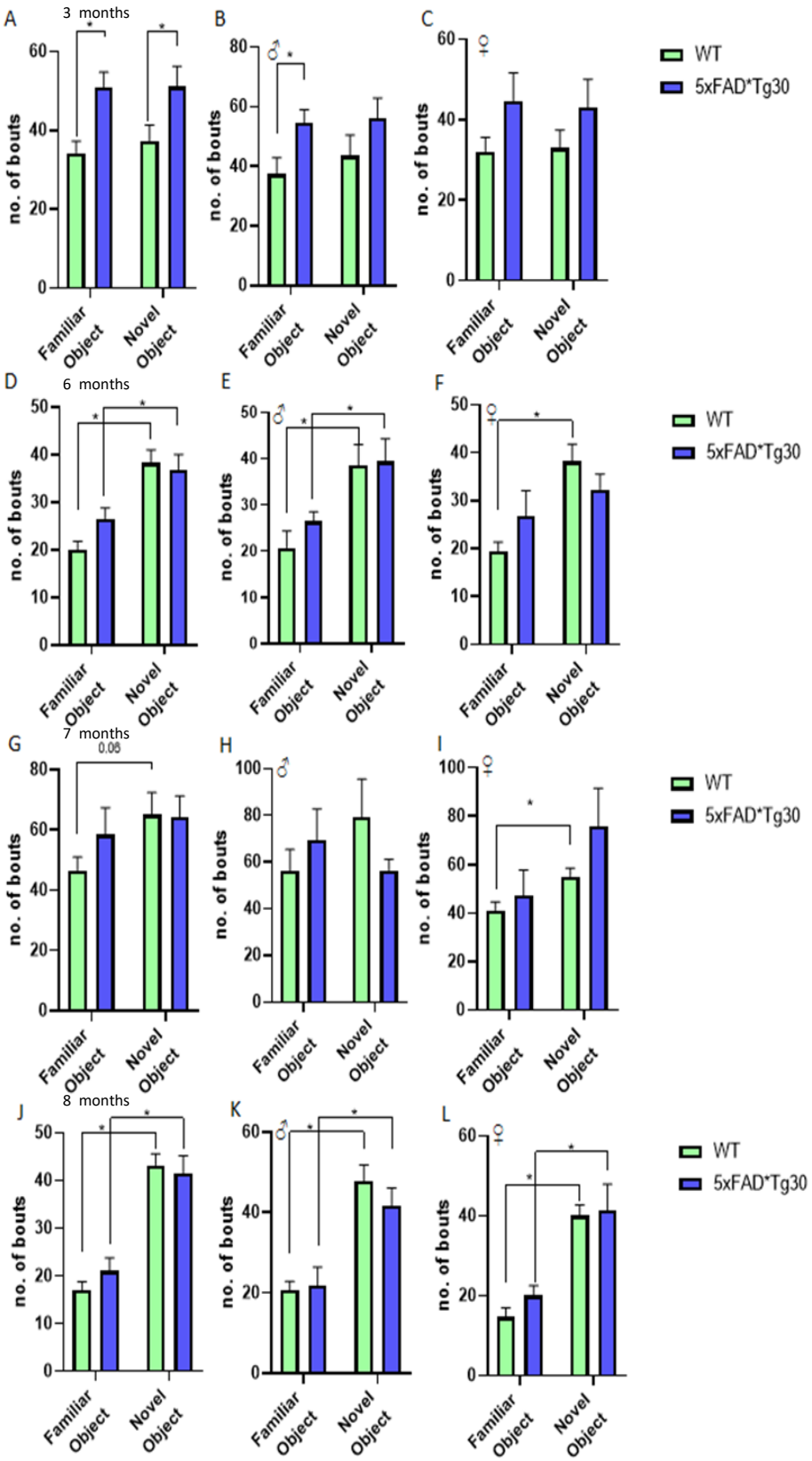

Figure 2.5 ***Number of bouts of investigative behaviour of each object at 3-8 months of age.*** *(A-C) number of bouts at 3 months (D-F) number of bouts at 6 months (G-I) number of bouts at 7months (J-L) number of bouts at 8months. Animals had 10 minutes familiarisation with Object 1 and Object 2. Object 1 was then replaced with Novel Object and animals and a 10-minute test was recorded. (A,D,G,J) Total cohort, n=15-17 per group (B,E,H,K) Male animals only, n=7-10 per group (C,F,I,L) Female animals only, n=6-10 per group. 2tailed, type 2 students t-test performed *p<0.05 novel object effect within both genotypes. Graph represents Mean ± SEM*

2.3.5 Learning, spatial memory and recognition

Morris water maze was performed at 3 and 8 months of age to assess learning and spatial memory abilities. There were no genotype differences in the learning curve over 7 days of training at 3 months **(Figure 2.6 A-C)**. *5xFAD*Tg30* animals trended to spend more time in the quadrant area once the platform was removed on day 8, however this was not significant **(Figure 2.6 D-F)**. At 8 months, there is a marked difference in latency to platform in the *5xFAD*Tg30* animals, from training day 2 ($p<0.05$) **(Figure 2.6 G-I)**. This was attributable to the females' slower latency. Despite this, time spent in the quadrant area once the platform was removed for the probe trial, showed no genotype differences (although trended to be less time in *5xFAD*Tg30* mice) **(Figure 2.6 J-L)**. Due to this finding, a closer look into the learning curve was observed, where some learning, to an extent, was occurring within the *5xFAD*Tg30* mice.

Thus, there was no deficits in spatial memory in *5xFAD*Tg30* mice at 3 months, but by 8 months, deficits in learning are suggested, however it is more likely that these longer latencies are complicated due to the motor deficit as seen from 6-7 months of age.

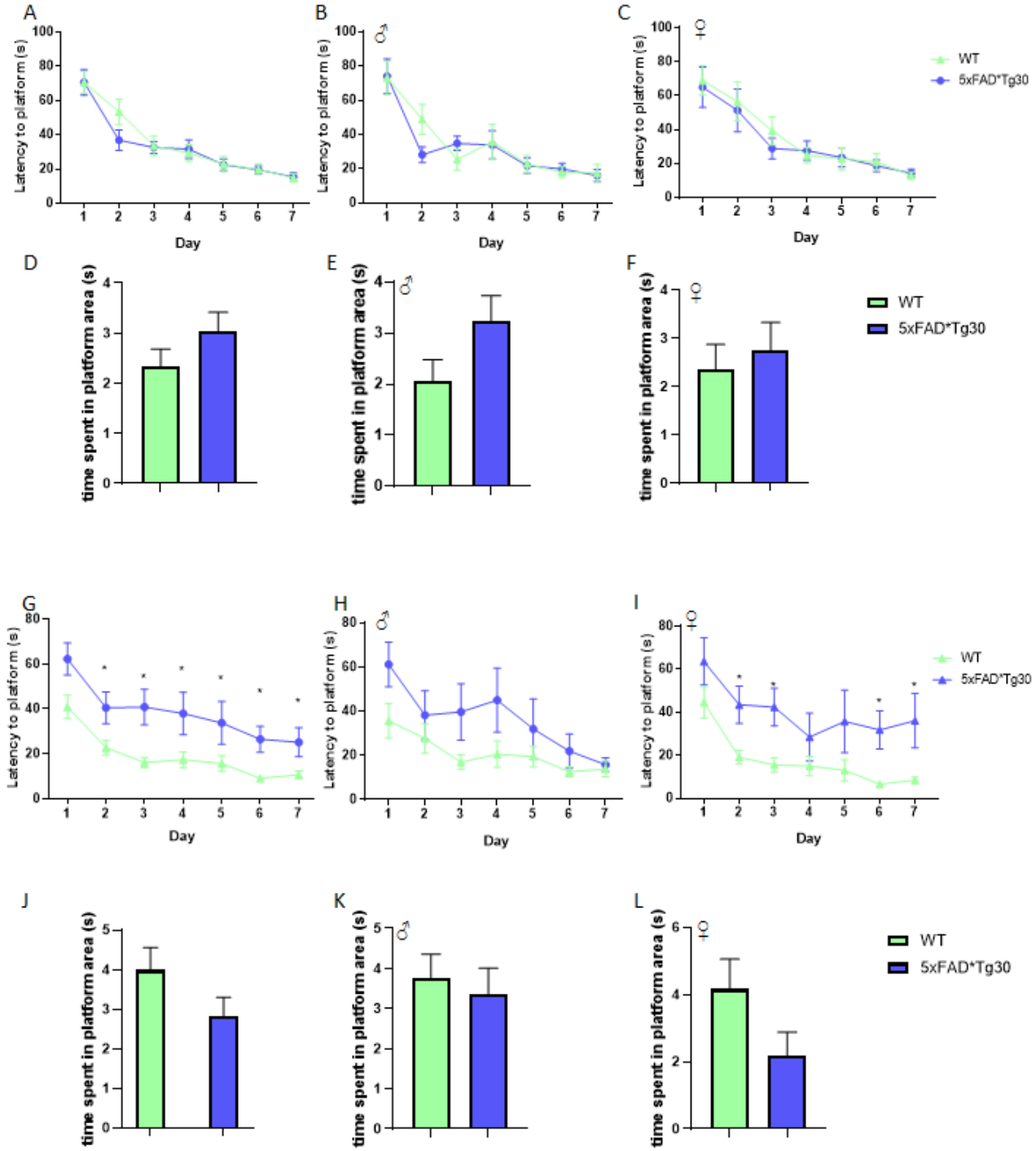

Figure 2.6 ***Learning curve, latency to platform over 7 days, at 3 and 8 months of age in the Morris water maze.*** *(A-C) learning curve at 3months (D-F) probe trial at 3months (G-I) learning curve at 8months (J-L) probe trial at 8months. Animals were given a maximum of 120 seconds to find platform. Probe Trial- time spent in platform quadrant. Platform was removed on Day 8 and animals swam for 60 seconds (A,D,G,J) Total cohort, n=16-17 per group (B,E,H,K) Male animals only, n=7-10 per group (C,F,I,L) Female animals only, n=6-10 per group. Graph represents Mean of 4 trials per day ± SEM. (A-C) and (G-I)Two-way repeated measures ANOVA with Holm-Sidak post-hoc analysis. Genotype effect at 8 months in latency to platform. (D-F) and (J-L) T-test.*

Upon closer inspection of the latency graph at 8 months, it was clear that while the lines were separated so there was a genotype effect, this difference was seen from day 1 and maintained so that each genotype indeed had similar learning curves. This could indicate a slower swim speed to the platform rather than impaired learning performance. This was further supported by no significant genotype difference on probe trial day, for time spent in the platform quadrant. Due to these findings, swim velocity was investigated, to test this hypothesis. Velocity was tracked at 8 months of age and was indeed significantly reduced in *5xFAD*Tg30* mice, irrespective of gender **(Figure 2.7 A-C)**. This result suggests the motor phenotype of the model may compound the effects on the latency data, rather than a true cognitive deficit.

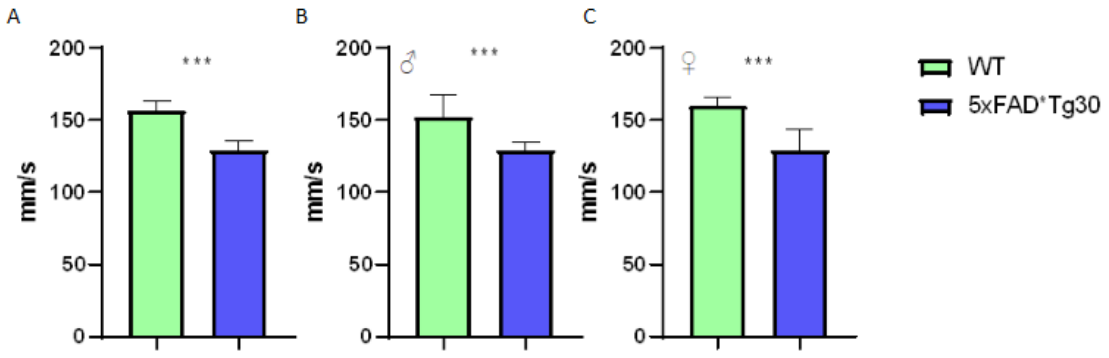

Figure 2.7 ***Swim Velocity***. *Graph represents average velocity over 4 trials on day 1 of MWM testing. (A) Total cohort, n=16-17 per group (B) Male animals only, n= 7-10 per group (C) Female animals only, n= 6-10 per group. Graph indicates mean ± SEM. ***p<0.001 students t-test*

Preface

A separate cohort of animals were utilised for all metabolic characterisation analyses from the behavioural characterisation analyses.

2.3.6 Body Composition analysis

As the initial characterisation paper observed a significant and progressive reduction in body weight, the next aim was to investigate the effects of tau accumulation in the presence of amyloid pathology on body composition. Body analysis was tracked over time including body weight, lean mass, fat mass and body fat percentage. Initial body weight **(Figure 2.8 A-C)** at 2 months of age trended to be smaller in *5xFAD*Tg30* mice and was significantly smaller in males at 2 months ($p<0.05$). Over time, as WT control animals increased body weight, *5xFAD*Tg30* animals remained stable and weight differences were markedly different ($p<0.001$).

Lean mass **(Figure 2.8 D-F)** was significantly lower in *5xFAD*Tg30* throughout their lifespan, suggesting lack of muscle and/or organ development compared to WT and perhaps a transition to muscle atrophy at later time points (post 6mths) coinciding with when we observed motor defects.

Fat mass **(Figure 2.8 G-I)** saw no genotype differences until 8 months, which progressed until endpoint at 10 months. Body fat % results were not different, with this data showing no differences by 10 months **(Figure 2.8 J-L)** indicating the relative proportion of fat to lean mass was maintained in the transgenic model despite the large differences in fat and lean mass size.

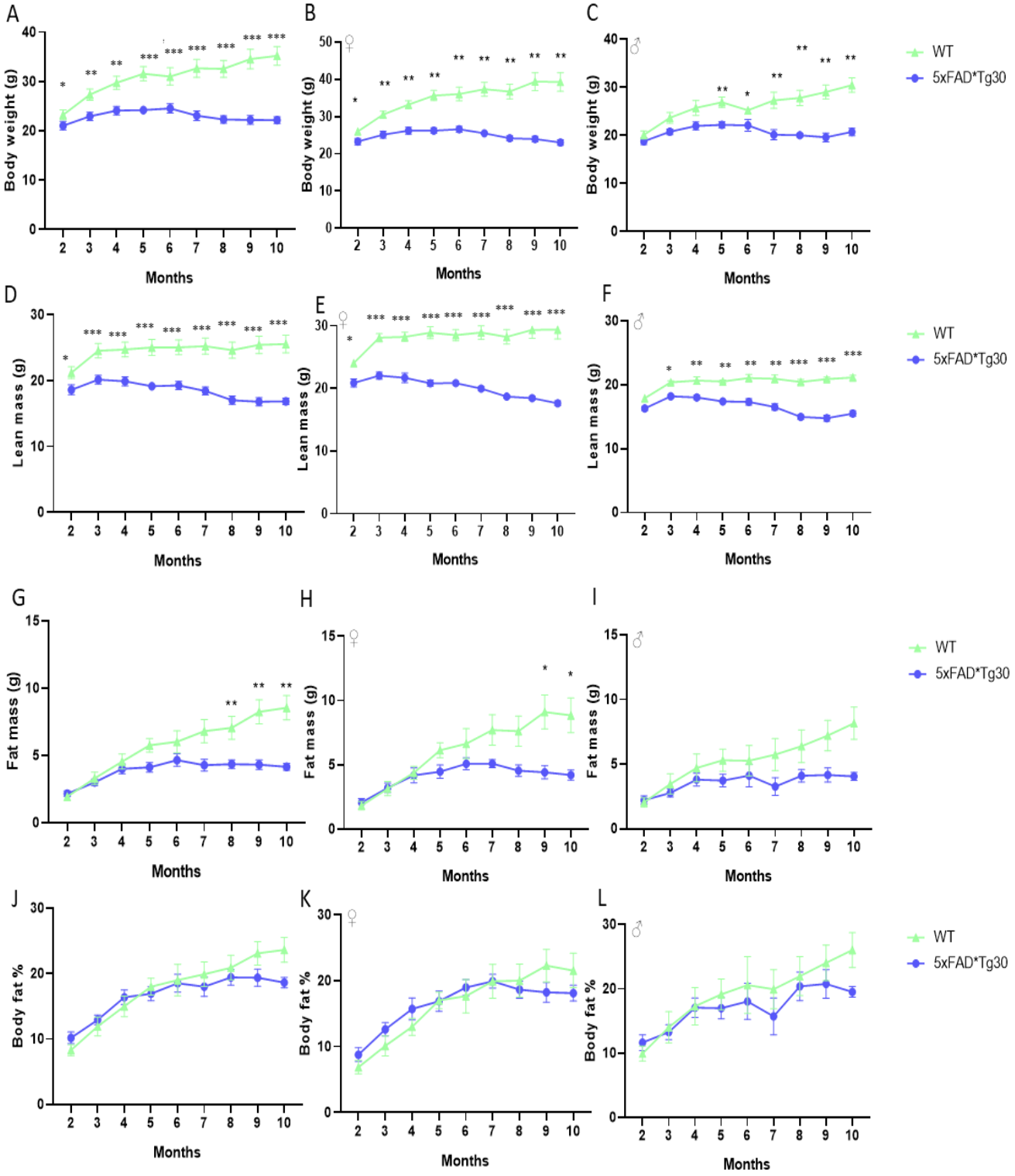

Figure 2.8 ***Body composition analysis in WT and 5xFAD*Tg30 mice over time***. *(A-C) Body weight, (D-F) lean mass, (G-I) fat mass (J-L) body fat percentage. (A,D,G,J) total cohort n=12-15 per group, (B,E,H,K) male animals only n=6-8 per group, (C,F,I,L) female animals only, n=6-7 per group. WT animals had a significantly higher body weight and lean mass compared to 5xFAD*Tg30 across lifespan. Fat mass was significantly different at 8 months of age between WT and 5xFAD*Tg30 animals. *p<0.05 **p<0.01 ***p<0.001 Graph indicates ± SEM*

2.3.7 Oral glucose tolerance test: Set dose vs. Lean mass dose

Due to AD being associated with metabolic disturbances such as obesity and T2D, we conducted two glucose tolerance tests (at 5 and 9mths of age). At 5 months, **(Figure 2.9 A-C)** we dosed the mice per their lean weight to account for the differences in their lean mass given skeletal muscle is a large driver of glucose disposal. There were no significant differences between genotypes on the oGTT curve at any specific time point. Fasting glucose levels were also the same between genotypes. While after an initial spike in blood glucose levels after initial glucose gavage, both genotypes had similar levels throughout the 120-minute test.

From there, animals were aged to 9 months and the oGTT performed again with a set dose of glucose. *5xFAD*Tg30* mice showed a lower fasting glucose level as shown at time point 0 **(Figure 2.9 D-F),** primarily from the female mice ($p<0.01$), where males almost reached significance ($p<0.06$). Over the 120-minute test, *5xFAD*Tg30* mice continued to have a lower blood glucose concentration than WT control, again, primarily attributable to the female animals. *5xFAD*Tg30* animals had a lower spike in blood glucose after the initial glucose load and continued to remain at a lower level, as time progressed. As mice each received the same quantity of glucose but the *5xFAD*Tg30* mice have markedly less lean mass, this improvement in the glucose tolerance despite receiving more glucose per unit of lean mass.

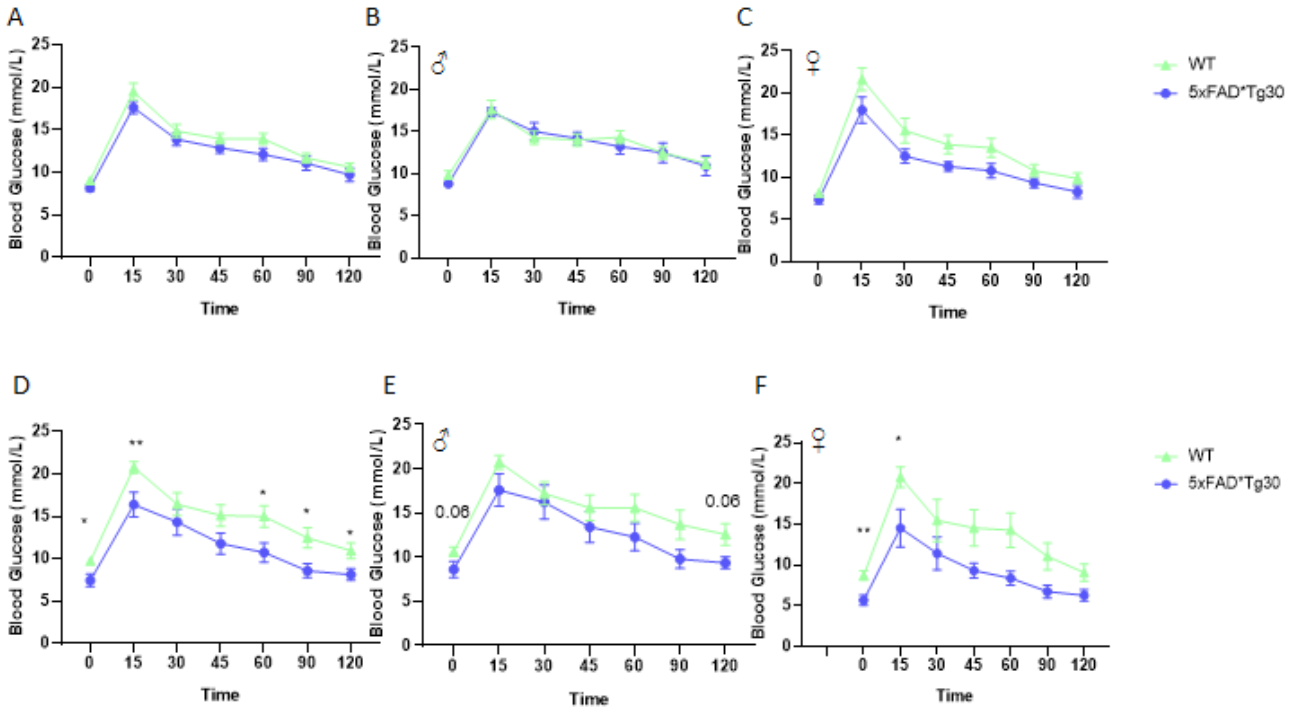

Figure 2.9 ***Whole-body glucose metabolism analysis***. *Fasting blood glucose levels after an oral gavage glucose tolerance test (2gm/kg LBM) at 5 and (50mg glucose) 9 months of age. (A-C) 5 months (D-F) 9months. (A,D) total cohort n=12-15 per group, (B,E) male animals only n=6-8 per group, (C,F) female animals only, n=6-7 per group. Fasting blood glucose was taken after a 6 hour fast and is the '0' time value represented in the OGTT. Genotype effects between WT and 5xFAD*Tg30 at 9months. *p = <0.05 **p = <0.01, One-way repeated measures ANOVA with Holm-Sidak post-hoc analysis. Graphs indicate mean ± SEM*

2.3.8 Metabolic caging analysis

*5xFAD*Tg30* animals were assessed for their metabolic function compared to WT control via the use of the Comprehensive Laboratory Animal Monitoring System (CLAMS). To do this, data was measured over 48 hours, but analysed over the last 24 hours, including respiratory exchange ratio (RER) (carbohydrates to lipid utilisation ratio), energy expenditure, total movement and VO_2 consumption. Raw oxygen consumption was significantly lower in *5xFAD*Tg30* males and trended to be lower in females **(Figure 2.10 A-D).** As VO_2 consumption is directly related to energy expenditure, consequently, *5xFAD*Tg30* males additionally demonstrated a significantly lower expenditure, with it trending to be lower in female *5xFAD*Tg30* animals **(Figure 2.10 M-P)**. Oxygen consumption when normalised to body weight saw marked genotype effects **(Figure 2.10 E-H)**, particularly in males ($p<0.001$) with *5xFAD*Tg30* mice having an increased VO_2. When this was adjusted to lean mass, female animals no longer saw significant genotype effects (trending to be higher) **(Figure 2.10 J,L)** , however male *5xFAD*Tg30* mice still displayed increased VO_2, in both light and dark cycles **(Figure 2.10 I, K)**. Again, this was consistent with an increased energy expenditure in male *5xFAD*Tg30* mice when adjusted for body weight **(Figure 2.10 Q-T)** and lean mass **(Figure 2.10 U-X).** The carbohydrate to lipid utilisation ratio (RER) remained the same between genotypes **(Figure 2.11 A-D)** as did overall activity in both the light and dark cycles **(Figure 2.11 E-H)**.

Results indicated that *5xFAD*Tg30* males have a significantly lower VO_2 consumption compared to WT control which was associated with a lower energy expenditure when looking at raw values. This makes sense as they are smaller and therefore have less metabolically active tissue. Females trended to have similar results but did not reach significance. However, when data was adjusted for body weight and lean mass, results were inverse, demonstrating a higher VO_2 and energy consumption in *5xFAD*Tg30* animals per unit body tissue or lean mass. This

suggests the significance of appropriate adjustments when comparing data- as the size difference between genotypes is vast, it can be difficult to normalise appropriately. RER and total movement were not affected by genotype, at time of experiment, 4 months of age.

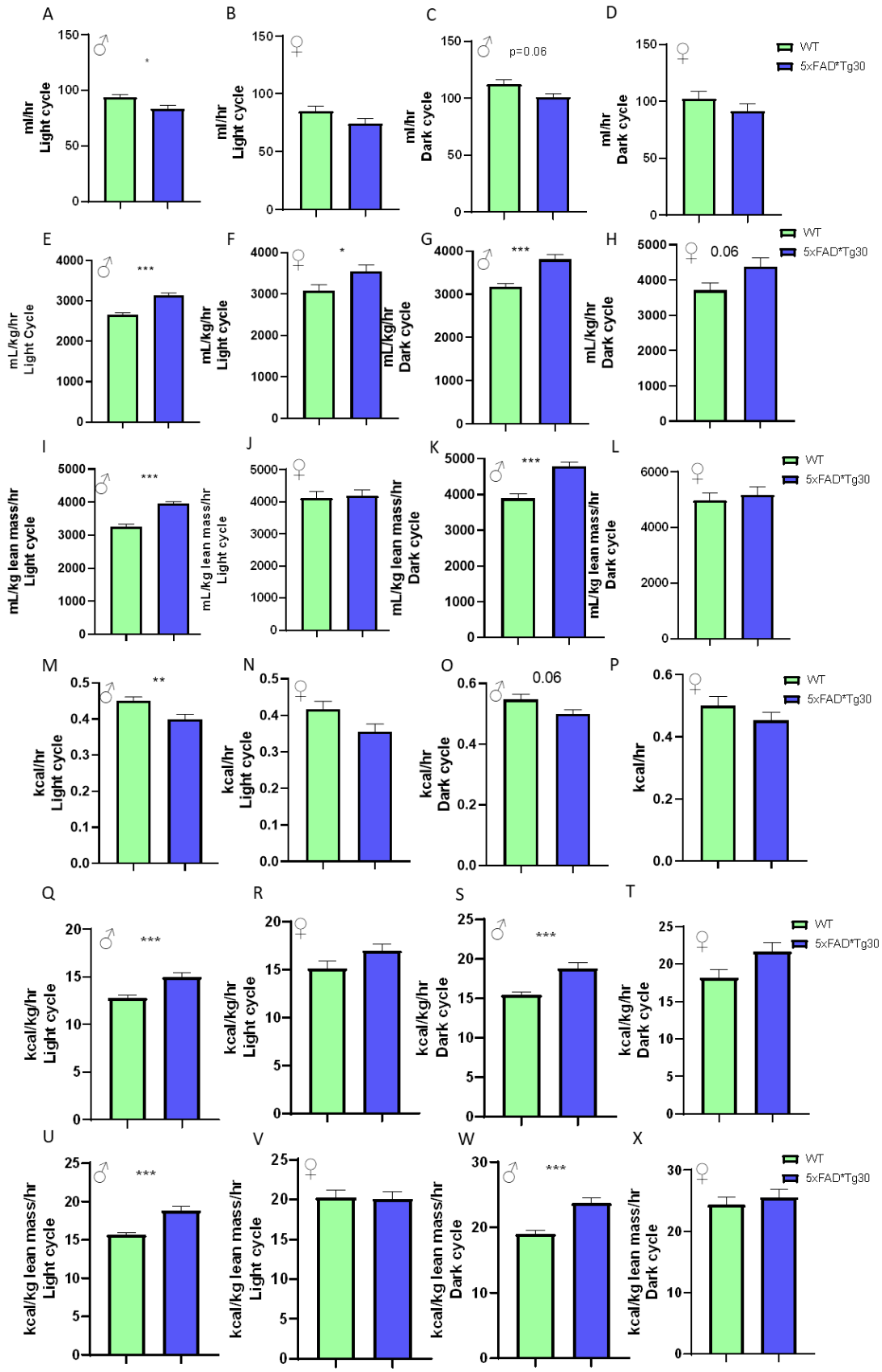

Figure 2.10 ***Aspects of whole-body energy metabolism measured in a CLAMs system for WT control and 5xFAD*Tg30 mice.*** ***(A-D)*** *Raw VO_2 data, Male (A,C) Female (B,D)* ***(E-H)*** *VO_2 data normalised to body weight, Male (E,G) Female (F,H)* ***(I-L)*** *VO_2 normalised to lean body mass, Male (I,K) Female (J,L)* ***(M-P)*** *Raw Energy expenditure (Heat), Male (M,O) Female (N,P)* ***(Q-T)*** *Energy expenditure (Heat) adjusted to body mass, Male (Q,S) Female (R,T)* ***(U-V)*** *Energy expenditure (Heat) adjusted to lean mass, Male (U,W) Female (V,X) Genotype effects in oxygen consumption rate, as well as energy expenditure in males. *p<0.05 ***p = <0.001 data assessed by a students t-test n=5-8 per group. Graphs indicate mean ± SEM.*

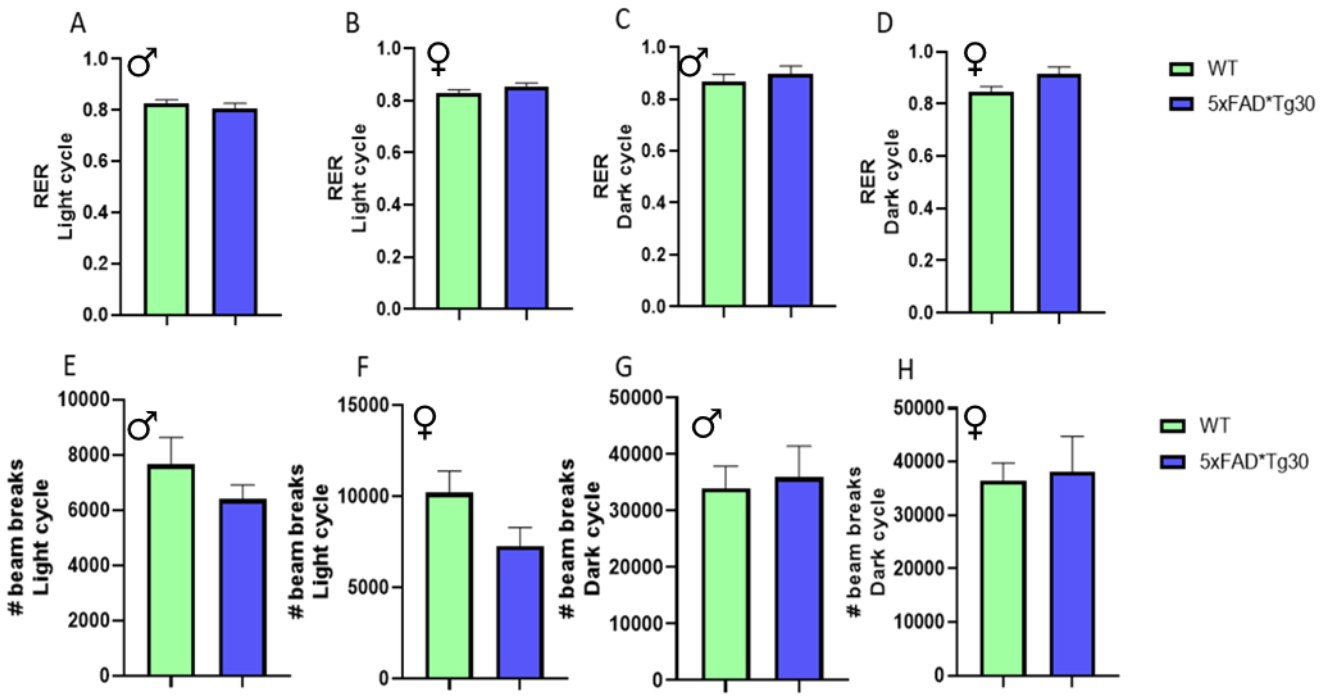

Figure 2.11 ***Aspects of whole-body energy metabolism measured in a CLAMs system for WT control and 5xFAD*Tg30 mice. (A-D)*** *Respiratory exchange ratio (RER), Male (A,C) Female (B,D)* ***(E-H)*** *Total movement/activity as measured via beam breaks (x + Y ambulatory plus z breaks), Male (E,G) Female (F,H).No genotype effects. n=5-8 per group. Graphs indicate mean ± SEM, data assessed by a students t-test.*

2.3.9 End point measures

As the previous study on *5xFAD*Tg30* mice indicated a decreased survival and brain weight, these measures were also analysed as well as further end point measures. In agreement with Heraud, *5xFAD*Tg30* mice had a 37% reduction in survival rate by 10 months of age (7/19 *5xFAD*Tg30* mice suddenly died compared to 0/17 WT's) **(Figure 2.12 M)** and trended to have a smaller brain weight compared to WT control **(Figure 2.12 A&B).** There was a significant reduction in liver weight, tibialis anterior weight and tibia length **(Figure 2.12 C,D,G,H,I,J).** The ratio of tibialis anterior weight to tibia length was also analysed, which showed a significant reduction in *5xFAD*Tg30* animals **(Figure 2.12 K,L)**. Additionally, *5xFAD*Tg30* mice displayed a significant difference in % change of body weight from beginning of analyses at 3 months to end point at 10 months **(Figure 2.12 E,F).** Together, these data suggest that the *5xFAD*Tg30* mice are prone to early death and are smaller in stature.

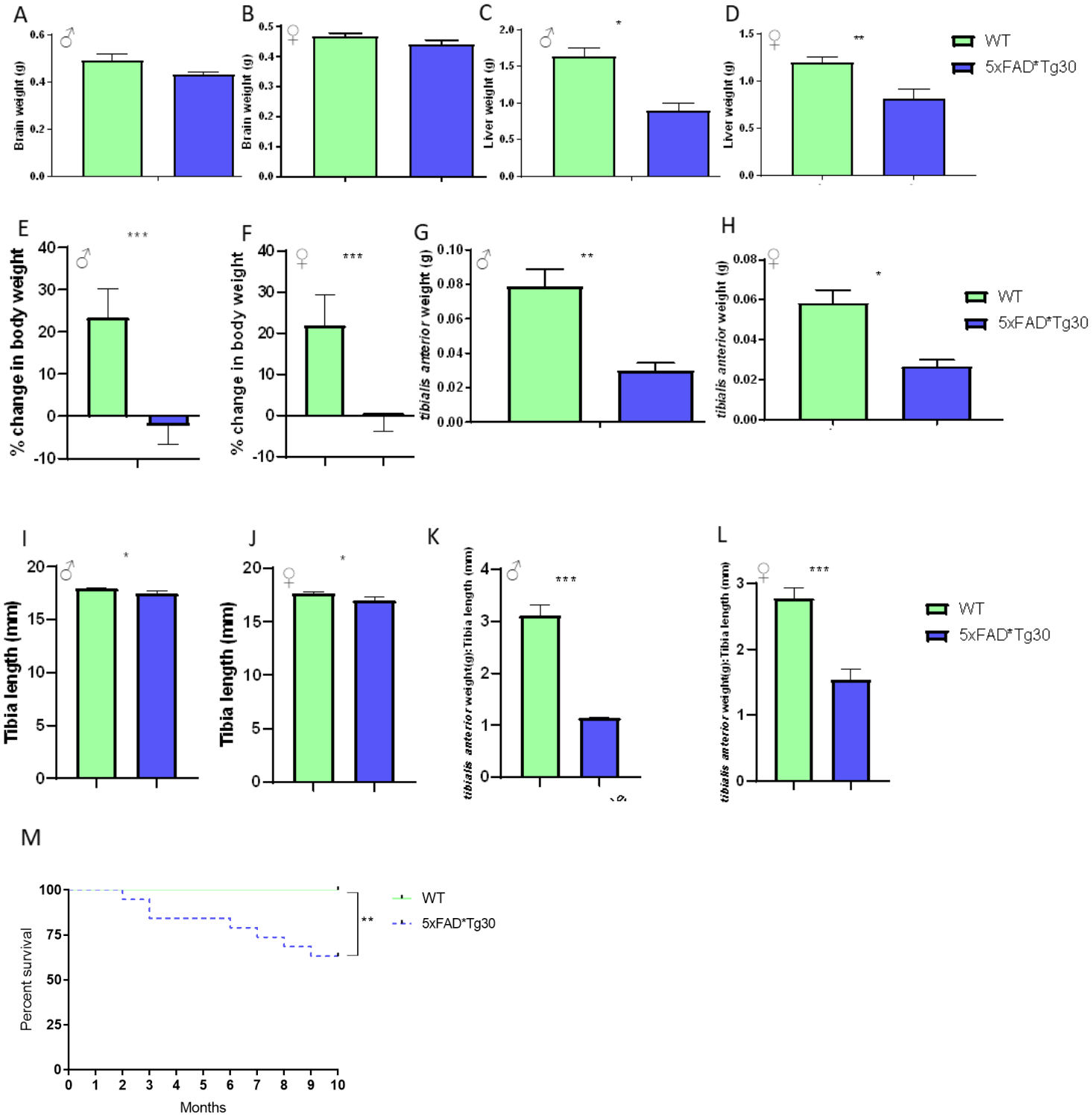

Figure 2.12 ***End point measures for*** *(A & B) Brain weight, n=4-8 per group (C & D) Liver weight, n=4-8 per group (E & F) % change in body weight, n=5-10 per group (G & H) tibialis anterior weight, n=4-8 per group (I & J) Tibia length, n=7-10 per group and (K & L) tibialis anterior: tibia length at 8months of age, n= 7-10 per group. (M) Kaplan–Meier survival percentage survival curve, evaluating males and females from Behavioural cohort only, by a Gehan Breslow Wilcoxon test. N=17-19. Genotype trend effect on brain weight between WT and 5xFAD*Tg30 animals. Genotype effect on liver weight, %change in body weight, tibialis anterior weight, tibia length and tibialis anterior weight: tibia length and survival between WT and 5xFAD*Tg30 and WT. *p = <0.05 **p = <0.01 ***p= <0.001 genotype effects. Data assessed by students t-test. Graphs indicate mean ± SEM*

2.3.10 Protein Expression

To verify the model, and that APP and tau protein expression was increased in *5xFAD*Tg30*, as in the original Heraud paper, protein expression via western blot was performed. To replicate Heraud, whole brain homogenates were probed for APP and human tau. Results showed indeed an elevated level of APP and human tau in *5xFAD*Tg30* animals compared to WT-control.

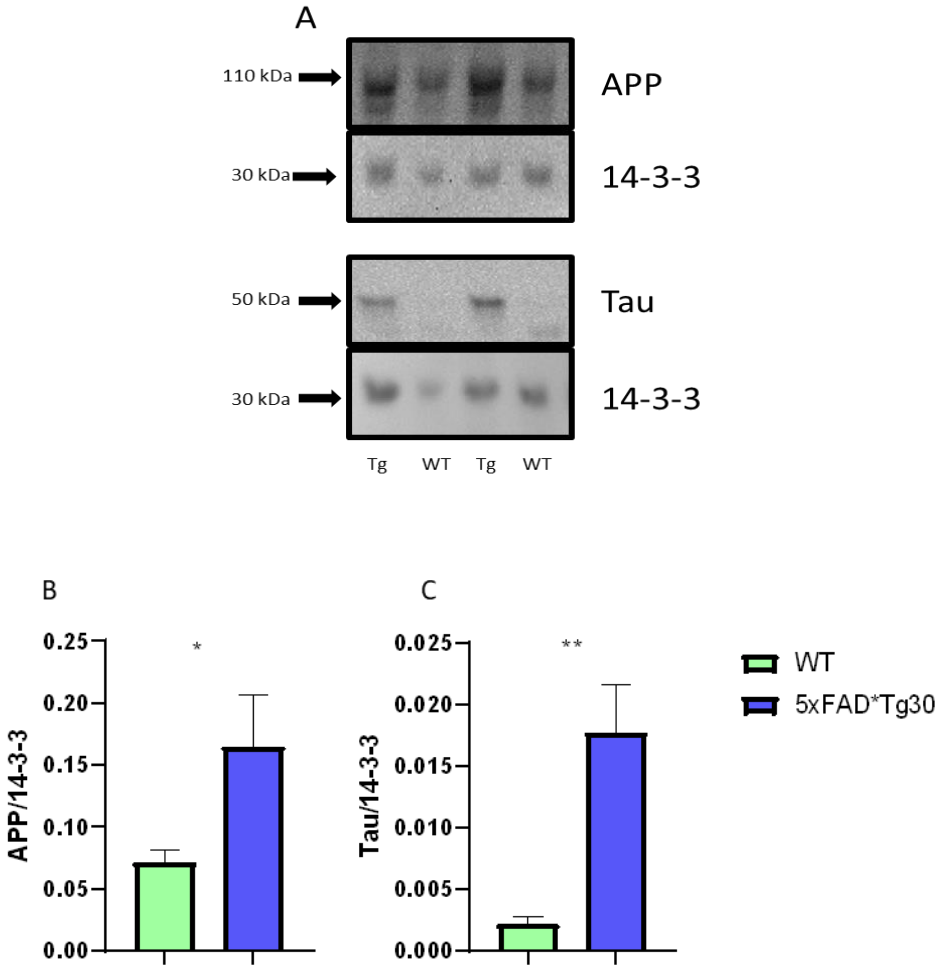

Figure 2.13 ***APP and tau protein expression*** ***(A)*** *Representative western blots, the expression of human APP and tau in 5xFAD*Tg30. Brain was harvested at 10 months and whole brain homogenates processed.* ***(B)*** *Quantification of tau/14-3-3* ***(C)*** *Quantification of APP/14-3-3. Graph indicates mean ± SEM. N=8-11 per group *p<0.05 **p<0.01 t-test*

2.3.11 Lipidomics

As a recent study demonstrated vast differences in plasma lipidomic profiles between AD patients and healthy controls (Huynh et.al 2020), plasma lipidomic analysis was performed to investigate any recapitulation in the *5xFAD*Tg30* model of AD.

After identification of 768 plasma lipid species, 266 species were found to be significantly different between WT and *5xFAD*Tg30* animals after correction for multiple comparisons **(Figure 2.14).** For most species, *5xFAD*Tg30* animals demonstrated a decreased abundance, namely Phosphatidylcholine's (PC's), Phosphatidylethanolamine's (PE's) and Triglyceride's (TG's). Due to this vast difference, we then looked at total quantity of lipid classes. Out of 39 identified lipid classes, 20 were significantly different in *5xFAD*Tg30* animals. *5xFAD*Tg30* animals demonstrated significantly lower total lipids, including total free fatty acids **(Figure 2.15 A)**, total Sphingomyelin's **(Figure 2.15 L)** and total lysophosphatidylethanolamine's (LPE) **(Figure 2.15 J).**

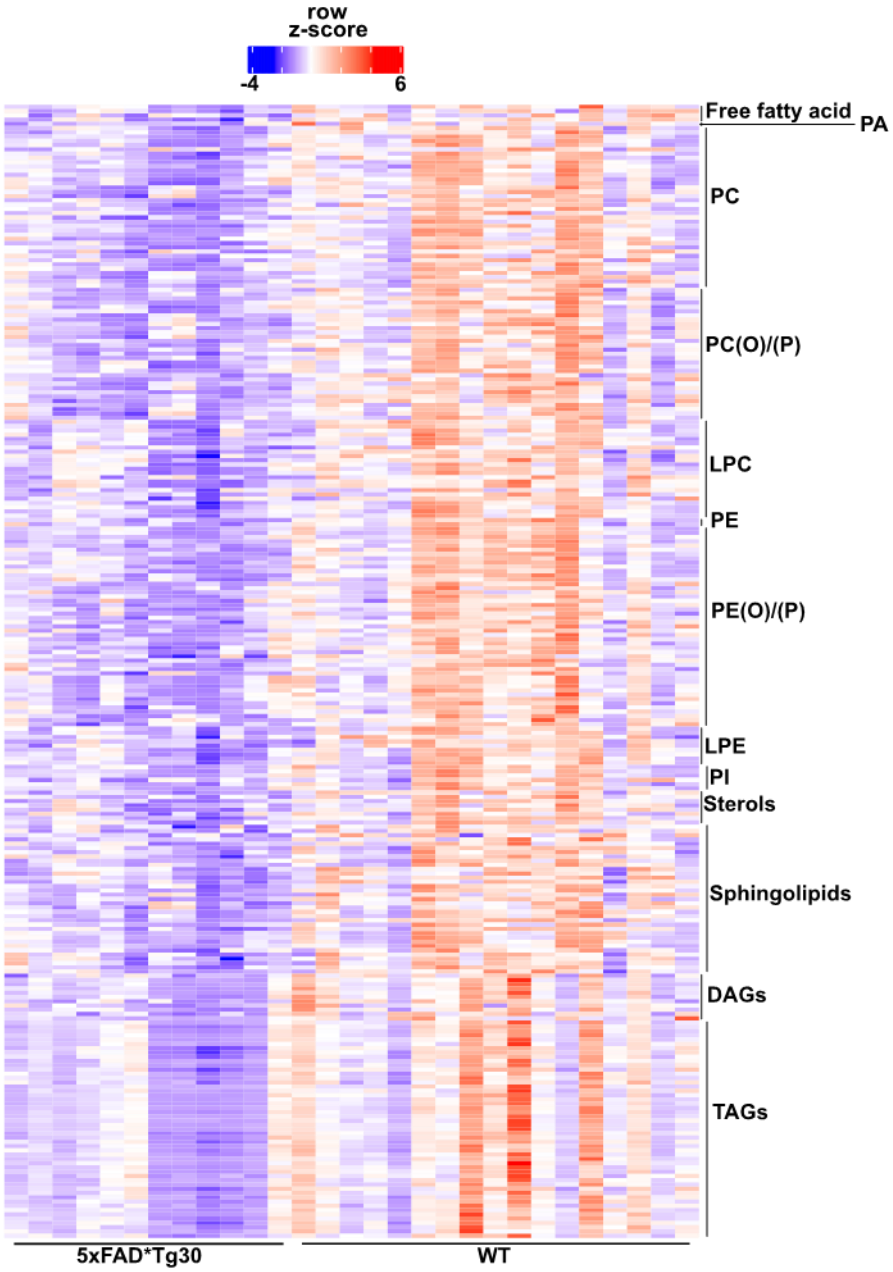

Figure 2.14 ***Heat map of the 266 significantly different lipid species from WT and 5xFAD*Tg30 animals.*** *Data expressed as pmol/ul plasma, significance determined by two-tailed t-test and corrected for multiple comparisons using the Benjamini-Hochberg false discovery rate correction set to 0.05. Lipids were significant if the FDR-corrected p-value < 0.05. Each column is an individual mouse, each row is an individual lipid species. N=12-17 per group*
(PA) *phosphatidic acid* ***(PC)****Phosphatidylcholines* ***(PC(O))****alkylphosphatidylcholine* ***(PC(P))*** *alkenylphosphatidylcholine* ***(LPC)*** *Total Lysophosphatidylcholines* ***(PE)****Total Phosphatidylethanolamine* ***(PE(O))****alkylphosphatidylethanolamine* ***(PE(P))****alkenylphosphatidylethanolamine* ***(LPE)****lysophosphatidylethanolamine* ***(PI)*** *Total Phosphatidylinositol* ***(DAGs)*** *Diacylglycerol* ***(TAGs)*** *Triacylglycerol*

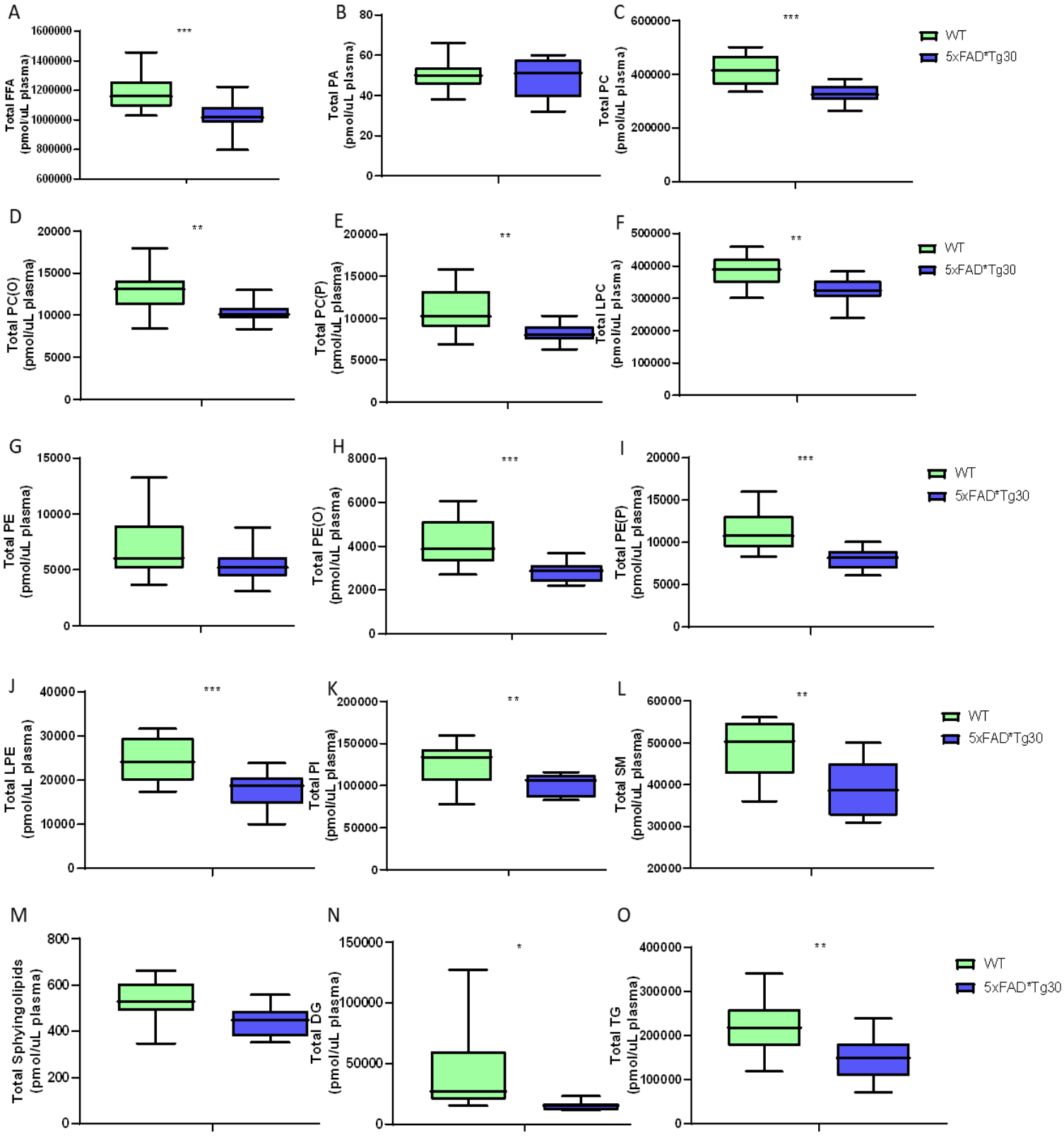

Figure 2.15 ***Total levels of lipid families in WT and 5xFAD*Tg30 animals.*** ***(A)*** *Total free fatty acids* ***(B)*** *Total phosphatidic acid (PA)* ***(C)*** *Total Phosphatidylcholines (PC)* ***(D)*** *Total* alkylphosphatidylcholine *(PC(O))* ***(E)*** *Total* alkenylphosphatidylcholine *(PC(P))* ***(F)*** *Total Lysophosphatidylcholines (LPC)* ***(G)*** *Total Phosphatidylethanolamine (PE)* ***(H)*** *Total* alkylphosphatidylethanolamine *(PE(O))* ***(I)*** *Total* alkenylphosphatidylethanolamine *(PE(P))* ***(J)*** *Total lysophosphatidylethanolamine (LPE)* ***(K)*** *Total Phosphatidylinositol (PI)* ***(L)*** *Total Sphingomyelin (SM)* ***(M)*** *Total Sphyingolipids* ***(N)*** *Total Diacylglycerol (DG)* ***(O)*** *Total Triacylglycerol (TG). Data expressed as pmol/ul plasma, significance determined by two-tailed t-test and corrected for multiple comparisons using the Benjamini-Hochberg false discovery rate correction set to 0.05. Lipids were significant if the FDR-corrected p-value< 0.05 n=12-17 per group*

2.4 Discussion

A suite of animal models modelling AD have been established over the years since the amyloid hypothesis became a leading target for AD research in the 1990's. Transgenic mouse models allow scientists to study key pathological hallmarks of disease, as well as trial therapeutic experiments pre-clinically. Efforts into therapies for AD have struggled and despite a multitude of factors hampering efforts, a recent review has shone the spotlight on the animal models that are used in the initial stages of drug development (King, 2018). Historically, while animal models have brought about astounding insights to the disease and its mechanisms, it does not reflect the entire biology of the disease. The creation of the first transgenic mouse model and subsequent AD models have expressed high levels of mutant APP and/or PS1, developing plaques and cognitive deficits. However, most mouse models struggle to replicate the other dysfunctional protein, tau. Many models loaded with Aβ plaques do not end up developing NFT's, hence models expressing physiological levels of both human APP and human tau would be ideal for testing potential drugs.

To date, there are several mouse models that display both amyloid and tau pathology, including the Tg2576/JNPL3 cross, hAPP (Swe)/wildtype human Tau and the 3xTg-AD mouse (Oddo, 2003). The 3xTg-AD model also contains mutations in PS1. Recently, a new model was generated expressing mutant human APP/PS1 and human tau, called *5xFAD*Tg30* which was the basis of the studies in this chapter. This chapter describes the phenotypic reproduction of the original work in this model of AD, and its extended behavioural and metabolic characterisation.

The data demonstrate that the *5xFAD*Tg30* mouse model displays a significant motor deficit phenotype, is smaller in size and has potential initiation of cognitive decline. Additionally, this study showed a significant difference in survival between WT and *5xFAD*Tg30* animals,

validating Heraud's 2014 initial description (Heraud *et.al* 2014) and contributing a rationale to use this model for the therapeutic studies presented in *Chapter 3* and *Chapter 4* of this thesis.

To analyse and adequately compare behavioural and metabolic phenotypes of the transgenic model, behavioural assessments from Heraud's publication were repeated and extended over the animals' lifetime, as well as a battery of gold standard behavioural tests. By 8 months, *5xFAD*Tg30* animals displayed signs of elevated risk-taking behaviour and decreased novel object recognition but no differences in memory function. Learning and spatial awareness was impeded, however, was presumed affected by the gross motor phenotype.

Metabolically, *5xFAD*Tg30* animals displayed severely reduced body weight, lean mass and, towards later life, fat mass. This supports the severe motor impairment, suggesting a reduced muscle mass results in poor muscle power, strength and endurance and consequently rotarod performance. This is likely to come from the Tg30 mutation, as this tauopathy model is well known for its motor deficits (Audouard, 2015). Despite links between T2D and AD, *5xFAD*Tg30* animals had a significantly lower fasting glucose level which was more prominent in females than in males.

The standard protocol for administering a GTT to mice is calculating a glucose concentration based on their body weight or lean mass. If animals have a substantially different lean mass, errors may occur in results. This is due to lean mass being the principal site for glucose disposal. The second GTT performed, using a set dose of glucose, was performed to appreciate the difference between the two procedures. Using a set dose of glucose does not consider the differing lean mass between the genotypes, and more glucose may be required to be taken up relative to lean muscle available.

At 9 months however, WT animals had more lean mass. Despite receiving the same amount of glucose, their glucose levels were higher, when it was expected to be lower due to the increased muscle mass. It would have been valuable to perform both a set dose and dose-per-lean-mass

experiments at this time point. This higher glucose curve could be attributed to the higher fasting glucose levels of WT animals, indicating a higher blood glucose level prior to the experiment.

*5xFAD*Tg30* animals also have a higher VO_2 consumption, when adjusted for body weight and lean mass as well as a higher adjusted energy expenditure. Raw values for VO_2 and energy expenditure were, however, significantly lower, which raises the question on appropriate normalisation. Liver, *tibilias anterior* and tibia were all significantly reduced matching the overall decreased size of the mice. While the Heraud publication showed a significant reduction in brain weight, our study could not reproduce this statistically, although a strong trend was seen.

Finally, a full lipid profile was conducted on the *5xFAD*Tg30* model. As a result, *5xFAD*Tg30* animals were shown to have a significantly decreased plasma lipid abundance, in 20 out of 39 total lipid classes. Investigating into individual species saw a significant difference in 266 out of 768 species. In agreeance with Huynh and colleagues, who showed clinical significance in a number of plasma lipids, we demonstrated significant decreases in the majority of ether lipid classes such as alkylphosphatidylcholine (PC(O)), alkenylphosphatidylcholine (PC(P)), alkylphosphatidylethanolamine (PE(O)) and alkenylphosphatidylethanolamine (PE(P)). Unlike the examination of the Australian Imaging, Biomarker & Lifestyle Flagship Study of Ageing (AIBL) study, we saw no differences in GM3 species which have reported positive associations with AD, accelerating Aβ aggregation leading to deposition in the brain (Hoshino *et.al* 2013).

While the *5xFAD*Tg30* model did not display a significant amount of cognitive decline at 8 months when characterised further, it still gives us great insight into how the co-expression of

mutants APP and PS1 in a tau mutant mouse affect whole body phenotype. Mild cognitive impairments in AD transgenic animals are not usually seen until at least 8-10 months of age (Pepeu 2004). This makes it difficult to determine cognitive decline in the *5xFAD*Tg30* model due to their early death, however, the initiation is apparent.

Pathologically, Heraud noted dramatically increased formation of NFT's in the brain, increased phosphorylated soluble and insoluble tau, and neuronal loss. Additionally, while *5xFAD*Tg30* mice showed additional conformational, phosphorylation, and truncation changes in insoluble tau (compared to single mutant Tg30), Aβ load was lower when compared to the single 5xFAD model. Because the post-translational changes of PHF-tau mimic more closely what happens in AD, it is suggested that this model might be more beneficial to study the misprocessing of tau in the presence of Aβ, as normally seen in AD, and consequent cognitive behaviour and whole-body phenotypes.

Together, we have reproduced aspects of the findings of Heraud and colleagues in relation to early death and rotorod impairment in this model and expanded on these findings to also demonstrate a decrease in lean mass, muscle size and initiation of decline in cognitive performance with aging. While noting the likely complication of the motor defect on the outcome of behavioural tests that involve movement in determining cognition status, we concluded that the model was viable to test our hypothesis of increasing Hsp72.With the AD brain pathology already described in (Heraud *et.al* 2014), this model is appropriate for our further studies as it contains both tau and Aβ brain associated pathology, and a physical phenotype consistent with frailty - smaller muscle size, impaired motor co-ordination, decreased physical performance and increased risk of death. All factors with the potential to be improved with Hsp72 overexpression. Given this phenotype, we utilised this model to

investigate if BGP-15 treatment or genetic overexpression of Hsp72 is effective in preventing or treating this AD-like pathology and/or frailty.

3 The effect of transgenic overexpression of Hsp72 on the *5xFAD*Tg30* mouse model of AD

Preface

The aim of Chapter 3 was to investigate the effect of transgenic overexpression of Hsp72 on the phenotypic traits of the *5xFAD*Tg30* mice presented in *Chapter 2*. In *Chapter 1* the potential therapeutic benefits of Hsp72 was discussed, providing a rationale as to why we wished to investigate the benefits in a mouse model containing both amyloid and tau pathology. We utilised a Hsp72 Tg mouse model, which has been primarily used for its skeletal muscle overexpression, but also known to overexpress Hsp72 in the brain (Marshall et.al 2018) and bred it with the *5xFAD*Tg30* model. This triple transgenic model was, therefore, appropriate to assess Hsp72 transgenic overexpression in a model of AD.

3.1 Introduction

The overexpression of Hsp72 has previously been used to study skeletal muscle insulin resistance (Chung 2008), mitochondrial dysfunction (Suzuki 2002; Wu *et.al* 2015), inflammatory markers (Gabai, 1997; Park, 2001) and fibrosis (Gehrig *et al*, 2014, Sapra *et al*., 2015) due to its chaperoning ability and cytoprotective action. Despite being first proposed in 1991 (Hamos 1991), the role of Hsp72 has only recently become a more popular area of interest in the scope of neurodegenerative diseases and aging.

It was initially hypothesized that Hsp72 was induced as an early response to the formation of abnormal proteins such as in AD, when it was found that Hsp72 levels in the brain increased dramatically in AD patients while remaining low in healthy controls (Hamos, 1991). Due to their targeted clustering around plaques and tangles, it was thought that this was an attempt to restore homeostasis. Since then, as described in *Chapter 1*, Hsp72 has been found to provide an array of protective and preventative effects on the pathogenesis of AD.

Considering that the main cause of toxicity is the aggregation of proteins (being Aβ and tau), it is no wonder that the molecular chaperoning abilities of Hsp72 have been explored. In healthy individuals, this phenomenon of protein misfolding is naturally prevented by HSP's (Liberek, 2008). Many *in vitro* studies have shown positive results, certainly suggesting that the expression of Hsp72 could suppress the progression of AD (Magrane, 2004; Muchowski, 2005; Evans, 2006; Kumar, 2007; Yoshiike, 2008). Additionally, several *in vivo* studies have also observed positive effects of the overexpression of Hsp72 not only in the pathogenesis, but also the functional phenotype of AD (Hoshino, 2011; Sun, 2017). Spatial learning and memory, as well as pathological features were ameliorated through the overexpression of HSP70 in these models of AD. Despite this, previous animal models used had mutations in PS1/APP genes, therefore only expressing Aβ. As described in *Chapter 1* and *Chapter 2*, this does not accurately mimic human AD pathology.

We crossed two transgenic models the *Hsp72 Tg* mouse and *5xFAD*Tg30* mouse to produce a triple transgenic, expressing Aβ, tau and Hsp72 in the brain. This chapter aims to investigate the effects of genetically overexpressing Hsp72 in a mouse model of AD containing both elevated Aβ and tau.

3.2 Materials and Methods

3.2.1 Generation of 5xFAD*Tg30*Hsp72Tg mice

All activities involving the use of animals for research were approved by the Alfred Medical Research Education Precinct Animal Ethics Committee (AMREP AEC) and conducted according to the guidelines of the National Health and Medical Research Council of Australia for animal experimentation. Heterozygous *5xFAD* and *Tg30* mice were crossed to produce the double transgenic, *5xFAD*Tg30* as described in *Chapter 2*. *5xFAD*Tg30* animals were subsequently crossed with heterozygous *Hsp72 Tg* mice to create the triple transgenic, *5xFAD*Tg30*Hsp72 Tg*. The mice were all on a C57/Bl6 genetic background and were compared with wildtype littermate control mice and the double transgenic *5xFAD*Tg30* **(See Supp 3 for animal flow charts)**. Mice were genotyped from tail samples performed by Transnetyx (TN, USA) using real-time PCR. Mice were fed a normal chow diet (NC) (14.0MJ/kg, 75.2% kJ from carbohydrate, 4.8% from fat, 20% from protein; Specialty Feeds, Glen Forrest, Western Australia, Australia) during their lifespan. During the experiment, mice had free access to food and water (except for in fasting periods before a glucose tolerance test) and were housed at 22±1°C on a 12 h light/dark cycle. All animals were culled at 10months age.

3.2.2 Behavioural Characterisation

A similar battery of behavioural experiments was performed in Chapter 3 as in Chapter 2, with some additional tests and some tests substituted. Since behavioural differences could not be seen until 6 months in Chapter 2, behavioural experiments did not start until 7 months for this current study. An updated timeline is as below, with protocol descriptions of experiments not described in Chapter 2, following.

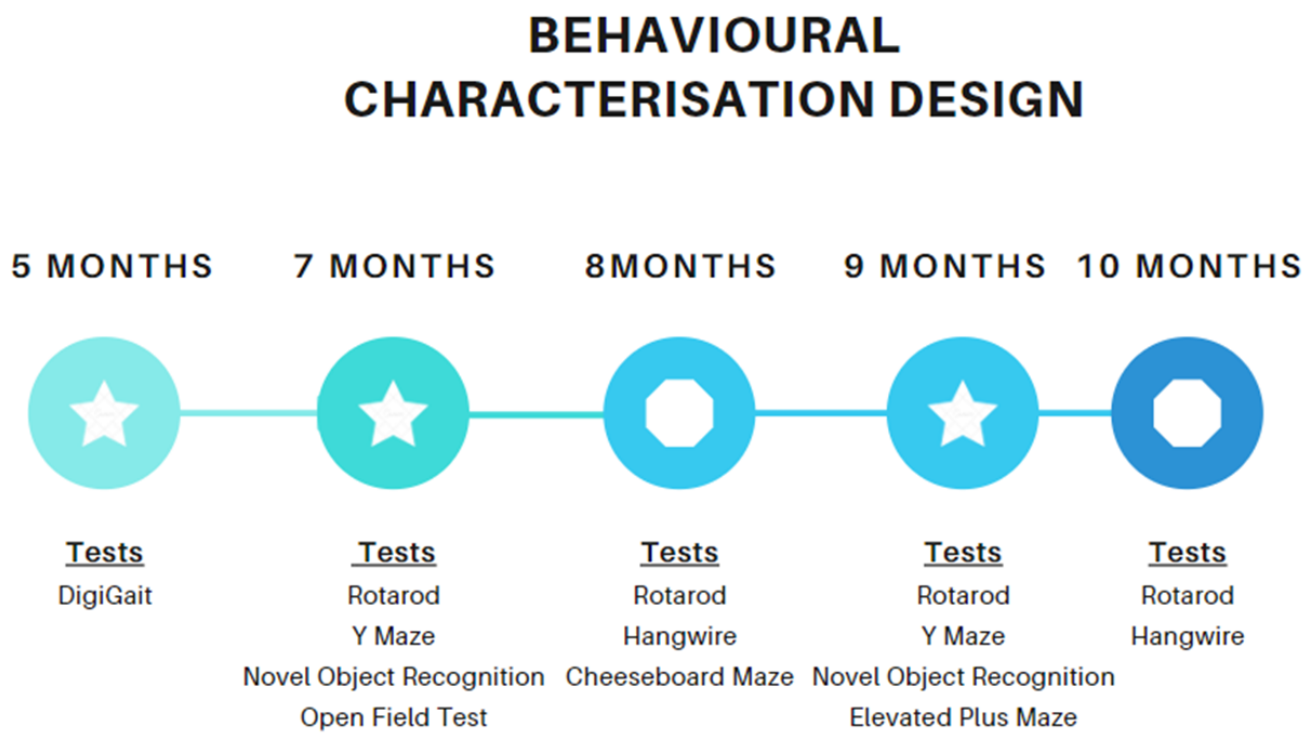

Figure 3.i *Behavioural characterisation timeline design.* *A comprehensive battery of behavioural tests was performed at 5, 7, 8, 9 and 10 months of age. At 9 months, the anxiety-like behaviour test was substituted from Open Field to Elevated Plus Maze. At 6 months, animals were not assessed. Animals were kept at the Baker Institute for the duration of their life.*

Hangwire

To assess whole-body muscle strength (specifically forelimb strength), endurance and coordination, a Hangwire test was performed. A wire rod was suspended horizontally between two vertical beams, ~45 cm from a padded surface. Mice were encouraged to grasp the rod with their forepaws. Once forepaws firmly grasp the rod, animals were allowed to hang freely without the help of their hind legs. Latency-to-fall onto a padded surface was recorded in three successive trials with at least 5 min to rest between trials.

Cheeseboard Maze

To assess spatial memory, learning and recognition- we switched from the Morris Water Maze used in Chapter 2, to the Cheeseboard maze. In addition to attempting to alleviate motor deficit confounding effects, the Cheeseboard maze was utilized to assess if there were differences in motivational factors to assess cognition. While the Morris Water Maze utilizes aversion/fear, the Cheeseboard uses a reward as its end goal. Animals are fasted and food restricted until they reach a percentage of weight loss, to optimize interest of a food reward.

The maze was constructed from a circular table (94cm diameter) that was painted white. Caps (Corning 50mL polypropyl tube caps, 3.25cm diameter, 1cm depth) were painted the same colour and were superglued to the table to be used as wells. 32 wells were spread evenly in a radial pattern of 8 lines of 4 wells. The inner most well of each line was 14cm from the centre of the maze and the outer most well was 5cm from the edge. Along each line, every well was separated from the next by 5cm. A semitransparent cylindrical start cage (28cm diameter) was attached to a pulley system and was placed in the centre of the maze. High contrast spatial cues (A3 size) were attached to the interior of the faraday cage (“North”, “South”, “East”, “West”).

Food restriction

Baseline weights of the mice were obtained by taking the average weight over three days before commencement of food restriction. Food restriction was introduced gradually over 3 days prior to testing. Animals were fed approximately 80% of free feeding amount (determined in a preliminary test on a separate cohort of mice) to obtain a total weight loss of 10%. The weights of the mice were recorded every day during the CB task and individually weighed food pellets were supplied to maintain their weights at 90%.

Protocol

Mice were habituated to strawberry milk food reward from 3 days prior to testing, during their acclimatization days. Testing and acclimatization for all mice across trials was conducted in the same room.

During acclimatization, animals were given 5minutes to roam the cheeseboard freely, then were given the opportunity to lick a cotton tip with a film of strawberry milk on it. Maze was unbaited.

The 4 corners of the maze were brushed with strawberry milk prior to testing phase to minimise the effect of odour cues. The maze was cleaned with diluted ethanol (approx. 10%) after each trial.

During the testing phase, two 60sec trials with an inter trial time of 20 minutes were conducted on each day, for 6 days. One well was baited with a cap full of strawberry milk reward. The location of the baited well was conserved across trials and days for each mouse.

On the 7^{th} day, the probe trial occurred where no well was baited. Mice with an intact spatial memory are expected to spend more time in the target quadrant during this test.

Behavioural analysis

Cheeseboard maze trials were analysed using video tracking software (Topscan CleverSys, VA, USA). The maze was sectioned into zones between each line of wells, totaling 8 equal wedge-shaped zones. Two adjacent zones were combined to create quadrants, depending on the location of the baited well. The centre zone (circular, reaching the inner-most well of each line of wells) was included for measurement of distance travelled but was excluded for quadrant-based analysis. The software detected when the mice reached the baited well and was able to output latencies, distance travelled, time spent in zones and path trace images.

Elevated plus maze

As an additional way to assess anxiety-like behaviour, the elevated plus maze was substituted in for the large open field test, at 9 months. The elevated plus maze has a smaller overall area than the large open field, which was a concern due to the severe progressive motor phenotype displayed from 6 months onwards.

The elevated plus maze is comprised of two open arms and two closed arms that extend from a common central platform elevated to a height of 40cm above the floor. The closed arms provide protection via a 15cm high wall with a passageway 4.5cm wide. The open arms have no walls and are the same width. Mice are placed on the centre square, facing an open arm and allowed to freely explore the apparatus for a 10-minute period. A greater relative occupation in the closed arms is considered indicative of anxiety-like behaviour. Trials were tracked and analysed using video tracking software (Topscan CleverSys, VA, USA).

3.2.2 Metabolic Characterisation

In order to assess the effects of transgenic overexpression of Hsp72 on the baseline metabolic results of *5xFAD*Tg30* animals as seen in *Chapter 2*, the same battery of metabolic assessments was performed. The timeline for the metabolic characterisation was as per *Chapter 2*.

Metabolic Caging (Promethion)

We used the Promethion System (Sable Systems International, North Las Vegas, NV, USA) as opposed to the CLAMS machine for this cohort, to measure oxygen consumption (VO_2), respiratory exchange ratio (RER), Energy expenditure (heat) and total movement (beam breaks). The Promethion system also measured total activity as measured by all meters travelled, voluntary activity as measured by total exercise wheel meters and food intake. Measurements were recorded over 48hrs with the first 24hrs serving as an acclimatisation period and the final 24 hrs serving as the period analysed.

3.2.3 Western Blotting

Tissue samples were homogenised in protein lysis buffer (50mM HEPES, 2mM EDTA, 50mM β-glycerophosphate, 1mM DL-Dithiothreitol (DTT), 1mM Na3VO4, 1.0% Triton X-100, 10% glycerol), 1mM NaF, 1mM PMSF, 0.05% protease inhibitor cocktail (P8340; Sigma, St.Louis, MO, USA), 0.05% phosphatase inhibitor cocktail (P5726; Sigma, St. Louis, MO, USA). The protein concentration was determined using the Pierce BCA Protein Assay Kit (Life Technologies, Carlsbad, CA, USA). Absorbance was read at 560nm. Equal amounts of protein were solubilised in 4X Laemmeli's buffer (40% glycerol, 8.2% SDS, 50% 0.5M Tris-HCl (pH 6.8), 0.5mL 1% Bromophenol blue, 10% H2O and 20mM DTT). Proteins were denatured at 85˚C for 5-10min.

Samples were then run on a precast 12% bis tris gel (Nupage, Life technology, CA USA). Proteins were transferred onto a membrane using the iBlot/PVDF stack (Life technology, CA USA) on a MARKG2 setting for 13minutes. Gel was initially bathed in 20% EtOH before transfer. Membranes were washed in TBST (137mM NaCl, 20mM Tris with 0.1% Tween), blocked in TBST with 5% skim milk powder, washed again and incubated with the appropriate primary antibody (22c11, 1:2000 in TBST,gifted by Prof Ashley Bush [made in house]; anti-human tau, 1:2000 in TBST, Dako; Hsp72, 1:2000, Enzo Life Sciences, Farmingdale, NY, USA; GAPDH, 1:2000, Sigma Aldrich, St. Louis, MO, US) overnight at 4˚C. After washing, membranes were incubated again at RT for 30 minutes with the appropriate LiCor fluorescent secondary antibody (1:10,000) in TBST + 0.01% SDS (IRDye 800CW Goat anti-Rabbit; IRDye 680RD Goat anti-Rabbit; IRDye 680RD Goat anti-Mouse).

Membranes were washed again in TBST and visualized using LICOR Odyssey Scanner. Quantification was performed using Image Studio Lite Analysis Software.

3.3 Results

3.3.1 Protein expression

To assess if Hsp72 was indeed over expressed in the *5xFAD*Tg30*Hsp72 Tg* mice, protein expression via western blotting was analysed. Animals were culled at 10 months of age and both hippocampus and cerebellum regions of the brain were probed for Hsp72. There was a significant over expression of Hsp72 in both the hippocampus and cerebellum in *5xFAD*Tg30*Hsp72 Tg* animals compared to *5xFAD*Tg30* and WT-control animals **(Figure 3.1)**. Levels of protein expression was normalised against GAPDH expression.

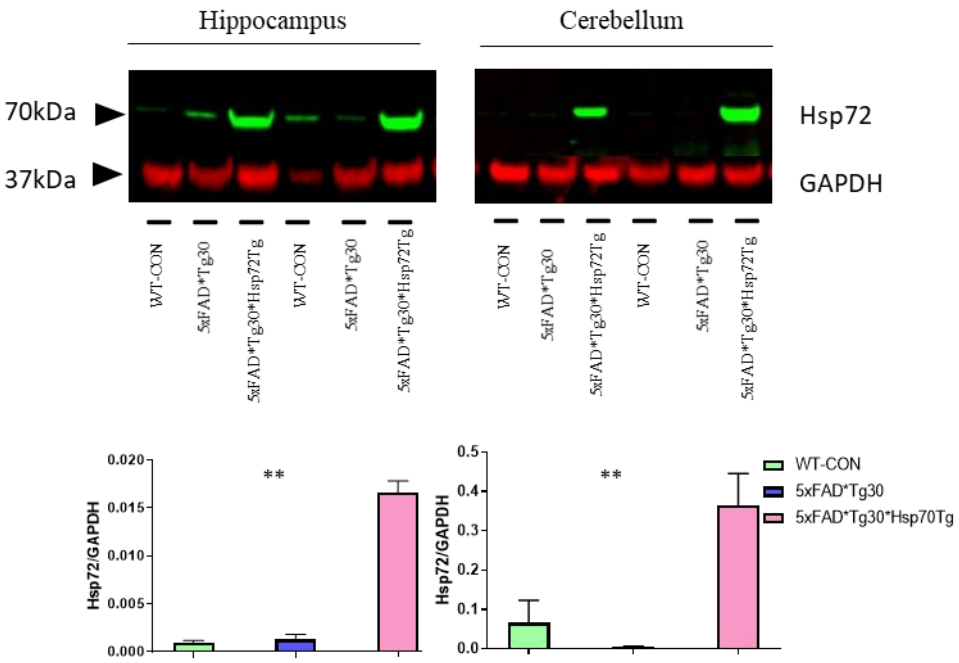

Figure 3.1 ***Hsp72 protein expression.*** *Representative western blots, overexpressing Hsp72 in the 5xFAD*Tg30 mouse model, using transgenic overexpression. Brain was harvested at 10 months and dissected into hippocampus and cerebellum. Quantification performed using GAPDH as loading control **p<0.01 WT vs. 5xFAD*Tg30*Hsp70Tg and 5xFAD*Tg30 vs 5xFAD*Tg30*Hsp70Tg one- way ANOVA with post hoc. Graph indicates mean ± SEM. N=6 per group*

Since Hsp72 was successfully overexpressed in the hippocampus and cerebellum, and we (Chapter 2) and the Heraud paper (Heraud *et.al* 2014) demonstrated overexpression of human tau and APP in the whole brains of *5xFAD*Tg30* animals, we next checked regional expression of APP and tau in the hippocampus and cerebellum.

There was a significant overexpression of APP in the hippocampus of *5xFAD*Tg30* and *5xFAD*Tg30*Hsp72 Tg* compared to WT-control, however there were no effects of Hsp72 Tg overexpression **(Figure 3.2)**. There was no significant overexpression of APP in the cerebellum region of both *5xFAD*Tg30* and *5xFAD*Tg30*Hsp72 Tg* animals.

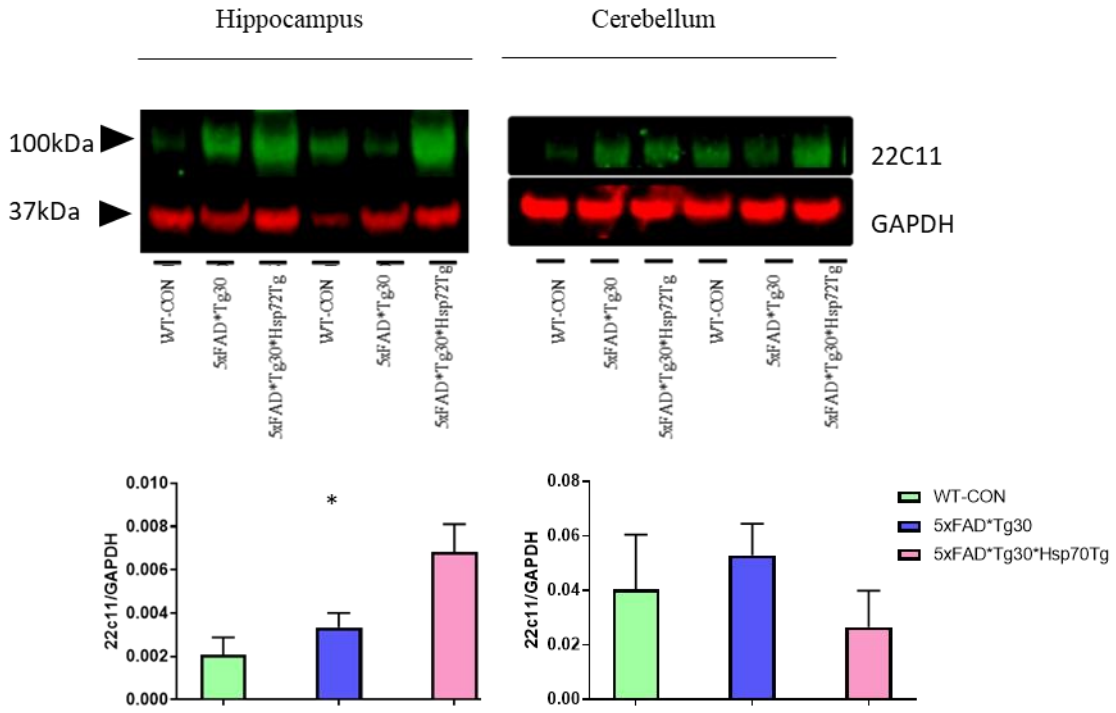

Figure 3.2 ***APP protein expression.*** *Representative western blots, the expression of APP in 5xFAD*Tg30 and 5xFAD*Tg30*Hsp72Tg. Brain was harvested at 10 months and dissected into hippocampus and cerebellum. Quantification was performed using GAPDH as loading control *p<0.05 one-way ANOVA WT vs 5xFAD*Tg30*Hsp70Tg and 5xFAD*Tg30 vs 5xFAD*Tg30*Hsp70Tg, with post hoc. Graph indicates mean ± SEM. N=6 per group*

Additionally, the levels of human tau were significantly overexpressed in the hippocampus in *5xFAD*Tg30* animals, as well as *5xFAD*Tg30*Hsp72 Tg* compared to WT-control **(Figure 3.3)** but there was no difference in the cerebellum. There were no effects of Hsp72 Tg overexpression on the levels of human tau, although quantification showed levels trended to be lower than *5xFAD*Tg30* in the hippocampus, as indicated by the difference between WT and *5xFAD*Tg30* but no significant difference between *5xFAD*Tg30* and *5xFAD*Tg30*Hsp70Tg.*

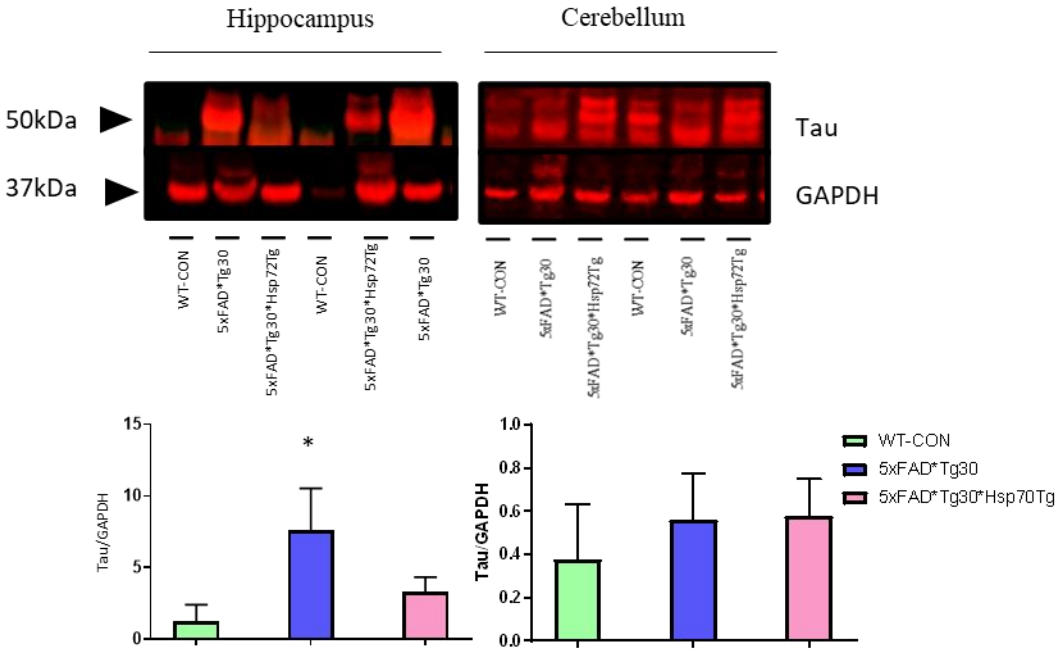

Figure 3.3 ***Human tau protein expression.*** *Representative western blots, the expression of human tau in 5xFAD*Tg30 and 5xFAD*Tg30*Hsp72Tg. Brain was harvested at 10 months and dissected into hippocampus and cerebellum. Quantification was performed using GAPDH as loading control *p<0.05 One-way ANOVA WT vs 5xFAD*Tg30. Graph indicates mean ± SEM. N=6 per group*

3.3.1 Gross motor strength and control

Since Hsp72 preserves muscle function and slows progression of a model that phenocopies Duchenne muscular dystrophy (Gehrig, 2012) gross motor strength and control was assessed through rotarod performance and hangwire testing in *5xFAD*Tg30*Hsp72 Tg* mice. Additionally, it has been found that *Hsp72 Tg* animals have a superior running performance (Henstridge, 2014), so the effect of Hsp72 overexpression on *5xFAD*Tg30* animals' motor performance was assessed, during their lifespan.

Over time, between 7-10 months of age, WT animals displayed a slightly improved but generally steady rotarod performance with a slight decrease in Hangwire performance. There were no genotype effects between *5xFAD*Tg30* and *5xFAD*Tg30*Hsp72 Tg* animals in either rotarod performance **(Figure 3.4 A-C)** or hangwire performance **(Figure 3.4 D-F).** There were no sex differences between male and female animals.

Hence, Hsp72 overexpression was not able to rescue the severe motor phenotype as seen in *5xFAD*Tg30*.

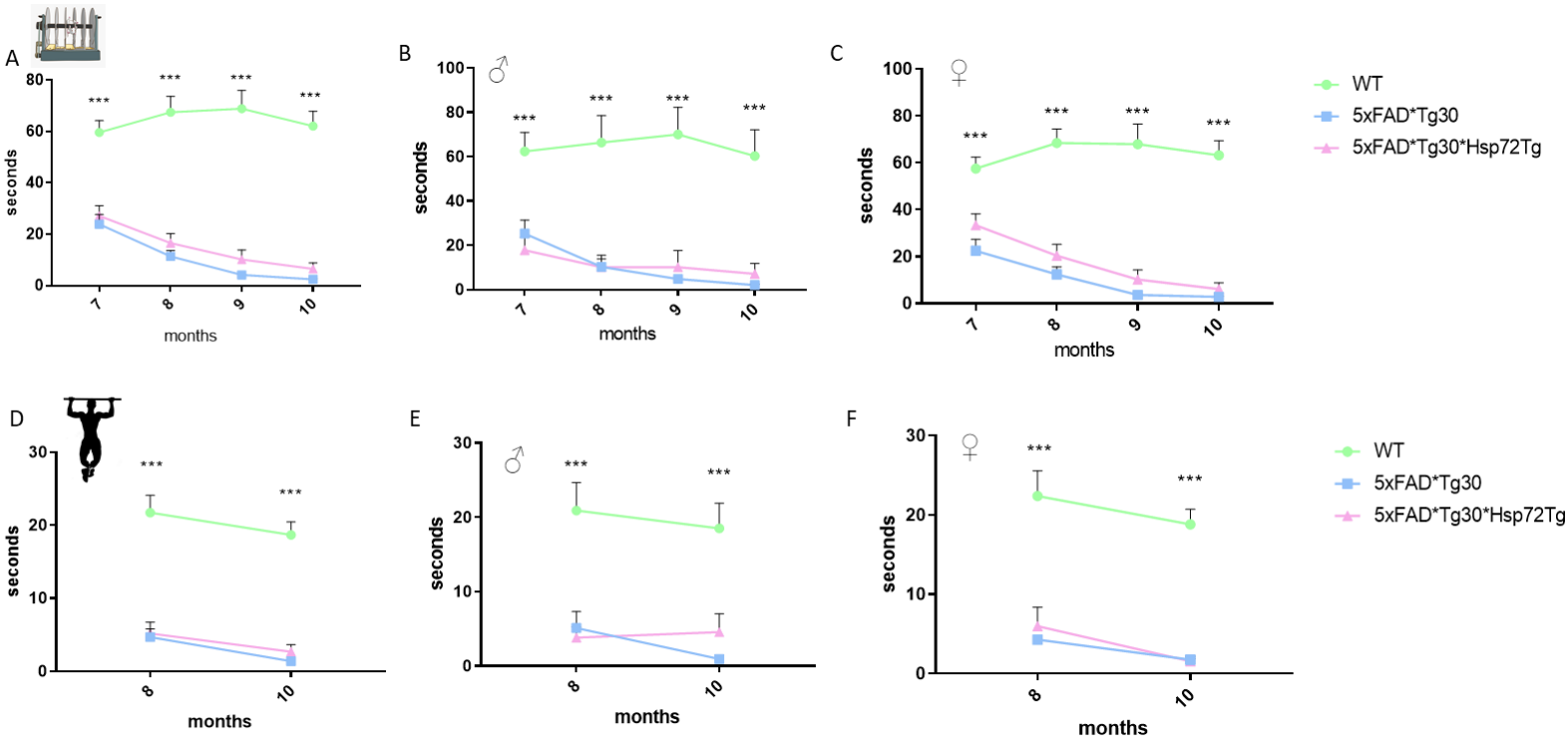

Figure 3.4 ***Measuring gross motor strength and control over time, displayed between 7-10months of age***. *5xFAD*Tg30 and 5xFAD*Tg30*Hsp72Tg animals displayed a significant motor phenotype from 7 months onwards, compared to WT. Average of three trials per month, latency to fall off. (A) Rotarod Total cohort, n=25-26 per group (B) Rotarod Male animals only, n=11-13 per group (C) Rotarod Female animals only, n=13-15 per group. (D) Hangwire Total cohort, n=25-26 per group (E) Hangwire Male animals only, n=11-13 per group (F) Hangwire Female animals only, n=13-15 per group. One-way repeated measures ANOVA with Holm-Sidak post-hoc analysis. ***p<0.001. Graph represents Mean ± SEM*

3.3.2 Memory Function

As Hsp72 treatment has previously been shown to prevent memory decline (in a post-operative general anaesthesia mouse model) (Vizcaychipi, 2011), memory was assessed in *5xFAD*Tg30*Hsp72 Tg* mice over time. The analysis of memory with the Y-maze test was carried out at 7 and 9 months of age. WT animals showed a significant preference of time to the *novel arm* at 7 months as expected, but this did not carry over to 9 months.

At 7 months, *5xFAD*Tg30*Hsp72 Tg* showed a significant preference of time to the *novel arm* compared to the *familiar arm*, which can be attributed to the male animals as females displayed no preference. There were no genotype effects between *5xFAD*Tg30* and *5xFAD*Tg30*Hsp72 Tg* **(Figure 3.5)**.

At 9 months, similar to WT, there was no preference towards the *novel arm*, however there was significant preference to *home arm*, for both *5xFAD*Tg30* and *5xFAD*Tg30*Hsp72 Tg* **(Figure 3.6)**. It is important to note by 9 months, a severe motor phenotype can be seen, so it is assumed the lack of animal movement can account for this result. Females showed no significance to any maze arm.

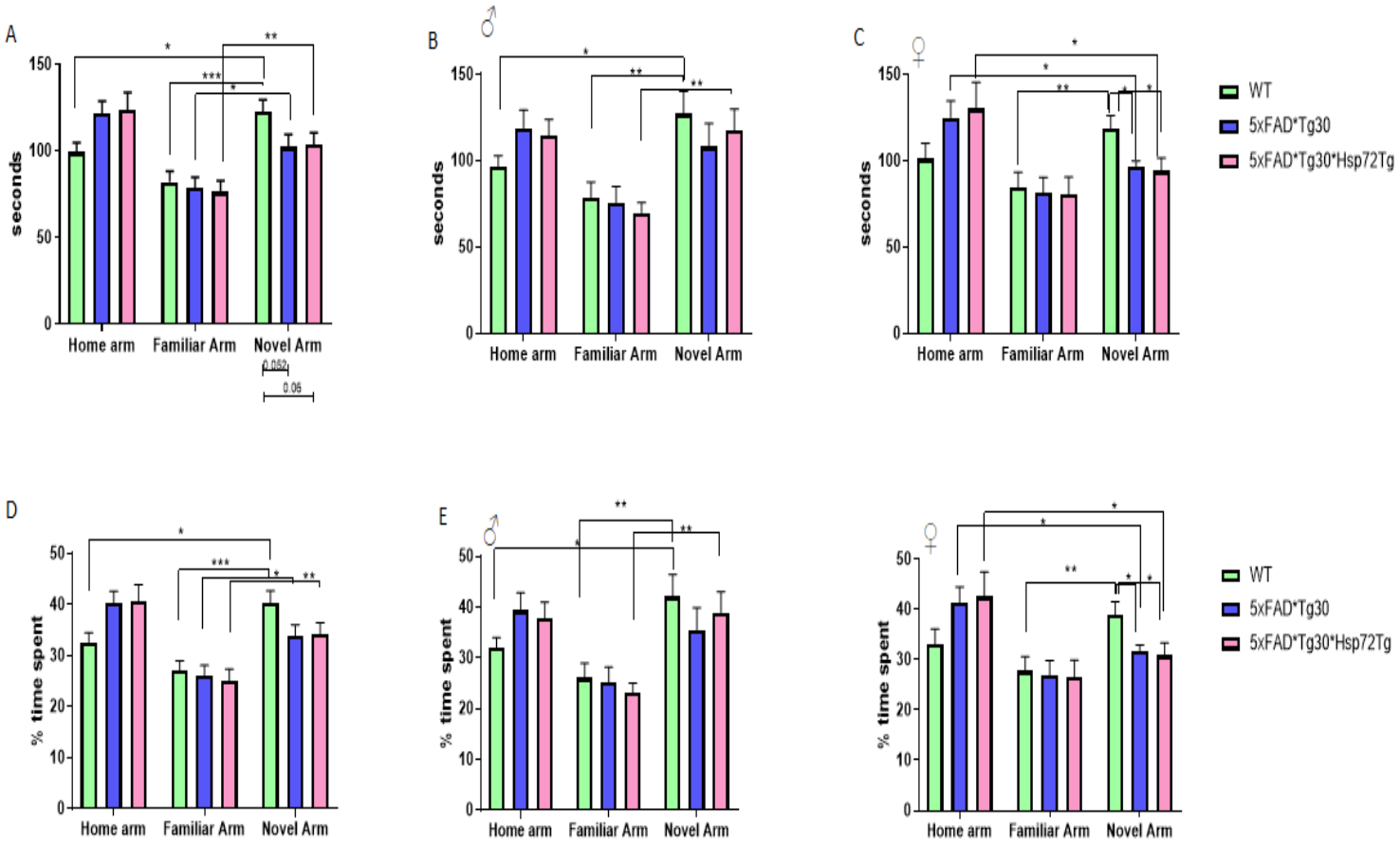

Figure 3.5 ***Duration of overall time and percentage of time spent in each arm of a Y-maze at 7 months of age***. *Animals had 10 minutes familiarisation, before a 5-minute trial, 2 hours later. (A) Total cohort, n=25 per group (B) Male animals only, n=10-13 per group (C) Female animals only, n=12-15 per group (D) %time spent total cohort, n=25 per group (E) %time spent Male animals only, n=10-13 per group, (F) %time spent Female animals only, n=12-15 per group. WT animals spent significantly (females; trended in males and overall) more time in the Novel arm compared to 5xFAD*Tg30 but Hsp72 Tg did not rescue this memory deficit. One-way ANOVA performed in the arm of interest, the Novel arm. 2tailed, type 2 students t-test performed between arms. *p<0.05 **p<0.01 ***p<0.001 Graph represents Mean ± SEM*

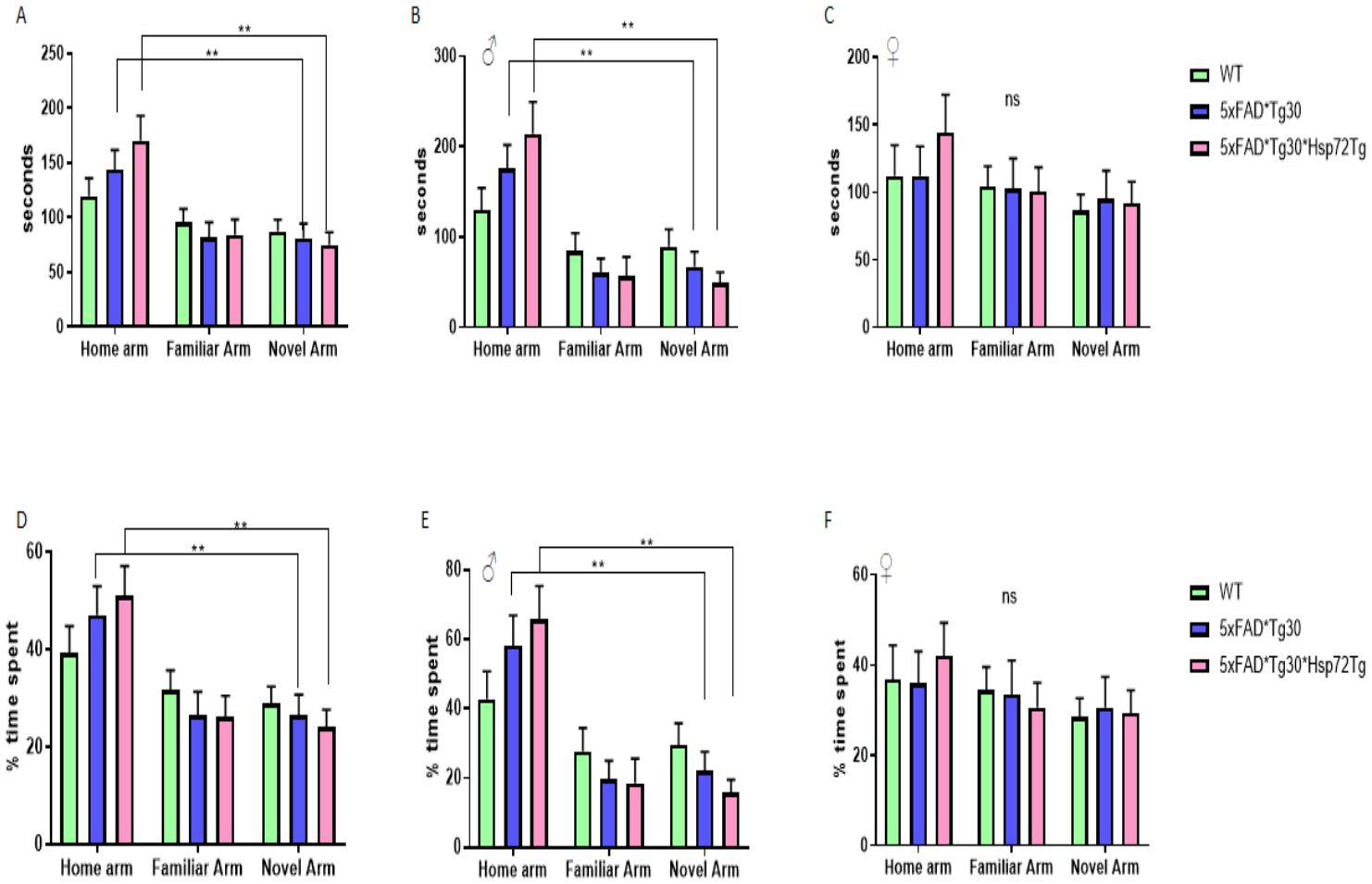

Figure 3.6 ***Duration of overall time and percentage spent in each arm of a Y-Maze at 9 months of age.*** *Animals had 10 minutes familiarisation, before a 5-minute trial, 2 hours later. (A) Total cohort, n=24-25 per group (B) Male animals only, n=9-13 per group (C) Female animals only, n=12-15 per group (D) %time spent total cohort, n=25 per group (E) %time spent Male animals only, n=10-13 per group, (F) %time spent Female animals only, n=12-15 per group. 5xFAD*Tg30 and 5xFAD*Tg30*Hsp72Tg animals spent significantly less time in the Novel*

3.3.3 Anxiety-like behaviour

As *5xFAD*Tg30* mice previously appeared to display more risk-taking behaviour **(Figure 2.4)**, the effect of Hsp72 overexpression was assessed on anxiety-like behaviour. Interestingly, animals spent a significant amount of time in the *corners* of the field, as usually expected, but not as resulted previously in *Chapter 2*. Both *5xFAD*Tg30* and *5xFAD*Tg30*Hsp72Tg* animals spent their time in the *corner's* areas preferentially over the *centre* area, and there were no genotype differences between WT and *5xFAD*Tg30* and WT and *5xFAD*Tg30*Hsp72Tg* **(Figure 3.7)**. Interestingly, female *5xFAD*Tg30*Hsp72 Tg* trended to have a genotype effect within the *corners* area between *5xFAD*Tg30* females ($p<0.056$) **(Figure 3.7 C and F)**.

In an attempt to alleviate motor phenotype effects that may be present in the open field test, at 9 months, animals were placed in an elevated plus maze, as an anxiety-like behaviour test substitute. This maze is smaller than the large open field and requires less motor ability. Similar to *Chapter 2* results, *5xFAD*Tg30* animals appeared to display more risk-taking behaviour, by spending significantly more time in the *open arm* than WT **(Figure 3.8)**. This behaviour suggests the inability to recognise danger to remove themselves from a vulnerable position. Interestingly, *5xFAD*Tg30*Hsp72 Tg* also spent significantly more time in the *open arm* than WT, but it was significantly less than *5xFAD*Tg30*. What is even more interesting, is that looking into the number of bouts of exploratory behaviour into the *open arm*, it can be seen that WT animals displayed more nose bouts into the *open arm* than *5xFAD*Tg30* and *5xFAD*Tg30*Hsp72 Tg* **(Figure 3.8 G-I)**. A nose bout could represent exploratory behaviour, without actual risk taking. This is called appropriate decision making in the animal behaviour field. Again,

*5xFAD*Tg30*Hsp72 Tg* were also significantly different to *5xFAD*Tg30*. This could suggest an effect of Hsp72 Tg on the behaviour of *5xFAD*Tg30* but not effective enough to recover to WT-like behaviours. This overall genotype finding however, was primarily driven by female performance **(Figure 3.8 I)**.

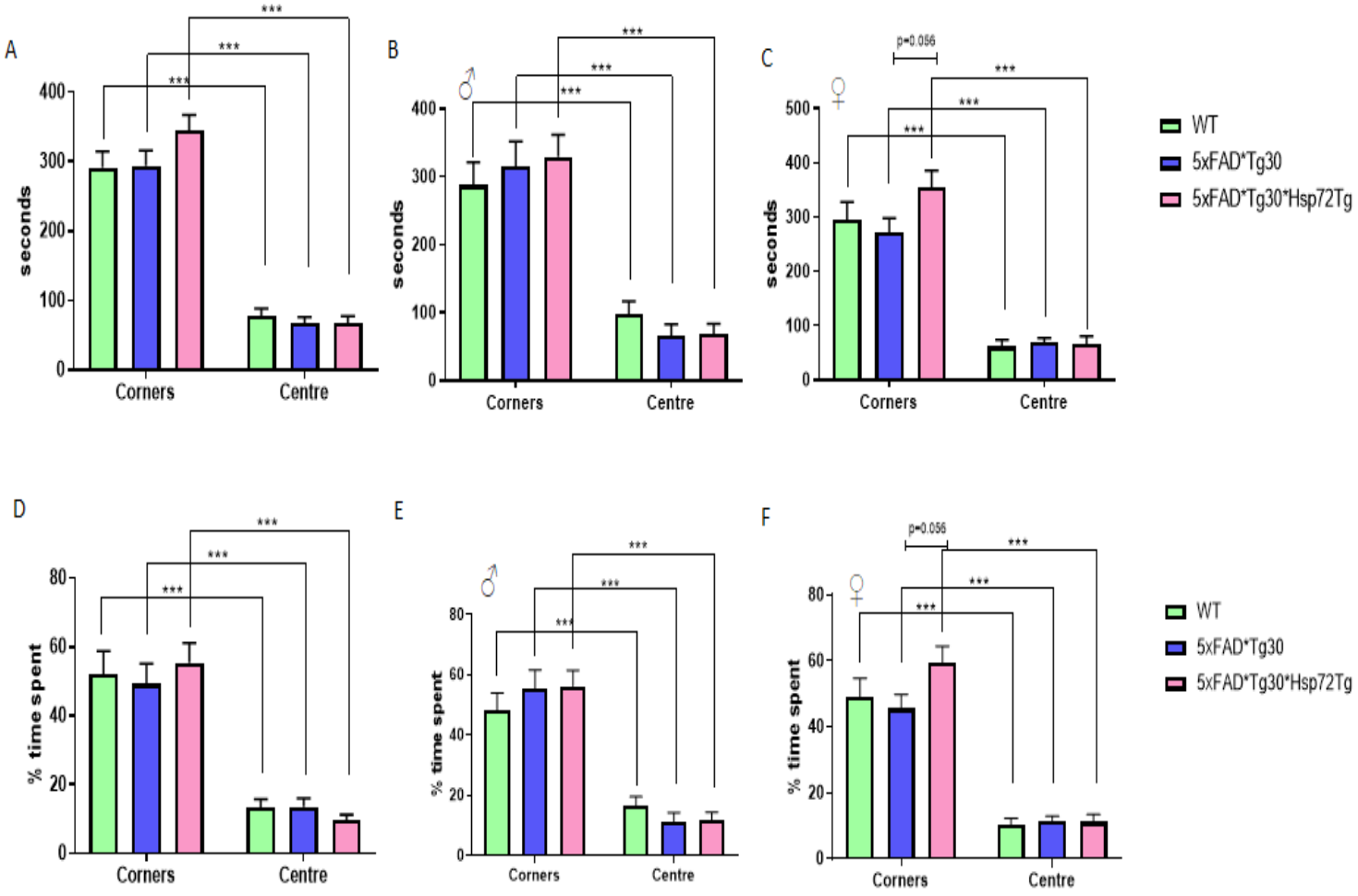

Figure 3.7 ***Duration of time and percentage of time spent in areas of a large open field at 7 months of age***. *Animals had 10 minutes in the arena lit with bright lights, corners and centre of arena tracked (A) Total cohort, n=25 per group (B) Male animals only, n=10-13 per group (C) Female animals only, n=12-15 per group (D) %time spent total cohort, n=25 per group (E) %time spent Male animals only, n=10-13 per group, (F) %time spent Female animals only, n=12-15 per group. Animals spent significantly more time in the corner areas of field compared to the centre of the field. No genotype differences. One-way ANOVA performed in each area of interest. 2tailed, type 2 students t-test performed between arms * $p<0.05$ Graph represents Mean ± SEM*

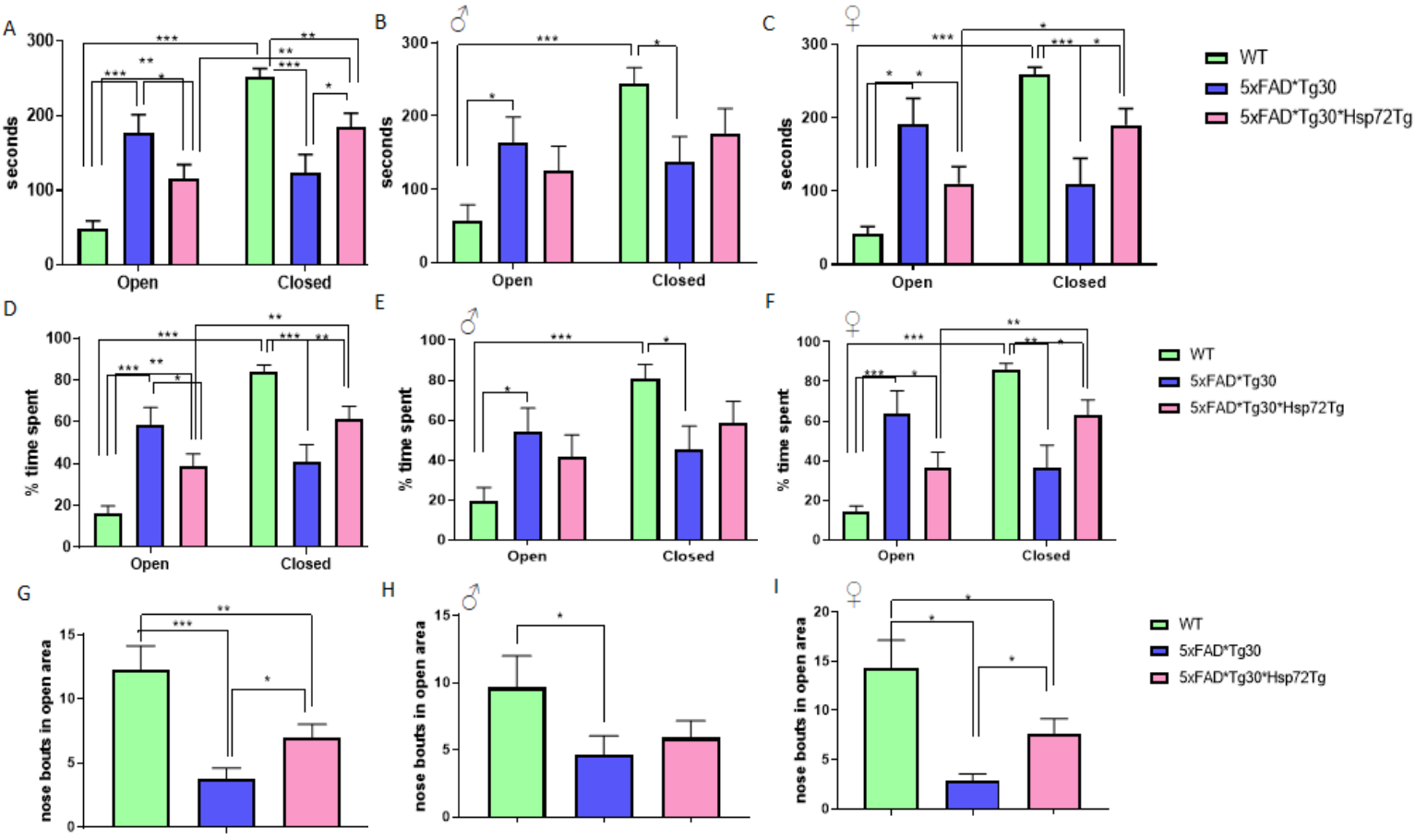

Figure 3.8 ***Anxiety-like behaviour assessed via elevated plus maze.*** *(A-F) Duration of overall time and percentage spent at 9 months of age in an elevated plus maze. Animals spent 10 minutes in an elevated plus maze, consisting of open arms and closed arms. (A) Total cohort, n=24-25 per group (B) Male animals only, n=9-13 per group (C) Female animals only, n=12-15 per group (D) %time spent total cohort, n=25 per group (E) %time spent Male animals only, n=10-13 per group, (F) %time spent Female animals only, n=12-15 per group. WT animals spent significantly more time in the closed area compared to the open area, and significantly more time in the closed area compared to 5xFAD*Tg30 and 5xFAD*Tg30*Hsp72Tg animals. Within the open area and closed areas, there were genotype differences. One-way ANOVA performed in each area of interest. 2tailed, type 2 students t-test performed between arms *p<0.05 **p<0.01 ***p<0.001. Graph represents Mean ± SEM*

*(G-I) Nose bouts in open area. WT animals showed greater nose bouts in the open area compared to 5xFAD*Tg30 animals. 5xFAD*Tg30*Hsp72Tg animals showed greater nose bouts in the open area compared to 5xFAD*Tg30 animals (G) Total cohort, n=24-15 per group (H) Male animals only, n=9-13 (I) Female animals only, n=12-15 per group*

3.3.4 Novel object recognition

Next, we assessed novel object recognition and the effect of Hsp72 on the ability to recognise and explore new or familiar objects. At 7 months, there was no genotype difference in preference to the *novel object* over *familiar object. 5xFAD*Tg30* animals had a greater number of exploratory bouts in the *novel object* compared to WT **(Figure 3.9 A-C)**, driven by female performance **(Figure 3.9 C)**.

At 9 months, *5xFAD*Tg30* had reduced novel object recognition and *5xFAD*Tg30*Hsp72 Tg* did not rescue this deficit **(Figure 3.9 D-F)**. WT animals were still able to recognise the *novel object,* however male animals were less likely to do so. Hence, at 7 months, *5xFAD*Tg30* and *5xFAD*Tg30*Hsp72 Tg* animals have in-tact novel object recognition, but this is altered by 9 months. Hsp72 overexpression does not rescue this decline in function.

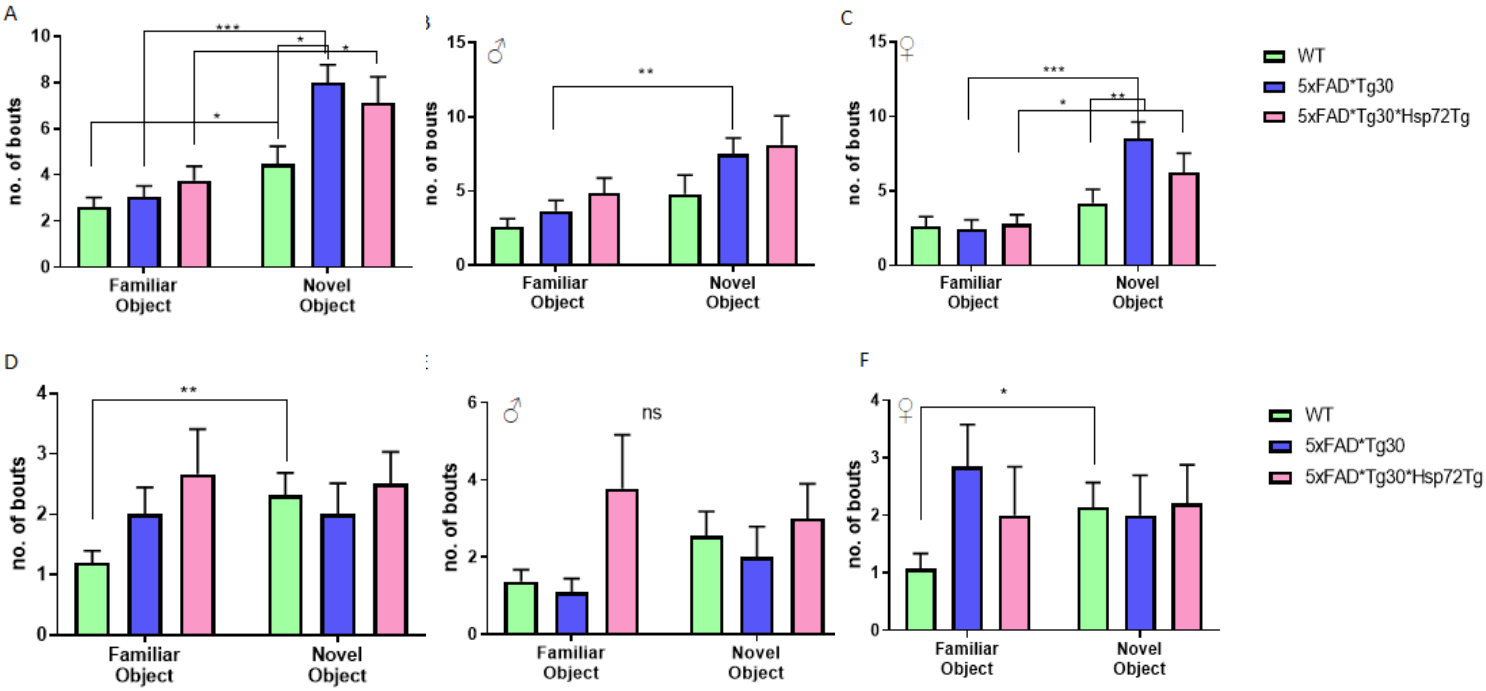

Figure 3.9 ***Number of bouts of investigative behaviour of each object*** *at 7 months (A-C) and 9 months (D-F) of age. Animals had 10 minutes familiarisation with Object 1 and Object 2. Object 1 was then replaced with Novel Object and animals had a 5 minute test (A) Total cohort, n=16-17 per group (B) Male animals only, n=7-10 per group (C) Female animals only, n=6-10 per group. WT animals observed the Novel Object significantly more than the Familiar Object and both 7 and 9 months. 5xFAD*Tg30 and 5xFAD*Tg30*Hsp72Tg animals observed the Novel Object significantly more than the Familiar Object at 7 months, but this did not translate at 9 months. One-way ANOVA performed in the object of interest, the Novel object. 2tailed, type 2 students t-test performed between arms *p<0.05 **p<0.01 ***p<0.001 Graph represents Mean ± SEM*

3.3.5 Learning, spatial memory and recognition

Learning has previously been associated with the increase in *heat shock cognate 70* (Hsc70) mRNA and protein expression (Pizarro, 2003). While Hsp70 is a stress induced protein and Hsc70 is a constitutively expressed protein, they share common structures and functions. Hence, learning was assessed with Hsp72 overexpression with the *5xFAD*Tg30* model of AD.

In *Chapter 2* of this thesis, learning, spatial memory and recognition was assessed via the widely used task, the Morris Water Maze. This uses spatial learning and aversive stress related swimming, which, due to the severe motor phenotype we identified in this model carried potential risk. Therefore, as an alternative, the Cheeseboard maze was utilised. The cheeseboard maze assesses learning, spatial memory and recognition similarly to the Morris Water Maze; however, it uses reward over aversion. It is also performed on a table instead of in water, which aids in the safety and wellbeing of the animals.

The Cheeseboard maze was performed at 8months of age, with male animals only. Mice took less time to reach and find the baited well on the second and third day, but their latency increased slightly on the fourth day **(Figure 3.10 A)**. The fifth and sixth day continued to lessen their latencies. On the fourth day, a genotype effect could be seen between WT and *5xFAD*Tg30*; *5xFAD*Tg30*Hsp72 Tg* ($p<0.01$). There was no genotype effect between *5xFAD*Tg30* and *5xFAD*Tg30*Hsp72 Tg*. Interestingly, when the baited well was removed, both WT and *5xFAD*Tg30*Hsp72 Tg* animals trended to spend more time in the baited well areas, compared to *5xFAD*Tg30* but this did not reach significance **(Figure 3.10 B)**.

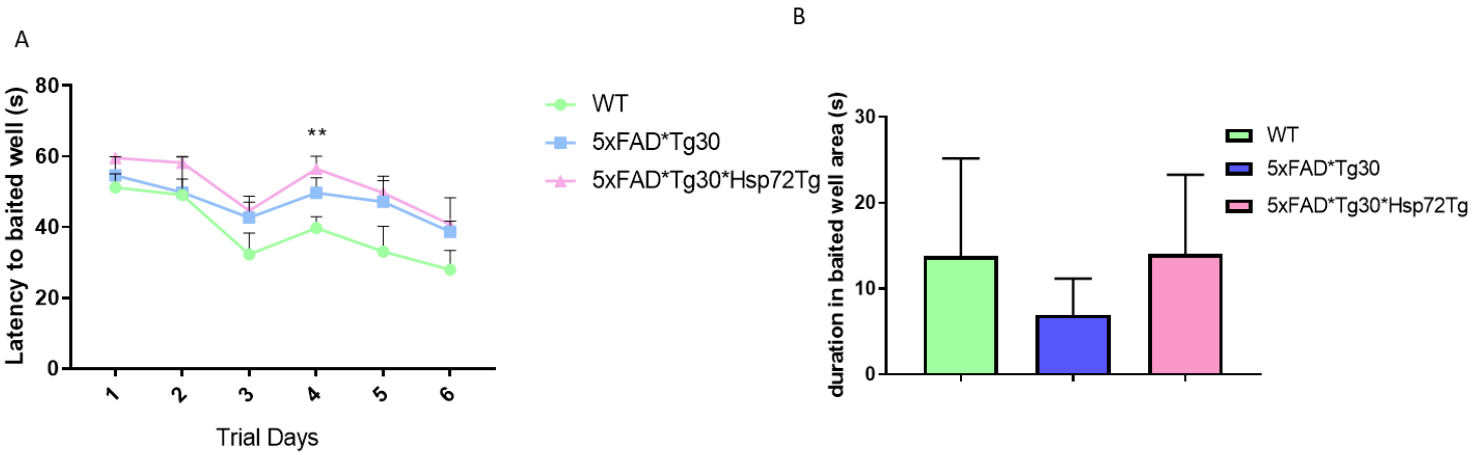

Figure 3.10 ***Learning curve, latency to baited well on a Cheeseboard maze***. *(A) Over a 6-day training period, male animals were given 60 seconds to find a baited well with a hidden reward, and latency was recorded. (B) On the last day, the reward was removed, and the duration spent in the previously baited well was recorded. Day 4 observed a difference in latency between WT and 5xFAD*Tg30*Hsp72Tg but did not translate to any other days. There were no differences during the probe trial. Graph represents Mean of 4 trials per day ± SEM. Two-way repeated measures ANOVA with Holm-Sidak post-hoc analysis. **p<0.01 genotype effect n=4-5 per group. Graph indicates ± SEM*

3.3.6 Body composition

As *5xFAD*Tg30* animals displayed a significant body weight and lean mass phenotype throughout their lifespan, as well as fat mass towards the end of life, lifespan body composition was assessed with Hsp72 Tg overexpression.

As in *Chapter 2*, body weight was significantly different between WT and *5xFAD*Tg30*, and Hsp72 Tg overexpression did not rescue this **(Figure 3.11 A-C).**

Lean mass in WT animals was significantly higher than *5xFAD*Tg30* and *5xFAD*Tg30*Hsp72 Tg*. Interestingly, *5xFAD*Tg30*Hsp72 Tg* trended to have a slightly higher lean mass than *5xFAD*Tg30* and in males, at later stages, was significantly higher **(Figure 3.11 D-F)**. Females showed no genotype effects.

Fat mass and body fat percentage were significantly lower in *5xFAD*Tg30*, as in *Chapter 2*, but Hsp72 Tg overexpression did not rescue this effect **(Figure 3.11 G-L)**.

Animals, but could not be recovered with Hsp72 Tg overexpression. There could, however, be a potential for a slight effect in male lean mass.

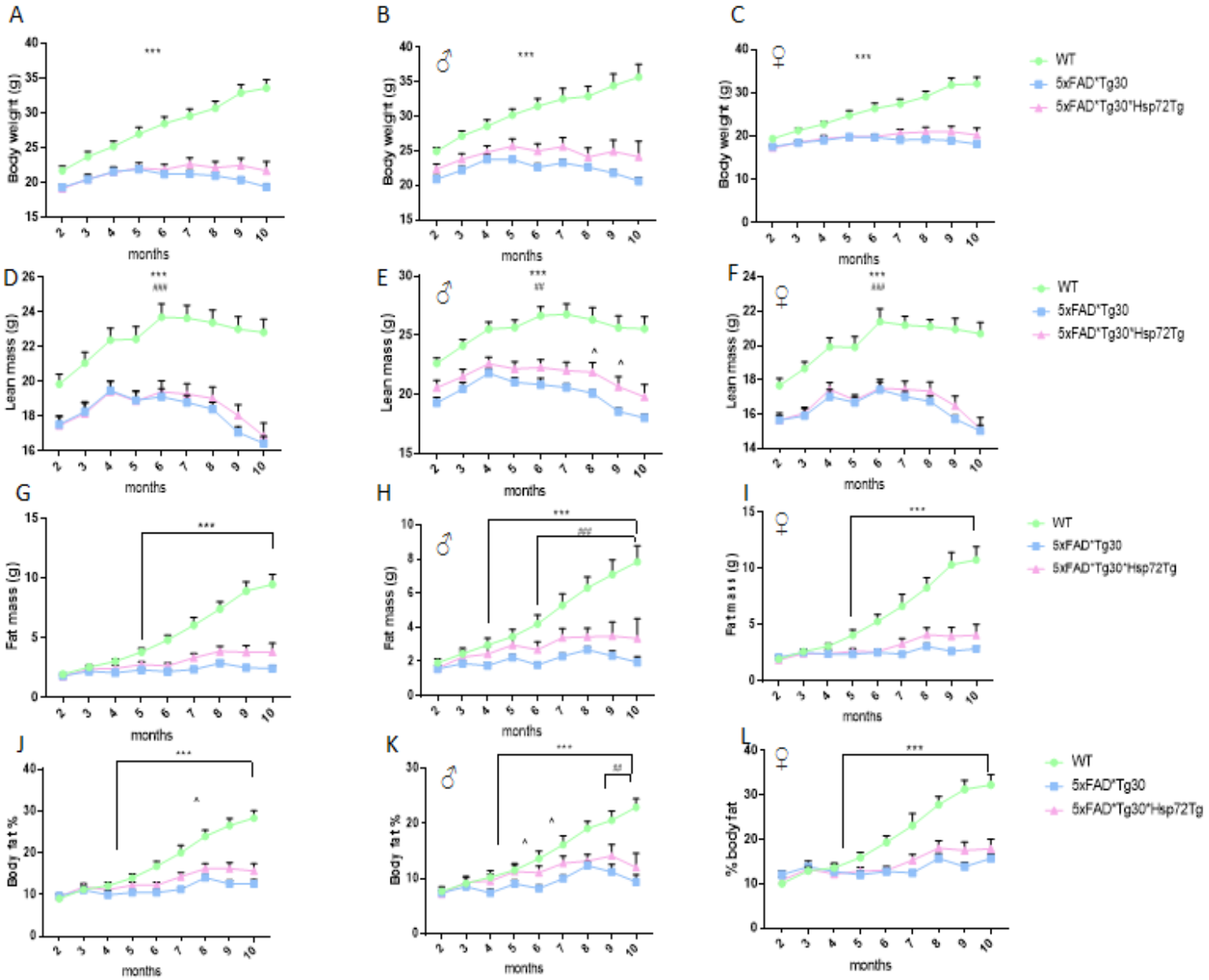

Figure 3.11 ***Body composition analysis in WT, 5xFAD*Tg30 and 5xFAD*Tg30*Hsp72Tg mice over time***. *(A-C) Body weight, (D-F) lean mass, (G-I) fat mass (J-L) body fat percentage. (A,D,G,J) total cohort n=24-28 per group, (B,E,H,K) male animals only n=10-14 per group, (C,F,I,L) female animals only, n=13-17 per group. WT animals had a significantly higher body weight and lean mass compared to 5xFAD*Tg30 and 5xFAD*Tg30*Hsp72Tg across lifespan. Fat mass and body fat percentage was significantly different at 5 months of age between WT and 5xFAD*Tg30 animals, but not until 6months and 9 months respectively for Male 5xFAD*Tg30*Hsp72Tg animals. One-way repeated measures ANOVA with Holm-Sidak post-hoc analysis ***p<0.05 #p<0.05 WT vs 5xFADTg30*Hsp72Tg ^p<0.05 5xFAD*Tg30 vs 5xFAD*Tg30*Hsp72Tg. Graph indicates ± SEM*

3.3.7 Glucose Tolerance

Since Hsp72 overexpression has previously been shown to provide protective benefits when glucose challenged (Chung, 2008), an oral gavage glucose tolerance test was next performed. The test was performed at 5 months of age, to avoid any effects from behavioural testing. Genders combined, *5xFAD*Tg30* and *5xFAD*Tg30*Hsp72 Tg* mice had a significantly lower fasting blood glucose level and this lowered blood glucose remained over the period of the test **(Figure 3.12)**. Both male and female *5xFAD*Tg30* and *5xFAD*Tg30*Hsp72 Tg* had a lower initial spike in glucose after the glucose bolus, compared to WT **(Figure 3.12 B-C)**. There were no genotype effects between *5xFAD*Tg30* and *5xFAD*Tg30*Hsp72 Tg*. Thus, there were no effects of Hsp72 Tg overexpression on the *5xFAD*Tg30* mouse model.

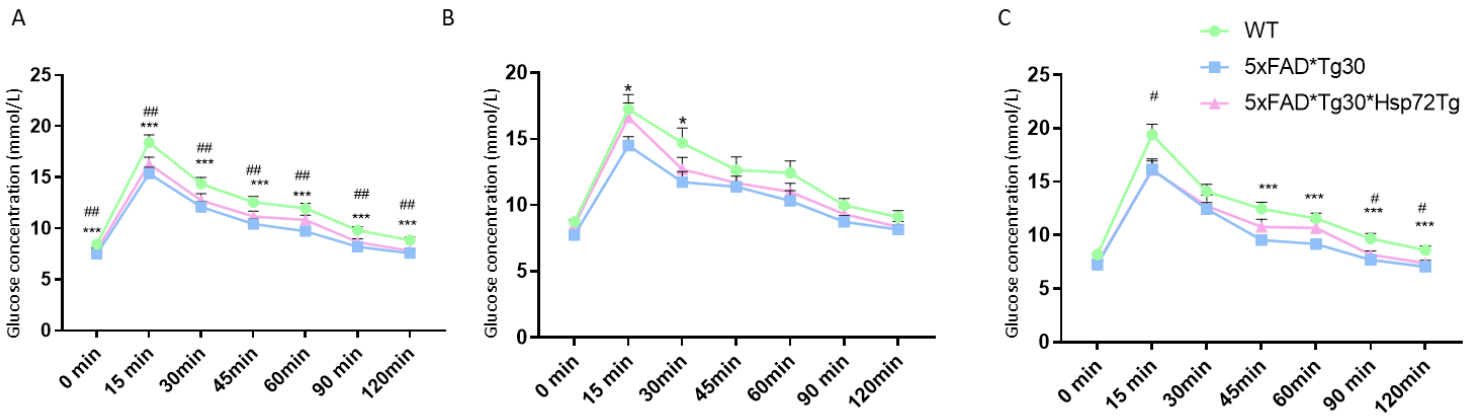

Figure 3.12 ***Whole-body glucose metabolism analysis***. *Fasting blood glucose levels after an oral gavage glucose tolerance test (2gm/kg LBM) at 5months of age. (A) total cohort n=24-26 per group (B) males only n=10-12 per group (C) females only n=13-14 per group. Fasting blood glucose was taken after a 6 hour fast and is the '0' time value represented in the OGTT. Genotype effects between WT and 5xFAD*Tg30 and WT and 5xFAD*Tg30*Hsp72Tg. One-way repeated measures ANOVA with Holm-Sidak post-hoc analysis *p = <0.05 ***p = <0.001, # p= <0.05 WT vs 5xFAD*Tg30*Hsp72Tg. Graphs indicate mean ± SEM*

3.3.8 Metabolic caging analysis

In *Chapter 2,* metabolic caging analyses indicated that *5xFAD*Tg30* males have higher VO_2 consumption and energy expenditure when adjusted for both body weight and lean mass compared to WT control. Raw VO_2 and energy expenditure however, showed a significantly reduced rate. To test if Hsp72 Tg overexpression had any effect on these measures, animals were placed inside a metabolic cage and aspects of whole-body energy metabolism was recorded over 48hrs, with the last 24hrs analysed.

Gender combined **(Figure 3.13A)** and male **(Figure 3.13B)** raw VO_2 rates saw no genotype effects, but female *5xFAD*Tg30* and *5xFAD*Tg30*Hsp72 Tg* displayed a small period in the dark cycle where they had a significantly lower oxygen consumption **(Figure 3.13 C).** When adjusted for both body weight and lean mass, VO_2 rates were again, significantly higher in male *5xFAD*Tg30* animals and there was no effect of Hsp72 Tg overexpression on this **(Figure 3.13 D-I)**. Female *5xFAD*Tg30* and *5xFAD*Tg30*Hsp72 Tg* animals also displayed a higher VO_2 when adjusted for body weight **(Figure 3.13 F).**

In *Chapter 2,* female *5xFAD*Tg30* animals trended to have a lower energy expenditure compared to WT which came out significant in this chapter **(Figure 3.13 L).** Interestingly, unlike in *Chapter 2* this did not show significance for male animals **(Figure 3.13 K)**. Therefore, when adjustment for body weight and lean mass was analysed, male *5xFAD*Tg30* animals displayed a higher energy expenditure **(Figure 3.13 N, Q)**. There were no genotype effects of Hsp72 Tg overexpression on these measures.

Interestingly, males displayed a higher RER compared to WT, and females a lower RER compared to WT **(Figure 3.14 A-C).**

Animals showed significant increased overall activity via beam breaks in the dark cycle, but there were no genotype effects **(Figure 3.14 D-F).** The Promethion also allows analysis of activity such as all meters travelled, as well as voluntary meters travelled via an exercise wheel. These two measures additionally saw no genotype effects, which was expected as motor phenotype is not seen until 6 months. Female *5xFAD*Tg30*Hsp72 Tg* however, showed an increase in all meters travelled, compared to WT **(Figure 3.14 I).** Additionally, the Promethion system allows for measurement of food intake, however there were no genotype effects present **(Figure 3.14 M-O).**

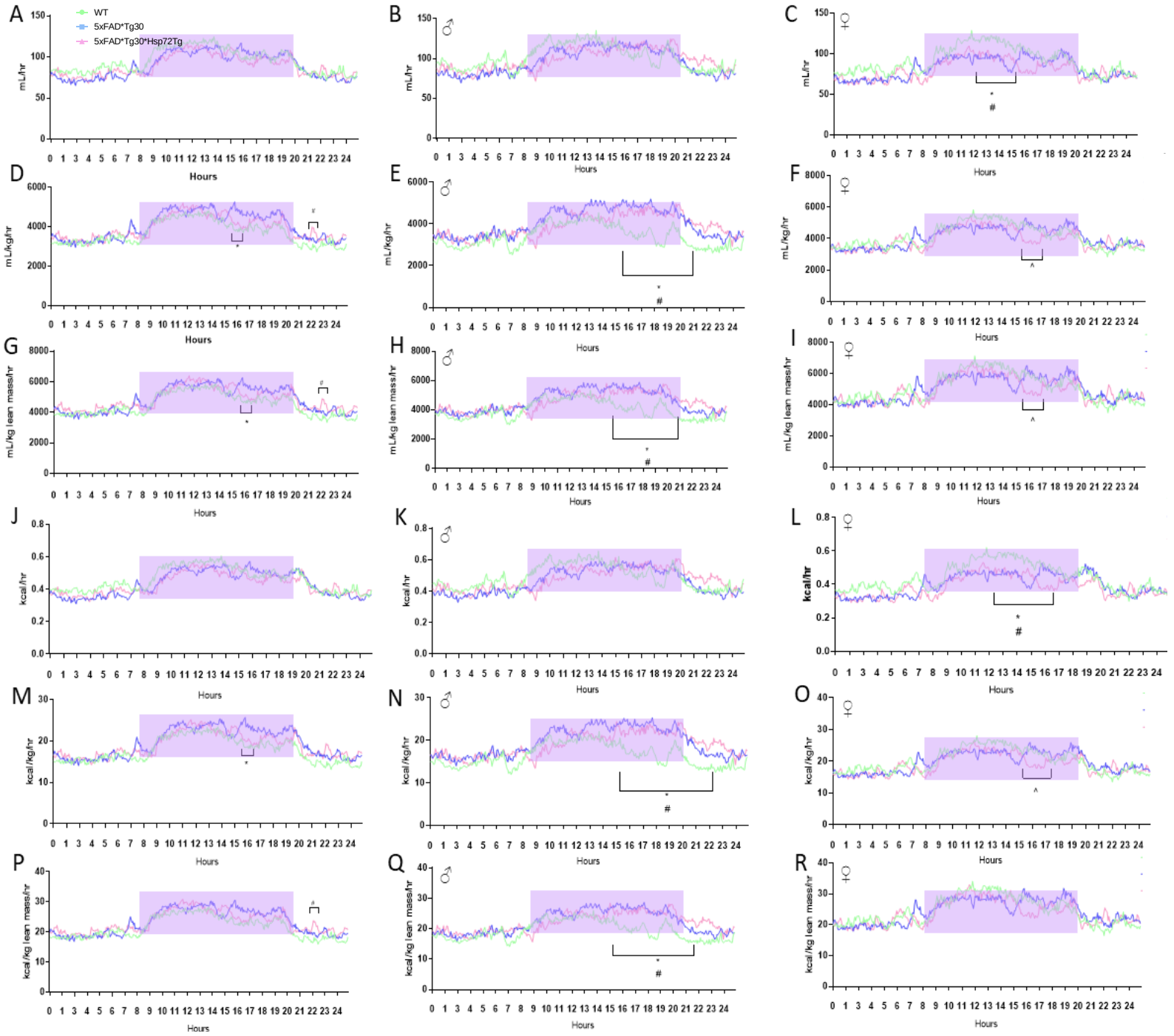

Figure 3.13 ***Aspects of whole-body energy metabolism measured in a CLAMs system for WT control, 5xFAD*Tg30 and 5xFAD*Tg30*Hsp72Tgmice over a 24hour period.*** *Total cohort (A,D,G,J,M,P), Male (B,E,H,K,N,Q), Female (C,F,I,L,O,R) (A-C) Raw oxygen consumption (VO_2) unadjusted for any factor during light cycle, dark cycle and over the total 24 hour measurement period. Genotype effects between female WT and 5xFAD*Tg30, and WT and 5xFAD*Tg30*Hsp72Tg. (D-F) VO_2 data normalised to body weight. Genotype effects between WT and 5xFAD*Tg30, and WT and 5xFAD*Tg30*Hsp72Tg (G-I) VO_2 normalised to lean body mass. Genotype effects between WT and 5xFAD*Tg30, and WT and 5xFAD*Tg30*Hsp72Tg (J-L) Raw energy expenditure (heat) unadjusted for any factor. Genotype effects between female WT and 5xFAD*Tg30, and WT and 5xFAD*Tg30*Hsp72Tg (M-O) Energy expenditure data normalised to body weight. Genotype effects between WT and 5xFAD*Tg30, and WT and 5xFAD*Tg30*Hsp72Tg (P-R) Energy expenditure normalised to lean body mass. Genotype effects between male WT and 5xFAD*Tg30, and WT and 5xFAD*Tg30*Hsp72Tg *p<0.05 WT vs 5xFAD*Tg30 #p<0.05 WT vs 5xFAD*Tg30*Hsp72Tg. One-way ANOVA; n=11-13 per group. Graphs indicate mean ± SEM. Shading refers to dark 12-hr cycle*

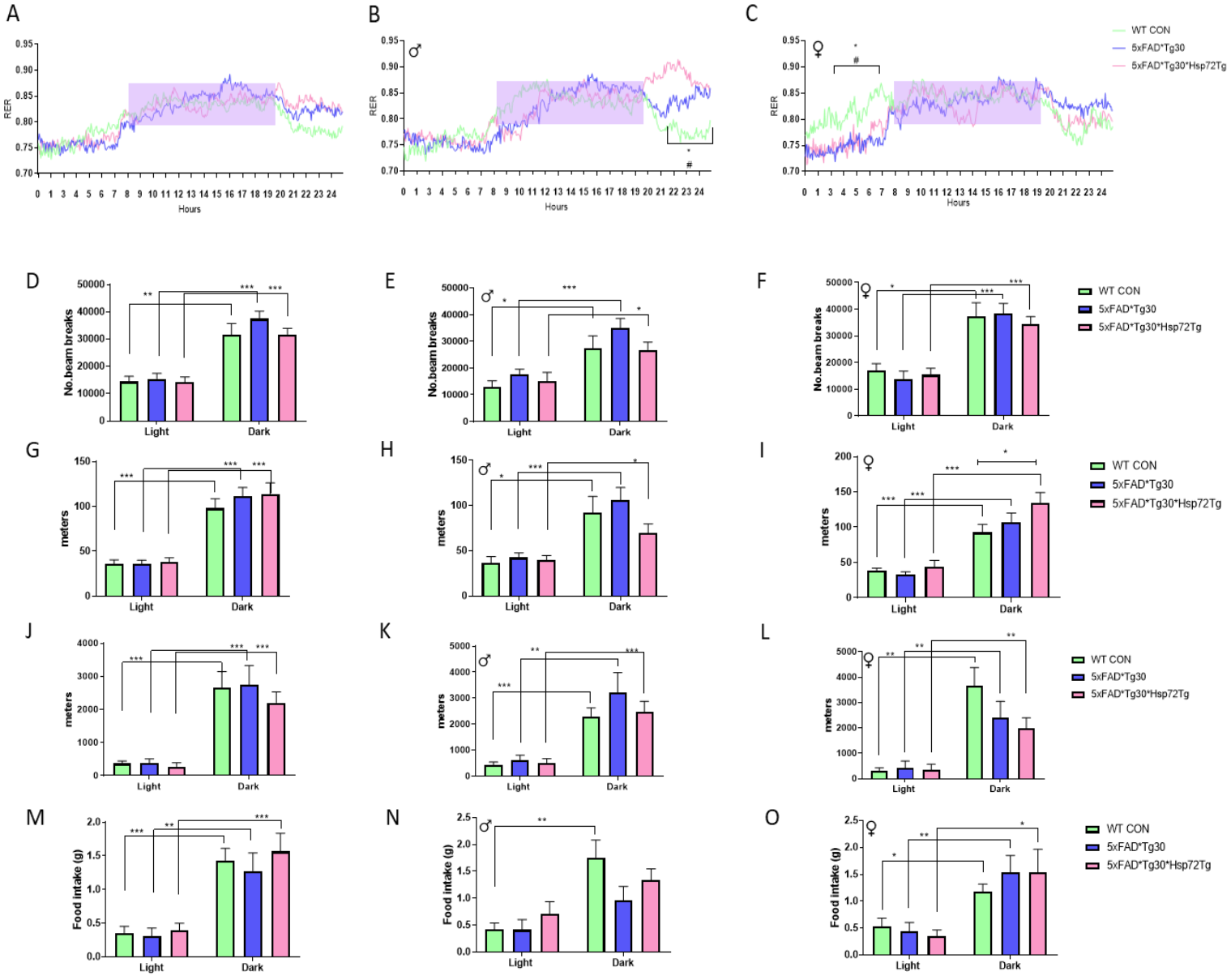

Figure 3.14 ***Aspects of whole-body energy metabolism measured in a Promethion system for WT control, 5xFAD*Tg30 and 5xFAD*Tg30*Hsp72Tg mice over a 24hour period***. *Total cohort (A,D,G,J,M,), Male (B,E,H,K,N,), Female (C,F,I,L,O,)* ***(A-C)*** *Respiratory exchange ratio (RER), genotype effects in male and female between WT and 5xFAD*Tg30, and WT and 5xFAD*Tg30*Hsp72Tg* ***(D-F)*** *Total movement/activity as measured via beam breaks (x + Y ambulatory plus z breaks). No genotype effects.* ***(G-I)*** *Total activity as measured by all meters travelled. Genotype effects during the dark cycle in female between WT and 5xFAD*Tg30*Hsp72Tg.* ***(J-L)*** *Voluntary activity as measured by total exercise wheel meters. No genotype effects.* ***(M-O)*** *Total food intake *p<0.05 **p<0.01 ***p<0.001 #p<0.05 WT vs 5xFAD*Tg30*Hsp72Tg n=11-13 per group. Graphs indicate mean ± SEM. Shading refers to dark 12-hr cycle*

3.3.9 End point measures

As *5xFAD*Tg30* animals show a significant decrease in brain weight and *tibialis anterior* weight compared with WT at end point, this was next assessed with Hsp72 Tg overexpression. In agreement with *Chapter 2,* brain weight was significantly decreased in *5xFAD*Tg30* animals but did not reach significance with *5xFAD*Tg30*Hsp72 Tg*. When data was split between genders, this did not reach significance **(Figure 3.15 A-C)**. *Tibialis anterior* weights were significantly decreased in both *5xFAD*Tg30* and *5xFAD*Tg30*Hsp72 Tg* animals compared with WT. Thus, Hsp72 Tg overexpression did not rescue the decrease in brain weight or *tibialis anterior* weight as seen in *5xFAD*Tg30* animals.

*5xFAD*Tg30* animals additionally display a decreased survival, and while *5xFAD*Tg30*Hsp72 Tg* animals trended to have an increased survival, this did not reach significance **(Figure 3.16).** In terms of total numbers of survival vs deaths, there were 6 deaths out of 28 (21%) in the *5xFAD*Tg30* group and 3 deaths out of 27 (11%) in the *5xFAD*Tg30*Hsp72 Tg*.

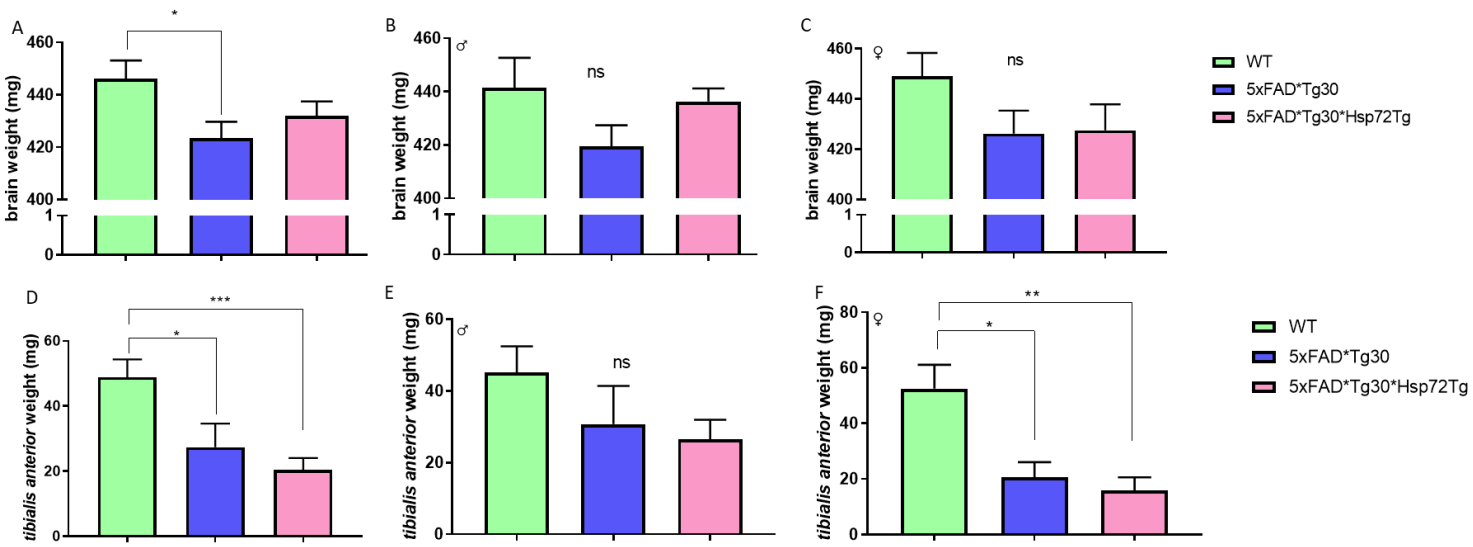

Figure 3.15 ***End point brain weight and tibialis anterior weight, at 10months of age.*** *(A,D) total cohort n=12-16 per group (B, E) males only n=6 per group (C, F) females only n=6-10 per group. Genotype effect in brain weight between WT and 5xFAD*Tg30 animals and genotype effect in tibialis anterior weight between WT and 5xFAD*Tg30 and WT and 5xFAD*Tg30*Hsp72Tg. One-way repeated measures ANOVA *p = <0.05 **p = <0.01 ***p= <0.001. Graphs indicate mean ± SEM*

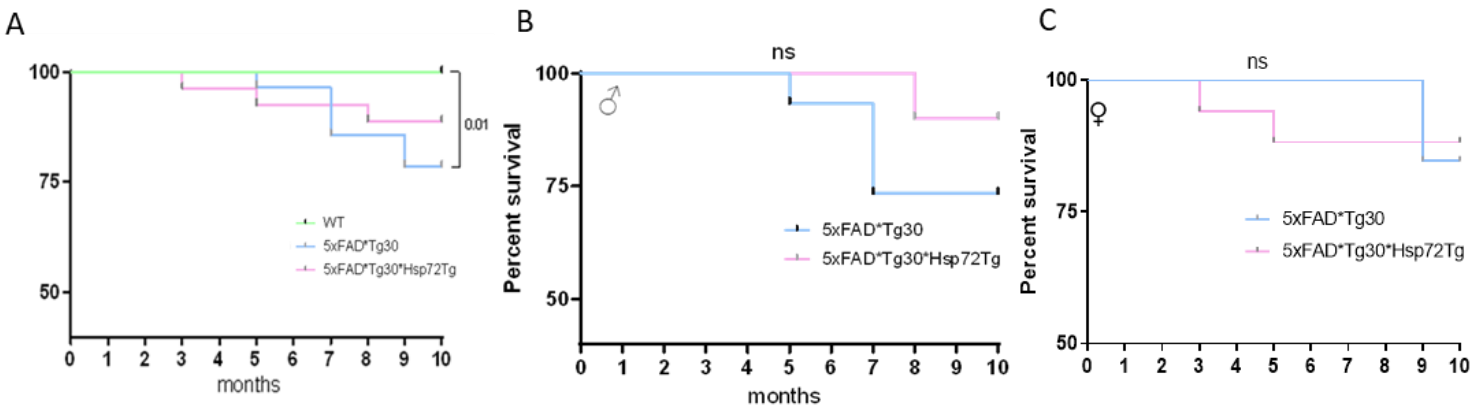

Figure 3.16 ***Decreased survival in5xFAD*Tg30mice Kaplan–Meier survival curves***. *(A) Decreased survival of 5xFAD*Tg30 mice compared to WT n=24-28 per group. (B) No genotype effect between 5xFAD*Tg30 and 5xFADTg30*Hsp72 animals, males only n=10-15 per group. (C) No genotype effect between 5xFAD*Tg30 and 5xFAD*Tg30*Hsp72Tg animals, females only n=13-17 per group. The statistical difference was evaluated by a Gehan Breslow Wilcoxon test*

3.4 Conclusions

Hsp72, a protein implicated in AD, is now a potential target for therapeutic treatment of neurodegenerative diseases. Previous research into Hsp72 overexpression found protective treatment effects; effectively protecting neurons from intracellular accumulation of Aβ through promoting the clearance of Aβ (Hoshino 2011) and promoting tau homeostasis (Dou, 2003; Shimura, 2004; Petrucelli, 2004; Jinwal, 2010; Miyata, 2011; Wang, 2010).

This study was aimed at overexpressing Hsp72 genetically, driving elevated levels in the brain. Further, we aimed to determine the effects of this overexpression on the behavioural and metabolic phenotype of the *5xFAD*Tg30* mouse model of AD. Using transgenic overexpression, we confirmed Hsp72 overexpression in the brain via western blotting analysis **(Figure 3.1)**.

Behaviourally, Hsp70 mRNA and protein has been found to increase following learning (Porto, 2018) and overexpression has been shown to prevent memory decline induced by surgery under general anaesthesia in mice (Vizcaychipi, 2011). Results from this chapter indicated that Hsp72 Tg overexpression could not ameliorate any memory or learning deficits in *5xFAD*Tg30* mice, however, evidence was found to suggest a behavioural effect in fear and reasoning. In the elevated plus maze performance, *5xFAD*Tg30*Hsp72 Tg* mice had a significantly lower risk performance compared to *5xFAD*Tg30* **(Figure 3.8)**. This could suggest that Hsp72 overexpression improved the ability for *5xFAD*Tg30* mice to recognise when they are in vulnerable situations and therefore remove themselves from danger. It must also be taken into consideration the inference of each experiment- primarily, does risk taking behaviour relate to exploratory behaviour?

Should we be associating the NOR experiment with risk taking too; rather than testing memory, could it also infer the readiness to risk seeking an unknown object. It is clear that the exact relationship between Hsp72 expression and learning/memory has yet to be elucidated, as contrasting studies have shown Hsp72 levels are lower in DBA mice that had learned a radial maze, unchanged in C57Bl6 mice after learning the maze (Ambrosini, 2005), but increased (Hsp cognate) in rats learning the Morris water maze (Pizarro, 2003). This chapters' Cheeseboard maze results saw no Hsp72 effect.

Interestingly, brain weight trended to improve with Hsp72 overexpression (specifically in the males, p=0.1) which could indicate protection against neuronal loss. Since Hsp72 has been shown to protect against neuronal apoptosis (Mailhos 1994), this slight improvement cannot be ruled out. There were no significant differences in survival rate, despite previous correlations with Hsp72 and longer lifespan (Salway, 2011). While statistically, there were no differences, considering the raw values, there is an impressive trend to suggest that Hsp72 overexpression extended survival- 6 out of 28 *5xFAD*Tg30* animals died prematurely compared to 3 out of 27 *5xFAD*Tg30*Hsp72Tg* **(Figure 3.16, p=0.2)**.

Previous data had demonstrated superior running performance in Hsp72 Tg mice, which coincided with an increase in VO_2 and mitochondria number (Henstridge et.al 2014). Hsp72 overexpression has also been shown to improve rotarod performance in a cerebral ischemic model (Xu, 2011). Since Hsp72 Tg mice also overexpress Hsp72 in the skeletal muscle alongside the brain (Marshall, 2018), one of this chapter's assessments was if Hsp72 Tg could ameliorate motor deficits as seen in the *5xFAD*Tg30* mouse model. This

study did not find any difference in rotarod or hangwire performance with Hsp72 Tg overexpression **(Figure 3.4)**. There was, however, slight genotype effects on VO_2 consumption and meters travelled (**Figure 3.13 and 3.14 I)**. Despite not ameliorating gross motor strength, there appeared to be a potential improvement in maintenance of lean muscle mass for male *5xFAD*Tg30*Hsp72 Tg* mice, who showed a significantly higher lean muscle mass towards their end of life compared to *5xFAD*Tg30* mice **(Figure 3.11 E)**. No other body composition data were affected. The slight preservation of muscle mass could be in support of a data shown by Gehrig and colleagues, demonstrating Hsp72 overexpression decreases muscle breakdown (Gehrig et.al 2012). While promising results were demonstrated by Gehrig and colleagues (Gehrig et.al 2012) regarding Hsp72 overexpression in a model of Duschenne muscular dystrophy (DMD), it is important to note the methods of this publication. Gehrig and colleagues used the *dmx* model of (DMD), which portrays a mild phenotype. The *5xFAD*Tg30* model, as previously demonstrated displays a much more severe motor phenotype which perhaps was too severe to show a similar rescue with Hsp72 overexpression. Additionally, Gehrig's publication used animals at 5 and 12 weeks of age, which are difficult to compare with the *5xFAD*Tg30* model, as they were aged to up to 10 months. Further to this, when Kennedy and colleagues repeated this experiment in older *dmx* animals, results could not be replicated (Kennedy et.al 2016).

Hsp72 Tg studies have shown mice are protected from HFD-induced obesity and insulin resistance, however, intriguingly even on a NC diet, Hsp72 Tg mice showed enhanced glucose tolerance (Henstridge et.al 2014). This was unaltered between *5xFAD*Tg30* and *5xFAD*Tg30*Hsp72 Tg*.

Chapter 3 aimed to investigate the behavioural and metabolic effects of Hsp72 overexpression on the AD mouse model, *5xFAD*Tg30*. We found Hsp72 overexpression improved the cognitive ability to recognise dangerous or vulnerable positions. We demonstrated lean mass in males was maintained with Hsp72 Tg overexpression in the later stages of life, as well as significantly lowering body mass and lean mass adjusted VO_2 during small periods of the dark cycle. We also found a significant genotype difference in all meters travelled during the dark cycle between WT and *5xFAD*Tg30*Hsp72 Tg*. Interestingly, in males, both brain weight and survival trended to improve with Hsp72 Tg overexpression, however, neither reached significance.

Chapter 4 aims to investigate targeting Hsp72 via the use of a co-activator of Hsp72, the compound BGP-15. While Hsp72 transgenic overexpression improved some, but not all, phenotypic traits in the *5xFAD*Tg30* mice, pharmacological intervention with an Hsp72 co-inducer that also targets multiple other pathways related to AD, may be sufficient to provide additional benefits.

4 The effect of Hsp72 co-inducing compound, BGP-15 on the *5xFAD*Tg30* mouse model of AD

Preface

The primary aim of *Chapter 4* was to determine whether BGP-15 treatment improves the phenotypic traits observed in the *5xFAD*Tg30* mice. Secondly, from observations made during the studies from *Chapter 2* and *Chapter 3*, we assessed the *5xFAD*Tg30* mice for epilepsy-like traits. The prevalence of epilepsy in patients with AD is 10-fold higher than the age-matched general population, and up to 64% of AD patients will develop at least one unprovoked seizure (Hauser 1986; Risse 1990). While handling and observing the *5xFAD*Tg30* animals in the previously conducted studies, it was noticed that some mice would display tremor-like movements. Potentially, this was a cause of the observed sudden and unexpectant death in the model. Consequently, an additional cohort of *5xFAD*Tg30* mice were generated to assess whether these animals exhibit spontaneous seizures and characterise this susceptibility. Despite glaring statistics, there is little known about the biological mechanisms associated with AD which might create such a vulnerability to epilepsy, nor are there any anti-epileptic treatments which are specific for epilepsy in AD. A sub-cohort of animals were also treated with BGP-15, to assess if this drug could have any effects on their seizure susceptibility and was conducted as a separate study to the rest of the data seen in *Chapter 4*.

4.1 Introduction

Despite over 400 clinical trials that have been conducted for the treatment of AD (King, 2018), there has yet to be a drug found both efficacious and/or safe. The neuroprotective effects of Hsp72 due to the initiation of Aβ clearance and the anti-aggregation of tau both *in vitro,* as well as the cognitive rescue effects *in vivo* begin to suggest that inducers of Hsp72 may be a potential therapeutic target in the treatment of AD.

BGP-15, originally utilised as an insulin sensitising drug, increases HSP induction via inhibiting the acetylation of heat shock factor 1, prolonging the duration of it binding to heat shock elements activating Hsp72 (Gombos et al. 2011). Despite its initial use as an Hsp72 co-inducer, it is now well known to be a multi-action drug, inhibiting the HDAC and PARP-1 pathways as well as increasing the IGF-1 receptor (Szabados 2000; Budzynski 2017; Sapra 2014). A recent review concluded that while multiple groups around the world are investigating this molecule, the exact mechanisms of its effects are still quite unknown (Peto, 2020). Other mechanisms of effects discovered have been blocking JNK, increasing insulin sensitivity and remodelling lipid rafts increasing membrane fluidity and therefore cellular stress response potential (Sarszegi et.al 2012; Literati-Nagy et.al 2009; Gombos et.al 2011).

Due to its multi-modal nature, its potential for multiple effects on disease models is appreciable. BGP-15 shows several beneficial cardiovascular effects, including cardioprotective effects on ischemic heart disease (Szabados, 2000) and repairing diastolic dysfunction in diabetic cardiomyopathy (Bombicz, 2019). Additionally, it has been found to protect against heart failure and atrial fibrillation, but interestingly, protects independently of Hsp72 (Sapra, 2014). Other disease models that have seen protective effects with BGP-15 treatment include DMD (Gehrig 2012; Kennedy 2016), liver injury

(Nagy 2010), skin injury (Farkas 2002), traumatic brain injury (Eroglu, 2014) and gynaecological diseases such as Polycystic Ovarian Syndrome (Takahashi, 2017).

While BGP-15 has not been used in the space of AD therapy, it is a derivative of a similar compound called Arimoclomol, which has been previously shown successful results in ALS pre-clinical research (Kieran *et.al* 2004) as well as shown to be a potential therapy clinically (Lanka *et.al* 2009), thus supporting the principle of Hsp72 co-inducers having therapeutic relevance on neurodegenerative diseases more broadly. Additionally, it has a promising potential due to its multiple mechanisms of effect that have links to AD, as well as prior evidence that BGP-15 treatment has the potential to help promote the survival or neurons (Eroglu 2014). As a complex disease, with a multitude of pathways affected, it is reasonable to assume that a drug that similarly targets multiple mechanisms may be required. Many pathways that have been shown to be altered via BGP-15 are implicated in AD progression. Not only is Hsp72 (the interest of this thesis) affected by both BGP-15 and AD, so too HDAC, PARP-1, JNK, IGF-1. The potential for BGP-15 to play a protective role in AD via the Hsp72 pathway or its various other mechanisms of action is of great interest. Hence, this chapter aims to investigate the effects of BGP-15 on the progression of the AD mouse model, *5xFAD*Tg30.*

4.2 Materials and methods

4.2.1 Generation of 5xFAD*Tg30 mice

All activities involving the use of animals for research were approved by the Alfred Medical Research Education Precinct Animal Ethics Committee (AMREP AEC) and conducted according to the guidelines of the National Health and Medical Research Council of Australia for animal experimentation. *5xFAD* and *Tg30* animals were crossed to produce the double transgenic, *5xFAD*Tg30* as described in Heraud et.al 2014 and as in *Chapter 2.* Mice were genotyped from tail samples performed by Transnetyx (TN, USA) using real-time PCR. WT animals were littermate controls **(See Supp 4-6 for animal flow charts)**. At 6 months of age, animals were relocated to Florey Institute of Neuroscience and Mental Health (Melbourne, Australia) for behavioural tests, with a one-month familiarisation period before initiation.

4.2.2 Use of BGP-15

BGP-15 was administered via drinking water (100mg/kg/day) in a randomised design. The quantity of drug was calculated and drinking water changed on a weekly basis which was determined by the average weight of mice and quantity of water consumed per cage. Animals were split into cages determined by genotype to account for large differences in body mass (and associated water intake) we had observed in our initial pilot study between WT and 5xFAD*Tg30 mice to allow for correct administration of compound. However, the investigator was blinded at all times to which treatment the mice were on.

4.2.3 Behavioural Characterisation

To keep experimental consistency, the battery of behavioural tests were similar to *Chapter 2* and *Chapter 3*, with slight alterations with the added experiments of DigiGait and seizure monitoring for a separate cohort. An updated timeline describing the procedures is presented below.

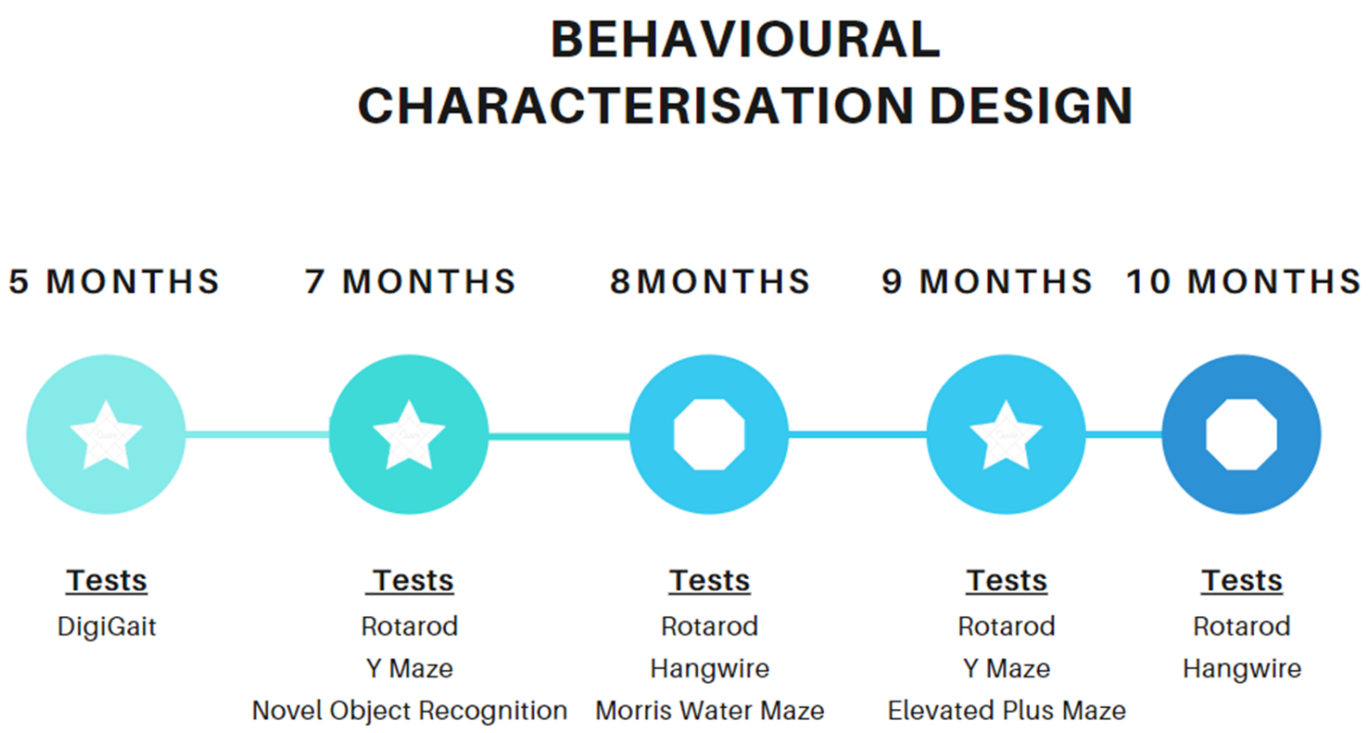

Figure 4.i *Behavioural characterisation timeline design.* *A comprehensive battery of behavioural tests was performed at 7, 8, 9 and 10 months of age. At 5 months of age, animals were tested on a DigiGait analysis machine, before being transported to the Florey Neuroscience Institute at 6 months, with 1-month acclimatisation period.*

4.2.4 DigiGait

To assess the manner of walking and to determine subtle disturbances in gait, the DigiGait analysis system was utilised (Mouse Specifics Inc, MA USA).

For tests, each mouse was placed into a Perspex chamber that is fitted on to a transparent treadmill. The treadmill was run at 10cm/sec for a short period of time in order to get acceptable video footage of 3-8 seconds. Images were collected at 157 frames per second and stored in audio video interleaved format. Acceptable footage meant that all four paws remained within frame for the duration and that the mouse did not hit the back bumper. Mice that were unable to walk at 10cm/sec without hitting the back bumper were excluded, following 3 attempts. Data taken from the Digigait videos are edited using data analysis software to ensure that each recorded foot placement is indeed a true placement. The data analysis software then takes this corrected step data to produce time and spatial parameters for each paw. The software is used to analyse each video and determine a host of spatial and temporal gait indices for each limb, including the stance and swing components of stride as well as stride length, duration and frequency.

4.2.5 Seizure study

At 6 months of age, a separate cohort of animals were taken to the Monash Neuroscience facility within AMREP to measure the difference in kindling rate between *5xFAD*Tg30*, *5xFAD*Tg30* treated with BGP-15 and WT mice by comparing the number of kindling stimulations that triggered the first class V seizure.

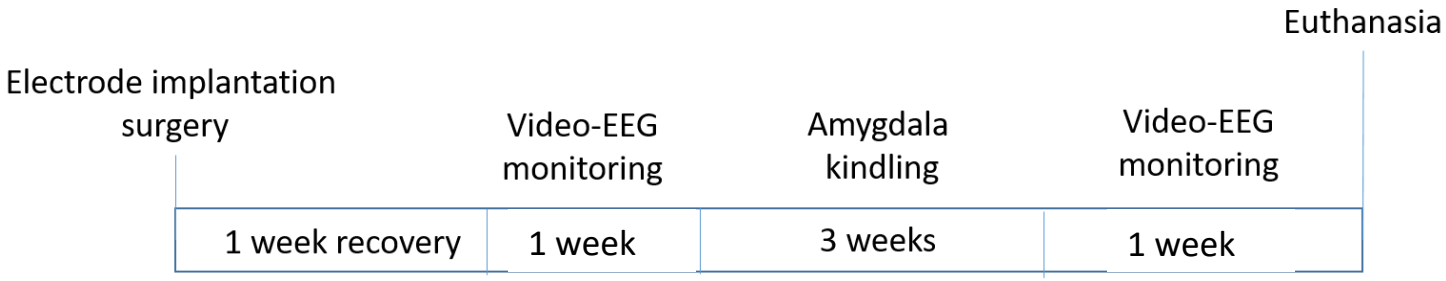

Figure 4.ii *Seizure study timeline design.* *At 6 months of age, animals underwent electrode implantation surgery before 1-week recovery and video monitoring for 1 week. Electrical stimulation via amygdala kindling was performed daily for 3 weeks, with another week of monitoring post kindling, before euthanasia.*

Surgical Implantation

Surgical implantation of stimulating and recording electrodes facilitates the stimulation of the brain to trigger seizures.

Animals were given Buprenorphine (0.05mg/kg) and carprofen (5mg/kg) before induction of anaesthesia then fur clipped and skin disinfected. A midline incision through the skin is made to expose the top of the skull between lambda and bregma (suture lines on skull). The surface of the skull is cleaned using the sharp edge of a scalpel blade and then lightly swabbed with sodium peroxide to remove any fat on the surface of the skull. 1mm holes are drilled through the skull at the locations where the electrodes will be implanted. These correspond to regions above the left amygdala and right hippocampus, as well as two holes over the cerebellum. Stainless steel electrodes are then gently lowered into the brain through the holes to reside in the appropriate locations. Two stainless steel screw electrodes are placed into the cerebellum holes to act as reference and ground electrodes. Electrodes are connected to an electrical connector socket, and the whole exposed area of the skull and wires are then covered in dental cement to ensure the structural integrity of the electrodes.

Kindling

Kindling is a process whereby repeated electrical stimulation of the brain results in increasingly severe seizures.

Animals were connected to the stimulator and EEG amplifier using cables linking the headpiece to a computer. Electrical stimulation of the brain occurs using a 200uA stimulus of 1 second duration with a frequency of 60Hz. Initially this triggers a sub

convulsive seizure, only detectable from view of the EEG. Animals are then returned to their home cages for 24 hours. During this period, they undergo video-EEG monitoring.

This process is repeated 5 days a week for 3 weeks (total of 15 stimulations). As the number of stimulations increase, animals should start to experience mild convulsive (partial) seizures which increase in duration. At the end of the experiment, animals are normally experiencing convulsive seizures lasting ~1 minute. This is referred to as 'kindling' and represents the transition of a normal brain into an epileptic brain.

This is quantified by two measures: increasing duration of each seizure and the severity of each seizure, as scored using the Racine scale (Racine, 1972). During each rest period, animals are continuously monitored for any spontaneous seizures which might occur, or other epileptiform abnormalities in the EEG. If an animal experiences 5 consecutive convulsive seizures as a result of the stimulation, they have reached the end-stage of kindling, and receive no more stimulations. Alternatively, once the 15 stimulations have occurred, the procedure is complete.

Video-EEG monitoring

During the whole experimental period animals are video recorded to document any spontaneously occurring seizures (as opposed to those triggered by electrical stimulation) which are determined by offline review of the recordings. This procedure is conducted for 5 consecutive weeks – one week prior to the onset of kindling, then continues for the 3-week period of kindling whenever the mice are not being stimulated, followed by another week period occurring after the completion of kindling.

4.2.6 Metabolic characterisation

To assess the effects of BGP-15 on the baseline metabolic results of *5xFAD*Tg30* animals as seen in *Chapter 2*, the same battery of metabolic assessments was performed. The timeline for the metabolic characterisation was as per *Chapter 2*.

4.2.7 Seahorse Analysis

To assess mitochondrial metabolism in neurons in response to BGP-15, we utilised the Seahorse XF96 Analyser (Agilent, CA USA) which allows real-time measures of oxygen consumption and glycolysis. Glycolysis was assessed via analysing extracellular acidification rate (ECAR) and mitochondrial oxygen consumption via oxygen consumption rate (OCR), on live primary neuronal cells derived from mice at a density of 75,000 cells per well.

Cells were exposed to a series of mitochondrial agents. Oligomycin inhibits ATP synthase to decrease OCR and can be used to assess ATP-linked respiration. 2-[2-[4-(trifluoromethoxy)phenyl]hydrazinylidene]-propanedinitrile (FCCP) is an uncoupling agent that disrupts the mitochondrial membrane potential, resulting in the electron flow through the electron transport chain (ETC) being uninhibited and being able to achieve maximal respiration. This also allows for the calculation of the spare capacity- the OCR between basal and maximal OCR. Finally, Rotenone and Antimycin are Complex 1 and 3 inhibitors, respectively, which shuts down mitochondrial respiration.

Additionally, the extracellular acidification rate (ECAR) was directly measured, with different doses of BGP-15. Briefly, the conversion of glucose to pyruvate, then on to lactate in the cytoplasm causes an increase of protons in the extracellular medium. This results in the acidification of the medium surrounding the cell.

Glucose induces glycolysis, increasing the ECAR- this induced response is relative to the cells' basal glycolysis rate. Oligomycin inhibits mitochondrial ATP production, shifting all energy production into glycolysis, further increasing ECAR. The final injection of 2-

deoxy-glucose completely inhibits glycolysis through the competitive binding with glucose hexokinase. This acts as a confirmation that ECAR produced is from glycolysis.

OCR Media

Seahorse base media was prepared with 2mM glutamine, 1mM sodium pyruvate and 25mM glucose. It was then warmed to 37˚C, pH adjusted to 7.4 then sterilised using 0.22uM filter.

The XF 96 calibrant plate was prepared with 200 µL of calibrant and placed in a non-CO_2 incubator overnight.

OCR experiment

Briefly, primary cells were used and measurements of oxygen consumption were made continuously and averaged over a period of three minutes. Cells were initially treated with BGP-15 at varying doses (5µM, 50µM and 500µM) and incubated at room temperature for 1 hr. After incubation, cells were sequentially treated with 1.5 µM oligomycin (ATP synthase inhibitor), FCCP (0.75µM) (Carbonyl cyanide-4 (trifluoromethoxy) phenylhydrazone; an uncoupling agent), and 0.5 µM rotenone/antimycin A (inhibitors of complex I/III of the ETC).

Glycolytic capacity test media

Seahorse base media was prepared with 2mM glutamine and warmed to 37˚C, pH adjusted to 7.4 and sterilised using a 0.22µM filter.

For Glycolysis

Briefly, primary cells were used and measurements of extracellular acidification were made continuously and averaged over a period of three minutes while cells were sequentially treated with 10µM glucose, 1µM oligomycin (ATP synthase inhibitor) and 50mM 2-deoxy-glucose.

Cells used were primary neuronal cells, received 24 hours after culture and used at 7-14 days in culture. Cells were prepared as per Ray *et.al* 2011. Briefly, neurons from individual pups were maintained in Neurobasal medium (Gibco) containing 10% fetal calf serum, at 37°C in humidified air containing 5% CO2. The culture medium was replaced with serum- and glutamic acid-free culture medium after 24 hours.

4.2.8 Measuring BGP-15

The measuring of BGP-15 was conducted by Dr. Phil Wright at the Monash Institute of Pharmaceutical Sciences

Bioanalytical Method Summary

LC-MS analysis was performed on a Shimadzu 8030 triple quadrupole instrument coupled with a Shimadzu Nexera UHPLC. MS analysis was conducted in positive mode electrospray ionisation and quantitation of the analytes performed in MRM mode. Table A1 details the MS acquisition parameters and LC retention times. Representative chromatograms are provided in Figures A1 and A2. The column employed was a Phenomenex Kinetex EVO C18 column (2.6 µm particle size, 50 x 2.1 mm i.d.) equipped with a Phenomenex Security Guard column with C18 packing material. The column was maintained at 40°C. The mobile phase consisted of 10mM ammonium acetate in water (pH adjusted to 9.5) (Mobile Phase A) and 100% acetonitrile (Mobile Phase B). Separations were conducted using a flow rate of 0.4 mL/min and an injection volume of 3 µL. Samples were controlled in the autosampler at a temperature of 10ºC.

Standard and Sample Preparation

Extraction of the BGP-15 from plasma was conducted using protein precipitation with acetonitrile (3-fold volume ratio). Plasma standards were freshly prepared on the day of analysis with the calibration curve comprising at least 10 different analyte concentrations. Solution standards were diluted from the stock solution (5mg/mL in methanol) with 50% acetonitrile in water. Plasma standards were prepared by spiking blank mouse plasma (provided by the Garvan Institute, 20µL) with solution standards (4µL) before protein precipitation by the addition of 100% acetonitrile (containing internal standard; diazepam, 0.025µg/mL). Standards were then vortexed and centrifuged (10,000 rpm, 3mins). The supernatant was subsequently separated, transferred to a HPLC vial and injected for LC-MS analysis. Plasma samples were similarly prepared except blank 50% acetonitrile in water (4µL) was added instead of the solution standard.

Assay Validation and Quality Control

Validation of the bioanalytical assay was conducted to support discovery stage sample analysis. The plasma assay was assessed with respect to calibration range, linearity, accuracy, precision, extraction efficiency and matrix effect. The accuracy, precision, extraction efficiency and matrix effect of the assay were evaluated at nominal concentrations of 10, 50, 100 and 500 ng/mL. Quantification was performed using an external standard method as the response for the internal standard differed from standards to samples. Quality Control (QC) samples were analysed as part of the batch analysis and were conducted at nominal concentrations of 50, 100 and 500 ng/mL.

4.3 Results

4.3.1 Measuring BGP-15 in plasma and the brain and protein expression

We first quantified the plasma and brain concentration of BGP-15 after 8 months of treatment.

At 10 months of age, the plasma concentration of BGP-15 was elevated in both WT and *5xFAD*Tg30* animals administered BGP-15 **(Image 4.1A)**.

Next, the concentration of BGP-15 in the brain was assessed. At 10 months, significant levels of BGP-15 were found in the brain of both WT and *5xFAD*Tg30* animals **(Image 4.B)**. Similarly, to plasma concentrations, brain concentrations of BGP-15 saw no genotype effect, suggesting there were no significant effects of overall brain health on concentration levels. While the differences were not significant, BGP-15 concentration did trend to be lower in in *5xFAD*Tg30* mice for both plasma and brain perhaps reflecting the decreased size of the mice.

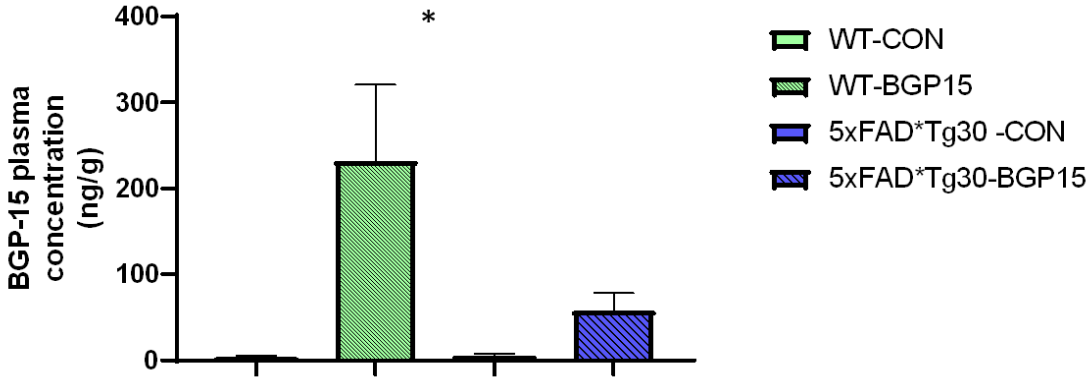

Figure 4.1A Plasma BGP-15 concentration (ng/g). BGP-15 concentration in the plasma of WT and *5xFAD*Tg30* animals on long-term BGP-15 or saline vehicle treatment. Graph represents mean ± SEM. N= 4-6 per group *p>0.05 for drug effect 2-way ANOVA

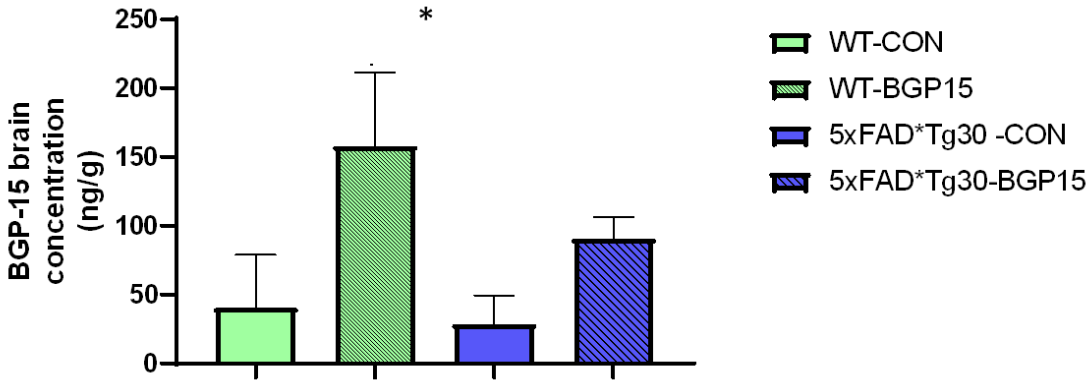

Figure 4.1B Brain BGP-15 concentration (ng/g). BGP-15 concentration in the brains of WT and *5xFAD*Tg30* animals on long-term BGP-15 or saline vehicle treatment. Graph represents mean ± SEM. N= 4-6 per group *p>0.05 for drug effect 2-way ANOVA

To assess if long-term administration of BGP-15 co-induces Hsp72 overexpression in the brain, 10-month-old animals were culled, and brain regions dissected into hippocampus and cerebellum for western blot analysis. Protein expression of Hsp72 did not significantly increase with BGP-15 treatment, in either WT-control animals or *5xFAD*Tg30* treated animals **(Figure 4.1C)**. As BGP-15 is known to be a 'co-inducer', it is thought that cellular stress (such as the environment from AD pathology) is a requirement for BGP-15 to induce Hsp72. So, while we were not necessarily expecting an increase in WT mice, we were hypothesizing that the pathology of the brain in the AD model would provide sufficient conditions to induce Hsp72 with BGP-15 treatment.

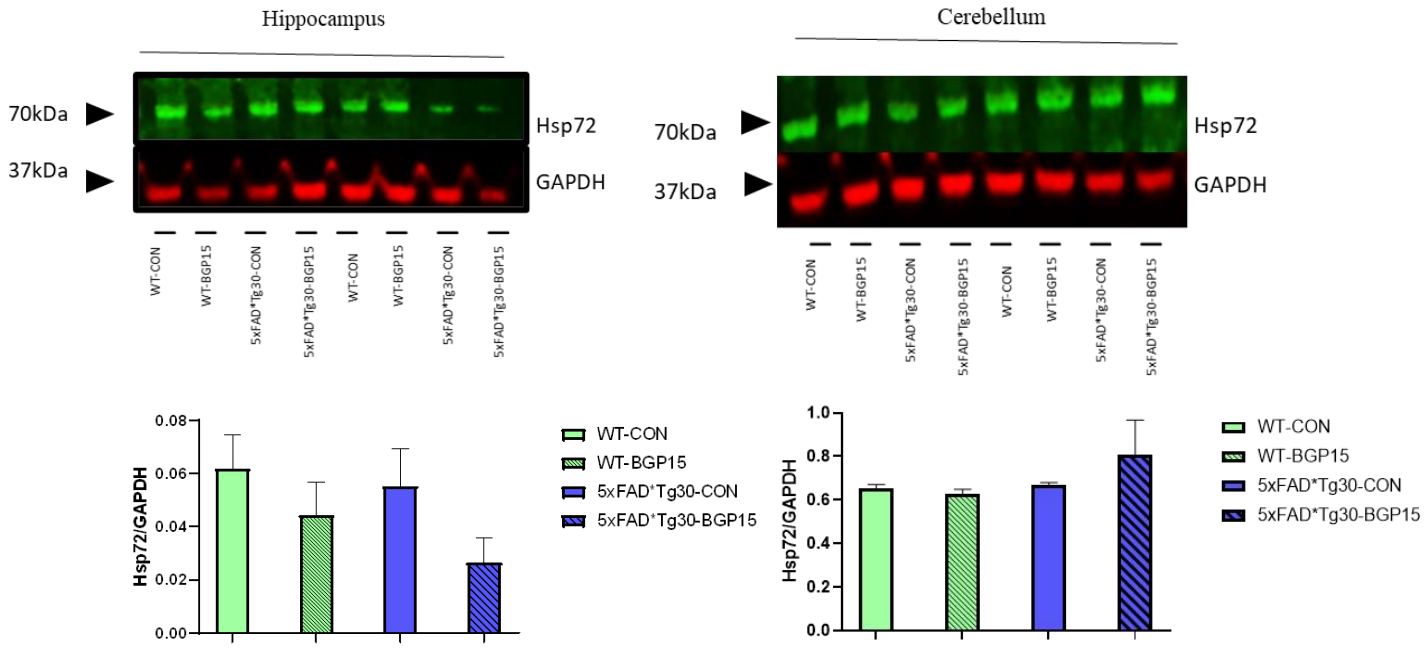

Figure 4.1C ***Hsp72 protein expression.*** *Representative western blots, Hsp72 in the 5xFAD*Tg30 mouse model, after long-term BGP-15 administration. Brain was harvested at 10 months and dissected into hippocampus and cerebellum. Quantification performed using GAPDH as loading control. Graph indicates mean ± SEM. N=4 per group, 2-way ANOVA*

It is important to note at this point the relevance of this western blot result. The initial aim of this chapter, and indeed the thesis, is to investigate the effects of Hsp72 overexpression in the brain and its effects on whole body phenotype and behaviour. In this chapter, the effects of Hsp72 was to be explored via its co-induction with BGP-15 treatment. However, despite the result of BGP-15 not significantly inducing overexpression of Hsp72 in the brain, BGP-15 still has an interesting therapeutic potential, due to its other mechanisms of actions, as mentioned in *Chapter 1*. Briefly, this includes the inhibition of PARP-1 and HDAC's and the suppression of inflammatory markers such as JNK and TNF-α.

The protein expression of APP was significantly increased in the hippocampus of 5xFAD*Tg30 mice compared to WT-control **(Figure 4.2)**. BGP-15 treatment did not significantly affect APP protein expression, although trended to reduce its expression in the hippocampus. Similarly, to *Chapter 3,* expression of APP was not elevated in the cerebellum of *5xFAD*Tg30* animals and BGP-15 had no effect on protein levels.

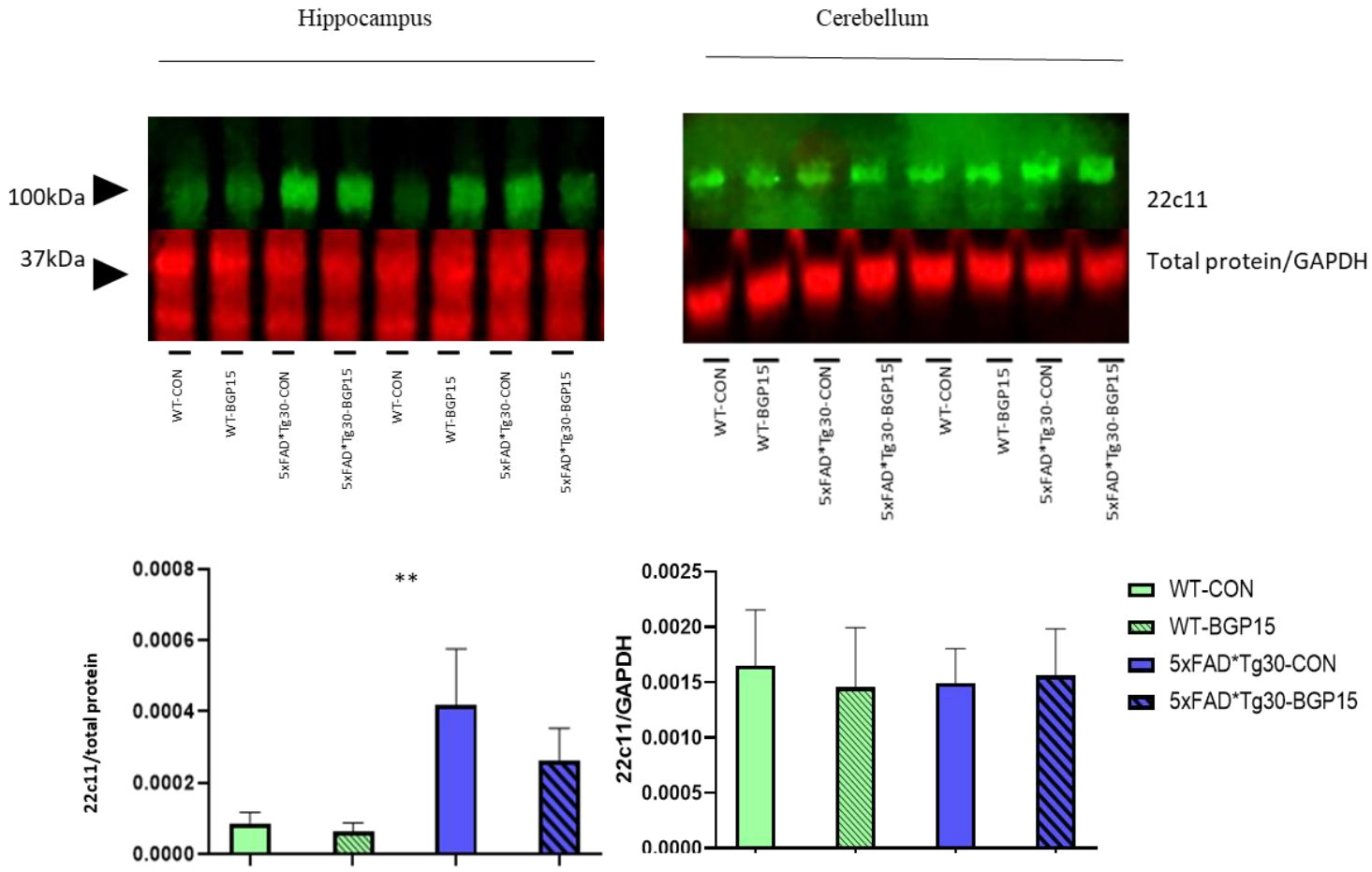

Figure 4.2 ***APP protein expression levels.*** *Representative western blots, measuring protein expression levels of APP in hippocampus and cerebellum of 5xFAD*Tg30 mice treated and untreated with BGP-15. Brain was harvested at 10 months and dissected into hippocampus and cerebellum. Significant expression levels in the hippocampus of 5xFAD*Tg30 animals compared to WT-control. BGP-15 trended to reduce APP levels but did not reach significance. Expression normalised to total protein. No overexpression of APP in the cerebellum of 5xFAD*Tg30 and no effect of BGP-15. Quantification performed using GAPDH or total protein as loading control. Graph indicates mean ± SEM. **p<0.01 2-way for genotype effect. ANOVA, n=4 per group*

Protein expression of human tau was significantly increased in 5xFAD*Tg30 animals, in both the hippocampus and cerebellum regions of the brain **(Figure 4.3)** reproducing our findings from *Chapter3*. There was no effect of BGP-15 on tau protein levels.

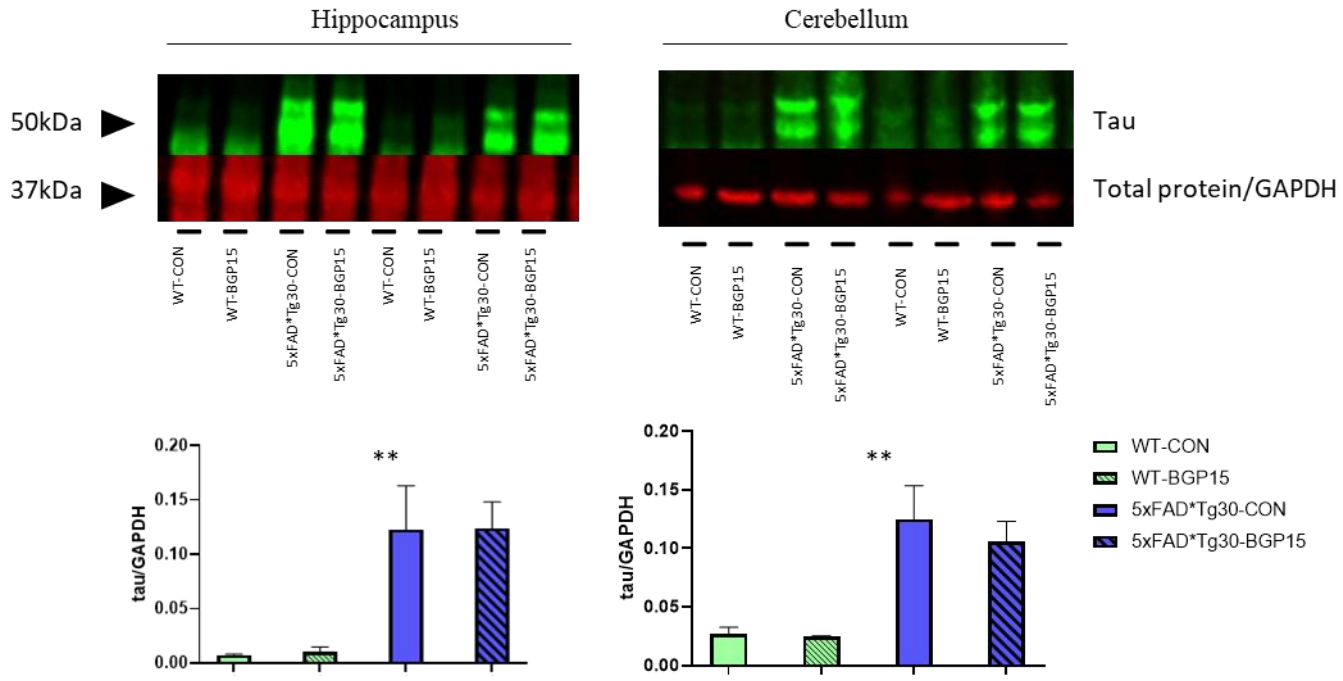

Figure 4.3 ***Human tau protein expression levels.*** *Representative western blots, measuring protein expression levels of tau in hippocampus and cerebellum of 5xFAD*Tg30 mice treated with or without BGP-15. Brain was harvested at 10 months and dissected into hippocampus and cerebellum. Significant expression levels in both the hippocampus and cerebellum of 5xFAD*Tg30 animals compared to WT-control. No effect of BGP-15 on expression of tau. Expression normalised to total protein or GAPDH. Graph indicates mean ± SEM. **p<0.01 for genotype effect 2-way ANOVA. n=5 per group*

4.3.2 Gross motor strength and control

As mentioned in *Chapter 3,* Hsp72 preserves muscle function and slows progression of a model that phenocopies Duchenne muscular dystrophy (Gehrig, 2012). This paper additionally demonstrated that BGP-15 treatment exhibited the same effects. Hence, gross motor strength and control was assessed through rotarod performance and hangwire testing on *5xFAD*Tg30* mice. Despite Hsp72 Tg overexpression not displaying any phenotype in *Chapter 3,* BGP-15 has had beneficial effects in skeletal muscle previously, so it was assessed if its long-term administration improved rotarod and hangwire performances.

As expected, at 7 months, WT animals had a significantly higher rotarod performance compared to *5xFAD*Tg30,* which continued to diverge until 10 months. By 10months, *5xFAD*Tg30* mice have a severely impacted motor impairment. Animals treated with BGP-15 did not have an improved rotarod performance and followed performances of untreated animals **(Figure 4.4 A-C).**

The hangwire test was performed at 8 and 10 months of age and followed a similar pattern of motor degeneration over time in *5xFAD*Tg30's.* WT animals were, again, significantly unimpaired and the treatment of BGP-15 did not affect either genotypes for their performance **(Figure 4.4 D-F).**

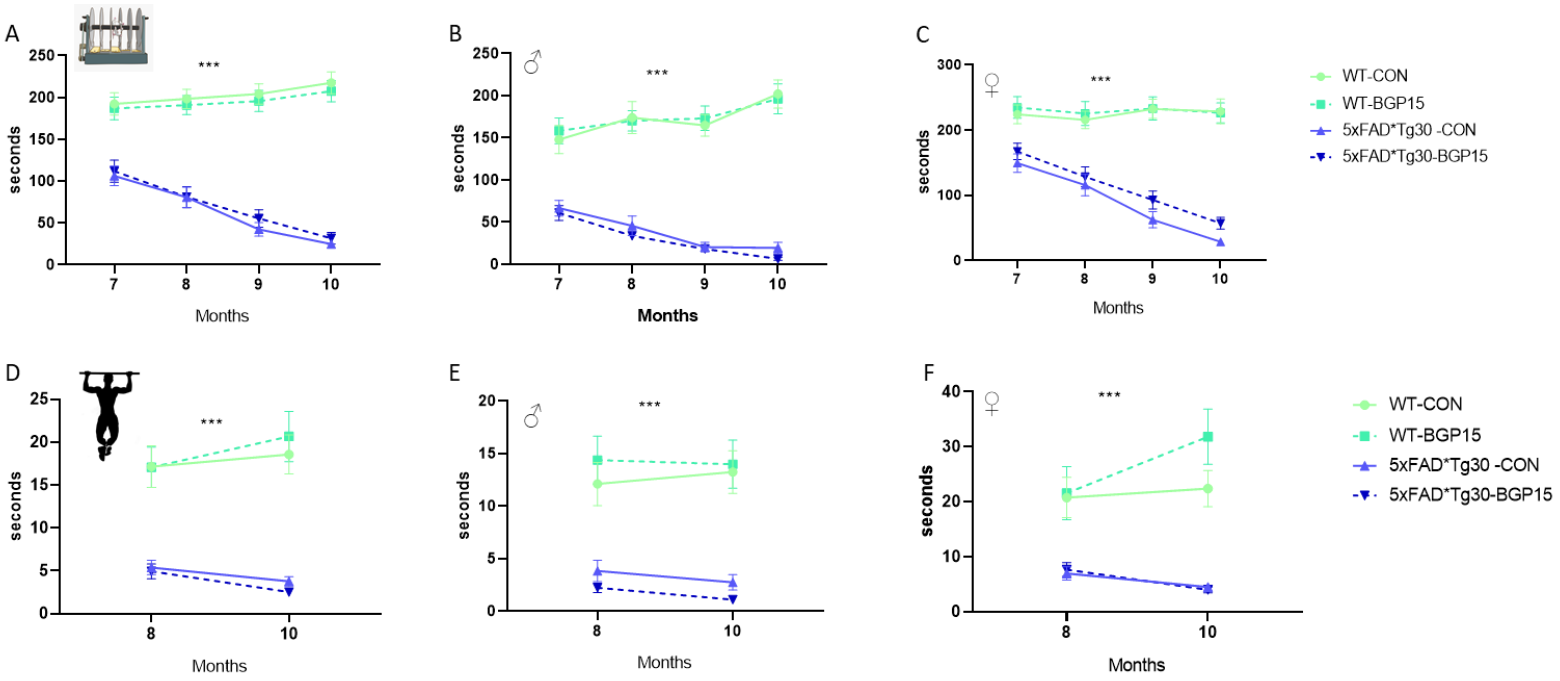

Figure 4.4 ***Measuring gross motor strength and control over time, displayed between 7-10months of age***. *5xFAD*Tg30 animals displayed a significant motor phenotype from 7 months onwards, compared to WT. There was no effect of treatment with BGP-15. Average of three trials per month, latency to fall off. (A) Rotarod Total cohort, n=24-27 per group (B) Rotarod Male animals only, n=10-15 per group (C) Rotarod Female animals only, n=9-14 per group. (D) Hangwire Total cohort, n=24-27 per group (E) Hangwire Male animals only, n=10-15 per group (F) Hangwire Female animals only, n=9-14 per group. Two-way repeated measures ANOVA with Holm-Sidak post-hoc analysis. ***p<0.001 for genotype effect Graph represents Mean ± SEM*

4.3.3 Memory function

Along with the co-induction of Hsp72, BGP-15 has other targets including being a known inhibitor of HDAC's (Budzynski, 2017), which are implicated in AD and memory function. Therefore, it was next assessed if treatment of BGP-15 could improve memory function in *5xFAD*Tg30* animals.

At 7 months, a deficit in memory function could be seen in *5xFAD*Tg30* animals, who spent a significantly reduced amount of time (seconds and % of time) in the *novel* arm compared to WT and their own time in the *familiar* arm **(Figure 4.5).** Females had a more impaired performance whereas males trended to be impaired but did not reach significance. There were no effects of BGP-15 treatment.

At 9 months, female *5xFAD*Tg30* animals continued to show an impaired memory function, compared to WT animals within the *novel* arm, but males did not reach significance **(Figure 4.6)**. However, comparing this to their own durations in the *familiar* arm, it does appear that even the male WT animals are failing to investigate the *novel* arm more often. BGP-15 treatment in females trended to improve time spent in the *novel* arm of the maze compared to untreated *5xFAD*Tg30* females. This may suggest a trend in improved memory function, but this did not reach significance nor increase their time spent in *novel* compared to their time in *familiar* arms.

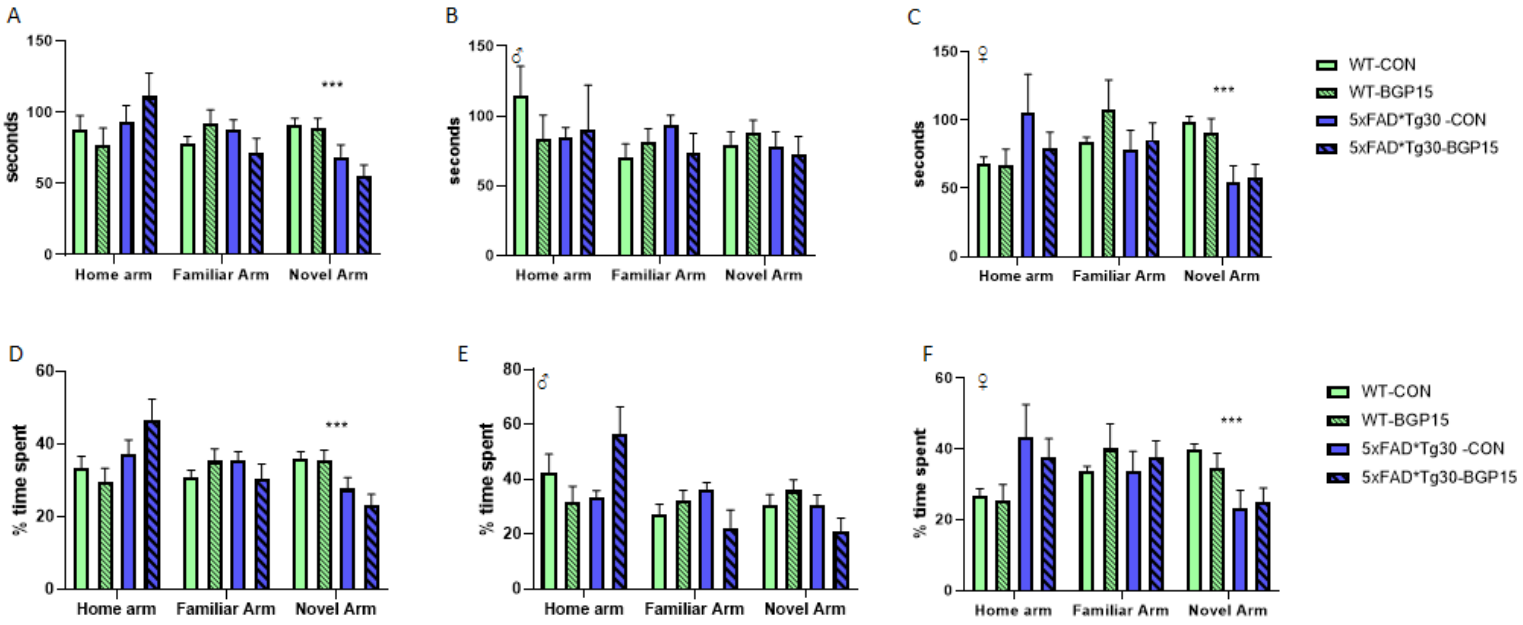

Figure 4.5 ***Duration of overall time and percentage of time spent in each arm of a Y-maze at 7 months of age***. *Animals had 10 minutes familiarisation, before a 5-minute trial, 2 hours later. (A-C) Total time spent. (D-F) % time spent (A) Total cohort, n=23-24 per group (B) Male animals only, n=10-15 per group (C) Female animals only, n=9-15 per group (D) Total cohort, n=23-24 per group (E) Male animals only, n=10-15 per group, (F) Female animals only, n=9-15 per group. WT animals spent significantly (females; trended in males) more time in the Novel arm compared to 5xFAD*Tg30 but BGP-15 did not rescue this memory deficit. 2-way ANOVA was performed in the arm of interest, the Novel arm***p<0.001 for genotype effect Graph represents Mean ± SEM.*

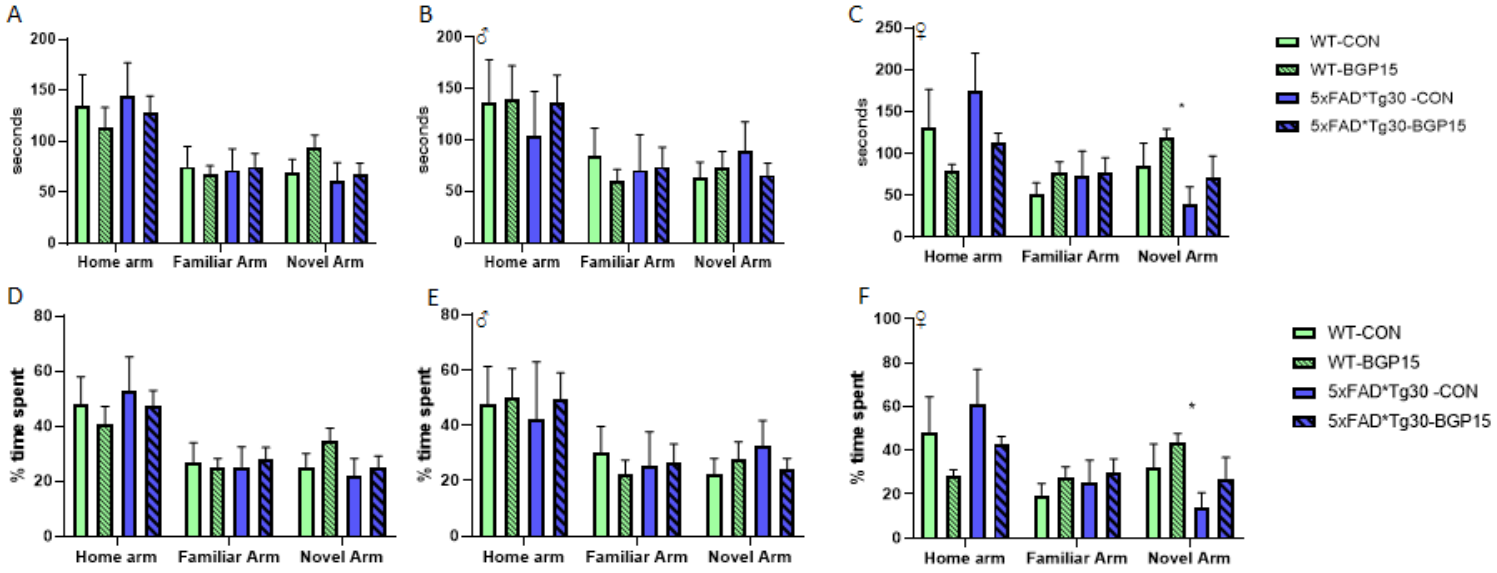

Figure 4.6 ***Duration of overall time and percentage of time spent in each arm of a Y-maze at 9 months of age.*** *Animals had 10 minutes familiarisation, before a 5-minute trial, 2 hours later. (A-C) Total time spent. (D-F) % time spent (A) Total cohort, n=7-9 per group (B) Male animals only, n=3-5 per group (C) Female animals only, n=2-4 per group (D) Total cohort, n=7-9 per group (E) Male animals only, n=3-5 per group, (F) Female animals only, n=2-4 per group. WT animals spent significantly (females) more time in the Novel arm compared to 5xFAD*Tg30 but BGP-15 did not rescue this memory deficit. 2-way ANOVA was performed in the arm of interest, the Novel arm *p<0.05 for genotype effect Graph represents Mean ± SEM*

4.3.4 Anxiety-like behaviour

To assess anxiety-like behaviour with the treatment of BGP-15, the large open field test was performed at 7 months and the elevated plus maze, at 9 months.

At 7 months, a genotype effect could be seen between WT and *5xFAD*Tg30* animals, as well as an effect for the area of maze. While all animals showed preference to *corners, 5xFAD*Tg30* animals spent more time in the *centre* of the maze, compared to WT. The duration and percentage of time were higher for *5xFAD*Tg30* than WT which agreed with results in *Chapter 2* which were not reproduced in *Chapter 3.* There was no effect of BGP-15 **(Figure 4.7).** It is important to note that in this *Chapter,* as well as in *Chapter 2,* tests were conducted at the Florey Institute and *Chapter 3* at the AMREP site, this discrepancy could be a consequence of the different location and/or different equipment utilised. The large open field arena at the Florey Institute was markedly different to the one used at the AMREP site, in terms of size and layout.

At 9 months, *5xFAD*Tg30* mice displayed similar anxiety-like behaviour, spending the most time in the *open* area of the elevated plus maze. Again, there was no effect of BGP-15 **(Figure 4.8)**.

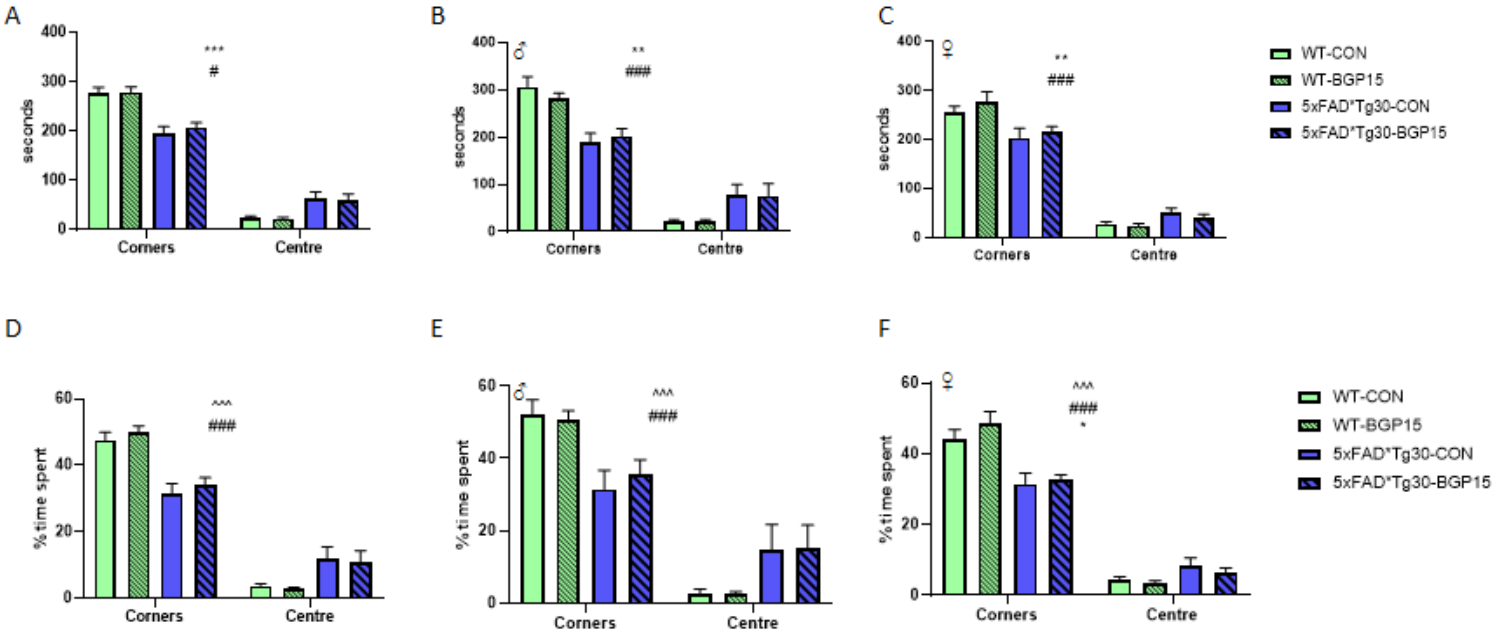

Figure 4.7 ***Anxiety-like behaviour assessed via large open field at 7 months.*** *(A-C) Duration of time spent in areas of a large open field at 7 months of age. Animals had 10 minutes in the arena lit with bright lights, corners and centre of arena tracked (C-D) Percentage of time in areas of an elevated plus maze at 7 months of age. (A,D) Total cohort n= 24-27 per group (B,E) Males only, n=10-15 per groups (C,F) Females only, n=9-14. Area of maze effect, between corners and centre as well as genotype effect between WT and 5xFAD*Tg30. Interaction with genotype and area of maze. Treatment with BGP-15 had no effect. *p<0.05genotype effect **p<0.01 genotype effect ***p<0.001 genotype effect ###p<0.001 area effect ^^^p<0.001 interaction genotype x area. 2-way ANOVA performed in each area. T-test performed between areas for each group. Graph indicates ± SEM*

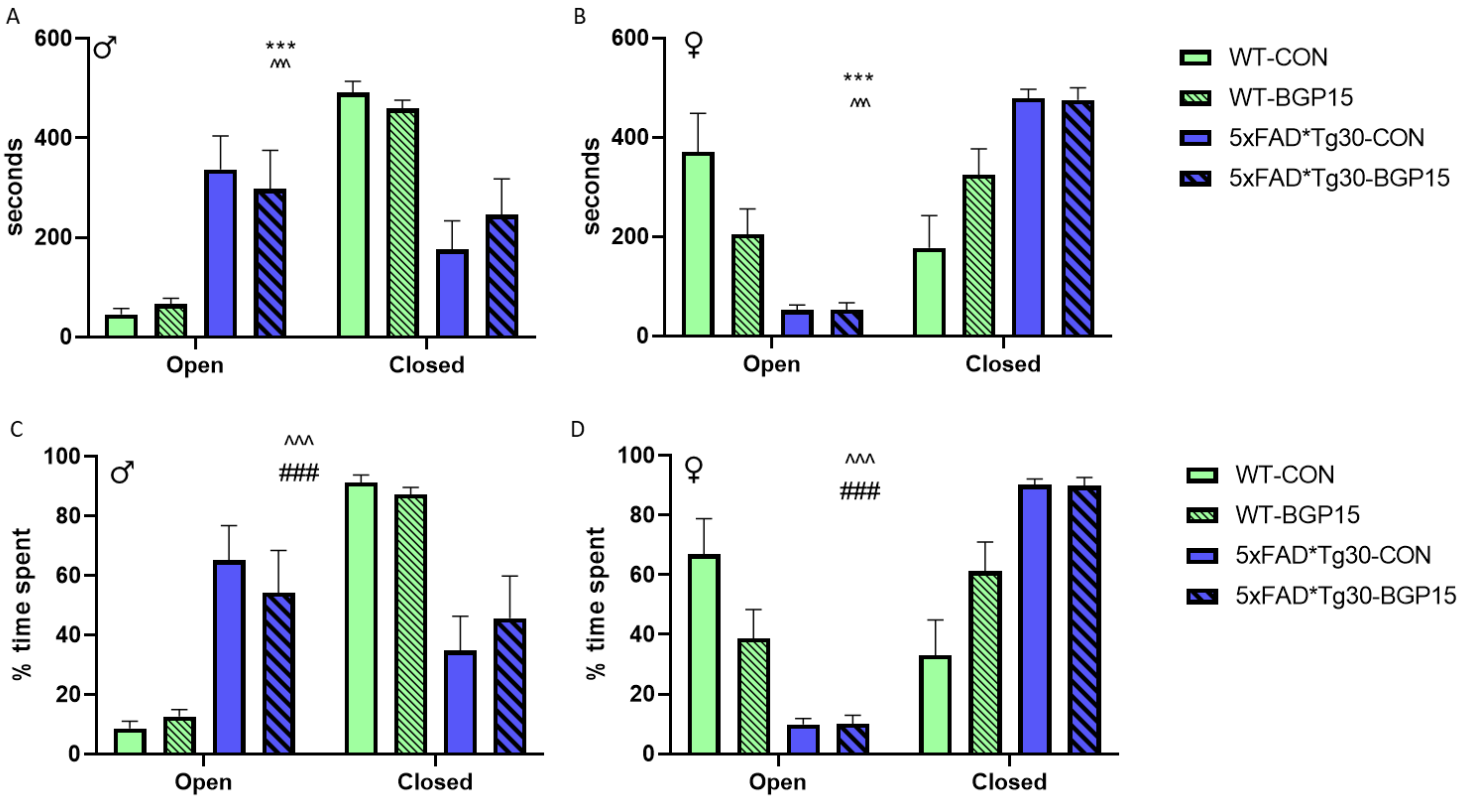

Figure 4.8 ***Anxiety-like behaviour assessed via an elevated plus maze at 9 months.*** *(A-B) Duration of overall time in areas of an elevated plus maze at 9 months of age. (C-D) Percentage of time spent in areas of an elevated plus maze. Animals spent 10 minutes in an elevated plus maze, consisting of open arms and closed arms. (A,C) Male animals only, n= 5 per group (B,D) Female animals only, n=4 per group. Genotype effect between WT and 5xFAD*Tg30. Area effect between open and closed areas. Interaction effect between genotype and area of maze. ***p<0.001 genotype ###p<0.001 area effect ^^^p<0.001 interaction effect. 2-way ANOVA performed in each area. T-test performed between areas for each group. Graph indicates ± SEM*

4.3.5 Novel object recognition

To assess short term memory and novel object recognition, the test was completed at 7 months to determine if BGP-15 treatment improved performance. Mice displayed a preference to the novel object over the familiar object, after a 10-minute familiarisation period and a 5-minute test period. Surprisingly, although WT-CON animals trended to show this preference, it did not reach significance **(Figure 4.9 A)**. After separating for sex, only *5xFAD*Tg30-CON* animals showed significant preference to the novel object in females **(Figure 4.9 C)**, whereas male animals displayed a preference to the *novel* object **(Figure 4.9 B)**. There were no effects of BGP-15 treatment on novel object recognition.

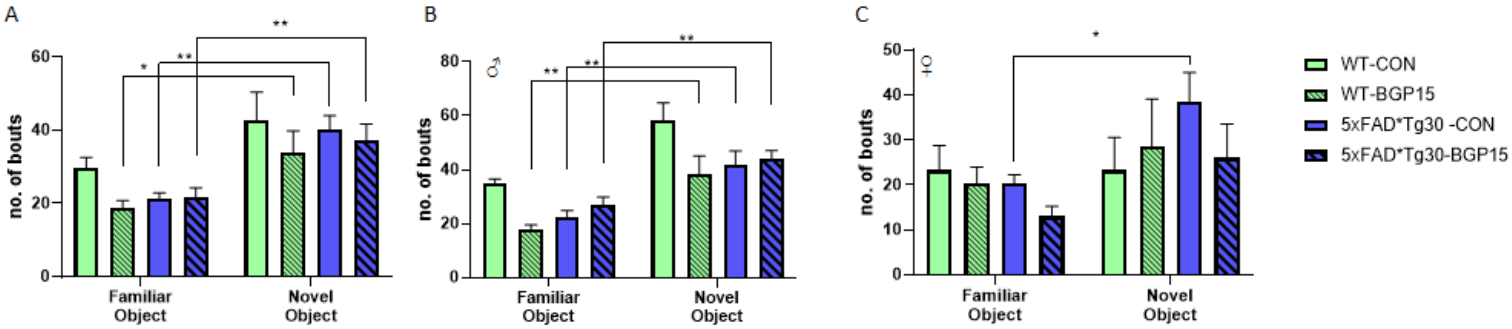

Figure 4.9 ***Number of bouts of investigative behaviour of each object at 7 months of age***. *Animals had 10 minutes familiarisation with Object 1 and Object 2. Object 1 was then replaced with Novel Object and animals had a 10 minute test (A) Total cohort, n=16-18 per group (B) Male animals only, n=8-10 per group (C) Female animals only, n=6-8 per group. WT animals and 5xFAD*Tg30 animals observed the Novel Object significantly more than the Familiar Object. There was no effect of BGP-15. 2-way ANOVA performed in object of interest, the Novel Object. T-test performed between each object for each group. *p<0.05 **p<0.01 Graph represents Mean ± SEM*

4.3.6 Learning, spatial memory and recognition

Learning, spatial memory and recognition was assessed as per *Chapter 2* with the Morris Water Maze in a sub-set of the cohort. By the 6th trial day, both male and female WT animals halved their latency from day 1 to the hidden platform. Although latencies were significantly different between genotypes, and female *5xFAD*Tg30* animals did not show a learning curve, male *5xFAD*Tg30* animals also halved their latency **(Figure 4.10 A-B)**. Genotype effects for time spent in quadrant area on probe trial day **(Figure 4.10 C-D)** were observed. In *Chapter 2*, by 8 months, deficits in learning were also noted, however it was more likely that these longer latencies are due to the motor deficit as seen by 6 months of age. Hence, swim velocity was additionally recorded and despite latency to platform being significantly different, so too was swim velocity, which could suggest latency is due to motor ability rather than learning impairment **(Figure 4.10 E-F).** There were no effects of BGP-15 on learning curve, probe trial or swim velocity.

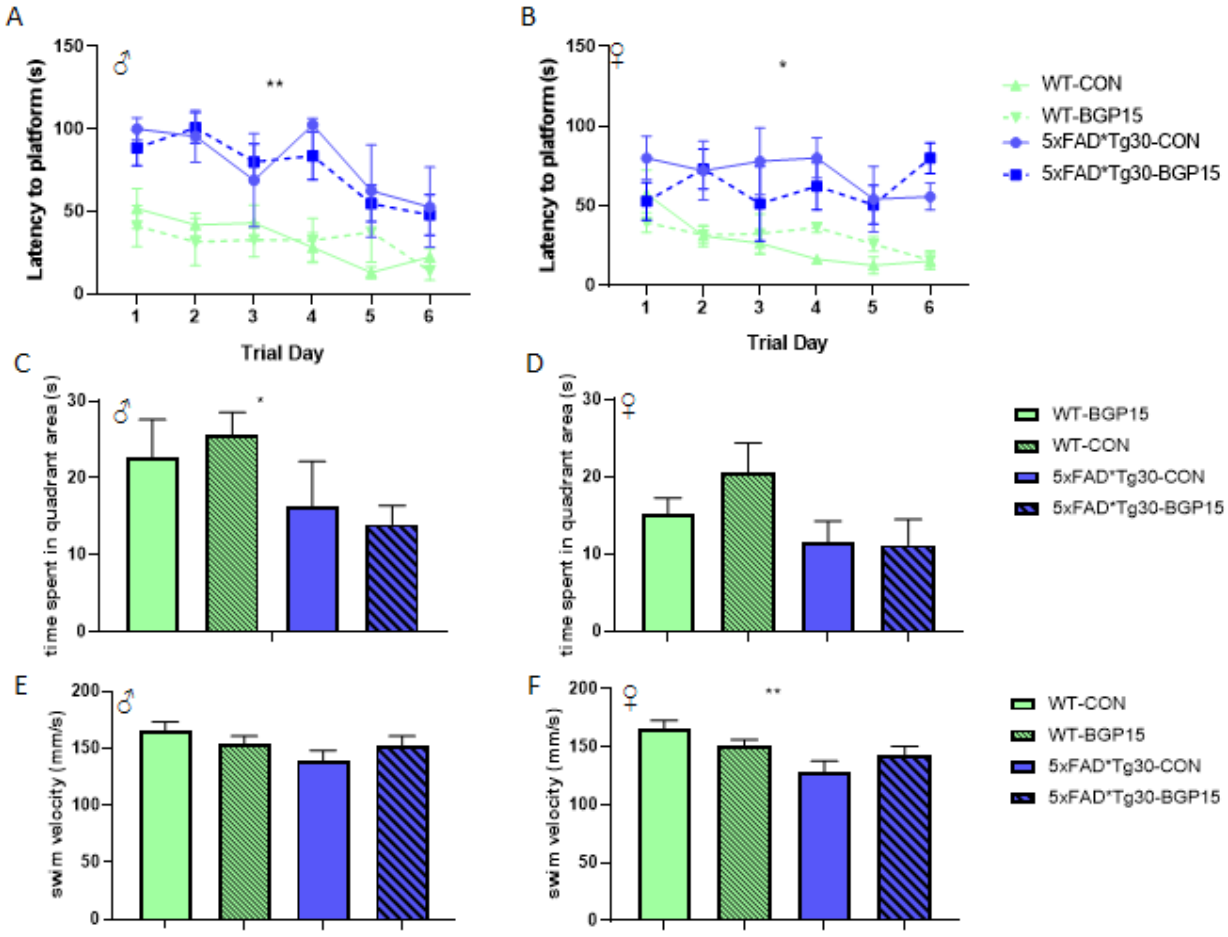

Figure 4.10 ***Learning curve, latency to platform over 6 days, at 8 months of age***. *(A-B) learning curve at 8 months, male and female respectively (C-D) probe trial at 8months, male and female respectively (E-F) Average swim velocity and 8 months, male and female, respectively. Animals were given a maximum of 120 seconds to find platform. Probe Trial- time spent in platform quadrant. Platform was removed on Day 7 and animals swam for 60 seconds. N=8-15 males per group, 9-14 females per group. Graph represents Mean of 4 trials per day ± SEM. Two-way repeated measures ANOVA with Holm-Sidak post-hoc analysis. Genotype effect at 8 months in latency to platform. *p<0.05 **p<0.01*

4.3.7 Gait Analysis

Due to the marked differences in rotarod performance and hangwire ability in *Chapter 2* and *Chapter 3*, further gait abilities were assessed via DigiGait analysis. Analysis of swing duration confirmed a weak walk in *5xFAD*Tg30* animals, with all four limbs displaying a reduced swinging paw compared to WT **(Figure 4.11 A, D. Figure 4.12 A, D)**. Similarly, *5xFAD*Tg30* mice displayed a lower propulsion duration in each limb, confirming a weak lifting of paw movement **(Figure 4.11 B, E. Figure 4.12 B, E).** This suggests that the *5xFAD*Tg30* mice have significantly weaker gait movements than WT mice, likely due to muscle weakness. The treatment of BGP-15 did not rescue swing duration or propulsion duration deficits in any limb, nor enhance the performance in WT animals. Additionally, *5xFAD*Tg30* animals displayed a higher frequency of steps per second, compared to WT **(Figure 4.11 C, F. Figure 4.12 C, F).** This is most likely due to the significant size difference between the two genotypes, resulting in *5xFAD*Tg30* mice needing to move their smaller legs faster, in order to keep up with the moving DigiGait belt. Similarly, these results were not affected with the treatment of BGP-15.

It is interesting to note, that at this timepoint, these gait differences are apparent despite rotarod deficits not appearing until a month later, at 6 months. At 5 months, *5xFAD*Tg30* animals do not have a significantly impaired rotarod performance, yet more precise gait analysis from the DigiGait system was able to pick up on these underlying impairments. As such, on the rotarod at 5 months of age, the mice must be able to compensate for these weaknesses but with further deterioration the system is overwhelmed and rotarod impairment is detected.

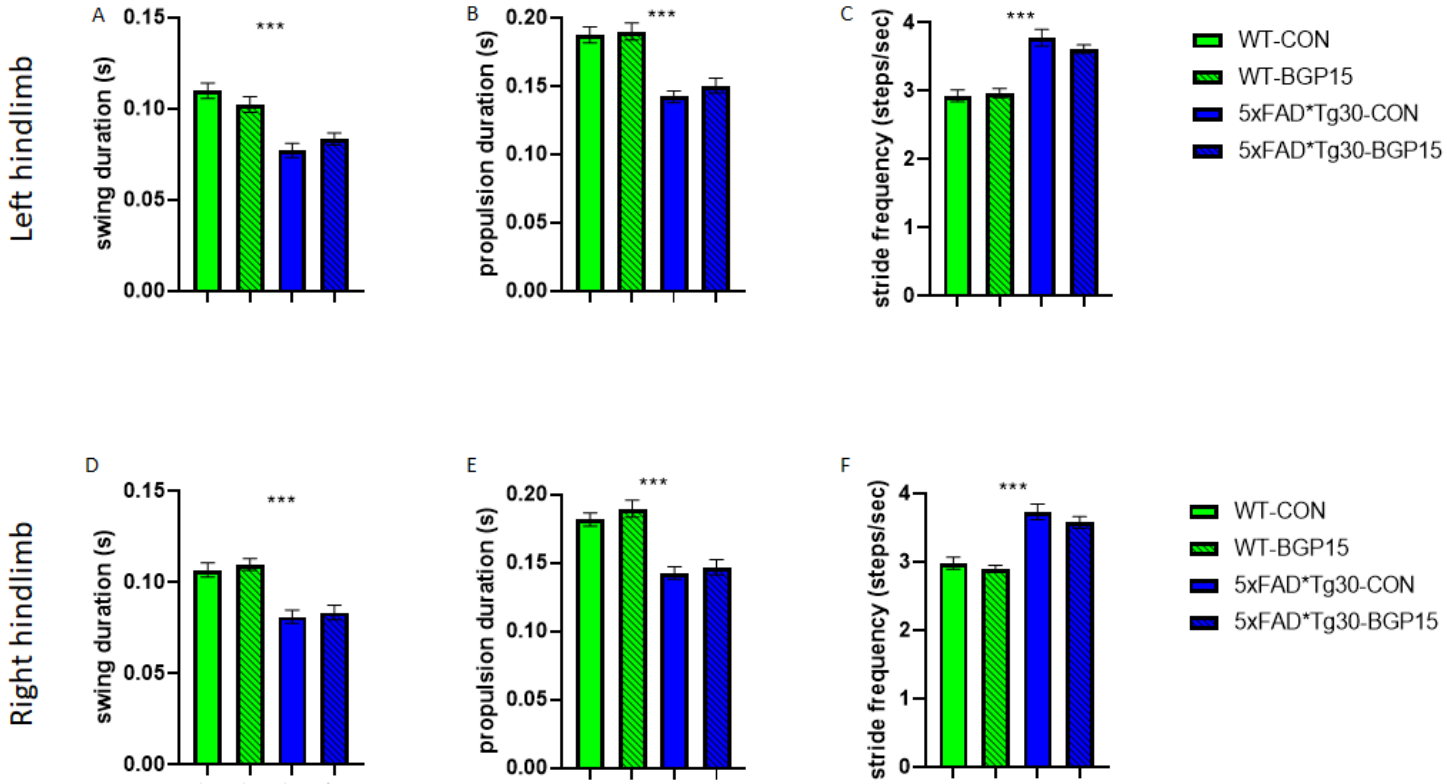

Figure 4.11 ***DigiGait analysis.*** *(A,D) Swing duration, (B, E) propulsion duration and (C, F) stride frequency measured in steps per second of the left and right hindlimb of WT and 5xFAD*Tg30 animals with and without BGP-15 treatment. Analysis was performed on male animals only, at 5 months of age. Swing and propulsion duration were significantly reduced in 5xFAD*Tg30 animals indicating an impaired, weaker gait. Stride frequency was significantly increased in 5xFAD*Tg30 animals, likely from smaller stature. No treatment differences with BGP-15. N= 12-21 per group ***p<0.001 2-way ANOVA Graph indicates mean ± SEM*

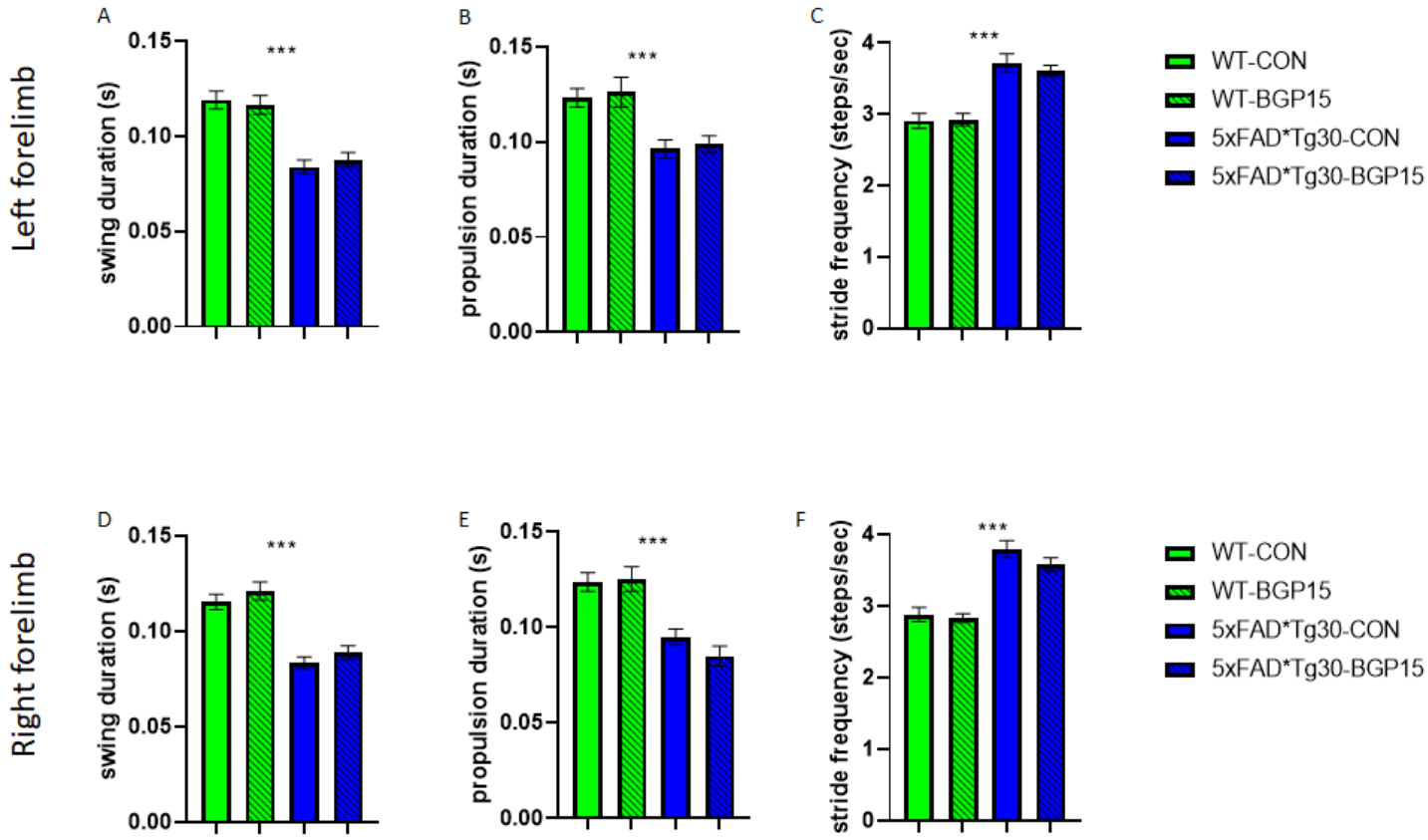

Figure 4.12 ***DigiGait analysis.*** *(A,D) Swing duration, (B, E) propulsion duration and (C, F) stride frequency measured in steps per second of the left and right forelimb of WT and 5xFAD*Tg30 animals with and without BGP-15 treatment. Analysis was performed on male animals only, at 5 months of age. Swing and propulsion duration were significantly reduced in 5xFAD*Tg30 animals indicating an impaired, weaker gait. Stride frequency was significantly increased in 5xFAD*Tg30 animals, likely from smaller stature. No treatment differences with BGP-15. N= 12-21 per group ***p<0.001 2-way ANOVA Graph indicates mean ± SEM*

4.3.8 Body composition

BGP-15 has previously been shown to ameliorate dystrophic muscle wasting in a model of Duchenne muscular dystrophy (Gehrig 2012). Therefore, it was of interest to investigate any BGP-15 effect on lean mass given the lower lean mass in the *5xFAD*Tg30* model.

As in *Chapter 2* and *Chapter 3*, vast genotype differences were observed in body mass, lean mass, fat mass and body fat percentages. As mice were transported to a different location at 6 months of age that did not have body composition equipment, lean mass, fat mass and body fat percentage was only recorded up to 6 months.

Body weight and lean mass continue to increase as WT animals aged, but this did not occur in *5xFAD*Tg30* animals, who already have a significantly smaller weight and lean mass at just 2 months of age. BGP-15 treatment did not rescue this deficit **(Figure 4.13 A-F).**

Fat mass and body fat percentage showed the same trends as in *Chapter 2* and *Chapter 3*, not showing significant divergence until around 5 months of age. Again, BGP-15 treatment did not rescue this deficit **(Figure 4.13 G-L).**

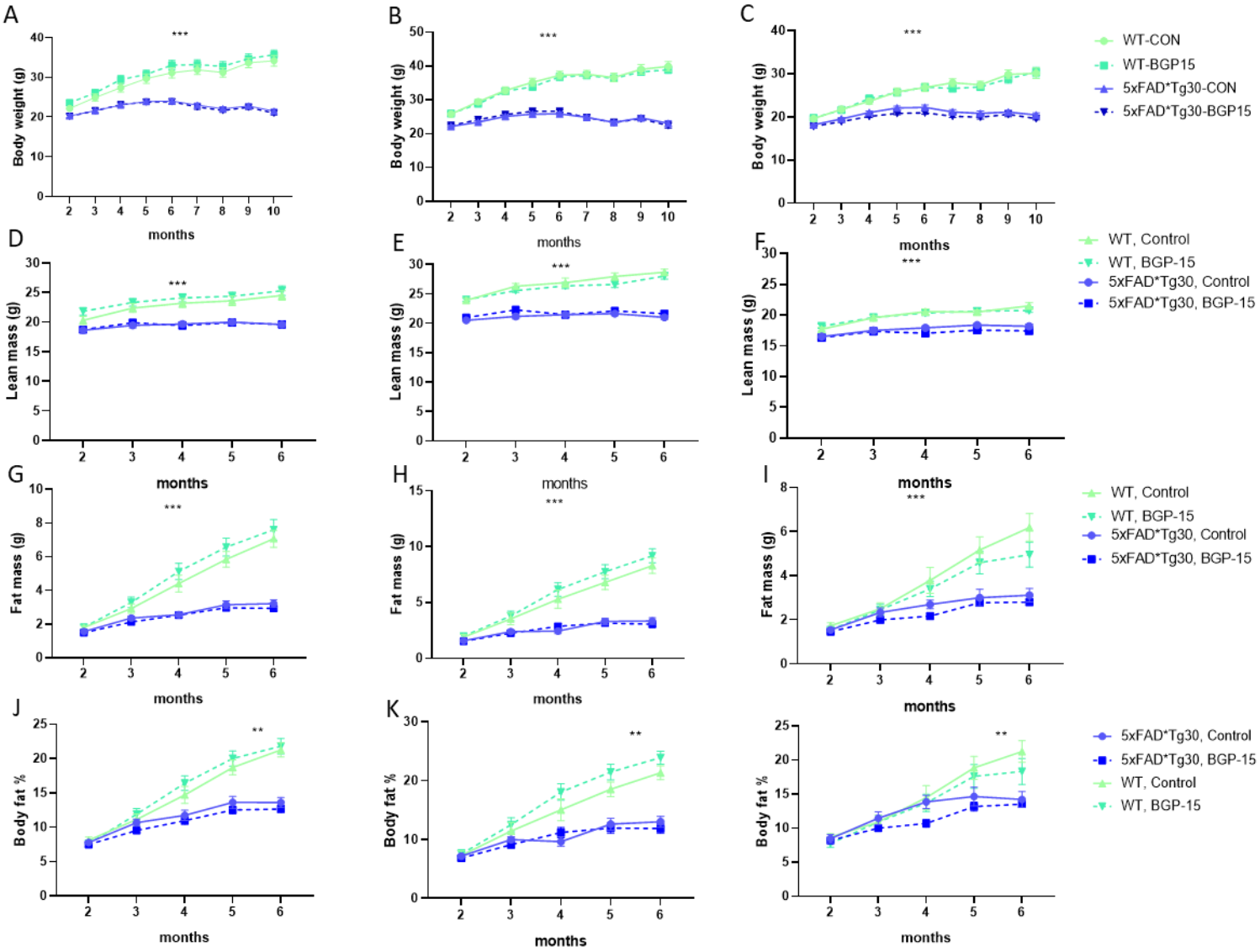

Figure 4.13 ***Body composition analysis in WT-CON, WT-BGP15, 5xFAD*Tg30-CON and 5xFAD*Tg30-BGP15 mice over time.*** *(A-C) Body weight, (D-F) lean mass, (G-I) fat mass (J-L) body fat percentage. (A,D,G,J) total cohort n=24-30 per group, (B,E,H,K) male animals only n=10-16 per group, (C,F,I,L) female animals only, n=9-14 per group. WT animals had a significantly higher body weight and lean mass compared to 5xFAD*Tg30 from 2 months onwards and a higher fat mass and body fat percentage from 5 months onwards. **p<0.01 ***p<0.001. Two-way repeated measures ANOVA with Holm-Sidak post-hoc analysis. Graph indicates ± SEM*

4.3.9 Glucose tolerance

BGP-15 has previously been shown to improve insulin sensitivity (Literati-Nagi 2009) and is currently in clinical trials for the treatment of T2D. At 5 months of age, an oral gavage glucose tolerance test was performed to see the effects of BGP-15 on the *5xFAD*Tg30* model of AD.

Similar to results in *Chapter 2* and *Chapter 3*, *5xFAD*Tg30* animals showed a lower oGTT curve compared to WT, in both males and females, however there was a larger discrepancy in the females **(Figure 4.14)**. Analysing the female curve, there was an additional BGP-15 treatment effect, which elevated the oGTT curve of both WT and *5xFAD*Tg30* female mice.

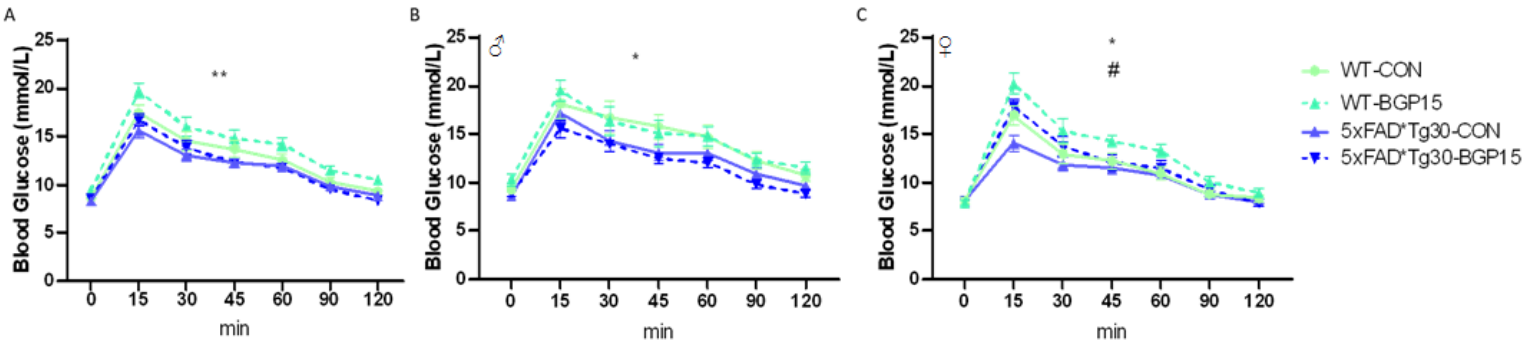

Figure 4.14 ***Whole-body glucose metabolism analysis at 5 months of age***. *Fasting blood glucose levels after an oral gavage glucose tolerance test (2gm/kg LBM) at 5months of age. (A) total cohort n=24-28 per group (B) males only n=10-15 per group (C) females only n=9-14 per group. Fasting blood glucose was taken after a 6 hour fast and is the '0' time value represented in the OGTT. Genotype effects between WT and 5xFAD*Tg30. *p = <0.05 **p = <0.01, # p= <0.05 drug effect in females. Two-way ANOVA. Graphs indicate mean ± SEM*

4.3.10 Metabolic caging analysis

As in *Chapter 2* and *Chapter 3*, metabolic caging was used to determine if BGP-15 altered metabolic measures such as VO_2 consumption, energy expenditure, respiratory exchange ratio (RER) and total movement. Results were analysed over the 24-hr period and showed *5xFAD*Tg30* animals had a significantly lower raw oxygen consumption, particularly during the dark cycle (active part) of their day. When adjusted for body mass, these differences were not apparent, however when adjusted for lean mass the opposite effect occurred, where a higher VO_2 rate was observed. This higher VO_2 result complemented what was seen in *Chapter 2* and *Chapter 3* **(Figure 4.15i G-I).** There was no effect of BGP-15 on any VO_2 measurements.

In *Chapter 2* and *Chapter 3*, *5xFAD*Tg30* animals showed a lower energy expenditure which was reproduced in this chapter **(Figure 4.15ii J-L).** This predominately came from male *5xFAD*Tg30* animals, as female animals did not show any differences compared to WT. There was no effect of BGP-15 on energy expenditure.

There was a vast difference in RER (utilisation of carbohydrates to fat ratio) between *5xFAD*Tg30* and WT animals **(Figure 4.15ii M-O).** In *Chapter 2*, *5xFAD*Tg30* animals trended to have a higher RER however this did not reach significance and in *Chapter 3*, there were no apparent differences. Results in this chapter suggest that *5xFAD*Tg30* animals indeed have a vastly higher RER compared to WT animals across a large period of the 24hr cycle. This indicates carbohydrates are predominately being used over lipid metabolism, compared to WT. There were no effects of BGP-15 on RER.

Overall activity was additionally assessed via the number of beam breaks, and *5xFAD*Tg30* animals had a significantly decreased activity level, which was largely accounted for the vast difference in female animals **(Figure 4.15ii P-R)**. Male

*5xFAD*Tg30* animals had similar activity level to WT animals at this time point (5 months). There was no effect of BGP-15 on activity levels.

Thus, it was confirmed that *5xFAD*Tg30* animals have a lower lean mass adjusted VO_2 consumption, lower energy expenditure and higher RER. There were no effects of BGP-15 on any of these metabolic measures.

As a caveat to these results, it is important to recognise the difficulty in comparing mice of difference sizes for these measures. As the size difference between genotypes is so vast, it can be difficult to normalise the data appropriately- there is both an overall size difference as well as a body composition difference. Normalising may not consider different organ sizes, which were demonstrated in *Chapter 2*, such as brain and liver, which are highly metabolic organs. One way around this could be to measure the metabolic activity of every single organ, which would be extremely difficult. Another could be to take WT animals at a younger age and compare them to *5xFAD*Tg30* animals at an older age, with a similar body composition.

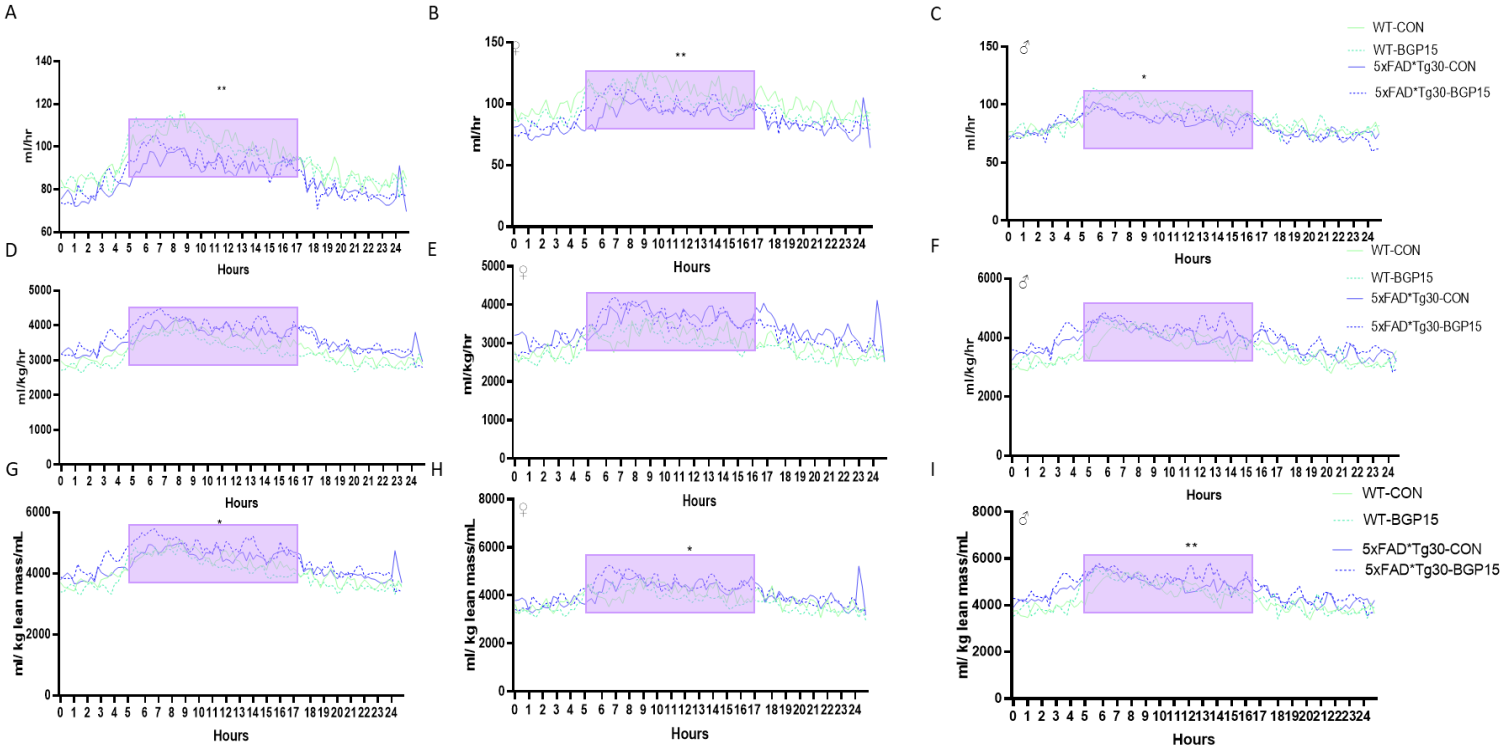

Figure 4.15i ***Aspects of whole-body energy metabolism measured in a CLAMs system for WT control, 5xFAD*Tg30 BGP-15 treated and untreated animals over a 24hr period.*** *Total cohort (A, D, G, J, M, P) n=22-30 per group, Male (B, E, H, K, N, Q) n=10-19 per group, Female (C, F, I, L, O, R) n=9-15 per group.* ***(A-C)*** *Raw oxygen consumption (VO_2) unadjusted for any factor. Genotype effects between 5xFAD*Tg30 and WT animals.* ***(D-F)*** *VO_2 data normalised to body weight. No genotype effects.* ***(G-I)*** *VO_2 normalised to lean body mass. Genotype effects between WT and 5xFAD*Tg30 *p<0.05 **p<0.01 t-test. Graphs indicate mean ± SEM. Shading indicates dark 12hr cycle.*

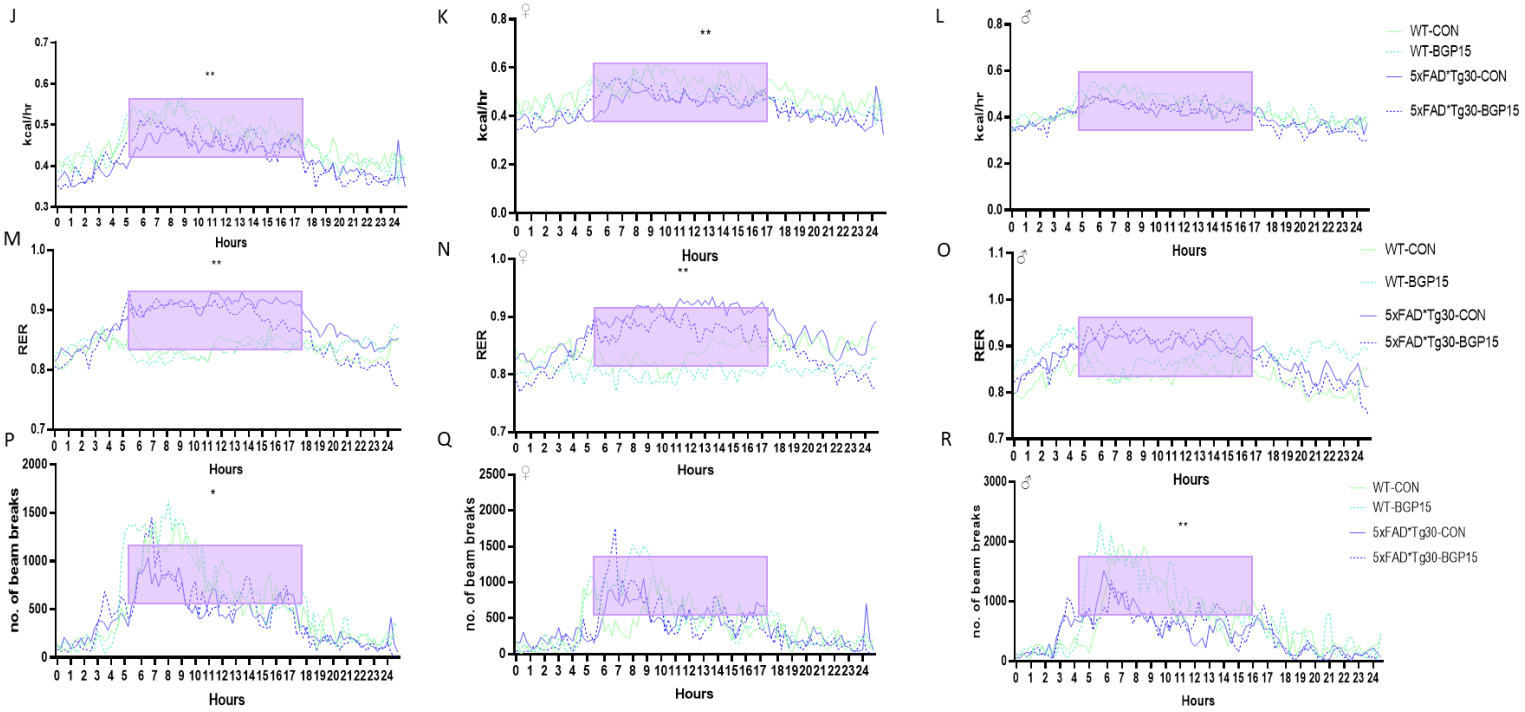

Figure 4.15ii ***Aspects of whole-body energy metabolism measured in a CLAMs system for WT control, 5xFAD*Tg30 BGP-15 treated and untreated animals over a 24hr period.*** *Total cohort (A, D, G, J, M, P) n=22-30 per group, Male (B, E, H, K, N, Q) n=10-19 per group, Female (C, F, I, L, O, R) n=9-15 per group.* ***(J-L)*** *Raw energy expenditure (heat). Genotype effects in total cohort and in males between WT and 5xFAD*Tg30* ***(M-O)*** *Respiratory exchange ratio (RER), genotype effects in total cohort and males between WT and 5xFAD*Tg30,* ***(P-R)*** *Total movement/activity as measured via beam breaks (x + Y ambulatory plus z breaks).Genotype effects in total cohort and female animals between WT and 5xFAD*Tg30. *p<0.05 **p<0.01 t-test. Graphs indicate mean ± SEM. Shading indicates dark 12hr cycle.*

4.3.11 End point measures

As in *Chapter 2* and *Chapter 3, tibialis anterior* weight was significantly reduced in *5xFAD*Tg30* mice, at almost half the weight of WT control littermates. Despite BGP-15 previously rescuing muscle atrophy in a model of Duchenne muscular dystrophy, there was no effect on muscle atrophy in *5xFAD*Tg30* animals **(Figure 4.16).**

A Kaplan-Meir survival curve was analysed after 10 months, which was determined as end point. After 10 months, *5xFAD*Tg30-CON* animals had a significantly reduced survival compared to WT, as in *Chapter 2* and *Chapter 3*, with a survival of approximately 60%. *5xFAD*Tg30* animals treated with BGP-15 appeared to have an increased survival rate, improving to a survival rate above 85% **(Figure 4.17 A).** Sexes were then split, to account for any sex differences and it was determined that female *5xFAD*Tg30* mice did not show an improved survival and BGP-15 treatment had no effects **(Figure 4.17 B).** It was determined that differences in survival rates in the whole cohort were attributed to male *5xFAD*Tg30* mice, so an additional lifespan study was performed to increase experimental numbers. Male *5xFAD*Tg30-CON* mice saw a 72% survival rate, which was improved by BGP-15 treatment to 88% **(Figure 4.17 C).** In total numbers of survival vs death, there were 11 deaths out of 40 (27.5%) in the *5xFAD*Tg30-CON* group, vs 4 deaths out of 34 (12%) in the 5xFAD*Tg30-BGP15 group. Specifically, in males, there were 10 deaths out of 26 (38%) in the *5xFAD*Tg30-CON* group, vs 3 deaths out of 21 (14%). Despite this, this result did not prove to be statistically significant, but does suggest potential benefits for increased survival with BGP-15 treatment.

Thus, BGP-15 did not rescue muscular atrophy in tibialis anterior but trended to improve lifespan in male *5xFAD*Tg30* mice.

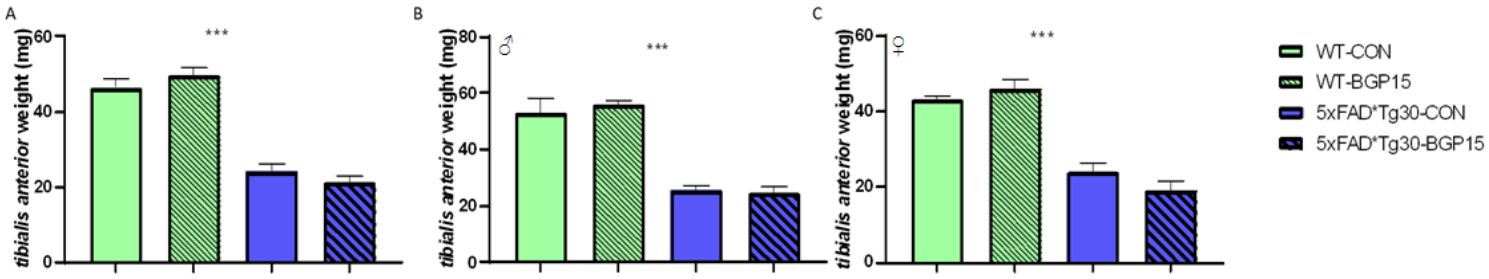

Figure 4.16 ***End-point Tibialis anterior weight of BGP-15 treated and untreated animals.*** ***(A)*** *Total cohort n=9-12 per group* ***(B)*** *Male only n=4 per group* ***(C)*** *Female only n=7-8 per group. Genotype differences in weight between WT and 5xFAD*Tg30 animals. No effect of BGP-15 ***p<0.001 2-way ANOVA. Graphs indicate mean ± SEM.*

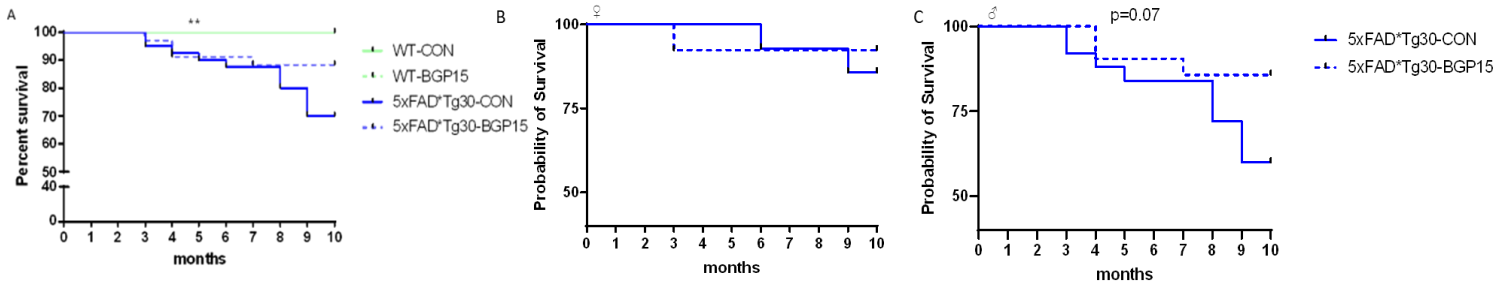

Figure 4.17 ***Kaplan-Meir survival curves (A)*** *5xFAD*Tg30 animals show a significant decreased survival. BGP-15 increased their survival from 72% to 88%. Total cohort n=24-40 per group* ***(B)*** *BGP-15 treatment in female 5xFAD*Tg30 mice does not alter survival n=13-14 per group* ***(C)*** *BGP-15 treatment in male 5xFAD*Tg30 mice trends to improve survival n=21-26 per group. Graph represents mean ±SEM **p<0.01 evaluated by a Gehan Breslow Wilcoxon test*

4.3.12 Seizure study

Preface

This seizure study was conducted in conjunction with Prof. Nigel Jones and Ms. Anna Harutyunyan at Monash Neuroscience.

As there was a trend in longevity with animals treated with BGP-15, an additional cohort of male mice were used in a seizure study to measure the difference in kindling rate between *5xFAD*Tg30*, *5xFAD*Tg30* treated with BGP-15 and WT mice. By comparing the number of kindling stimulations that triggered the first-class V seizure, this would give an indication if male *5xFAD*Tg30* mice were more susceptible to seizures/fatal seizures and if BGP-15 was rescuing this susceptibility and therefore improving their survival through this mechanism.

A class V seizure is considered when the animal is fully kindled and are compared with the secondary generalised seizure found in human epilepsies. The behavioural manifestation from this type of seizure includes both rearing and falling. The number of stimulations required for *5xFAD*Tg30* mice to reach a class V seizure was significantly less than the required number for WT animals. While WT animals required around 10 stimulations, *5xFAD*Tg30* animals required less than 5. There was no effect of BGP-15 treatment **(Figure 4.18 A).** When graphed over time, it is clear that WT animals require a linear progression to reach class V seizures, whereas *5xFAD*Tg30* animals reach this class rapidly, and continue to seize as so, for the remainder of the kindling process **(Figure 4.19 A).**

The average seizure duration was also recorded throughout the kindling process, and indeed, *5xFAD*Tg30* mice experienced longer seizures than their WT control.

*5xFAD*Tg30* animals that were treated with BGP-15 showed no differences in seizure duration to those untreated **(Figure 4.18 B).** Interestingly, when analysed over time, it appears that although the genotypes display different seizure durations, the rate of change over time is similar, with WT animals slowly increasing the seizure duration after each successive stimulation. Similarly, *5xFAD*Tg30* animals slowly see an increase in seizure duration, until around stimulation 8, where we then see a spike until it levels out after stimulation 11 **(Figure 4.19 B).**

Additionally, throughout the kindling process, the average class of seizures were recorded. As expected, *5xFAD*Tg30* mice, both untreated and treated, had an average class seizure of V and there were no treatment effects. WT animals displayed on average a seizure class of III **(Figure 4.18 C).**

Thus, *5xFAD*Tg30* male animals have a significantly reduced kindling rate compared to WT animals. After characterising differences in seizure duration, *5xFAD*Tg30* animals display significantly longer seizures and an increased seizure severity. There were no effects on any measures with BGP-15 treatment.

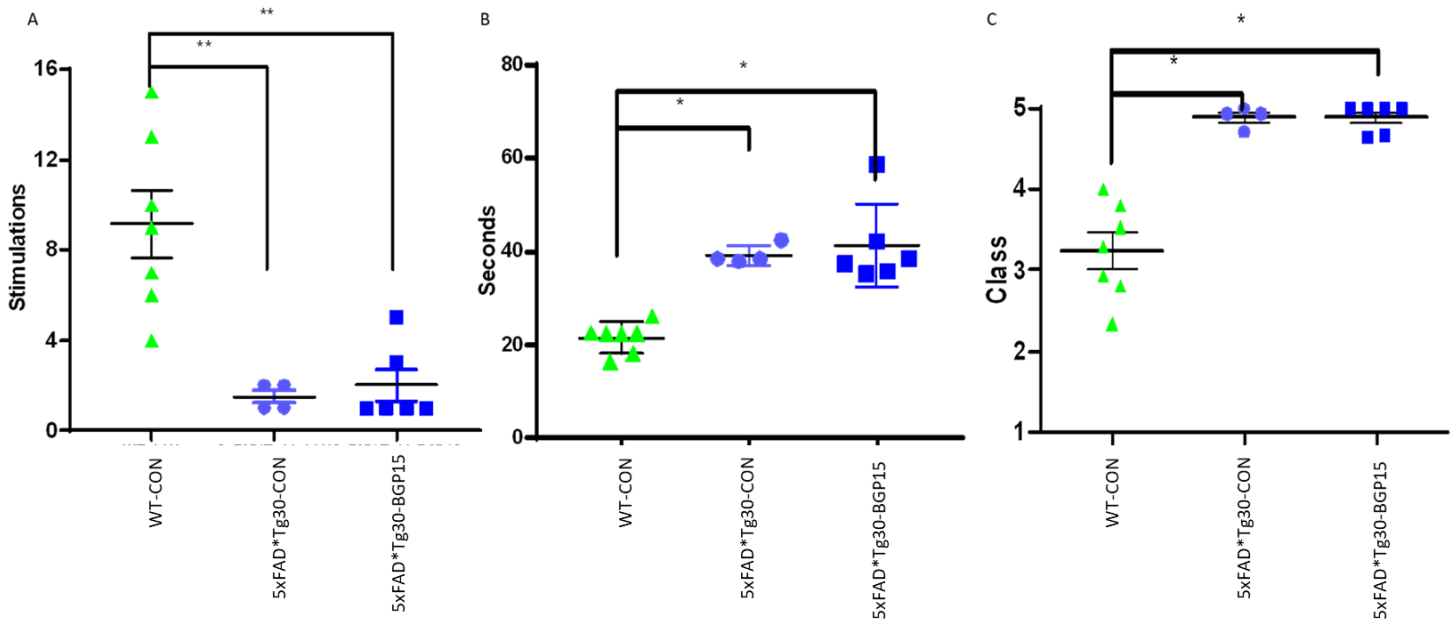

Figure 4.18 (*A) Number of kindling stimulations delivered to trigger the first, class V seizure in each animal*. *Kruskal-Wallis test **p<0.01* ***(B) Average seizure duration***. *Two-way ANOVA and Tukey HSD *p<0.05* ***(C) Average seizure class***. *Two-way ANOVA and Tukey HSD **p<0.01 n= 4-7 per group*

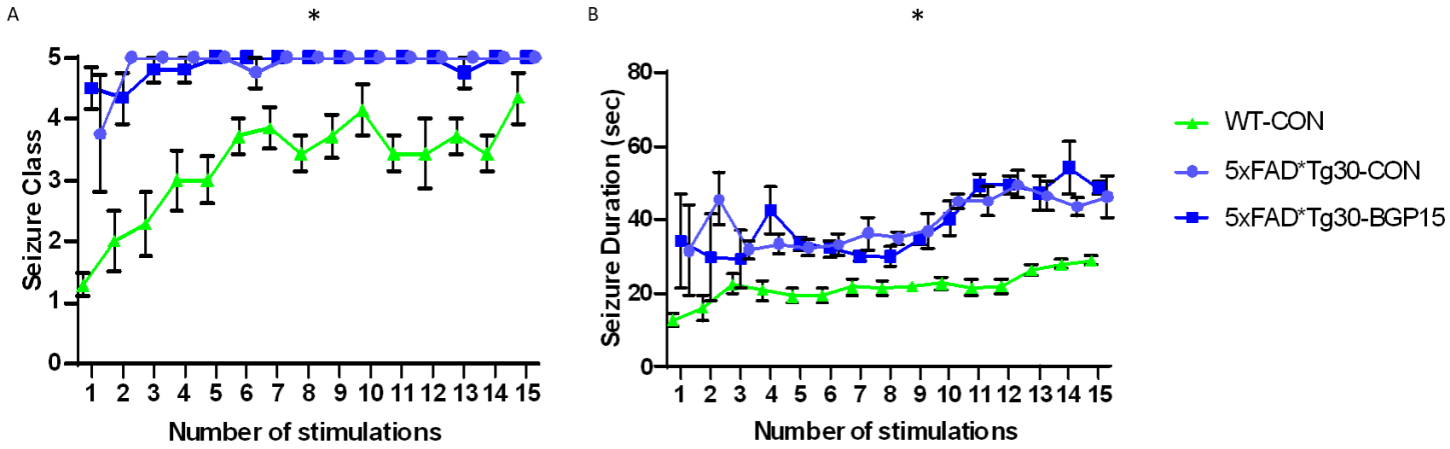

Figure 4.19 (*A) Seizure class progression*. *Significant genotype differences in overall seizure class* ***(B) Seizure duration.*** *Significant genotype differences in over seizure duration *p<0.05 n= 4-7 per group. One-way ANOVA with Tukey's post hoc analysis performed. Graph represents mean ± SEM*

4.3.13 Seahorse Analysis

To assess if BGP-15 alters key parameters of mitochondrial function in neurons, OCR was directly measured, with a range of doses of BGP-15. Included below is a diagram from Agilent Seahorse XF, displaying the key parameters of mitochondrial function that the assay measures

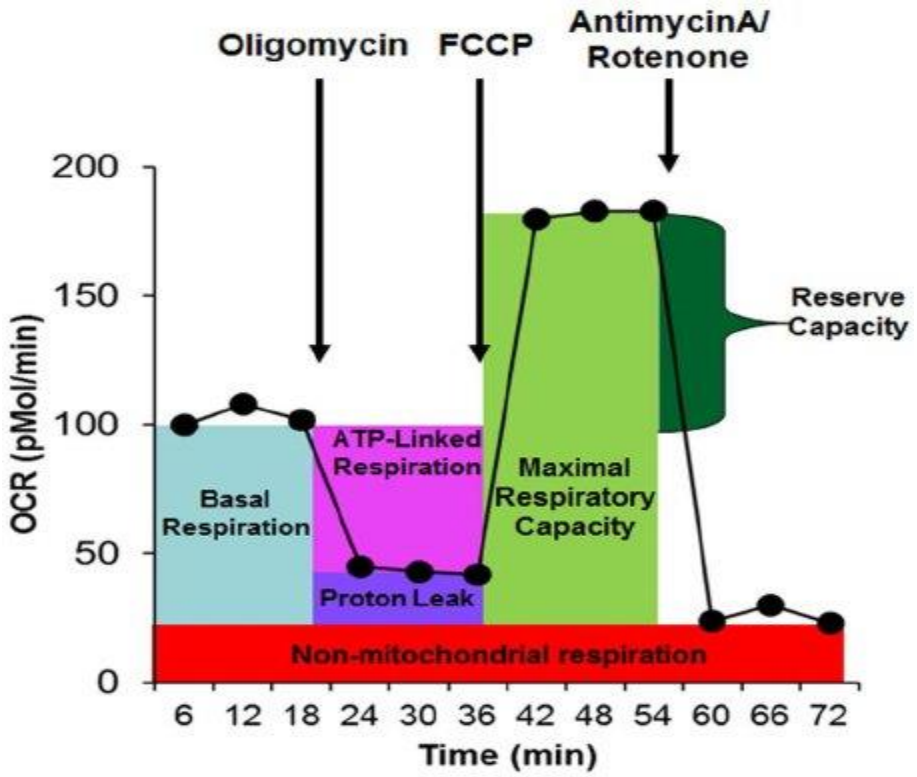

Figure 4.20 ***Mito stress test profile.*** *Key parameters of mitochondrial function, including basal respiration, ATP-linked respiration and maximal respiration. Source: Agilent, CA USA*

Basal respiration and respiration post BGP-15 treatment showed no OCR differences between BGP-15 treatments and control. The injection of Oligomycin reduced OCR in each condition, (ATP linked respiration), however there was no significant difference between treatment groups. Similarly, uncoupled respiration showed no differences between treatments. BGP-15 treatment trended to increase the maximal respiration, compared to control, with the lowest dose producing the highest OCR, but this did not reach significance. Consequently, the spare respiratory capacity trended to increase with BGP-15 treatment, with 5uM yielding the greatest results.

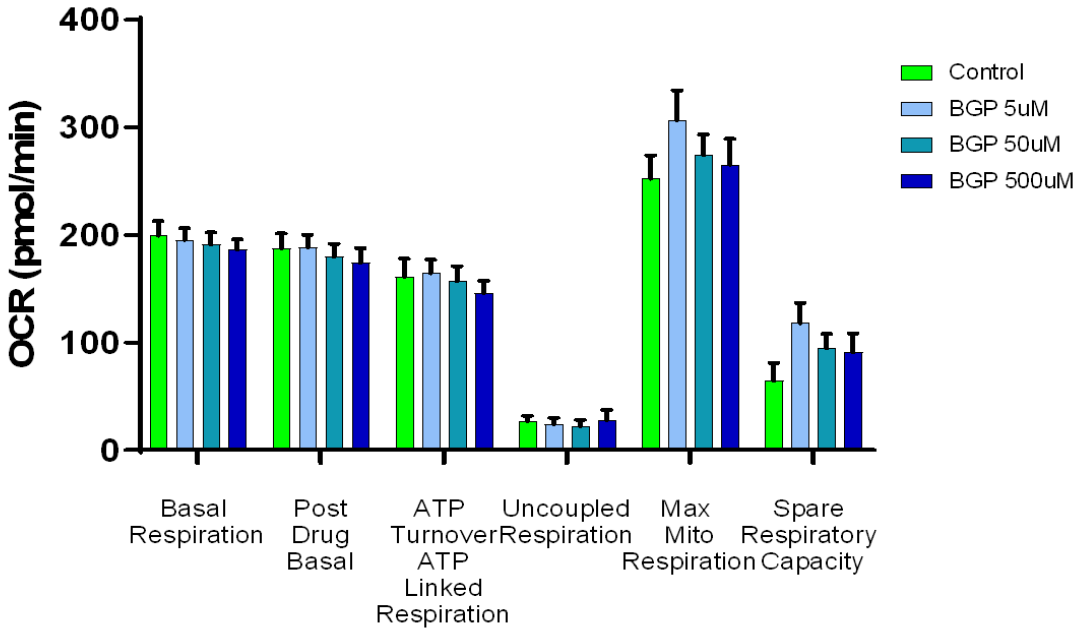

Figure 4.21 ***Oxidative capacity rate (pmol/min) of neuronal cells treated with BGP-15.*** *Basal respiration, ATP-linked respiration and uncoupled respiration saw no effects with BGP-15 on OCR. BGP-15 trended to increase maximal respiration and spare respiratory capacity. Graph represents average of 3 individual experiments, conducted in triplicates mean ±SEM.*

Next, to assess if BGP-15 had effects on glycolytic function, ECAR was directly measured, with a range of doses of BGP-15. Included below is a diagram from Agilent Seahorse XF, displaying the key parameters of mitochondrial function that the assay measures.

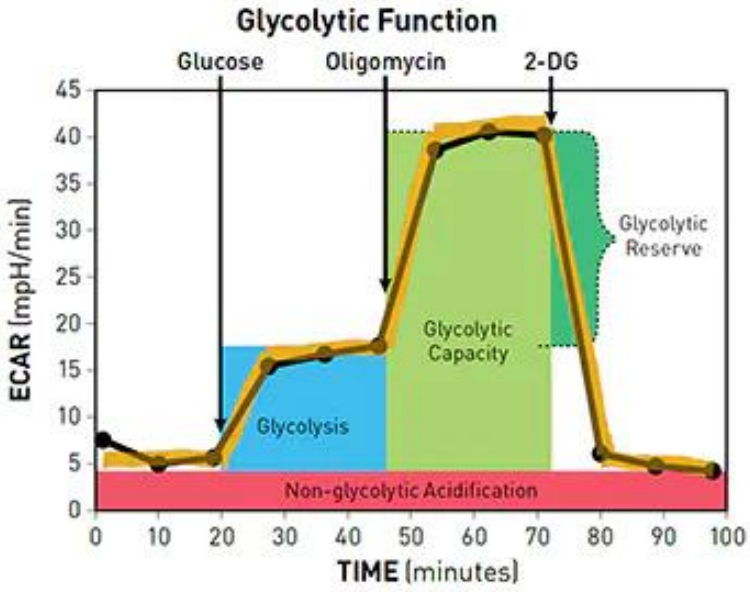

Figure 4.22 ***Glycolysis stress test profile.*** *Key parameters of glycolytic function, including basal glycolytic rate and maximal glycolytic capacity. Source: Agilent, CA USA*

Glucose-induced basal glycolysis had no effect with 5uM BGP-15 treatment compared to control. However, higher doses of BGP-15 treatment trended to decrease ECAR and basal glycolysis. This did not reach statistical significance **(Figure 4.23 A).** Glycolytic capacity trended to increase slightly with 5uM BGP-15 treatment but showed no difference with higher doses of BGP-15uM. There was no statistical significance **(Figure 4.23 C).** Despite maximal glycolytic capacity showing no differences between treatment groups, as there were slight differences in basal glycolysis, this resulted in trended differences in glycolytic reserve. BGP-15 treatment trended to increase the reserve, compared to control **(Figure 4.23 B),** however this result is most likely from the reduced basal rate.

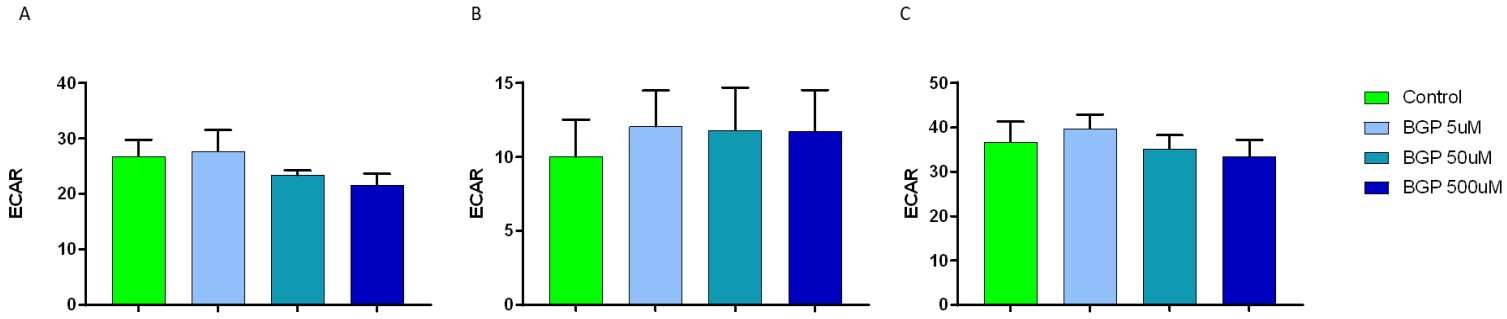

Figure 4.23 Glycolysis stress test. (A) *Glucose induced glycolysis post drug treatment***.** *BGP-15 trended to decrease basal glycolysis at higher doses (50uM and 500uM).* ***(B)*** *BGP-15/DMSO induced glycolytic reserve***.** *Glycolytic reserve trended to increase with BGP-15 treatment, however, could be put down to decreased glycolysis.* ***(C)*** *BGP-15/DMSO induced glycolytic capacity- maximal glycolytic capacity did not increase. Changes were not statistically significant, 2-way ANOVA performed. Graph represents average of 3 individual experiments, conducted in triplicates, mean ±SEM.*

Despite BGP-15 treatment, at multiple doses not improving neuronal mitochondrial oxidative capacity and glycolytic capacity, this group of experiments suggests, at the least, that BGP-15 treatment is non-toxic to neuronal cells.

4.4 Discussion

BGP-15, a small hydroxylamine derivative, is a potential target for therapeutic treatment of neurodegenerative diseases. Previous research into models of injury, stress, and disease have demonstrated its involvement with several intracellular pathways (Szabados, 2000; Halmosi, 2001; Racz, 2002; Chung, 2008; Bárdos, 2003; Nagy, 2010; Sarszegi, 2012; Gehrig, 2012; Sapra, 2014; Henstridge, 2014; Wu, 2015; Salah, 2016; Kennedy, 2016; Sumegi, 2017), including the Hsp72, HDAC, PARP1 and IGF-1 pathways. Despite not having been studied extensively in the space of AD or neurodegeneration, BGP-15 has the promising potential due to its multiple mechanisms of effect that have links to AD.

This study was devised to increase Hsp72 via pharmacological intervention with BGP-15 treatment. Further, we aimed to determine the effects of this elevation on the behavioural and metabolic phenotype of the *5xFAD*Tg30* mouse model of AD. As BGP-15 has been shown to activate several pathways, this study did not rule out other mechanisms of action other than Hsp72. Hence, results did not cause perturbation when Hsp72 protein expression was found to have not significantly overexpressed in the brain via western blot analysis.

Previous studies demonstrated protective effects on dystrophic muscle wasting in a model of Duschenne muscular dystrophy with BGP-15 treatment (Gehrig 2012), so it was assessed if BGP-15 treatment could ameliorate motor deficits as seen in the *5xFAD*Tg30* mouse model. Frailty has been associated with several clinical outcomes including dementia and a more rapid cognitive decline (Avila-Funes *et.al* 2009; Montero- Odasso *et.al* 2016) which, additionally, was a part of the rationale behind assessing the effects of BGP-15 on this model. This study did not find any difference in rotarod or hangwire

performance with BGP-15 treatment. Similarly, BGP-15 did not alter any body composition. Despite promising results from the Gehrig paper, we did not see similar positive effects with the *5xFAD*Tg30* model which could be due to several reasons. The animals used in *Chapter 4* were aged to 2 months before treatment commenced, and were aged to 10 months, whereas animals used in the DMD study were administered BGP-15 at a young age (3-4 weeks). The age difference between the two models are considerable, as was the severity of the muscle phenotype. The *mdx* model of muscular dystrophy is known to cause a mild phenotype, with minimal clinical symptoms and a life span reduction of only 25% (Chamberlain *et al*., 2007; Li *et al*., 2009).

The initial use of BGP-15 came when primary studies showed its ability to increase insulin sensitivity (Literati-Nagy 2009). Since then, it has also been shown to markedly decreased olanzapine-induced insulin resistance (Literati-Nagy 2010) and ameliorate cholesterol-fed induced insulin resistance (Literati-Nagy 2014). 5xFAD*Tg30 females treated with BGP-15 had a significantly elevated oGTT curve compared to those of WT females. Similar to results in *Chapter 2* and *Chapter 3, 5xFAD*Tg30* untreated animals showed a lower oGTT curve compared to WT, in both males and females, which BGP-15 was able to elevate in females. Interestingly, BGP-15 elevated this in WT females also. As these BGP-15 effects were only seen in female animals, this suggests potential sex differences in drug efficacy. In 2008 when Chung and colleagues showed BGP-15 improved glucose tolerance (Chung et.al 2008), these experiments were only conducted in male mice. These unexpected results in *Chapter 4* strongly indicate the importance of considering both male and female animals in the experimental design for metabolic testing, as sex differences can occur. This concept is further supported by a recent review,

highlighting the possibility that metabolic responses can be altered in a sex-dependent manner (Henstridge et.al 2019). It is not clear why these sex differences have occurred in response to BGP-15, as there are no drug effects on body composition, however, it does suggest sex-specific research and/or treatments should be considered in the future.

The activity of several mitochondrial specific enzymes is also reduced in AD and has therefore encouraged the hypothesis that AD is a disease of perturbed brain energy metabolism (Blass *et al*., 2002, Gibson *et al*., 1998, Sorbi *et al*., 1983). While it was confirmed that *5xFAD*Tg30* animals have a lower lean mass adjusted VO_2 consumption, lower energy expenditure and higher RER, there were no effects of BGP-15 on any metabolic measures as seen by the CLAMS metabolic caging.

On a cellular level, mitochondrial oxidative capacity and glycolytic capacity were assessed via Agilent Seahorse XF. There were no effects of BGP-15 treatment on any key mitochondrial functions except for a trend in the increased max respiratory rate for the lowest BGP-15 dose, 5uM. Similarly, there were no effects of BGP-15 during the glycolytic stress test, except for a trend in reduced basal glycolytic basal rate for the highest BGP-15 treatment doses (50uM and 500uM). Despite no significant alterations to mitochondrial function or glycolytic capacity in neurons, these results nevertheless show BGP-15 treatment, at varying doses, is not toxic to neuronal cells.

Behaviourally, minimal research has been conducted in the space of BGP-15 treatment and cognitive decline. Research into the protective effects of BGP-15 have shown it has potential in TBI treatment to help promote the survival of neurons (Eroglu 2014), however this does not necessarily translate to working memory function. Results from

this chapter indicated that BGP-15 treatment could not ameliorate any cognitive deficits in *5xFAD*Tg30* including memory, anxiety-like behaviour, novel object recognition or spatial memory.

Interestingly, despite the improved brain weight trend with Hsp72 overexpression in *Chapter 3*, there was no effect of BGP-15 on any end-point measures. There was however, an extremely strong trend for an improved lifespan with BGP-15 treatment. While this did not reach statistical significance, a 30% mortality rate by 10 months of age was improved to a 12% mortality rate in *5xFAD*Tg30* animals treated with BGP-15 suggesting a genuine improvement.

It is critical to note the limitation of a lifespan survival study when utilizing animals with a severe phenotype. Due to welfare reasons it was not appropriate to continue to age the mice out longer than 10 months. Essentially, the consequence of this was fewer vehicle treated *5xFAD*Tg30* animals dying as they naturally would, had they been left to age out further. This may have limited the true potential of BGP-15 improving survival rates. Additionally, from 7 months of age, zero BGP-15 treated *5xFAD*Tg30* mice experienced sudden death **(Figure 4.17C)** which could suggest BGP-15 was having more of an effect as age increased- precisely when the majority of *5xFAD*Tg30-CON* mice began to die. This further suggests if the lifespan study could have been prolonged, there may have been a true effect of BGP-15 on survival.

Due to the trend in improved lifespan, which was also suggested in the Gehrig paper (Gehrig 2012), the elucidation of this protection was of interest. During the characterisation study in *Chapter 2*, it was noticed that several *5xFAD*Tg30* animals

were displaying tremor-like behaviour. As such, it was then hypothesised that spontaneous seizures could be responsible for the premature deaths of *5xFAD*Tg30* animals, and BGP-15 protected against this in males. After completing the kindling experiments, it was confirmed that *5xFAD*Tg30* males had a significantly lower threshold to reach a class V seizure, shown by a significantly reduced kindling rate compared to WT animals. Additionally, *5xFAD*Tg30* animals display significantly longer seizures and an increased seizure severity. Despite this, there were no effects on any measures with BGP-15 treatment. This suggests that seizure protection was not the mechanism of life span extension as seen in BGP-15 treatment and opens other avenues for experimentation.

In terms of AD-like pathology and previous seizure susceptibility research, it is difficult to accurately portray a model of epilepsy in AD for several reasons. There are many different types of epilepsy as well as ways to model it. The two standard ways include those that examine acute seizure susceptibility and those that examine chronic epilepsy or epileptogenic change. For this study, the second approach was used- looking at a genetic model. For the epilepsy readout, it was assessed how quickly the animal transitions from a (presumably) non-epileptic brain into a highly seizure-prone brain using the amygdala kindling model. The advantage of this model is that epileptogenesis progresses in a readily quantifiable manner, to assess which animal (either treated with BGP-15 or saline) are more susceptible to this process. Generally, via the criteria used in epilepsy research, models that are considered acceptable as seizure models are those that exhibit spontaneous seizures (Scharfman 2012). There are two such models with AD pathology that display spontaneous seizures; the hAPP and APde9 model (Palop *et.al* 2007; Minkeviciene *et.al* 2009). As with most AD research, these models display APP

overexpression and Aβ pathology, without displaying tau pathology or NFT's. Interestingly though, a post-mortem study in 2011 used a staging criterion in chronic epilepsy in relation to traumatic brain injury and hippocampal sclerosis, based on NFT's, suggesting an important link between NFT pathology and seizures (Thom *et.al* 2011). Therefore, it could be suggested, in order to sufficiently make comparisons between AD and epilepsy to identify novel opportunities for mechanistic insight and therapeutic strategies, a more advanced model is required.

On the contrary, the *5xFAD*Tg30* model, while more advanced in its pathology, did not exhibit spontaneous seizures. Kindling does, however, appear to be a beneficial and well-accepted way to model epilepsy (Scharfman 2012), which was the methods utilized in *Chapter 4.*

Chapter 4 aimed to investigate the effects of BGP-15 treatment and its resultant Hsp72 induction on the AD mouse model, 5xFAD*Tg30. It was shown that BGP-15 can be detected in the brains of animals administered the drug long-term, however this did not result in significant elevations in Hsp72.

A strong trend for increased lifespan specifically in males was observed, as well as an elevation in the glucose tolerance curve in female animals.

5. Discussion

With the rising incidence of dementia and AD in society, the need for identifying potential targets for therapeutic benefits in the disease is increasingly necessary. It is also imperative that pre-clinical models accurately mimic human pathology associated with AD, in order to study the pathological hallmarks, underlying cellular processes and provide a realistic model for pharmacological trials.

Since their discovery almost 60 years ago, HSP's have been implicated in numerous physiological processes and disease states including in cardiovascular disease, diabetes and obesity research, neuroscience, mitochondrial function, cell survival and inflammation to name a few. HSP's, in particular for this thesis Hsp72, play a pivotal role in cellular homeostasis, and we are only just beginning to appreciate the importance of its role in repairing and/or removing damaged or aggregated proteins in the space of AD. This thesis aimed to address the effects of increasing Hsp72 on a dual pathological mouse model of AD, via transgenic overexpression as well as pharmacological overexpression. Together, these experiments have furthered our understanding on the therapeutic potential of Hsp72, long term BGP-15 treatment, and the use of the *5xFAD*Tg30* mouse model of AD. Specifically, we found:

1. Reproducibility from the Heraud et al. study in that the *5xFAD*Tg30* model, is characterised by early death, rotarod impairment and APP/tau protein expression.
2. The *5xFAD*Tg30* model contains a severe motor phenotype as evidenced by altered gait (DigiGait analysis), hangwire test (muscular endurance) and swimming velocity (muscular power).
3. While complicated by the motor phenotype, the *5xFAD*Tg30* model has signs of initiation of cognitive deficits particularly in regard to fear/anxiety testing.

4. The *5xFAD*Tg30* mice are smaller in stature. They have lower body weight, fat mass, lean mass, and smaller organs such as skeletal muscle, brain, liver and tibia length. The decreased muscle size if a likely mechanism for the impairments in rotarod, hangwire and swim velocity tests.
5. The *5xFAD*Tg30* model has an increased seizure susceptibility and severity.
6. The *5xFAD*Tg30* model displays a distinct plasma lipidomic signature, characterised by alterations in lipids such as total free fatty acids, total phosphatidic acid, total phosphatidylcholines, total sphingomyelin, total sphyingolipids, total diacylglycerol and total triacylglycerol.
7. Hsp72 Tg overexpression reduced fear/anxiety as evidenced by the elevated plus maze data and while not statistically significant, half the number of *5xFAD*Tg30*Hsp72 Tg* mice had died before endpoint as compared to the number of *5xFAD*Tg30* mice. Male *5xFAD*Tg30*Hsp72 Tg* mice maintained their lean mass with aging compared to *5xFAD*Tg30* mice.
8. BGP-15 treatment did not activate Hsp72 in the brain. *5xFAD*Tg30* mice were more likely to survive to endpoint on BGP-15 with 1 mouse every 3.3 mice dying if untreated and 1 mouse every 8.5 mice dying if treated with BGP-15.

These findings indicate that Hsp72 overexpression is not adequate to fully protect against the resultant phenotype of a model with severe AD pathology. BGP-15 showed it has the potential to increase survival in our model, but this finding was independent of Hsp72 brain overexpression. Additionally, this thesis provides extensive new insights into the relatively unknown *5xFAD*Tg30* mouse model. In this chapter, we discuss the implications of these findings, with recommendations for future directions.

5.1 The *5xFAD*Tg30* Model

The use of transgenic mouse models in the space of AD has been an interesting journey. Since the 1990's the leading hypothesis for the development of the disease has been involving Aβ deposits aggregating in the brain and brainstem. Consequently, therapeutics have been attempting to target the removal or impeding the development/aggregation of these plaques; however, until 1995, no animal models were available to test such therapeutics. In 1995, a transgenic mouse carrying a single gene mutation associated with the less common, inherited form of AD was successfully developed (Games *et.al* 1995). Since then, several models of AD have been developed using genetic mutations from familial AD, but with stark limitations. While transgenic models can provide great insights to the disease, they do not reflect the entire biology of the human condition. According to the amyloid cascade hypothesis, the hyperphosphorylation of tau and its aggregation occurs post Aβ cleavage, yet transgenic animals expressing mutated APP and/or PS1 gene(s) do not develop NFT's like in human AD (Boutajangout *et al*., 2004). To combat this, dual pathological transgenic models began to be developed, modelling both amyloid and tau pathology, including the Tg2576/JNPL3 cross, hAPP (Swe)/wildtype human Tau and the 3xTg-AD mouse. Despite these models expressing both amyloid and tau, they have been described as slow developing and relatively modest. Additionally, they may lack the PS1 gene (Paulson *et al*. 2008, Perez *et al.* 2005, Seino *et al*. 2010, Terwel *et al.* 2008) and still do not develop NFT's.

In 2014, Heraud and colleagues developed and published a new model named *5xFAD*Tg30* where in-depth pathological analysis showed transgenic animals expressing NFT's, phosphorylated tau and Aβ pathology. This model was not fully characterised, in terms of its cognitive and holistic phenotype, hence the first chapter of

this thesis (and aspects of *Chapter 3* and *4)* aimed to extensively further characterise the *5xFAD*Tg30* model and extended this to female animals to investigate any sex differences.

In agreement with the Heraud study, we observed a significant rotarod impairment from 6 months of age onwards **(Figure 2.1)** and we were able to further confirm a gross motor control and strength phenotype via conducting Hangwire test, swim velocity and DigiGait analysis. We observed a significant impairment on the Hangwire test which was performed at 8 and 10 months of age **(Figure 3.1)** with these results being consistent at these age points given the rotarod findings. Interestingly, the DigiGait analysis gave us deeper insights into the gait of the *5xFAD*Tg30* which showed impaired performance at 5 months, prior to rotarod performance being impaired. In depth analysis showed us swing duration, propulsion and speed frequency were significantly different between *5xFAD*Tg30* and WT-control, indicating a weaker, impaired gait **(Figure 4.12).**

The impaired rotarod performance and reduced motor phenotype could be attributed to the tau mutation, which is known to cause progressive motor impairment with neurogenic muscle atrophy (Leroy 2007). While no other publications have assessed body composition on the *Tg30* model, Leroy and colleagues showed severely reduced cross-sectional areas of muscle fibres and severe muscle atrophy in their hindlimbs which extended to their axial muscles and forelimbs. Impaired performance stemming from the *Tg30* mutation is further supported by the data from Heraud in 2014 showing rotarod performance was significantly worse in *Tg30* than *5xFAD*, however was compounded further in the double *5xFAD*Tg30*. As we know from the Heraud study, there is a reduced Aβ load in the *5xFAD*Tg30* compared to *5xFAD*, and a higher tau load compare to *Tg30*. Together, these indicate that the combined tau and amyloid pathology accelerates the

motor deficits of the *5xFAD*Tg30*. This may additionally indicate that a good model of AD would incorporate frailty, as this is a common symptom in AD patients and data has suggested an association between these two conditions. Recent studies have shown cases of frailty impacted several clinical outcomes including dementia and a more rapid cognitive decline (Avila-Funes *et.al* 2009; Montero- Odasso *et.al* 2016) suggesting that AD and/or dementia and frailty share some type of common biological mechanism or etiology. Complementing this finding is a study of 165 older persons with AD pathology post-mortem, which demonstrated their last frailty test was associated with AD pathology, but was not related to other common age-related pathologies such as the presence of cerebral infarcts or Lewy body disease (Buchman *et.al* 2008). These findings raise the possibility that AD pathology may be a contributing factor to frailty or that frailty and AD pathology share a common etiopathogenesis. Therefore, a common physiological mechanism that could be targeted for both conditions concurrently would be optimal.

A similar consequence is the severe reduction in body weight due to a reduced lean and fat mass **(Figure 2.7)**. The lean mass effect, again, likely can be attributed to the neurogenic muscular atrophy seen in the Tg30 model, however, compounded by the added amyloid pathology. In agreeance with Heraud, we found a 60-70% survival rate of *5xFAD*Tg30* animals out to 10 months of age, with early death suggested by Heraud and colleagues to be related to their severe motor deficits.

We however, through close observation, suggested the early death could be associated with spontaneous seizures. Consequently, we performed several experiments to investigate this hypothesis and while we were unable to observe spontaneous seizures, we indeed found that *5xFAD*Tg30* mice have a severely reduced kindling rate, indicating

greater susceptibility to seizures. Additionally, we discovered *5xFAD*Tg30* animals displayed significantly more severe and lengthier seizures **(Figure 4.18).**

There has been previous evidence that alterations in phospholipids (Goodenowe *et.al* 2017; Igarashi *et.al* 2011; Mapstone *et.al* 2014), plasmalogens (Han *et.al* 2001), ceramides (Cheng et.al 2010), gangliosides (Yamamoto *et.al* 2004) and sulfatides (Han *et.al* 2002; Cheng *et.al* 2011) occur in AD, as well as alterations associated with AD pathogenesis observed in the blood (Mapstone *et.al* 2014; Chatterjee *et.al* 2016; Whiley *et.al* 2014). Because of this and a recent study published on AD patients showing distinct plasma lipidomes (Huynh *et.al* 2020) we aimed to recapitulate this in *5xFAD*Tg30* animals. Through in-depth plasma lipid analysis, we demonstrated that indeed *5xFAD*Tg30* too, have a distinct plasma lipidome signature **(Figure 2.13-2.14).** While we were not able to recapitulate every aspect of the comprehensive lipidomic analysis from Huynh and colleagues, we supported their findings that Ether classes were negatively associated with AD (Huynh *et.al* 2020).

Limitations and considerations

During the behavioural characterisation of the *5xFAD*Tg30* model, it became apparent that there were complications assessing markers of cognition due to the confounding nature of their motor phenotype. While we potentially saw the initiation of cognitive deficits, through the Y-Maze **(Figure 2.3)** and Large Open Field **(Figure 2.4)** the early death and severe motor impairments make it difficult to establish this fully as we could not age the mice out longer as it was necessary from an animal welfare perspective to

cease the study by 10 months of age. The Y-Maze data suggested impaired memory recognition as *5xFAD*Tg30* trended to spend less time in the novel arm, however, this assessment requires movement which is reduced. Additionally, the Large Open Field showed significant genotype differences, which could suggest impaired reasoning due their inability to recognise the centre of an exposed area as a vulnerable location. However, strong considerations need to be made as part of experimental protocol, animals are initially placed in the middle of the arena. Considering *5xFAD*Tg30* animals have limited movement, they may not be as competent at removing themselves from this area regardless of if they could recognise danger. This motor phenotype limitation was evident during the MWM experiments **(Figure 2.6).** At 8 months there was a significant genotype difference in the latency to the platform, however the learning curve between the genotypes were almost identical. When investigated further, we showed it was indeed due to a significant decrease in swim velocity, due to the motor phenotype.

Despite the description of the brain pathology of the *5xFAD*Tg30* being more human-like in the Heraud paper, it was evident throughout our characterisation study that the cognition phenotype was not going to display all human AD traits. Many other AD models require the animal to be aged to at least 12 months (some even 18months – 2 years) before cognitive deficits can be seen, which could not be repeated in our studies due to early death and ethical considerations for the animals' welfare. Another consideration could be the type of experiments that were being conducted, particularly the MWM as an aversion test. Considering this, as well as ethical and safety considerations for the animal, we utilised a Cheeseboard maze to assess spatial memory and learning through a reward paradigm, in *Chapter 3*. Despite moving from aversion to reward-based analysis, this test still requires motor ability, and results were hampered.

Moving forward from *Chapter 2*, we attempted to alleviate these confounding factors as much as possible, by substituting in tests that assessed similar cognitive traits, but with smaller arenas. We believed the tests used were able to give a thorough overall assessment of cognitive deficits, should the animal be capable of movement, and this was evidently the limitation. It is worth noting that rotarod performance was not different until after 6 months of age, therefore any behaviour analysis performed prior to 6 months was not impacted by any motor phenotype. This confounding factor was unexpected when initially embarking on this project, as only one previous paper has been published on the *5xFAD*Tg30*, which did not include extensive behavioural characterisation. This demonstrates the reoccurring limitation of recapitulating AD pathology accurately, while also displaying significant behavioural deficits.

As mentioned, while brain pathology displayed similar characteristics to human AD brain pathology, whole body phenotype and cognition cannot be accurately mimicked in the *5xFAD*Tg30* model. However, evidence from our seizure study suggests that further investigation into the use of this model for epilepsy research is warranted. The prevalence of epilepsy in patients with AD is 10-fold higher than the age-matched general population, and up to 64% of AD patients will develop at least one unprovoked seizure (Hauser 1986; Risse 1990). Data suggests that pathology seen in AD, through unknown mechanisms, increases seizure susceptibility in human patients, which we were further able to support using the *5xFAD*Tg30* model. It has previously been suggested that the mechanisms of neuronal hyperexcitability as a consequence of Aβ or phosphorylated tau accumulation, as well as the structural changes in cortical and hippocampal regions are strongly involved in the link between AD and epilepsy (Miranda 2014). Despite evidence from population-based and observational studies, as well as studies using animal models that show this

significant susceptibility (Jenssen *et.al* 2010; Friedman *et.al* 2012; Ziyatdinova *et.al* 2011; Hommet *et.al* 2007), very little is known about the actual relationship between the two disorders. Due to this limitation in scientific knowledge, therapeutics for seizure control specifically in those with AD are not currently available and therefore treatment options are limited to traditional anti-epileptic drugs (AED). This poses problems due to the vulnerability of AD patients in terms of adverse effects of drugs with central nervous system activity, drug interactions and co-morbidities such as depression (Jenssen *et.al* 2010; Belcastro *et.al* 2007; Cumbo *et.al* 2010). Currently, the guidelines for choosing the best medication for AD patients with epilepsy is not succinct, with the choice of AED's made relatively empirically. Further research into the associated relationship of AD and epilepsy, perhaps using the *5xFAD*Tg30* model could help with biomarker discoveries, neurophysiological findings or potentially lead to improved guidelines for treating epilepsy in AD.

As discussed in *Chapter 4*, there are many ways to model epilepsy in animals. For this study, we looked at a genetic model and assessed how quickly the animal transitions from a (presumably) non-epileptic brain into a highly seizure-prone brain using the amygdala kindling model. There are additional models available with AD pathology that, unlike the *5xFAD*Tg30* model, display spontaneous seizures; the hAPP and APde9 model (Palop *et.al* 2007; Minkeviciene *et.al* 2009). However, as with most AD research, these models display APP overexpression and Aβ pathology, without displaying tau pathology or NFT's. Recently, a study was presented using the 3xTg model to assess seizure susceptibility (Vyver *et.al* 2020). The 3xTg model expresses APP/PS1/tau and has a closer AD-like pathology than previous Aβ only expressing models (Oddo *et.al* 2003). Similar to our findings, the 3xTg model demonstrated increased seizure susceptibility as

well as resistance to ASD's (Vyver *et.al* 2020). Future research should be conducted with a range of genotypes; WT, Aβ only expressing, tau only expressing and a double transgenic. Further, investigating the histology of these animals could be beneficial, to assess an association between the speed of kindling and Aβ/tau burden. It would also be interesting to preform seizure susceptibility experiments over the lifetime of 3xTg or *5xFAD*Tg30* mice- to assess if seizures are more inducible during the whole life of the animal.

While this area was not an initial aim of this thesis, through the thorough characterisation of the *5xFAD*Tg30* model, we have shown a robust candidate for a potential new epileptic-AD mouse model.

We have also shown the *5xFAD*Tg30* model has the potential to be a good model for certain aspects of AD, such as pathology (as seen in Heraud *et.al* 2014), frailty and early death. However, limitations exist for longer term cognitive studies due to the motor phenotype and early death.

5.2 Chaperoning to the Alzheimer's party: genetic targeting of Heat Shock Protein 72

Since its discovery, HSP's, specifically Hsp72, have been investigated actively due to their role as molecular chaperones and maintaining homeostasis in stress induced cellular environments. More recently, the role of Hsp72 has become a popular area of interest in the scope of neurodegeneration and treating AD. As AD is hypothesised to be characterised by the accumulation and aggregation of misfolded Aβ and tau proteins, the use of HSP's in their potential refolding and/or removal is of great interest.

Chapter 3 aimed at overexpressing Hsp72 genetically, driving elevated levels in the brain. Further, we aimed to determine the effects of this overexpression on the behavioural and metabolic phenotype of the *5xFAD*Tg30* mouse model of AD.

There were several ways to measure the efficacy of Hsp72 overexpression on the *5xFAD*Tg30* model. After confirming Hsp72 was indeed overexpressed in the brain of *5xFAD*Tg30* animals **(Figure 3.1)**, we then performed comprehensive cognitive experiments throughout their lifespan. As mentioned as part of *Chapter 2*, this measure of efficacy had its challenges, as cognition could not be accurately assessed due to the severe motor phenotype. Despite this, we saw a treatment effect on anxiety-like behaviour at 9 months during the elevated plus maze, which demonstrated a rescue in the suggested inability for *5xFAD*Tg30* animals to recognise dangerous/vulnerable situations **(Figure 3.8).** This rescue appeared to be more apparent in females **(Figure 3.8 C),** where female *5xFAD*Tg30*Hsp72 Tg* animals spent more time in the *closed arm* of the maze than *5xFAD*Tg30* mice.

Body composition and metabolic measures were assessed extensively, and we showed a slight rescue in lean mass for male *5xFAD*Tg30*Hsp72 Tg* animals, at the later stages of life once muscle atrophy appeared to develop **(Figure 3.11 E).** This improvement in lean mass did not however, translate to an improved rotarod **(Figure 3.4 A-C)** or hangwire **(Figure 3.4 D-F)** performance, which was an indicator of gross muscle strength and control. Hsp72 overexpression showed no significant effects on metabolic measures including VO_2, energy expenditure **(Figure 3.13)** or glucose tolerance **(Figure 3.12)**.

Interestingly, survival trended to improve with Hsp72 overexpression **(Figure 3.16)**, which correlated with a trend in improved brain weight, specifically in males **(Figure 3.15 B)**. Longer lifespan has previously been correlated with Hsp72 overexpression (Salway 2011), so the trend seen in *Chapter 3* could support this principle. Additionally, as Hsp72 overexpression has been shown to prevent neuronal apoptosis (Mailhos 1994), perhaps the trend in improved brain weight indicated lower neuronal loss and therefore premature death of the animal. Further research into the mechanisms of improved lifespan are warranted.

Considerations and Limitations

The largest limitation from *Chapter 3* is the lack of histology measuring amyloid and tau burden. Considering much of the rationale of using Hsp72 overexpression came from its positive effects in Aβ clearance, it is impossible to determine if Hsp72 overexpression had an effect pathologically on the *5xFAD*Tg30* model as this was not measured (due to COVID-19 restrictions). It is possible that Hsp72 overexpression had an impact on Aβ burden but did not translate to substantial behavioural/metabolic effects. COVID-19

lockdown laws in Melbourne prevented lab work for all non-essential research to be conducted for the majority of 2020, which prevented these data from being collected.

Much of the previous research from Hsp72 overexpression was in Aβ models or *in vitro* and it is possible that Hsp72 overexpression simply was not sufficient to overcome the extreme pathology associated with the *5xFAD*Tg30* model. As described in Heraud and colleagues' paper (Heraud et.al 2014), the *5xFAD*Tg30* mouse develops severe pathology, rapidly- much faster than standard AD models. Despite marked overexpression of Hsp72 in the brain, it is possible that the severity of pathology and its resultant phenotype was too harsh to alter. Possible future research could cross the 3xTg model with a Hsp72 Tg model, to assess Hsp72 overexpression in a less severe Aβ/tau model. This of course still has its limitations as it does not develop NFT's and is slower developing, however could still offer insights into elevated Hsp72 levels in the presence of Aβ and tau pathology.

A secondary promising effect of Hsp72 overexpression was its previous positive effects in skeletal muscle (Henstridge *et.al* 2014; Gehrig *et.al* 2012). While we showed signs of positive effects in lean mass in *5xFAD*Tg30*Hsp72 Tg* animals, this did not translate to improved motor performance. From previous knowledge, we know the motor effect comes primarily from the *Tg30* mutant, as it develops severe neurogenic muscle atrophy and axonopathy (Leroy et.al 2007). We know that Hsp72 Tg animals overexpress Hsp72 in muscle and brain (Marshall *et.al* 2018), but considering atrophy is neurogenic, there is the possibility that Hsp72 is needed in nerve cells to create this effect. It is well known clinically that muscle atrophy is associated with a severely reduced life expectancy (Wannamethee *et.al* 2007), which we were able to recapitulate in the *5xFAD*Tg30*

model, yet there are no drug treatments available, suggesting the complex relationship between the brain, muscle and nerves. Currently, exercise and increased protein intake are the intervention options available to slow the progression of neurogenic muscle loss (Sepulveda *et.al* 2015; Garber 2016), so it could be interesting to assess regular exercise trained animals and/or a high protein-fed cohort of *5xFAD*Tg30* mice.

5.3 BGP-15: are multi-mechanistic drugs the answer?

The race for scientists to find a therapeutic target that not only treats but slows down the progression and/or prevents AD has been challenging and multi-faceted. While it is well established that patients with AD experience mild-severe cognitive deficits, such as early-stage memory loss (Panegyres 2004), patients may also exhibit a range of other symptoms such as psychological symptoms (Ropacki *et.al* 2005, Shimabukuro *et.al* 2005), and attention deficits (Perry *et.al* 1999). Visuospatial deterioration (Cronin-Golomb *et al* 1995) and extreme motor dysfunction become more pronounced during the late stages of the disease (Suva *et al* 1999). The sophisticated nature of the disease may suggest the need for a multi-targeted approach, that has shown positive effects not only on cognition, but also on a holistic level.

BGP-15 is a nicotinic amidoxime derivate, developed as a Hsp72 co-inducer and has since been used by many research groups for its effects on a wide range of diseases and conditions (Peto *et.al* 2020). *Chapter 4* aimed at targeting Hsp72 via the co-induction using BGP-15 and investigating this long-term pharmacological treatment on the cognition, behaviour and metabolism of the *5xFAD*Tg30* model. We found that, despite knowledge of BGP-15 reaching the brain (unpublished data from developers, N-Gene), which we recapitulated **(Figure 4.1A, B)** -BGP-15 did not drive overexpression of Hsp72 in the brain. Due to its multi-target effects that have associations with AD, the long-term use of BGP-15 was nevertheless explored.

Similar to *Chapter 3*, there were several ways to measure the efficacy of BGP-15 treatment. Behaviourally, long-term administration of BGP-15 did not alter cognition or

behaviour via any measures, such as memory function **(Figure 4.5-4.6)**, anxiety-like behaviour **(Figure 4.7-4.8)**, novel object recognition **(Figure 4.9)** or spatial memory and learning **(Figure 4.10)**.

As BGP-15 treatment has previously shown positive effects against dystrophic muscle wasting in a model of Duschenne muscular dystrophy (Gehrig *et.al* 2012), we assessed if any measures of body composition or gross motor strength were affected. There were no treatment effects on lean muscle mass **(Figure 4.13 D-F)** which correlated to no effects on motor strength/control via the rotarod and hangwire tests **(Figure 4.4)**. To assess these deficits closer, we looked at gait analysis via the DigiGait analysis software which demonstrated a reduced swinging paw and lower propulsion **(Figure 4.11-4.12)**. This suggested at 5 months of age, impaired gait is prominent, however *5xFAD*Tg30* animals are able compensate for these weaknesses as shown by rotarod impairment only being detected at 6 months. BGP-15 treatment did not affect the gait of *5xFAD*Tg30* animals.

Metabolically, results were interesting. Despite BGP-15 not altering body composition **(Figure 4.13)** or metabolic caging analysis **(Figure 4.15)**, BGP-15 appeared to worsen the glucose tolerance of female animals, both WT and *5xFAD*Tg30* **(Figure 4.14).** This raised the importance of the use of different sexes in pre-clinical studies, as sex effects can play a role in metabolic processes.

Interestingly, like *Chapter 3* survival trended to improve with BGP-15 treatment (although, independent from Hsp72 overexpression) and in a male-specific fashion **(Figure 4.17)**. Longer lifespan has previously been correlated with BGP-15 treatment (Gehrig *et.al* 2012), but its mechanisms have not been elucidated. As a result, we then hypothesised spontaneous death was caused by spontaneous seizures, in which BGP-15 could have protective effects against. An extensive seizure study was then conducted,

which demonstrated, as previously mentioned, severe susceptibility to seizures in the *5xFAD*Tg30* mice, however, with no protective effects from BGP-15 treatment **(Figure 4.18-4.19)**.

Limitations and considerations

Similar to *Chapter 3* limitations and considerations, it is evident that for *Chapter 4* there is the lack of histology measuring amyloid and tau burden. While BGP-15 itself has not been researched in the context of AD, many pathways it is implicated with have. Considering this, it is impossible to determine if BGP-15 treatment had an effect pathologically on the *5xFAD*Tg30* model as this was not measured (due to COVID-19 restrictions). It is possible that long-term administration had an impact on Aβ/tau burden but did not translate to substantial behavioural/metabolic effects.

A large consideration was BGP-15 failing to co-induce Hsp72 overexpression in the brain **(Figure 4.1).** Despite showing a significant concentration of BGP-15 in both plasma and brain tissue of both genotypes **(Figure 4.24-4.25)**, this did not translate to overexpression of our protein of interest, Hsp72. There are several considerations for this- we know the drug passes through the blood brain barrier, but it remains unclear how, or how much would be required to effect expression levels. It is possible that BGP-15 requires a further cellular assault, to co-induce the Hsp72 expression pathway- and we saw signs of this with the trended increased expression in *5xFAD*Tg30* animals compared to WT **(Figure 4.1).** A secondary stressor, perhaps elevated temperature could be tested together with BGP-15 treatment. While BGP-15 was found in the brain tissue, we were not able to analyse which specific cell types its accumulated in.

Another consideration could be the relevance of dosing. We used a dose (100mg/kg/day) which was recommended by the developers of the drug which was previously shown in Wistar Rat studies to lead to elevation of BGP-15 in the brain. Previously, BGP-15 has increased tissue insulin-sensitivity in different animal models of metabolic disorders at 10–30 mg/kg doses (Literati-Nagy *et.al* 2014; Chung *et.al* 2008). In other disease settings, a 10-day treatment of BGP-15 at a dose of 40 mg/kg per day to Sprague-Dawley rats improved diaphragm muscle fibre function (Ogilvie *et.al* 2016). To compare, Gehrig and colleagues used a dose of 15 mg/kg per day to improve muscle strength and endurance in *mdx* transgenic mice (Gehrig *et.al* 2012). In contrast to this dosage, Sapra and colleagues demonstrated at a 15mg/kg dose, BGP-15-treatment did not alter the levels of Hsp70 in the myocardial tissue, however, did increase the phosphorylation of IGF1R (Sapra *et.al* 2014).

In the clinical setting, BGP-15 has entered clinical phase I–II as an insulin-sensitizer and proved to increase tissue insulin-sensitivity in 200 mg/day and 400 mg/day doses (Literati-Nagy *et.al* 2009). Dosing used in *Chapter 4*, led to BGP-15 in brain tissues, but whether this concentration is most effective is unknown. Unlike in *Chapter 3* with tissue specific Hsp72 Tg overexpression (expressing in heart, muscle and brain), BGP-15 is not tissue specific. So as with any drug, there is also the possibility that it could have off target effects in other tissues.

There are several other critical considerations whenever a therapeutic strategy has not been effective. Perhaps the dosing of BGP-15 did not begin early enough, and a window of efficacy was missed. Genetic models, by their nature have a substantial amount of pathology, and it can take a lot to intervene in that process. From *Chapter 1,* we saw that phenotypically, genotype effects were not apparent until 6 months of age. Therefore,

dosing from 2 months of age seemed appropriate, however there is the possibility that too much damage was already done pathologically in the first 2 months of life. It would be beneficial for time-point experiments to be conducted, showing pathology with and without BGP-15 treatment from birth onwards. Additionally, it is possible that the Hsp72 regulator was impaired and therefore BGP-15 couldn't induce an effect.

It was evident from our lifespan study that there was a trend of BGP-15 on longevity of the *5xFAD*Tg30* animals **(Figure 4.17, p=0.07)**. Despite not reaching statistical significance using the tests we used, there is a strong trend for survival which must be considered. Within our limits and resources, and the way the analysis is measured (via a Kaplan Meir survival curve) we attempted to flesh out this trend as much as possible. Our biggest limitation was ethical standards- if we had the flexibility to continue to a later timepoint (further than 10 months) it is likely that there would have been greater effects seen. BGP-15 treated *5xFAD*Tg30* animals were ethically required to be culled at 10 months, despite most of them not reaching care form requirements. Many saline treated *5xFAD*Tg30* animals were on care forms at the time of end point, whom would have added to the statistical power had they been left past the required end point. It could be warranted to repeat a longevity study with perhaps the *Tg30* single mutant, whom also has a reduced lifespan but is not as severe as the double *5xFAD*Tg30* line and could therefore potentially be exposed to a longer experimental period.

5.4 Concluding remarks

In summary, the data presented in this thesis demonstrates the complexity of AD mouse models and has expanded our understanding of the phenotype of an Aβ model in the presence of tau pathology. We have extensively characterised the *5xFAD*Tg30* model as well as described its potential to be a mouse model of epilepsy with AD pathology. Future work on AD mouse models should continue exploring models that closely mimic the pathology as seen in human brains, as well as contain behaviour phenotypes such as memory loss, cognitive deficits and frailty- accurately mimicking the human form of disease.

These studies further provided insight into targeting Hsp72 both genetically and pharmacologically in the context of mouse behaviour and metabolism, as well as lifespan and muscle mass/strength and control. Future work should investigate the role of Hsp72 and BGP-15 on a less severe, Aβ/tau model using similar methods as presented here, investigating the model holistically including pathology, lipidomic profile, behaviour, metabolism and lifespan.

Supplementary Diagrams

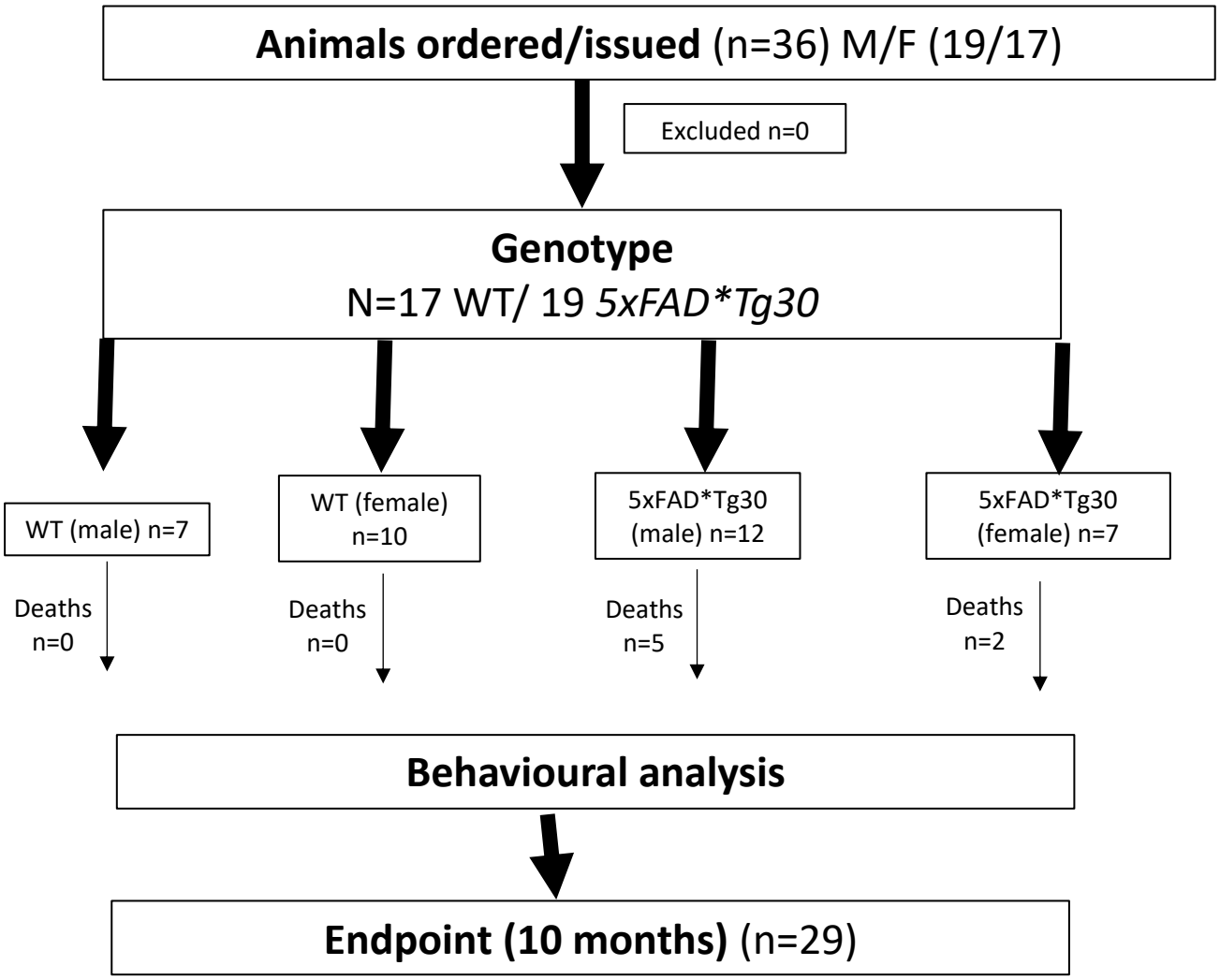

Supp.1: ***Animal flow chart of Chapter 2 behavioural cohort***

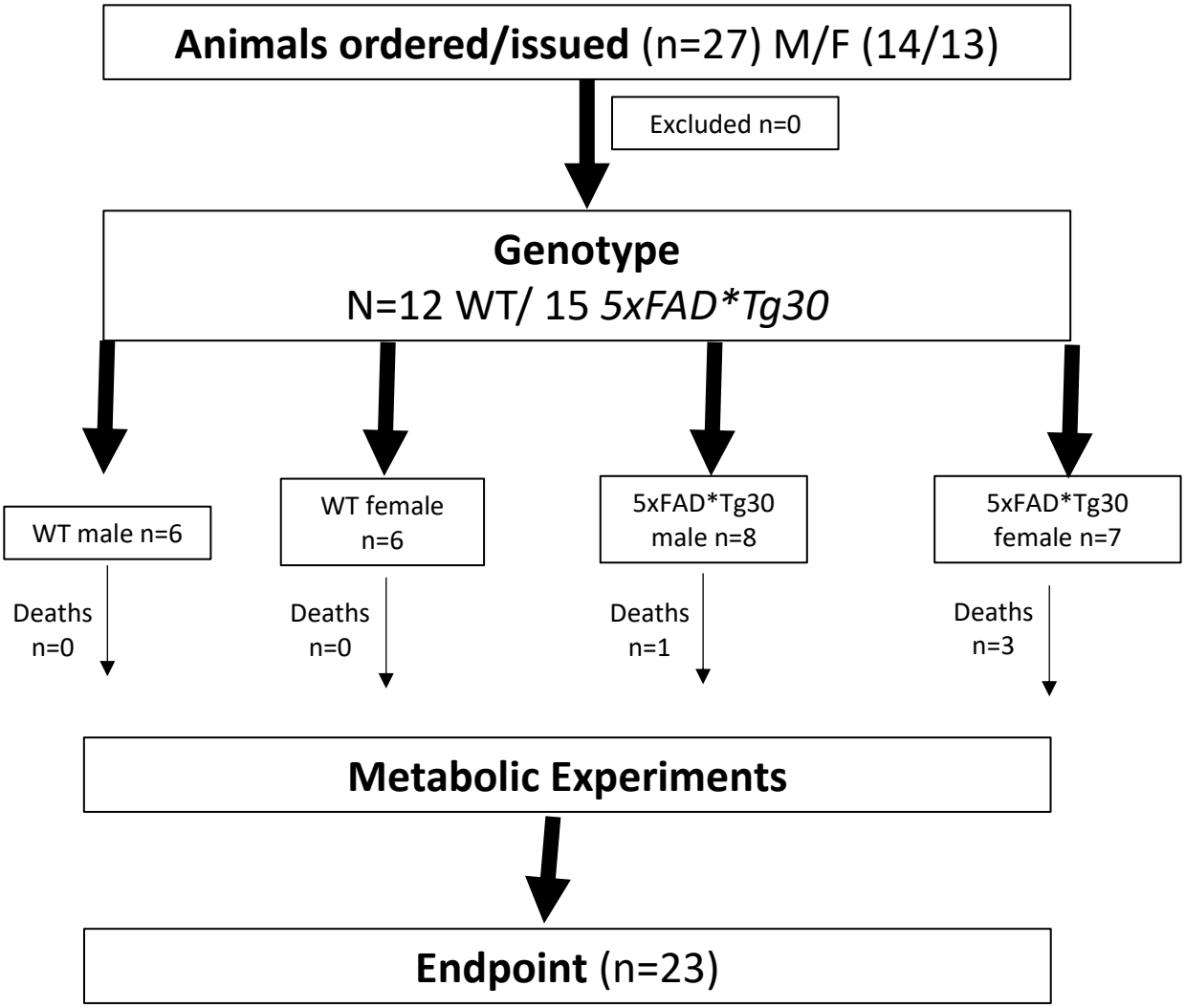

Supp.2: ***Animal flow chart of Chapter 2 metabolic cohort***

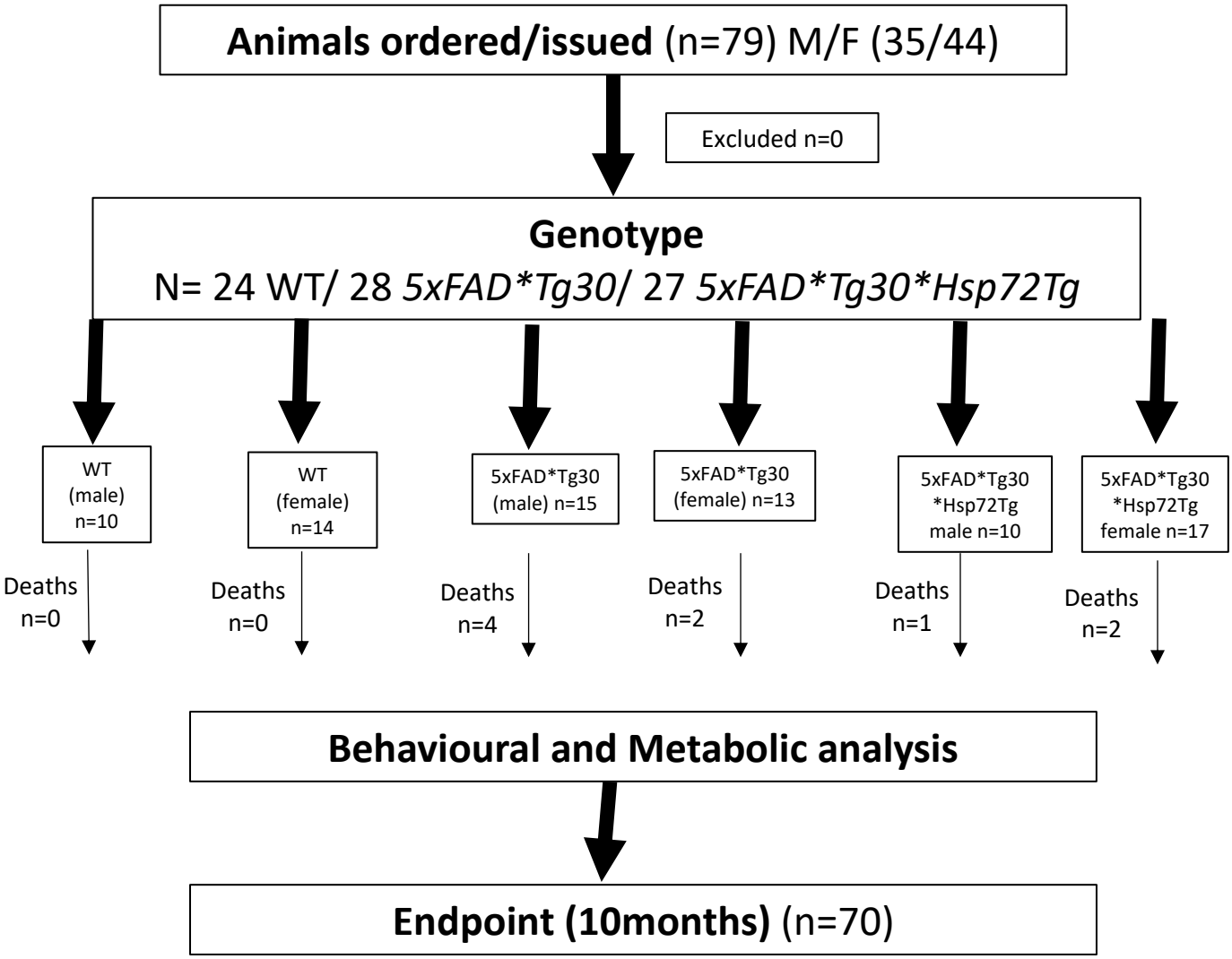

Supp.3: ***Animal flow chart of Chapter 3***

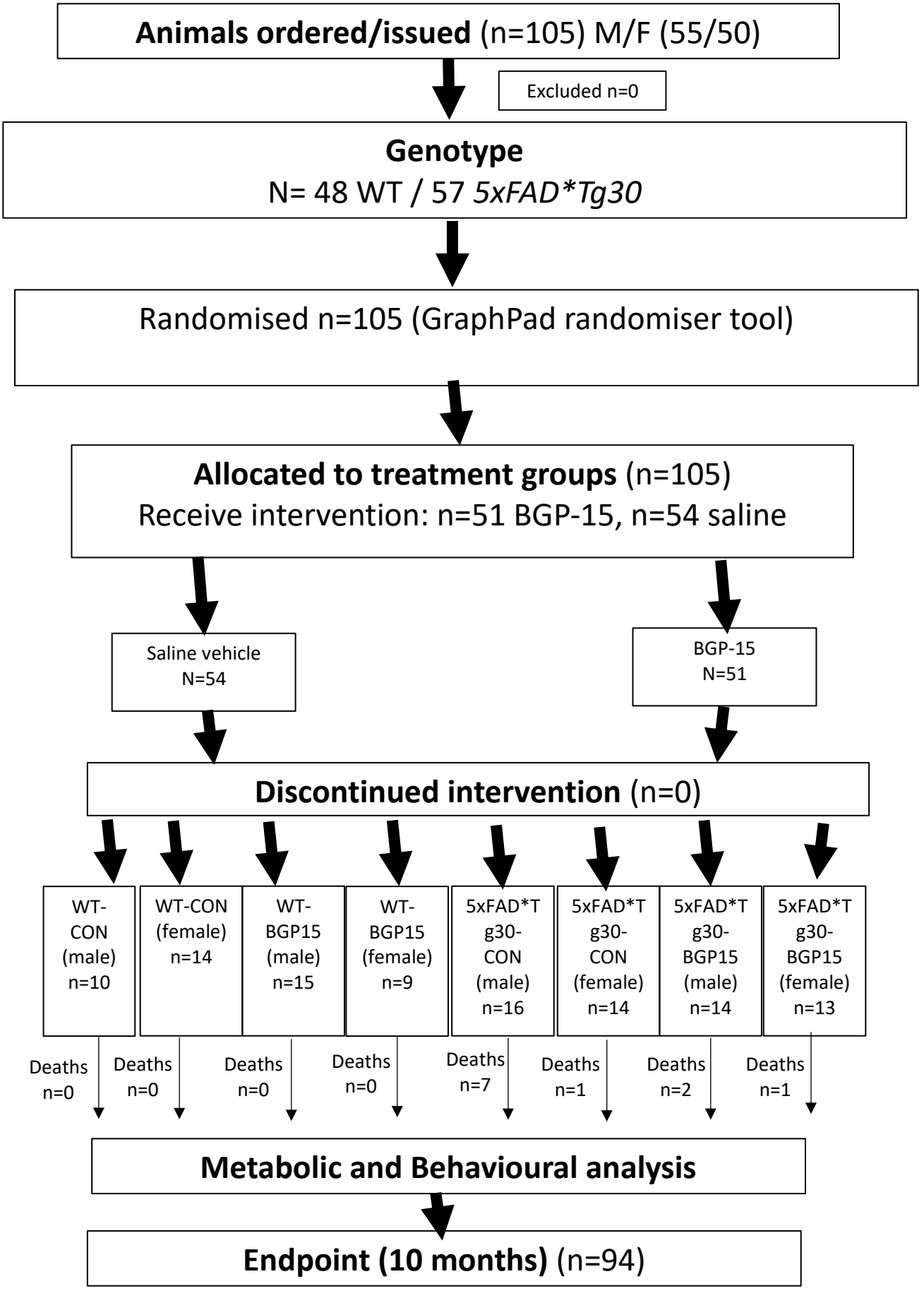

Supp.4: ***Animal flow chart of Chapter 4***

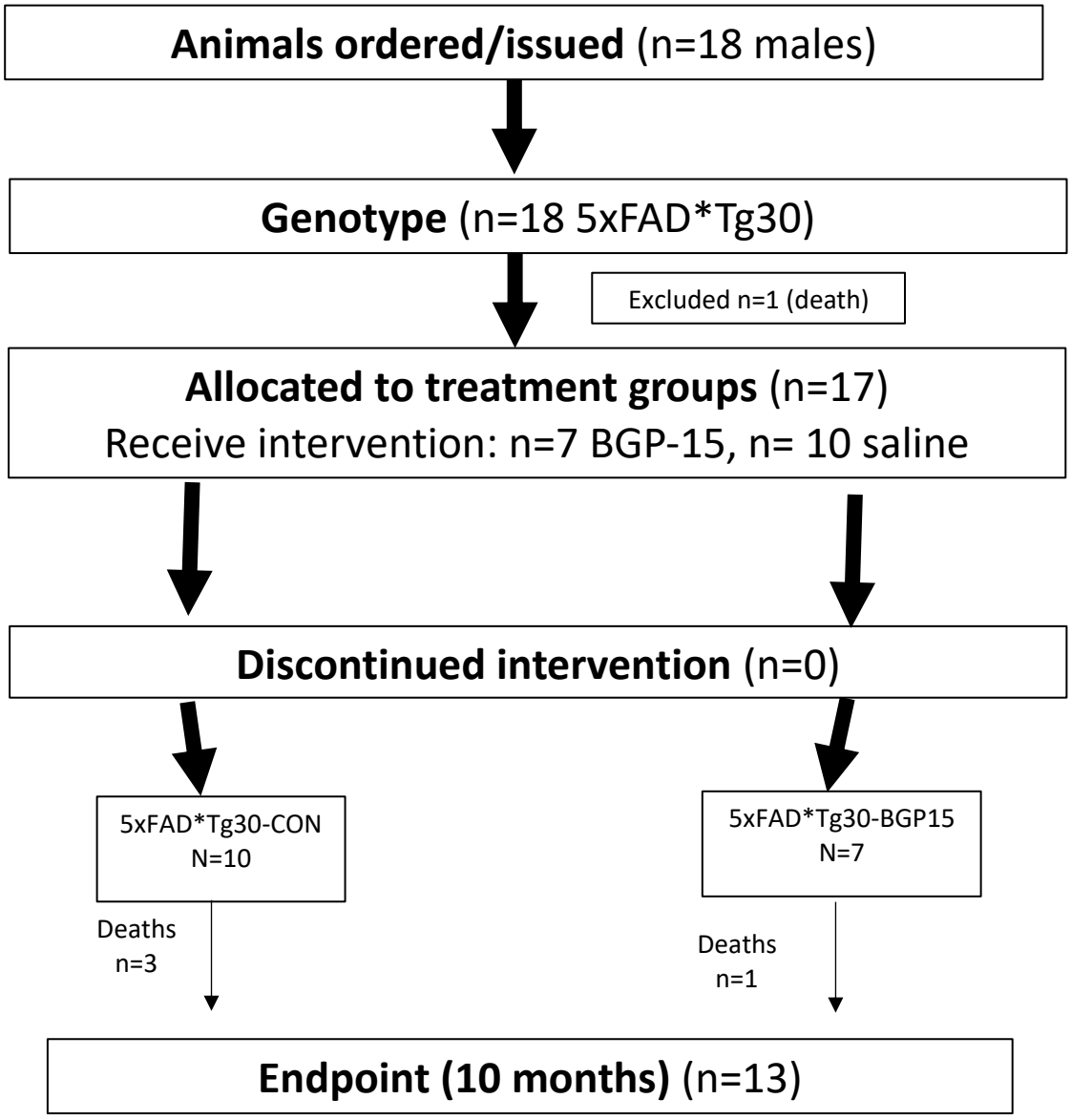

Supp.5: ***Animal flow chart of Chapter 4 repeat lifespan study, added to survival curve analysis***

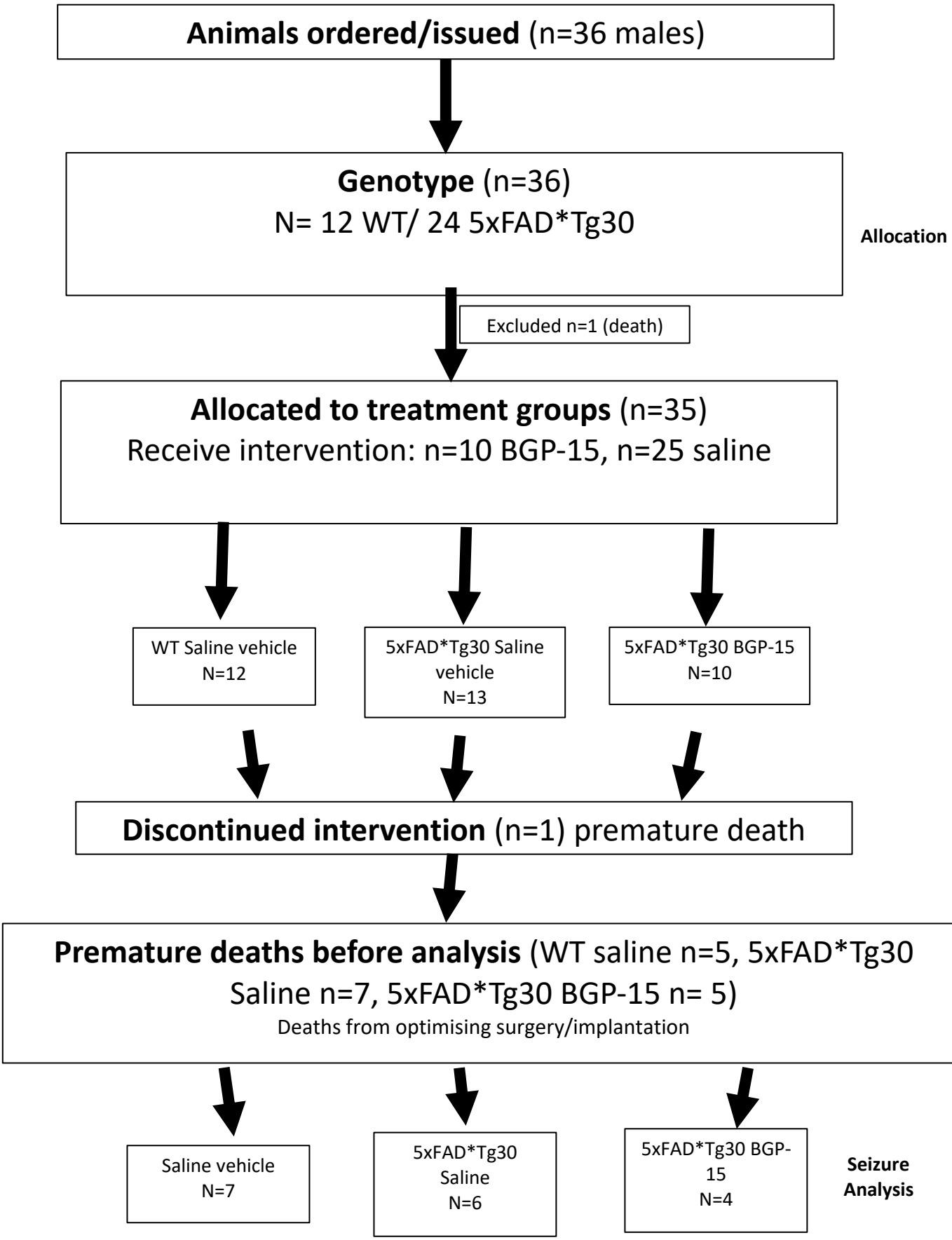

Supp.6: ***Animal flow chart of Chapter 4 seizure study***

Reference List

ABETI, R., ABRAMOV, A. Y. & DUCHEN, M. R. 2011. Beta-amyloid activates PARP causing astrocytic metabolic failure and neuronal death. Brain, 134, 1658-72.

ADACHI, H., KATSUNO, M., MINAMIYAMA, M., SANG, C., PAGOULATOS, G., ANGELIDIS, C., KUSAKABE, M., YOSHIKI, A., KOBAYASHI, Y., DOYU, M. & SOBUE, G. 2003. Heat shock protein 70 chaperone overexpression ameliorates phenotypes of the spinal and bulbar muscular atrophy transgenic mouse model by reducing nuclear-localized mutant androgen receptor protein. J Neurosci, 23, 2203-11.

AKERMAN, A. P., THOMAS, K. N., VAN RIJ, A. M., BODY, E. D., ALFADHEL, M. & COTTER, J. D. 2019. Heat therapy vs. supervised exercise therapy for peripheral arterial disease: a 12-wk randomized, controlled trial. Am J Physiol Heart Circ Physiol, 316, H1495-h1506.

AL-DELAIMY, W. K., VON MUHLEN, D. & BARRETT-CONNOR, E. 2009. Insulinlike growth factor-1, insulinlike growth factor binding protein-1, and cognitive function in older men and women. J Am Geriatr Soc, 57, 1441-6.

AMBROSINI, M. V., MARIUCCI, G., TANTUCCI, M., VAN HOOIJDONK, L. & AMMASSARI-TEULE, M. 2005. Hippocampal 72-kDa heat shock protein expression varies according to mice learning performance independently from chronic exposure to stress. Hippocampus, 15, 413-7.

ARIGA, T. 2017. The Pathogenic Role of Ganglioside Metabolism in Alzheimer's Disease-Cholinergic Neuron-Specific Gangliosides and Neurogenesis. Mol Neurobiol, 54, 623-638.

ARRIAGADA, P. V., MARZLOFF, K. & HYMAN, B. T. 1992. Distribution of Alzheimer-type pathologic changes in nondemented elderly individuals matches the pattern in Alzheimer's disease. Neurology, 42, 1681-8.

ARTIGA, M. J., BULLIDO, M. J., SASTRE, I., RECUERO, M., GARCIA, M. A., ALDUDO, J., VAZQUEZ, J. & VALDIVIESO, F. 1998. Allelic polymorphisms in the transcriptional regulatory region of apolipoprotein E gene. FEBS Lett, 421, 105-8.

AUDOUARD, E., VAN HEES, L., SUAIN, V., YILMAZ, Z., PONCELET, L., LEROY, K. & BRION, J. P. 2015. Motor deficit in a tauopathy model is induced by disturbances of axonal transport leading to dying-back degeneration and denervation of neuromuscular junctions. Am J Pathol, 185, 2685-97.

AULUCK, P. K. & BONINI, N. M. 2002. Pharmacological prevention of Parkinson disease in Drosophila. Nat Med, 8, 1185-6.

AUSTRALIA, D. 2020. Dementia Statistics [Online]. Available: https://www.dementia.org.au/statistics [Accessed].

AUTRALIANBUREAUOFSTATISTICS 2018. Causes of Death, Australia. cat. no. 3303.0.

AVILA-FUNES, J. A., AMIEVA, H., BARBERGER-GATEAU, P., LE GOFF, M., RAOUX, N., RITCHIE, K., CARRIÈRE, I., TAVERNIER, B., TZOURIO, C., GUTIÉRREZ-ROBLEDO, L. M. & DARTIGUES, J. F. 2009. Cognitive impairment improves the predictive validity of the phenotype of frailty for adverse health outcomes: the three-city study. J Am Geriatr Soc, 57, 453-61.

BACHMAN, D. L., WOLF, P. A., LINN, R. T., KNOEFEL, J. E., COBB, J. L., BELANGER, A. J., WHITE, L. R. & D'AGOSTINO, R. B. 1993. Incidence of dementia

and probable Alzheimer's disease in a general population: the Framingham Study. Neurology, 43, 515-9.

BAI, P. 2015. Biology of Poly(ADP-Ribose) Polymerases: The Factotums of Cell Maintenance. Mol Cell, 58, 947-58.

BAI, P. & CANTÓ, C. 2012. The role of PARP-1 and PARP-2 enzymes in metabolic regulation and disease. Cell Metab, 16, 290-5.

BAMBERGER, M. E., HARRIS, M. E., MCDONALD, D. R., HUSEMANN, J. & LANDRETH, G. E. 2003. A cell surface receptor complex for fibrillar beta-amyloid mediates microglial activation. J Neurosci, 23, 2665-74.

BÁRDOS, G., MÓRICZ, K., JASZLITS, L., RABLOCZKY, G., TORY, K., RÁCZ, I., BERNÁTH, S., SÜMEGI, B., FARKAS, B., LITERÁTI-NAGY, B. & LITERÁTI-NAGY, P. 2003. BGP-15, a hydroximic acid derivative, protects against cisplatin- or taxol-induced peripheral neuropathy in rats. Toxicol Appl Pharmacol, 190, 9-16.

BATURE, F., GUINN, B. A., PANG, D. & PAPPAS, Y. 2017. Signs and symptoms preceding the diagnosis of Alzheimer's disease: a systematic scoping review of literature from 1937 to 2016. BMJ Open, 7, e015746.

BEAUQUIS, J., PAVÍA, P., POMILIO, C., VINUESA, A., PODLUTSKAYA, N., GALVAN, V. & SARAVIA, F. 2013. Environmental enrichment prevents astroglial pathological changes in the hippocampus of APP transgenic mice, model of Alzheimer's disease. Exp Neurol, 239, 28-37.

BELCASTRO, V., GAETANO, G., ITALIANO, D., OTERI, G., CACCAMO, D., PISANI, L. R., STRIANO, P., STRIANO, S., IENTILE, R. & PISANI, F. 2007. Antiepileptic drugs and MTHFR polymorphisms influence hyper-homocysteinemia recurrence in epileptic patients. Epilepsia, 48, 1990-4.

BERCOVICH, B., STANCOVSKI, I., MAYER, A., BLUMENFELD, N., LASZLO, A., SCHWARTZ, A. L. & CIECHANOVER, A. 1997. Ubiquitin-dependent degradation of certain protein substrates in vitro requires the molecular chaperone Hsc70. J Biol Chem, 272, 9002-10.

BLASS, J. P., GIBSON, G. E. & HOYER, S. 2002. The role of the metabolic lesion in Alzheimer's disease. J Alzheimers Dis, 4, 225-32.

BOBKOVA, N., GUZHOVA, I., MARGULIS, B., NESTEROVA, I., MEDVINSKAYA, N., SAMOKHIN, A., ALEXANDROVA, I., GARBUZ, D., NUDLER, E. & EVGEN'EV, M. 2013. Dynamics of endogenous Hsp70 synthesis in the brain of olfactory bulbectomized mice. Cell Stress Chaperones, 18, 109-18.

BOBKOVA, N. V., GARBUZ, D. G., NESTEROVA, I., MEDVINSKAYA, N., SAMOKHIN, A., ALEXANDROVA, I., YASHIN, V., KARPOV, V., KUKHARSKY, M. S., NINKINA, N. N., SMIRNOV, A. A., NUDLER, E. & EVGEN'EV, M. 2014. Therapeutic effect of exogenous hsp70 in mouse models of Alzheimer's disease. J Alzheimers Dis, 38, 425-35.

BOLMONT, T., CLAVAGUERA, F., MEYER-LUEHMANN, M., HERZIG, M. C., RADDE, R., STAUFENBIEL, M., LEWIS, J., HUTTON, M., TOLNAY, M. & JUCKER, M. 2007. Induction of tau pathology by intracerebral infusion of amyloid-beta -containing brain extract and by amyloid-beta deposition in APP x Tau transgenic mice. Am J Pathol, 171, 2012-20.

BOMBICZ, M., PRIKSZ, D., GESZTELYI, R., KISS, R., HOLLOS, N., VARGA, B., NEMETH, J., TOTH, A., PAPP, Z., SZILVASSY, Z. & JUHASZ, B. 2019. The Drug Candidate BGP-15 Delays the Onset of Diastolic Dysfunction in the Goto-Kakizaki Rat Model of Diabetic Cardiomyopathy. Molecules, 24.

BORK, P., SANDER, C. & VALENCIA, A. 1992. An ATPase domain common to prokaryotic cell cycle proteins, sugar kinases, actin, and hsp70 heat shock proteins. Proc Natl Acad Sci U S A, 89, 7290-4.

BOUTAJANGOUT, A., AUTHELET, M., BLANCHARD, V., TOUCHET, N., TREMP, G., PRADIER, L. & BRION, J. P. 2004. Characterisation of cytoskeletal abnormalities in mice transgenic for wild-type human tau and familial Alzheimer's disease mutants of APP and presenilin-1. Neurobiol Dis, 15, 47-60.

BRADSHAW, E. M., CHIBNIK, L. B., KEENAN, B. T., OTTOBONI, L., RAJ, T., TANG, A., ROSENKRANTZ, L. L., IMBOYWA, S., LEE, M., VON KORFF, A., MORRIS, M. C., EVANS, D. A., JOHNSON, K., SPERLING, R. A., SCHNEIDER, J. A., BENNETT, D. A. & DE JAGER, P. L. 2013. CD33 Alzheimer's disease locus: altered monocyte function and amyloid biology. Nat Neurosci, 16, 848-50.

BROADLEY, S. A. & HARTL, F. U. 2009. The role of molecular chaperones in human misfolding diseases. FEBS Lett, 583, 2647-53.

BRUCE, J. L., PRICE, B. D., COLEMAN, C. N. & CALDERWOOD, S. K. 1993. Oxidative injury rapidly activates the heat shock transcription factor but fails to increase levels of heat shock proteins. Cancer Res, 53, 12-5.

BRUNT, V. E., HOWARD, M. J., FRANCISCO, M. A., ELY, B. R. & MINSON, C. T. 2016. Passive heat therapy improves endothelial function, arterial stiffness and blood pressure in sedentary humans. J Physiol, 594, 5329-42.

BU, G. 2009. Apolipoprotein E and its receptors in Alzheimer's disease: pathways, pathogenesis and therapy. Nat Rev Neurosci, 10, 333-44.

BUCHMAN, A. S., SCHNEIDER, J. A., LEURGANS, S. & BENNETT, D. A. 2008. Physical frailty in older persons is associated with Alzheimer disease pathology. Neurology, 71, 499-504.

BUDZYŃSKI, M. A., CRUL, T., HIMANEN, S. V., TOTH, N., OTVOS, F., SISTONEN, L. & VIGH, L. 2017. Chaperone co-inducer BGP-15 inhibits histone deacetylases and enhances the heat shock response through increased chromatin accessibility. Cell Stress Chaperones, 22, 717-728.

CAIRO, G., BARDELLA, L., SCHIAFFONATI, L. & BERNELLI-ZAZZERA, A. 1985. Synthesis of heat shock proteins in rat liver after ischemia and hyperthermia. Hepatology, 5, 357-61.

CASTELLANI, R. J. & SMITH, M. A. 2011. Compounding artefacts with uncertainty, and an amyloid cascade hypothesis that is 'too big to fail'. J Pathol, 224, 147-52.

CHAMBERLAIN, J. S., METZGER, J., REYES, M., TOWNSEND, D. & FAULKNER, J. A. 2007. Dystrophin-deficient mdx mice display a reduced life span and are susceptible to spontaneous rhabdomyosarcoma. Faseb j, 21, 2195-204.

CHAN, R. B., OLIVEIRA, T. G., CORTES, E. P., HONIG, L. S., DUFF, K. E., SMALL, S. A., WENK, M. R., SHUI, G. & DI PAOLO, G. 2012. Comparative lipidomic analysis of mouse and human brain with Alzheimer disease. J Biol Chem, 287, 2678-88.

CHATTERJEE, A., CHAKRABARTI, A., SENGUPTA, M. B., CHATTOPADHYAY, P., MUKHOPADHYAY, D 2017. Study of comorbidities in Alzheimer's disease patients requiring inpatient care. Alzheimer's & Dementia: The Journal of the Alzheimer's Association, 13, 494-495.

CHATTERJEE, P., LIM, W. L., SHUI, G., GUPTA, V. B., JAMES, I., FAGAN, A. M., XIONG, C., SOHRABI, H. R., TADDEI, K., BROWN, B. M., BENZINGER, T.,

MASTERS, C., SNOWDEN, S. G., WENK, M. R., BATEMAN, R. J., MORRIS, J. C. & MARTINS, R. N. 2016. Plasma Phospholipid and Sphingolipid Alterations in Presenilin1 Mutation Carriers: A Pilot Study. J Alzheimers Dis, 50, 887-94.

CHENG, H., WANG, M., LI, J. L., CAIRNS, N. J. & HAN, X. 2013. Specific changes of sulfatide levels in individuals with pre-clinical Alzheimer's disease: an early event in disease pathogenesis. J Neurochem, 127, 733-8.

CHENG, H., ZHOU, Y., HOLTZMAN, D. M. & HAN, X. 2010. Apolipoprotein E mediates sulfatide depletion in animal models of Alzheimer's disease. Neurobiol Aging, 31, 1188-96.

CHIANG, H. L., TERLECKY, S. R., PLANT, C. P. & DICE, J. F. 1989. A role for a 70-kilodalton heat shock protein in lysosomal degradation of intracellular proteins. Science, 246, 382-5.

CHUNG, J., NGUYEN, A. K., HENSTRIDGE, D. C., HOLMES, A. G., CHAN, M. H., MESA, J. L., LANCASTER, G. I., SOUTHGATE, R. J., BRUCE, C. R., DUFFY, S. J., HORVATH, I., MESTRIL, R., WATT, M. J., HOOPER, P. L., KINGWELL, B. A., VIGH, L., HEVENER, A. & FEBBRAIO, M. A. 2008. HSP72 protects against obesity-induced insulin resistance. Proc Natl Acad Sci U S A, 105, 1739-44.

CORDER, E. H., SAUNDERS, A. M., STRITTMATTER, W. J., SCHMECHEL, D. E., GASKELL, P. C., SMALL, G. W., ROSES, A. D., HAINES, J. L. & PERICAK-VANCE, M. A. 1993. Gene dose of apolipoprotein E type 4 allele and the risk of Alzheimer's disease in late onset families. Science, 261, 921-3.

CRONIN-GOLOMB, A., CORKIN, S. & GROWDON, J. H. 1995. Visual dysfunction predicts cognitive deficits in Alzheimer's disease. Optom Vis Sci, 72, 168-76.

CUMBO, E. & LIGORI, L. D. 2010. Levetiracetam, lamotrigine, and phenobarbital in patients with epileptic seizures and Alzheimer's disease. Epilepsy Behav, 17, 461-6.

DE CALIGNON, A., FOX, L. M., PITSTICK, R., CARLSON, G. A., BACSKAI, B. J., SPIRES-JONES, T. L. & HYMAN, B. T. 2010. Caspase activation precedes and leads to tangles. Nature, 464, 1201-4.

DE LA MONTE, S. M. 2012. Therapeutic targets of brain insulin resistance in sporadic Alzheimer's disease. Front Biosci (Elite Ed), 4, 1582-605.

DE LA MONTE, S. M. & WANDS, J. R. 2008. Alzheimer's disease is type 3 diabetes-evidence reviewed. J Diabetes Sci Technol, 2, 1101-13.

DEANE, R., SAGARE, A., HAMM, K., PARISI, M., LANE, S., FINN, M. B., HOLTZMAN, D. M. & ZLOKOVIC, B. V. 2008. apoE isoform-specific disruption of amyloid beta peptide clearance from mouse brain. J Clin Invest, 118, 4002-13.

DELEO, A. M. & IKEZU, T. 2018. Extracellular Vesicle Biology in Alzheimer's Disease and Related Tauopathy. J Neuroimmune Pharmacol, 13, 292-308.

DIK, M. G., PLUIJM, S. M., JONKER, C., DEEG, D. J., LOMECKY, M. Z. & LIPS, P. 2003. Insulin-like growth factor I (IGF-I) and cognitive decline in older persons. Neurobiol Aging, 24, 573-81.

DOKLADNY, K., ZUHL, M. N., MANDELL, M., BHATTACHARYA, D., SCHNEIDER, S., DERETIC, V. & MOSELEY, P. L. 2013. Regulatory coordination between two major intracellular homeostatic systems: heat shock response and autophagy. J Biol Chem, 288, 14959-72.

DOU, F., NETZER, W. J., TANEMURA, K., LI, F., HARTL, F. U., TAKASHIMA, A., GOURAS, G. K., GREENGARD, P. & XU, H. 2003. Chaperones increase association of tau protein with microtubules. Proc Natl Acad Sci U S A, 100, 721-6.

DREW, B. G., RIBAS, V., LE, J. A., HENSTRIDGE, D. C., PHUN, J., ZHOU, Z., SOLEYMANI, T., DARAEI, P., SITZ, D., VERGNES, L., WANAGAT, J., REUE, K., FEBBRAIO, M. A. & HEVENER, A. L. 2014. HSP72 is a mitochondrial stress sensor critical for Parkin action, oxidative metabolism, and insulin sensitivity in skeletal muscle. Diabetes, 63, 1488-505.

DUYCKAERTS, C., COLLE, M. A., DESSI, F., PIETTE, F. & HAUW, J. J. 1998. Progression of Alzheimer histopathological changes. Acta Neurol Belg, 98, 180-5.

ELY, B. R., CLAYTON, Z. S., MCCURDY, C. E., PFEIFFER, J., NEEDHAM, K. W., COMRADA, L. N. & MINSON, C. T. 2019. Heat therapy improves glucose tolerance and adipose tissue insulin signaling in polycystic ovary syndrome. Am J Physiol Endocrinol Metab, 317, E172-e182.

EROGLU, B., KIMBLER, D. E., PANG, J., CHOI, J., MOSKOPHIDIS, D., YANASAK, N., DHANDAPANI, K. M. & MIVECHI, N. F. 2014. Therapeutic inducers of the HSP70/HSP110 protect mice against traumatic brain injury. J Neurochem, 130, 626-41.

EVANS, C. G., WISÉN, S. & GESTWICKI, J. E. 2006. Heat shock proteins 70 and 90 inhibit early stages of amyloid beta-(1-42) aggregation in vitro. J Biol Chem, 281, 33182-91.

EVANS, D. A., BENNETT, D. A., WILSON, R. S., BIENIAS, J. L., MORRIS, M. C., SCHERR, P. A., HEBERT, L. E., AGGARWAL, N., BECKETT, L. A., JOGLEKAR, R., BERRY-KRAVIS, E. & SCHNEIDER, J. 2003. Incidence of Alzheimer disease in a biracial urban community: relation to apolipoprotein E allele status. Arch Neurol, 60, 185-9.

FARKAS, B., MAGYARLAKI, M., CSETE, B., NEMETH, J., RABLOCZKY, G., BERNATH, S., LITERÁTI NAGY, P. & SÜMEGI, B. 2002. Reduction of acute

photodamage in skin by topical application of a novel PARP inhibitor. Biochem Pharmacol, 63, 921-32.

FARRER, L. A., CUPPLES, L. A., HAINES, J. L., HYMAN, B., KUKULL, W. A., MAYEUX, R., MYERS, R. H., PERICAK-VANCE, M. A., RISCH, N. & VAN DUIJN, C. M. 1997. Effects of age, sex, and ethnicity on the association between apolipoprotein E genotype and Alzheimer disease. A meta-analysis. APOE and Alzheimer Disease Meta Analysis Consortium. JAMA, 278, 1349-56.

FASSBENDER, K., SIMONS, M., BERGMANN, C., STROICK, M., LUTJOHANN, D., KELLER, P., RUNZ, H., KUHL, S., BERTSCH, T., VON BERGMANN, K., HENNERICI, M., BEYREUTHER, K. & HARTMANN, T. 2001. Simvastatin strongly reduces levels of Alzheimer's disease beta -amyloid peptides Abeta 42 and Abeta 40 in vitro and in vivo. Proc Natl Acad Sci U S A, 98, 5856-61.

FOLEY, P. 2010. Lipids in Alzheimer's disease: A century-old story. Biochim Biophys Acta, 1801, 750-3.

FRANKLIN, T. B., KRUEGER-NAUG, A. M., CLARKE, D. B., ARRIGO, A. P. & CURRIE, R. W. 2005. The role of heat shock proteins Hsp70 and Hsp27 in cellular protection of the central nervous system. Int J Hyperthermia, 21, 379-92.

FRIEDMAN, D., HONIG, L. S. & SCARMEAS, N. 2012. Seizures and epilepsy in Alzheimer's disease. CNS Neurosci Ther, 18, 285-94.

FULLER, O. K., WHITHAM, M., MATHIVANAN, S. & FEBBRAIO, M. A. 2020. The Protective Effect of Exercise in Neurodegenerative Diseases: The Potential Role of Extracellular Vesicles. Cells, 9.

GABAI, V. L., MERIIN, A. B., MOSSER, D. D., CARON, A. W., RITS, S., SHIFRIN, V. I. & SHERMAN, M. Y. 1997. Hsp70 prevents activation of stress kinases. A novel pathway of cellular thermotolerance. J Biol Chem, 272, 18033-7.

GAMES, D., ADAMS, D., ALESSANDRINI, R., BARBOUR, R., BERTHELETTE, P., BLACKWELL, C., CARR, T., CLEMENS, J., DONALDSON, T., GILLESPIE, F. & ET AL. 1995. Alzheimer-type neuropathology in transgenic mice overexpressing V717F beta-amyloid precursor protein. Nature, 373, 523-7.

GARBER, K. 2016. No longer going to waste. Nat Biotechnol, 34, 458-61.

GASTPAR, R., GEHRMANN, M., BAUSERO, M. A., ASEA, A., GROSS, C., SCHROEDER, J. A. & MULTHOFF, G. 2005. Heat shock protein 70 surface-positive tumor exosomes stimulate migratory and cytolytic activity of natural killer cells. Cancer Res, 65, 5238-47.

GEHRIG, S. M., VAN DER POEL, C., SAYER, T. A., SCHERTZER, J. D., HENSTRIDGE, D. C., CHURCH, J. E., LAMON, S., RUSSELL, A. P., DAVIES, K. E., FEBBRAIO, M. A. & LYNCH, G. S. 2012. Hsp72 preserves muscle function and slows progression of severe muscular dystrophy. Nature, 484, 394-8.

GEIGER, P. C. & GUPTE, A. A. 2011. Heat shock proteins are important mediators of skeletal muscle insulin sensitivity. Exerc Sport Sci Rev, 39, 34-42.

GIANNAKOPOULOS, P., HERRMANN, F. R., BUSSIERE, T., BOURAS, C., KOVARI, E., PERL, D. P., MORRISON, J. H., GOLD, G. & HOF, P. R. 2003. Tangle and neuron numbers, but not amyloid load, predict cognitive status in Alzheimer's disease. Neurology, 60, 1495-500.

GIBSON, G. E., SHEU, K. F. & BLASS, J. P. 1998. Abnormalities of mitochondrial enzymes in Alzheimer disease. J Neural Transm (Vienna), 105, 855-70.

GOEDERT, M. & SPILLANTINI, M. G. 2006. A century of Alzheimer's disease. Science, 314, 777-81.

GOLDE, T. E., ECKMAN, C. B. & YOUNKIN, S. G. 2000. Biochemical detection of Abeta isoforms: implications for pathogenesis, diagnosis, and treatment of Alzheimer's disease. Biochim Biophys Acta, 1502, 172-87.

GOMBOS, I., CRUL, T., PIOTTO, S., GÜNGÖR, B., TÖRÖK, Z., BALOGH, G., PÉTER, M., SLOTTE, J. P., CAMPANA, F., PILBAT, A. M., HUNYA, A., TÓTH, N., LITERATI-NAGY, Z., VÍGH, L., JR., GLATZ, A., BRAMESHUBER, M., SCHÜTZ, G. J., HEVENER, A., FEBBRAIO, M. A., HORVÁTH, I. & VÍGH, L. 2011. Membrane-lipid therapy in operation: the HSP co-inducer BGP-15 activates stress signal transduction pathways by remodeling plasma membrane rafts. PLoS One, 6, e28818.

GOMEZ-ISLA, T., HOLLISTER, R., WEST, H., MUI, S., GROWDON, J. H., PETERSEN, R. C., PARISI, J. E. & HYMAN, B. T. 1997. Neuronal loss correlates with but exceeds neurofibrillary tangles in Alzheimer's disease. Ann Neurol, 41, 17-24.

GOODENOWE, D. B., COOK, L. L., LIU, J., LU, Y., JAYASINGHE, D. A., AHIAHONU, P. W., HEATH, D., YAMAZAKI, Y., FLAX, J., KRENITSKY, K. F., SPARKS, D. L., LERNER, A., FRIEDLAND, R. P., KUDO, T., KAMINO, K., MORIHARA, T., TAKEDA, M. & WOOD, P. L. 2007. Peripheral ethanolamine plasmalogen deficiency: a logical causative factor in Alzheimer's disease and dementia. J Lipid Res, 48, 2485-98.

GÖTZ, J. 2001. Tau and transgenic animal models. Brain Res Brain Res Rev, 35, 266-86.

GÖTZ, J., CHEN, F., VAN DORPE, J. & NITSCH, R. M. 2001. Formation of neurofibrillary tangles in P301l tau transgenic mice induced by Abeta 42 fibrils. Science, 293, 1491-5.

GRICIUC, A., SERRANO-POZO, A., PARRADO, A. R., LESINSKI, A. N., ASSELIN, C. N., MULLIN, K., HOOLI, B., CHOI, S. H., HYMAN, B. T. & TANZI, R. E. 2013. Alzheimer's disease risk gene CD33 inhibits microglial uptake of amyloid beta. Neuron, 78, 631-43.

GRIMM, M. O., GRIMM, H. S., PÄTZOLD, A. J., ZINSER, E. G., HALONEN, R., DUERING, M., TSCHÄPE, J. A., DE STROOPER, B., MÜLLER, U., SHEN, J. & HARTMANN, T. 2005. Regulation of cholesterol and sphingomyelin metabolism by amyloid-beta and presenilin. Nat Cell Biol, 7, 1118-23.

GUERREIRO, R., WOJTAS, A., BRAS, J., CARRASQUILLO, M., ROGAEVA, E., MAJOUNIE, E., CRUCHAGA, C., SASSI, C., KAUWE, J. S., YOUNKIN, S., HAZRATI, L., COLLINGE, J., POCOCK, J., LASHLEY, T., WILLIAMS, J., LAMBERT, J. C., AMOUYEL, P., GOATE, A., RADEMAKERS, R., MORGAN, K., POWELL, J., ST GEORGE-HYSLOP, P., SINGLETON, A. & HARDY, J. 2013. TREM2 variants in Alzheimer's disease. N Engl J Med, 368, 117-27.

GUPTE, A. A., BOMHOFF, G. L., SWERDLOW, R. H. & GEIGER, P. C. 2009. Heat treatment improves glucose tolerance and prevents skeletal muscle insulin resistance in rats fed a high-fat diet. Diabetes, 58, 567-78.

HAFEN, P. S., PREECE, C. N., SORENSEN, J. R., HANCOCK, C. R. & HYLDAHL, R. D. 2018. Repeated exposure to heat stress induces mitochondrial adaptation in human skeletal muscle. J Appl Physiol (1985), 125, 1447-1455.

HALES, K. G. 2004. The machinery of mitochondrial fusion, division, and distribution, and emerging connections to apoptosis. Mitochondrion, 4, 285-308.

HALMOSI, R., BERENTE, Z., OSZ, E., TOTH, K., LITERATI-NAGY, P. & SUMEGI, B. 2001. Effect of poly(ADP-ribose) polymerase inhibitors on the ischemia-reperfusion-induced oxidative cell damage and mitochondrial metabolism in Langendorff heart perfusion system. Mol Pharmacol, 59, 1497-505.

HAMOS, J. E., OBLAS, B., PULASKI-SALO, D., WELCH, W. J., BOLE, D. G. & DRACHMAN, D. A. 1991. Expression of heat shock proteins in Alzheimer's disease. Neurology, 41, 345-50.

HAN, X., D, M. H., MCKEEL, D. W., JR., KELLEY, J. & MORRIS, J. C. 2002. Substantial sulfatide deficiency and ceramide elevation in very early Alzheimer's disease: potential role in disease pathogenesis. J Neurochem, 82, 809-18.

HAN, X., HOLTZMAN, D. M. & MCKEEL, D. W., JR. 2001. Plasmalogen deficiency in early Alzheimer's disease subjects and in animal models: molecular characterization using electrospray ionization mass spectrometry. J Neurochem, 77, 1168-80.

HARTL, F. U. & HAYER-HARTL, M. 2002. Molecular chaperones in the cytosol: from nascent chain to folded protein. Science, 295, 1852-8.

HARTMANN, T., KUCHENBECKER, J. & GRIMM, M. O. 2007. Alzheimer's disease: the lipid connection. J Neurochem, 103 Suppl 1, 159-70.

HAUGABOOK, S. J., LE, T., YAGER, D., ZENK, B., HEALY, B. M., ECKMAN, E. A., PRADA, C., YOUNKIN, L., MURPHY, P., PINNIX, I., ONSTEAD, L., SAMBAMURTI, K., GOLDE, T. E., DICKSON, D., YOUNKIN, S. G. & ECKMAN, C. B. 2001. Reduction of Abeta accumulation in the Tg2576 animal model of Alzheimer's

disease after oral administration of the phosphatidyl-inositol kinase inhibitor wortmannin. Faseb j, 15, 16-18.

HAUSER, W. A., MORRIS, M. L., HESTON, L. L. & ANDERSON, V. E. 1986. Seizures and myoclonus in patients with Alzheimer's disease. Neurology, 36, 1226-30.

HAY, D. G., SATHASIVAM, K., TOBABEN, S., STAHL, B., MARBER, M., MESTRIL, R., MAHAL, A., SMITH, D. L., WOODMAN, B. & BATES, G. P. 2004. Progressive decrease in chaperone protein levels in a mouse model of Huntington's disease and induction of stress proteins as a therapeutic approach. Hum Mol Genet, 13, 1389-405.

HE, X., HUANG, Y., LI, B., GONG, C. X. & SCHUCHMAN, E. H. 2010. Deregulation of sphingolipid metabolism in Alzheimer's disease. Neurobiol Aging, 31, 398-408.

HEBERT, L. E., SCHERR, P. A., BECKETT, L. A., ALBERT, M. S., PILGRIM, D. M., CHOWN, M. J., FUNKENSTEIN, H. H. & EVANS, D. A. 1995. Age-specific incidence of Alzheimer's disease in a community population. JAMA, 273, 1354-9.

HECIMOVIC, S., WANG, J., DOLIOS, G., MARTINEZ, M., WANG, R. & GOATE, A. M. 2004. Mutations in APP have independent effects on Abeta and CTFgamma generation. Neurobiol Dis, 17, 205-18.

HECKMANN, B. L., TEUBNER, B. J. W., TUMMERS, B., BOADA-ROMERO, E., HARRIS, L., YANG, M., GUY, C. S., ZAKHARENKO, S. S. & GREEN, D. R. 2019. LC3-Associated Endocytosis Facilitates β-Amyloid Clearance and Mitigates Neurodegeneration in Murine Alzheimer's Disease. Cell, 178, 536-551.e14.

HENSOLD, J. O., HUNT, C. R., CALDERWOOD, S. K., HOUSMAN, D. E. & KINGSTON, R. E. 1990. DNA binding of heat shock factor to the heat shock element is

insufficient for transcriptional activation in murine erythroleukemia cells. Mol Cell Biol, 10, 1600-8.

HENSTRIDGE, D. C., ABILDGAARD, J., LINDEGAARD, B. & FEBBRAIO, M. A. 2019. Metabolic control and sex: A focus on inflammatory-linked mediators. Br J Pharmacol, 176, 4193-4207.

HENSTRIDGE, D. C., BRUCE, C. R., DREW, B. G., TORY, K., KOLONICS, A., ESTEVEZ, E., CHUNG, J., WATSON, N., GARDNER, T., LEE-YOUNG, R. S., CONNOR, T., WATT, M. J., CARPENTER, K., HARGREAVES, M., MCGEE, S. L., HEVENER, A. L. & FEBBRAIO, M. A. 2014. Activating HSP72 in rodent skeletal muscle increases mitochondrial number and oxidative capacity and decreases insulin resistance. Diabetes, 63, 1881-94.

HERAUD, C., GOUFAK, D., ANDO, K., LEROY, K., SUAIN, V., YILMAZ, Z., DE DECKER, R., AUTHELET, M., LAPORTE, V., OCTAVE, J. N. & BRION, J. P. 2014. Increased misfolding and truncation of tau in APP/PS1/tau transgenic mice compared to mutant tau mice. Neurobiol Dis, 62, 100-12.

HICKMAN, S. E., ALLISON, E. K. & EL KHOURY, J. 2008. Microglial dysfunction and defective beta-amyloid clearance pathways in aging Alzheimer's disease mice. J Neurosci, 28, 8354-60.

HIPPIUS, H. & NEUNDÖRFER, G. 2003. The discovery of Alzheimer's disease. Dialogues Clin Neurosci, 5, 101-8.

HOLTZMAN, D. M. 2001. Role of apoe/Abeta interactions in the pathogenesis of Alzheimer's disease and cerebral amyloid angiopathy. J Mol Neurosci, 17, 147-55.

HOLTZMAN, D. M., BALES, K. R., TENKOVA, T., FAGAN, A. M., PARSADANIAN, M., SARTORIUS, L. J., MACKEY, B., OLNEY, J., MCKEEL, D.,

WOZNIAK, D. & PAUL, S. M. 2000. Apolipoprotein E isoform-dependent amyloid deposition and neuritic degeneration in a mouse model of Alzheimer's disease. Proc Natl Acad Sci U S A, 97, 2892-7.

HOMMET, C., HUREAUX, R., BARRÉ, J., CONSTANS, T. & BERRUT, G. 2007. Epileptic seizures in clinically diagnosed Alzheimer's disease: report from a geriatric medicine population. Aging Clin Exp Res, 19, 430-1.

HONG, Y., BRISMAR, K., HALL, K., PEDERSEN, N. L. & DE FAIRE, U. 1997. Associations between insulin-like growth factor-I (IGF-I), IGF-binding protein-1, insulin and other metabolic measures after controlling for genetic influences: results from middle-aged and elderly monozygotic twins. J Endocrinol, 153, 251-7.

HONJO, K., BLACK, S. E. & VERHOEFF, N. P. 2012. Alzheimer's disease, cerebrovascular disease, and the beta-amyloid cascade. Can J Neurol Sci, 39, 712-28.

HOSHINO, T., MURAO, N., NAMBA, T., TAKEHARA, M., ADACHI, H., KATSUNO, M., SOBUE, G., MATSUSHIMA, T., SUZUKI, T. & MIZUSHIMA, T. 2011. Suppression of Alzheimer's disease-related phenotypes by expression of heat shock protein 70 in mice. J Neurosci, 31, 5225-34.

HOSHINO, T., SUZUKI, K., MATSUSHIMA, T., YAMAKAWA, N., SUZUKI, T. & MIZUSHIMA, T. 2013. Suppression of Alzheimer's disease-related phenotypes by geranylgeranylacetone in mice. PLoS One, 8, e76306.

HURTADO, D. E., MOLINA-PORCEL, L., IBA, M., ABOAGYE, A. K., PAUL, S. M., TROJANOWSKI, J. Q. & LEE, V. M. 2010. A{beta} accelerates the spatiotemporal progression of tau pathology and augments tau amyloidosis in an Alzheimer mouse model. Am J Pathol, 177, 1977-88.

IGARASHI, M., MA, K., GAO, F., KIM, H. W., RAPOPORT, S. I. & RAO, J. S. 2011. Disturbed choline plasmalogen and phospholipid fatty acid concentrations in Alzheimer's disease prefrontal cortex. J Alzheimers Dis, 24, 507-17.

ITTNER, A., CHUA, S. W., BERTZ, J., VOLKERLING, A., VAN DER HOVEN, J., GLADBACH, A., PRZYBYLA, M., BI, M., VAN HUMMEL, A., STEVENS, C. H., IPPATI, S., SUH, L. S., MACMILLAN, A., SUTHERLAND, G., KRIL, J. J., SILVA, A. P., MACKAY, J. P., POLJAK, A., DELERUE, F., KE, Y. D. & ITTNER, L. M. 2016. Site-specific phosphorylation of tau inhibits amyloid-β toxicity in Alzheimer's mice. Science, 354, 904-908.

ITTNER, L. M. & GOTZ, J. 2011. Amyloid-beta and tau--a toxic pas de deux in Alzheimer's disease. Nat Rev Neurosci, 12, 65-72.

ITTNER, L. M., KE, Y. D., DELERUE, F., BI, M., GLADBACH, A., VAN EERSEL, J., WÖLFING, H., CHIENG, B. C., CHRISTIE, M. J., NAPIER, I. A., ECKERT, A., STAUFENBIEL, M., HARDEMAN, E. & GÖTZ, J. 2010. Dendritic function of tau mediates amyloid-beta toxicity in Alzheimer's disease mouse models. Cell, 142, 387-97.

IWAKI, K., CHI, S. H., DILLMANN, W. H. & MESTRIL, R. 1993. Induction of HSP70 in cultured rat neonatal cardiomyocytes by hypoxia and metabolic stress. Circulation, 87, 2023-32.

JENSSEN, S. & SCHERE, D. 2010. Treatment and management of epilepsy in the elderly demented patient. Am J Alzheimers Dis Other Demen, 25, 18-26.

JIANG, Q., LEE, C. Y., MANDREKAR, S., WILKINSON, B., CRAMER, P., ZELCER, N., MANN, K., LAMB, B., WILLSON, T. M., COLLINS, J. L., RICHARDSON, J. C., SMITH, J. D., COMERY, T. A., RIDDELL, D., HOLTZMAN, D. M., TONTONOZ, P.

& LANDRETH, G. E. 2008. ApoE promotes the proteolytic degradation of Abeta. Neuron, 58, 681-93.

JINWAL, U. K., O'LEARY, J. C., 3RD, BORYSOV, S. I., JONES, J. R., LI, Q., KOREN, J., 3RD, ABISAMBRA, J. F., VESTAL, G. D., LAWSON, L. Y., JOHNSON, A. G., BLAIR, L. J., JIN, Y., MIYATA, Y., GESTWICKI, J. E. & DICKEY, C. A. 2010. Hsc70 rapidly engages tau after microtubule destabilization. J Biol Chem, 285, 16798-805.

JOHNSON, D. S., LI, Y. M., PETTERSSON, M. & ST GEORGE-HYSLOP, P. H. 2017. Structural and Chemical Biology of Presenilin Complexes. Cold Spring Harb Perspect Med, 7.

JOHNSON, G. V. 2006. Tau phosphorylation and proteolysis: insights and perspectives. J Alzheimers Dis, 9, 243-50.

KALMIJN, S., JANSSEN, J. A., POLS, H. A., LAMBERTS, S. W. & BRETELER, M. M. 2000. A prospective study on circulating insulin-like growth factor I (IGF-I), IGF-binding proteins, and cognitive function in the elderly. J Clin Endocrinol Metab, 85, 4551-5.

KATSUNO, M., SANG, C., ADACHI, H., MINAMIYAMA, M., WAZA, M., TANAKA, F., DOYU, M. & SOBUE, G. 2005. Pharmacological induction of heat-shock proteins alleviates polyglutamine-mediated motor neuron disease. Proc Natl Acad Sci U S A, 102, 16801-6.

KAUPPINEN, T. M., SUH, S. W., HIGASHI, Y., BERMAN, A. E., ESCARTIN, C., WON, S. J., WANG, C., CHO, S. H., GAN, L. & SWANSON, R. A. 2011. Poly(ADP-ribose)polymerase-1 modulates microglial responses to amyloid β. J Neuroinflammation, 8, 152.

KAVANAGH, K., FLYNN, D. M., JENKINS, K. A., ZHANG, L. & WAGNER, J. D. 2011. Restoring HSP70 deficiencies improves glucose tolerance in diabetic monkeys. Am J Physiol Endocrinol Metab, 300, E894-901.

KAWAS, C., GRAY, S., BROOKMEYER, R., FOZARD, J. & ZONDERMAN, A. 2000. Age-specific incidence rates of Alzheimer's disease: the Baltimore Longitudinal Study of Aging. Neurology, 54, 2072-7.

KENNEDY, T. L., SWIDERSKI, K., MURPHY, K. T., GEHRIG, S. M., CURL, C. L., CHANDRAMOULI, C., FEBBRAIO, M. A., DELBRIDGE, L. M., KOOPMAN, R. & LYNCH, G. S. 2016. BGP-15 Improves Aspects of the Dystrophic Pathology in mdx and dko Mice with Differing Efficacies in Heart and Skeletal Muscle. Am J Pathol, 186, 3246-3260.

KHACHATURIAN, A. S., CORCORAN, C. D., MAYER, L. S., ZANDI, P. P., BREITNER, J. C. & CACHE COUNTY STUDY, I. 2004. Apolipoprotein E epsilon4 count affects age at onset of Alzheimer disease, but not lifetime susceptibility: The Cache County Study. Arch Gen Psychiatry, 61, 518-24.

KIERAN, D., KALMAR, B., DICK, J. R., RIDDOCH-CONTRERAS, J., BURNSTOCK, G. & GREENSMITH, L. 2004. Treatment with arimoclomol, a coinducer of heat shock proteins, delays disease progression in ALS mice. Nat Med, 10, 402-5.

KIM, W. S., CHAN, S. L., HILL, A. F., GUILLEMIN, G. J. & GARNER, B. 2009. Impact of 27-hydroxycholesterol on amyloid-beta peptide production and ATP-binding cassette transporter expression in primary human neurons. J Alzheimers Dis, 16, 121-31.

KING, A. 2018. The search for better animal models of Alzheimer's disease. Nature, 559, S13-s15.

KNIGHT, E. M., MARTINS, I. V., GÜMÜSGÖZ, S., ALLAN, S. M. & LAWRENCE, C. B. 2014. High-fat diet-induced memory impairment in triple-transgenic Alzheimer's disease (3xTgAD) mice is independent of changes in amyloid and tau pathology. Neurobiol Aging, 35, 1821-32.

KREGEL, K. C. 2002. Heat shock proteins: modifying factors in physiological stress responses and acquired thermotolerance. J Appl Physiol (1985), 92, 2177-86.

KULIJEWICZ-NAWROT, M., VERKHRATSKY, A., CHVÁTAL, A., SYKOVÁ, E. & RODRÍGUEZ, J. J. 2012. Astrocytic cytoskeletal atrophy in the medial prefrontal cortex of a triple transgenic mouse model of Alzheimer's disease. J Anat, 221, 252-62.

KUMAR, P., AMBASTA, R. K., VEERESHWARAYYA, V., ROSEN, K. M., KOSIK, K. S., BAND, H., MESTRIL, R., PATTERSON, C. & QUERFURTH, H. W. 2007. CHIP and HSPs interact with beta-APP in a proteasome-dependent manner and influence Abeta metabolism. Hum Mol Genet, 16, 848-64.

LANKA, V., WIELAND, S., BARBER, J. & CUDKOWICZ, M. 2009. Arimoclomol: a potential therapy under development for ALS. Expert Opin Investig Drugs, 18, 1907-18.

LEROY, K., BRETTEVILLE, A., SCHINDOWSKI, K., GILISSEN, E., AUTHELET, M., DE DECKER, R., YILMAZ, Z., BUEE, L. & BRION, J. P. 2007. Early axonopathy preceding neurofibrillary tangles in mutant tau transgenic mice. Am J Pathol, 171, 976-92.

LEWIS, J., DICKSON, D. W., LIN, W. L., CHISHOLM, L., CORRAL, A., JONES, G., YEN, S. H., SAHARA, N., SKIPPER, L., YAGER, D., ECKMAN, C., HARDY, J., HUTTON, M. & MCGOWAN, E. 2001. Enhanced neurofibrillary degeneration in transgenic mice expressing mutant tau and APP. Science, 293, 1487-91.

LEWIS, M. J. & PELHAM, H. R. 1985. Involvement of ATP in the nuclear and nucleolar functions of the 70 kd heat shock protein. Embo j, 4, 3137-43.

LI, D., LONG, C., YUE, Y. & DUAN, D. 2009. Sub-physiological sarcoglycan expression contributes to compensatory muscle protection in mdx mice. Hum Mol Genet, 18, 1209-20.

LIBEREK, K., LEWANDOWSKA, A. & ZIETKIEWICZ, S. 2008. Chaperones in control of protein disaggregation. Embo j, 27, 328-35.

LIM, W. L. F., HUYNH, K., CHATTERJEE, P., MARTINS, I., JAYAWARDANA, K. S., GILES, C., MELLETT, N. A., LAWS, S. M., BUSH, A. I., ROWE, C. C., VILLEMAGNE, V. L., AMES, D., DREW, B. G., MASTERS, C. L., MEIKLE, P. J. & MARTINS, R. N. 2020. Relationships Between Plasma Lipids Species, Gender, Risk Factors, and Alzheimer's Disease. J Alzheimers Dis, 76, 303-315.

LITERÁTI-NAGY, B., KULCSÁR, E., LITERÁTI-NAGY, Z., BUDAY, B., PÉTERFAI, E., HORVÁTH, T., TORY, K., KOLONICS, A., FLEMING, A., MANDL, J. & KORÁNYI, L. 2009. Improvement of insulin sensitivity by a novel drug, BGP-15, in insulin-resistant patients: a proof of concept randomized double-blind clinical trial. Horm Metab Res, 41, 374-80.

LITERÁTI-NAGY, B., PÉTERFAI, E., KULCSÁR, E., LITERÁTI-NAGY, Z., BUDAY, B., TORY, K., MANDL, J., SÜMEGI, B., FLEMING, A., ROTH, J. & KORÁNYI, L. 2010. Beneficial effect of the insulin sensitizer (HSP inducer) BGP-15 on olanzapine-induced metabolic disorders. Brain Res Bull, 83, 340-4.

LITERÁTI-NAGY, B., TORY, K., PEITL, B., BAJZA, Á., KORÁNYI, L., LITERÁTI-NAGY, Z., HOOPER, P. L., VÍGH, L. & SZILVÁSSY, Z. 2014. Improvement of insulin

sensitivity by a novel drug candidate, BGP-15, in different animal studies. Metab Syndr Relat Disord, 12, 125-31.

LITERATI-NAGY, Z., TORY, K., LITERÁTI-NAGY, B., BAJZA, A., VÍGH, L., JR., VÍGH, L., MANDL, J. & SZILVÁSSY, Z. 2013. Synergic insulin sensitizing effect of rimonabant and BGP-15 in Zucker-obese rats. Pathol Oncol Res, 19, 571-5.

LIU, C. T. & BROOKS, G. A. 2012. Mild heat stress induces mitochondrial biogenesis in C2C12 myotubes. J Appl Physiol (1985), 112, 354-61.

LIU, Y., WALTER, S., STAGI, M., CHERNY, D., LETIEMBRE, M., SCHULZ-SCHAEFFER, W., HEINE, H., PENKE, B., NEUMANN, H. & FASSBENDER, K. 2005. LPS receptor (CD14): a receptor for phagocytosis of Alzheimer's amyloid peptide. Brain, 128, 1778-89.

LLORENS-MARTÍN, M., TORRES-ALEMÁN, I. & TREJO, J. L. 2010. Exercise modulates insulin-like growth factor 1-dependent and -independent effects on adult hippocampal neurogenesis and behaviour. Mol Cell Neurosci, 44, 109-17.

LO BIANCO, C., SHORTER, J., REGULIER, E., LASHUEL, H., IWATSUBO, T., LINDQUIST, S. & AEBISCHER, P. 2008. Hsp104 antagonizes alpha-synuclein aggregation and reduces dopaminergic degeneration in a rat model of Parkinson disease. J Clin Invest, 118, 3087-97.

LOVE, S., BARBER, R. & WILCOCK, G. K. 1999. Increased poly(ADP-ribosyl)ation of nuclear proteins in Alzheimer's disease. Brain, 122 (Pt 2), 247-53.

LUCHSINGER, J. A., PATEL, B., TANG, M. X., SCHUPF, N. & MAYEUX, R. 2007. Measures of adiposity and dementia risk in elderly persons. Arch Neurol, 64, 392-8.

MACCIONI, R. B., FARÍAS, G., MORALES, I. & NAVARRETE, L. 2010. The revitalized tau hypothesis on Alzheimer's disease. Arch Med Res, 41, 226-31.

MAGRANÉ, J., SMITH, R. C., WALSH, K. & QUERFURTH, H. W. 2004. Heat shock protein 70 participates in the neuroprotective response to intracellularly expressed beta-amyloid in neurons. J Neurosci, 24, 1700-6.

MAILHOS, C., HOWARD, M. K. & LATCHMAN, D. S. 1994. Heat shock proteins hsp90 and hsp70 protect neuronal cells from thermal stress but not from programmed cell death. J Neurochem, 63, 1787-95.

MAMBULA, S. S. & CALDERWOOD, S. K. 2006. Heat shock protein 70 is secreted from tumor cells by a nonclassical pathway involving lysosomal endosomes. J Immunol, 177, 7849-57.

MAPSTONE, M., CHEEMA, A. K., FIANDACA, M. S., ZHONG, X., MHYRE, T. R., MACARTHUR, L. H., HALL, W. J., FISHER, S. G., PETERSON, D. R., HALEY, J. M., NAZAR, M. D., RICH, S. A., BERLAU, D. J., PELTZ, C. B., TAN, M. T., KAWAS, C. H. & FEDEROFF, H. J. 2014. Plasma phospholipids identify antecedent memory impairment in older adults. Nat Med, 20, 415-8.

MARSHALL, J. P. S., ESTEVEZ, E., KAMMOUN, H. L., KING, E. J., BRUCE, C. R., DREW, B. G., QIAN, H., ILIADES, P., GREGOREVIC, P., FEBBRAIO, M. A. & HENSTRIDGE, D. C. 2018. Skeletal muscle-specific overexpression of heat shock protein 72 improves skeletal muscle insulin-stimulated glucose uptake but does not alter whole body metabolism. Diabetes Obes Metab, 20, 1928-1936.

MARTIRE, S., FUSO, A., ROTILI, D., TEMPERA, I., GIORDANO, C., DE ZOTTIS, I., MUZI, A., VERNOLE, P., GRAZIANI, G., LOCOCO, E., FARALDI, M., MARAS, B., SCARPA, S., MOSCA, L. & D'ERME, M. 2013. PARP-1 modulates amyloid beta peptide-induced neuronal damage. PLoS One, 8, e72169.

MARTIRE, S., MOSCA, L. & D'ERME, M. 2015. PARP-1 involvement in neurodegeneration: A focus on Alzheimer's and Parkinson's diseases. Mech Ageing Dev, 146-148, 53-64.

MASTERS, C. L., BATEMAN, R., BLENNOW, K., ROWE, C. C., SPERLING, R. A. & CUMMINGS, J. L. 2015. Alzheimer's disease. Nat Rev Dis Primers, 1, 15056.

MATSUOKA, Y., PICCIANO, M., MALESTER, B., LAFRANCOIS, J., ZEHR, C., DAESCHNER, J. M., OLSCHOWKA, J. A., FONSECA, M. I., O'BANION, M. K., TENNER, A. J., LEMERE, C. A. & DUFF, K. 2001. Inflammatory responses to amyloidosis in a transgenic mouse model of Alzheimer's disease. Am J Pathol, 158, 1345-54.

MATSUZAKI, K., KATO, K. & YANAGISAWA, K. 2010. Abeta polymerization through interaction with membrane gangliosides. Biochim Biophys Acta, 1801, 868-77.

MAWUENYEGA, K. G., SIGURDSON, W., OVOD, V., MUNSELL, L., KASTEN, T., MORRIS, J. C., YARASHESKI, K. E. & BATEMAN, R. J. 2010. Decreased clearance of CNS beta-amyloid in Alzheimer's disease. Science, 330, 1774.

MAXIME VANDE VYVER, C. V. C., GUY NAGELS, SEBASTIAAN ENGELBORGHS, DIMITRI DE BENDEL, ISLE SMOLDERS 2020. The 3xTg Alzheimer's disease mouse model is more susceptible to 6Hz corneal kindling.

MAYER, M. P. & BUKAU, B. 2005. Hsp70 chaperones: cellular functions and molecular mechanism. Cell Mol Life Sci, 62, 670-84.

MEDA, L., CASSATELLA, M. A., SZENDREI, G. I., OTVOS, L., JR., BARON, P., VILLALBA, M., FERRARI, D. & ROSSI, F. 1995. Activation of microglial cells by beta-amyloid protein and interferon-gamma. Nature, 374, 647-50.

MELDRUM, K. K., BURNETT, A. L., MENG, X., MISSERI, R., SHAW, M. B., GEARHART, J. P. & MELDRUM, D. R. 2003. Liposomal delivery of heat shock protein 72 into renal tubular cells blocks nuclear factor-kappaB activation, tumor necrosis factor-alpha production, and subsequent ischemia-induced apoptosis. Circ Res, 92, 293-9.

MERIIN, A. B. & SHERMAN, M. Y. 2005. Role of molecular chaperones in neurodegenerative disorders. Int J Hyperthermia, 21, 403-19.

MINJAREZ, B., CALDERÓN-GONZÁLEZ, K. G., RUSTARAZO, M. L., HERRERA-AGUIRRE, M. E., LABRA-BARRIOS, M. L., RINCON-LIMAS, D. E., DEL PINO, M. M., MENA, R. & LUNA-ARIAS, J. P. 2016. Identification of proteins that are differentially expressed in brains with Alzheimer's disease using iTRAQ labeling and tandem mass spectrometry. J Proteomics, 139, 103-21.

MINKEVICIENE, R., RHEIMS, S., DOBSZAY, M. B., ZILBERTER, M., HARTIKAINEN, J., FÜLÖP, L., PENKE, B., ZILBERTER, Y., HARKANY, T., PITKÄNEN, A. & TANILA, H. 2009. Amyloid beta-induced neuronal hyperexcitability triggers progressive epilepsy. J Neurosci, 29, 3453-62.

MIRANDA, D. D. C. & BRUCKI, S. M. D. 2014. Epilepsy in patients with Alzheimer's disease: A systematic review. Dement Neuropsychol, 8, 66-71.

MIYATA, Y., KOREN, J., KIRAY, J., DICKEY, C. A. & GESTWICKI, J. E. 2011. Molecular chaperones and regulation of tau quality control: strategies for drug discovery in tauopathies. Future Med Chem, 3, 1523-37.

MIZZEN, L. A. & WELCH, W. J. 1988. Characterization of the thermotolerant cell. I. Effects on protein synthesis activity and the regulation of heat-shock protein 70 expression. J Cell Biol, 106, 1105-16.

MONTERO-ODASSO, M. M., BARNES, B., SPEECHLEY, M., MUIR HUNTER, S. W., DOHERTY, T. J., DUQUE, G., GOPAUL, K., SPOSATO, L. A., CASAS-HERRERO, A., BORRIE, M. J., CAMICIOLI, R. & WELLS, J. L. 2016. Disentangling Cognitive-Frailty: Results From the Gait and Brain Study. J Gerontol A Biol Sci Med Sci, 71, 1476-1482.

MORINO, S., KONDO, T., SASAKI, K., ADACHI, H., SUICO, M. A., SEKIMOTO, E., MATSUDA, T., SHUTO, T., ARAKI, E. & KAI, H. 2008. Mild electrical stimulation with heat shock ameliorates insulin resistance via enhanced insulin signaling. PLoS One, 3, e4068.

MORRIS, J. K. & BURNS, J. M. 2012. Insulin: an emerging treatment for Alzheimer's disease dementia? Curr Neurol Neurosci Rep, 12, 520-7.

MORRIS, J. K., VIDONI, E. D., MAHNKEN, J. D., MONTGOMERY, R. N., JOHNSON, D. K., THYFAULT, J. P. & BURNS, J. M. 2016. Cognitively impaired elderly exhibit insulin resistance and no memory improvement with infused insulin. Neurobiol Aging, 39, 19-24.

MUCHOWSKI, P. J. & WACKER, J. L. 2005. Modulation of neurodegeneration by molecular chaperones. Nat Rev Neurosci, 6, 11-22.

MURPHY, M. E. 2013. The HSP70 family and cancer. Carcinogenesis, 34, 1181-8.

MUSTAFA, A., LANNFELT, L., LILIUS, L., ISLAM, A., WINBLAD, B. & ADEM, A. 1999. Decreased plasma insulin-like growth factor-I level in familial Alzheimer's disease patients carrying the Swedish APP 670/671 mutation. Dement Geriatr Cogn Disord, 10, 446-51.

NAGY, G., SZARKA, A., LOTZ, G., DÓCZI, J., WUNDERLICH, L., KISS, A., JEMNITZ, K., VERES, Z., BÁNHEGYI, G., SCHAFF, Z., SÜMEGI, B. & MANDL, J.

2010. BGP-15 inhibits caspase-independent programmed cell death in acetaminophen-induced liver injury. Toxicol Appl Pharmacol, 243, 96-103.

NAMBA, Y., TOMONAGA, M., KAWASAKI, H., OTOMO, E. & IKEDA, K. 1991. Apolipoprotein E immunoreactivity in cerebral amyloid deposits and neurofibrillary tangles in Alzheimer's disease and kuru plaque amyloid in Creutzfeldt-Jakob disease. Brain Res, 541, 163-6.

NEWCOMBE, E. A., CAMATS-PERNA, J., SILVA, M. L., VALMAS, N., HUAT, T. J. & MEDEIROS, R. 2018. Inflammation: the link between comorbidities, genetics, and Alzheimer's disease. J Neuroinflammation, 15, 276.

NORTON, S., MATTHEWS, F. E., BARNES, D. E., YAFFE, K. & BRAYNE, C. 2014. Potential for primary prevention of Alzheimer's disease: an analysis of population-based data. Lancet Neurol, 13, 788-94.

NOURHASHÉMI, F., DESCHAMPS, V., LARRIEU, S., LETENNEUR, L., DARTIGUES, J. F. & BARBERGER-GATEAU, P. 2003. Body mass index and incidence of dementia: the PAQUID study. Neurology, 60, 117-9.

OAKLEY, H., COLE, S. L., LOGAN, S., MAUS, E., SHAO, P., CRAFT, J., GUILLOZET-BONGAARTS, A., OHNO, M., DISTERHOFT, J., VAN ELDIK, L., BERRY, R. & VASSAR, R. 2006. Intraneuronal beta-amyloid aggregates, neurodegeneration, and neuron loss in transgenic mice with five familial Alzheimer's disease mutations: potential factors in amyloid plaque formation. J Neurosci, 26, 10129-40.

ODDO, S., CACCAMO, A., SHEPHERD, J. D., MURPHY, M. P., GOLDE, T. E., KAYED, R., METHERATE, R., MATTSON, M. P., AKBARI, Y. & LAFERLA, F. M.

2003. Triple-transgenic model of Alzheimer's disease with plaques and tangles: intracellular Abeta and synaptic dysfunction. Neuron, 39, 409-21.

OGILVIE, H., CACCIANI, N., AKKAD, H. & LARSSON, L. 2016. Targeting Heat Shock Proteins Mitigates Ventilator Induced Diaphragm Muscle Dysfunction in an Age-Dependent Manner. Front Physiol, 7, 417.

OHLEN, S. B., RUSSELL, M. L., BROWNSTEIN, M. J. & LEFCORT, F. 2017. BGP-15 prevents the death of neurons in a mouse model of familial dysautonomia. Proc Natl Acad Sci U S A, 114, 5035-5040.

OLABARRIA, M., NORISTANI, H. N., VERKHRATSKY, A. & RODRÍGUEZ, J. J. 2010. Concomitant astroglial atrophy and astrogliosis in a triple transgenic animal model of Alzheimer's disease. Glia, 58, 831-8.

OLABARRIA, M., NORISTANI, H. N., VERKHRATSKY, A. & RODRÍGUEZ, J. J. 2011. Age-dependent decrease in glutamine synthetase expression in the hippocampal astroglia of the triple transgenic Alzheimer's disease mouse model: mechanism for deficient glutamatergic transmission? Mol Neurodegener, 6, 55.

OLIVEIRA, T. G. & DI PAOLO, G. 2010. Phospholipase D in brain function and Alzheimer's disease. Biochim Biophys Acta, 1801, 799-805.

OSAWA, S., FUNAMOTO, S., NOBUHARA, M., WADA-KAKUDA, S., SHIMOJO, M., YAGISHITA, S. & IHARA, Y. 2008. Phosphoinositides suppress gamma-secretase in both the detergent-soluble and -insoluble states. J Biol Chem, 283, 19283-92.

OSENKOWSKI, P., YE, W., WANG, R., WOLFE, M. S. & SELKOE, D. J. 2008. Direct and potent regulation of gamma-secretase by its lipid microenvironment. J Biol Chem, 283, 22529-40.

PALOP, J. J., CHIN, J., ROBERSON, E. D., WANG, J., THWIN, M. T., BIEN-LY, N., YOO, J., HO, K. O., YU, G. Q., KREITZER, A., FINKBEINER, S., NOEBELS, J. L. & MUCKE, L. 2007. Aberrant excitatory neuronal activity and compensatory remodeling of inhibitory hippocampal circuits in mouse models of Alzheimer's disease. Neuron, 55, 697-711.

PANEGYRES, P. K. 2004. The contribution of the study of neurodegenerative disorders to the understanding of human memory. Qjm, 97, 555-67.

PARESCE, D. M., GHOSH, R. N. & MAXFIELD, F. R. 1996. Microglial cells internalize aggregates of the Alzheimer's disease amyloid beta-protein via a scavenger receptor. Neuron, 17, 553-65.

PARK, H. S., LEE, J. S., HUH, S. H., SEO, J. S. & CHOI, E. J. 2001. Hsp72 functions as a natural inhibitory protein of c-Jun N-terminal kinase. Embo j, 20, 446-56.

PATEL, N. S., PARIS, D., MATHURA, V., QUADROS, A. N., CRAWFORD, F. C. & MULLAN, M. J. 2005. Inflammatory cytokine levels correlate with amyloid load in transgenic mouse models of Alzheimer's disease. J Neuroinflammation, 2, 9.

PATTERSON, K. R., WARD, S. M., COMBS, B., VOSS, K., KANAAN, N. M., MORFINI, G., BRADY, S. T., GAMBLIN, T. C. & BINDER, L. I. 2011. Heat shock protein 70 prevents both tau aggregation and the inhibitory effects of preexisting tau aggregates on fast axonal transport. Biochemistry, 50, 10300-10.

PAULSON, J. B., RAMSDEN, M., FORSTER, C., SHERMAN, M. A., MCGOWAN, E. & ASHE, K. H. 2008. Amyloid plaque and neurofibrillary tangle pathology in a regulatable mouse model of Alzheimer's disease. Am J Pathol, 173, 762-72.

PEPEU, G. 2004. Mild cognitive impairment: animal models. Dialogues Clin Neurosci, 6, 369-77.

PEREZ, N., SUGAR, J., CHARYA, S., JOHNSON, G., MERRIL, C., BIERER, L., PERL, D., HAROUTUNIAN, V. & WALLACE, W. 1991. Increased synthesis and accumulation of heat shock 70 proteins in Alzheimer's disease. Brain Res Mol Brain Res, 11, 249-54.

PEREZ, S. E., LAZAROV, O., KOPRICH, J. B., CHEN, E. Y., RODRIGUEZ-MENENDEZ, V., LIPTON, J. W., SISODIA, S. S. & MUFSON, E. J. 2005. Nigrostriatal dysfunction in familial Alzheimer's disease-linked APPswe/PS1DeltaE9 transgenic mice. J Neurosci, 25, 10220-9.

PERRY, R. J. & HODGES, J. R. 1999. Attention and executive deficits in Alzheimer's disease. A critical review. Brain, 122 (Pt 3), 383-404.

PETANCESKA, S. S. & GANDY, S. 1999. The phosphatidylinositol 3-kinase inhibitor wortmannin alters the metabolism of the Alzheimer's amyloid precursor protein. J Neurochem, 73, 2316-20.

PETERSEN, N. S. & YOUNG, P. 1989. Effects of heat shock on protein processing and turnover in developing Drosophila wings. Dev Genet, 10, 11-5.

PETŐ, Á., KÓSA, D., FEHÉR, P., UJHELYI, Z., SINKA, D., VECSERNYÉS, M., SZILVÁSSY, Z., JUHÁSZ, B., CSANÁDI, Z., VÍGH, L. & BÁCSKAY, I. 2020. Pharmacological Overview of the BGP-15 Chemical Agent as a New Drug Candidate for the Treatment of Symptoms of Metabolic Syndrome. Molecules, 25.

PETRUCELLI, L., DICKSON, D., KEHOE, K., TAYLOR, J., SNYDER, H., GROVER, A., DE LUCIA, M., MCGOWAN, E., LEWIS, J., PRIHAR, G., KIM, J., DILLMANN, W. H., BROWNE, S. E., HALL, A., VOELLMY, R., TSUBOI, Y., DAWSON, T. M., WOLOZIN, B., HARDY, J. & HUTTON, M. 2004. CHIP and Hsp70 regulate tau ubiquitination, degradation and aggregation. Hum Mol Genet, 13, 703-14.

PIZARRO, J. M., HARO, L. S. & BAREA-RODRIGUEZ, E. J. 2003. Learning associated increase in heat shock cognate 70 mRNA and protein expression. Neurobiol Learn Mem, 79, 142-51.

PORTO, R. R., DUTRA, F. D., CRESTANI, A. P., HOLSINGER, R. M. D., QUILLFELDT, J. A., HOMEM DE BITTENCOURT, P. I., JR. & DE OLIVEIRA ALVARES, L. 2018. HSP70 Facilitates Memory Consolidation of Fear Conditioning through MAPK Pathway in the Hippocampus. Neuroscience, 375, 108-118.

POTTER, R. E. 2011. Amyloid-beta 42:40 metabolism is altered in autosomal dominant Alzheimer's disease (ADAD). Ann. Neurol., 70, S88-S89.

PRATT, W. B. & TOFT, D. O. 2003. Regulation of signaling protein function and trafficking by the hsp90/hsp70-based chaperone machinery. Exp Biol Med (Maywood), 228, 111-33.

PROFENNO, L. A., PORSTEINSSON, A. P. & FARAONE, S. V. 2010. Meta-analysis of Alzheimer's disease risk with obesity, diabetes, and related disorders. Biol Psychiatry, 67, 505-12.

QIU, W. Q., YE, Z., KHOLODENKO, D., SEUBERT, P. & SELKOE, D. J. 1997. Degradation of amyloid beta-protein by a metalloprotease secreted by microglia and other neural and non-neural cells. J Biol Chem, 272, 6641-6.

RACINE, R. J. 1972. Modification of seizure activity by electrical stimulation. II. Motor seizure. Electroencephalogr Clin Neurophysiol, 32, 281-94.

RACZ, I., TORY, K., GALLYAS, F., JR., BERENTE, Z., OSZ, E., JASZLITS, L., BERNATH, S., SUMEGI, B., RABLOCZKY, G. & LITERATI-NAGY, P. 2002. BGP-15 - a novel poly(ADP-ribose) polymerase inhibitor - protects against nephrotoxicity of

cisplatin without compromising its antitumor activity. Biochem Pharmacol, 63, 1099-111.

RAINGEAUD, J., GUPTA, S., ROGERS, J. S., DICKENS, M., HAN, J., ULEVITCH, R. J. & DAVIS, R. J. 1995. Pro-inflammatory cytokines and environmental stress cause p38 mitogen-activated protein kinase activation by dual phosphorylation on tyrosine and threonine. J Biol Chem, 270, 7420-6.

RAPOPORT, M., DAWSON, H. N., BINDER, L. I., VITEK, M. P. & FERREIRA, A. 2002. Tau is essential to beta -amyloid-induced neurotoxicity. Proc Natl Acad Sci U S A, 99, 6364-9.

RISSE, S. C., LAMPE, T. H., BIRD, T. D., NOCHLIN, D., SUMI, S. M., KEENAN, T., CUBBERLEY, L., PESKIND, E. & RASKIND, M. A. 1990. Myoclonus, seizures, and paratonia in Alzheimer disease. Alzheimer Dis Assoc Disord, 4, 217-25.

RITOSSA, F. 1962. A new puffing pattern induced by temperature shock and DNP in drosophila. Experientia, 18, 517-573.

RITOSSA, F. 1996. Discovery of the heat shock response. Cell Stress Chaperones, 1, 97-8.

ROGERS, R. S., MORRIS, E. M., WHEATLEY, J. L., ARCHER, A. E., MCCOIN, C. S., WHITE, K. S., WILSON, D. R., MEERS, G. M., KOCH, L. G., BRITTON, S. L., THYFAULT, J. P. & GEIGER, P. C. 2016. Deficiency in the Heat Stress Response Could Underlie Susceptibility to Metabolic Disease. Diabetes, 65, 3341-3351.

ROPACKI, S. A. & JESTE, D. V. 2005. Epidemiology of and risk factors for psychosis of Alzheimer's disease: a review of 55 studies published from 1990 to 2003. Am J Psychiatry, 162, 2022-30.

RYMAN, D. C., ACOSTA-BAENA, N., AISEN, P. S., BIRD, T., DANEK, A., FOX, N. C., GOATE, A., FROMMELT, P., GHETTI, B., LANGBAUM, J. B., LOPERA, F., MARTINS, R., MASTERS, C. L., MAYEUX, R. P., MCDADE, E., MORENO, S., REIMAN, E. M., RINGMAN, J. M., SALLOWAY, S., SCHOFIELD, P. R., SPERLING, R., TARIOT, P. N., XIONG, C., MORRIS, J. C., BATEMAN, R. J. & DOMINANTLY INHERITED ALZHEIMER, N. 2014. Symptom onset in autosomal dominant Alzheimer disease: a systematic review and meta-analysis. Neurology, 83, 253-60.

SABIRZHANOV, B., STOICA, B. A., HANSCOM, M., PIAO, C. S. & FADEN, A. I. 2012. Over-expression of HSP70 attenuates caspase-dependent and caspase-independent pathways and inhibits neuronal apoptosis. J Neurochem, 123, 542-54.

SALAH, H., LI, M., CACCIANI, N., GASTALDELLO, S., OGILVIE, H., AKKAD, H., NAMUDURI, A. V., MORBIDONI, V., ARTEMENKO, K. A., BALOGH, G., MARTINEZ-REDONDO, V., JANNIG, P., HEDSTRÖM, Y., DWORKIN, B., BERGQUIST, J., RUAS, J., VIGH, L., SALVIATI, L. & LARSSON, L. 2016. The chaperone co-inducer BGP-15 alleviates ventilation-induced diaphragm dysfunction. Sci Transl Med, 8, 350ra103.

SALWAY, K. D., GALLAGHER, E. J., PAGE, M. M. & STUART, J. A. 2011. Higher levels of heat shock proteins in longer-lived mammals and birds. Mech Ageing Dev, 132, 287-97.

SAPRA, G., THAM, Y. K., CEMERLANG, N., MATSUMOTO, A., KIRIAZIS, H., BERNARDO, B. C., HENSTRIDGE, D. C., OOI, J. Y., PRETORIUS, L., BOEY, E. J., LIM, L., SADOSHIMA, J., MEIKLE, P. J., MELLET, N. A., WOODCOCK, E. A., MARASCO, S., UEYAMA, T., DU, X. J., FEBBRAIO, M. A. & MCMULLEN, J. R.

2014. The small-molecule BGP-15 protects against heart failure and atrial fibrillation in mice. Nat Commun, 5, 5705.

SARAIVA, A. A., BORGES, M. M., MADEIRA, M. D., TAVARES, M. A. & PAULA-BARBOSA, M. M. 1985. Mitochondrial abnormalities in cortical dendrites from patients with Alzheimer's disease. J Submicrosc Cytol, 17, 459-64.

SARSZEGI, Z., BOGNAR, E., GASZNER, B., KÓNYI, A., GALLYAS, F., JR., SUMEGI, B. & BERENTE, Z. 2012. BGP-15, a PARP-inhibitor, prevents imatinib-induced cardiotoxicity by activating Akt and suppressing JNK and p38 MAP kinases. Mol Cell Biochem, 365, 129-37.

SCHARFMAN, H. E. 2012. Alzheimer's disease and epilepsy: insight from animal models. Future Neurol, 7, 177-192.

SCHEUNER, D., ECKMAN, C., JENSEN, M., SONG, X., CITRON, M., SUZUKI, N., BIRD, T. D., HARDY, J., HUTTON, M., KUKULL, W., LARSON, E., LEVY-LAHAD, E., VIITANEN, M., PESKIND, E., POORKAJ, P., SCHELLENBERG, G., TANZI, R., WASCO, W., LANNFELT, L., SELKOE, D. & YOUNKIN, S. 1996. Secreted amyloid beta-protein similar to that in the senile plaques of Alzheimer's disease is increased in vivo by the presenilin 1 and 2 and APP mutations linked to familial Alzheimer's disease. Nat Med, 2, 864-70.

SCOTT, M. P. & PARDUE, M. L. 1981. Translational control in lysates of Drosophila melanogaster cells. Proc Natl Acad Sci U S A, 78, 3353-7.

SEINO, Y., KAWARABAYASHI, T., WAKASAYA, Y., WATANABE, M., TAKAMURA, A., YAMAMOTO-WATANABE, Y., KURATA, T., ABE, K., IKEDA, M., WESTAWAY, D., MURAKAMI, T., HYSLOP, P. S., MATSUBARA, E. & SHOJI, M. 2010. Amyloid β accelerates phosphorylation of tau and neurofibrillary tangle

formation in an amyloid precursor protein and tau double-transgenic mouse model. J Neurosci Res, 88, 3547-54.

SELKOE, D. J. 2008. Soluble oligomers of the amyloid beta-protein impair synaptic plasticity and behavior. Behav Brain Res, 192, 106-13.

SEPULVEDA, P. V., BUSH, E. D. & BAAR, K. 2015. Pharmacology of manipulating lean body mass. Clin Exp Pharmacol Physiol, 42, 1-13.

SHANKAR, G. M., LI, S., MEHTA, T. H., GARCIA-MUNOZ, A., SHEPARDSON, N. E., SMITH, I., BRETT, F. M., FARRELL, M. A., ROWAN, M. J., LEMERE, C. A., REGAN, C. M., WALSH, D. M., SABATINI, B. L. & SELKOE, D. J. 2008. Amyloid-beta protein dimers isolated directly from Alzheimer's brains impair synaptic plasticity and memory. Nat Med, 14, 837-42.

SHIMABUKURO, J., AWATA, S. & MATSUOKA, H. 2005. Behavioral and psychological symptoms of dementia characteristic of mild Alzheimer patients. Psychiatry Clin Neurosci, 59, 274-9.

SHIMURA, H., MIURA-SHIMURA, Y. & KOSIK, K. S. 2004a. Binding of tau to heat shock protein 27 leads to decreased concentration of hyperphosphorylated tau and enhanced cell survival. J Biol Chem, 279, 17957-62.

SHIMURA, H., SCHWARTZ, D., GYGI, S. P. & KOSIK, K. S. 2004b. CHIP-Hsc70 complex ubiquitinates phosphorylated tau and enhances cell survival. J Biol Chem, 279, 4869-76.

SILVER, J. T. & NOBLE, E. G. 2012. Regulation of survival gene hsp70. Cell Stress Chaperones, 17, 1-9.

SIMONS, M., KELLER, P., DE STROOPER, B., BEYREUTHER, K., DOTTI, C. G. & SIMONS, K. 1998. Cholesterol depletion inhibits the generation of beta-amyloid in hippocampal neurons. Proc Natl Acad Sci U S A, 95, 6460-4.

SORBI, S., BIRD, E. D. & BLASS, J. P. 1983. Decreased pyruvate dehydrogenase complex activity in Huntington and Alzheimer brain. Ann Neurol, 13, 72-8.

STEWART, C. R., STUART, L. M., WILKINSON, K., VAN GILS, J. M., DENG, J., HALLE, A., RAYNER, K. J., BOYER, L., ZHONG, R., FRAZIER, W. A., LACY-HULBERT, A., EL KHOURY, J., GOLENBOCK, D. T. & MOORE, K. J. 2010. CD36 ligands promote sterile inflammation through assembly of a Toll-like receptor 4 and 6 heterodimer. Nat Immunol, 11, 155-61.

STEWART, R., MASAKI, K., XUE, Q. L., PEILA, R., PETROVITCH, H., WHITE, L. R. & LAUNER, L. J. 2005. A 32-year prospective study of change in body weight and incident dementia: the Honolulu-Asia Aging Study. Arch Neurol, 62, 55-60.

STOKES, C. E. & HAWTHORNE, J. N. 1987. Reduced phosphoinositide concentrations in anterior temporal cortex of Alzheimer-diseased brains. J Neurochem, 48, 1018-21.

STORTI, R. V., SCOTT, M. P., RICH, A. & PARDUE, M. L. 1980. Translational control of protein synthesis in response to heat shock in D. melanogaster cells. Cell, 22, 825-34.

STOVER, K. R., CAMPBELL, M. A., VAN WINSSEN, C. M. & BROWN, R. E. 2015. Early detection of cognitive deficits in the 3xTg-AD mouse model of Alzheimer's disease. Behav Brain Res, 289, 29-38.

SUMEGI, K., FEKETE, K., ANTUS, C., DEBRECENI, B., HOCSAK, E., GALLYAS, F., JR., SUMEGI, B. & SZABO, A. 2017. BGP-15 Protects against Oxidative Stress- or Lipopolysaccharide-Induced Mitochondrial Destabilization and Reduces Mitochondrial Production of Reactive Oxygen Species. PLoS One, 12, e0169372.

SUN, L., CHANG, J., KIRCHHOFF, S. R. & KNOWLTON, A. A. 2000. Activation of HSF and selective increase in heat-shock proteins by acute dexamethasone treatment. Am J Physiol Heart Circ Physiol, 278, H1091-7.

SUVÀ, D., FAVRE, I., KRAFTSIK, R., ESTEBAN, M., LOBRINUS, A. & MIKLOSSY, J. 1999. Primary motor cortex involvement in Alzheimer disease. J Neuropathol Exp Neurol, 58, 1125-34.

SUZUKI, K., MURTUZA, B., SAMMUT, I. A., LATIF, N., JAYAKUMAR, J., SMOLENSKI, R. T., KANEDA, Y., SAWA, Y., MATSUDA, H. & YACOUB, M. H. 2002. Heat shock protein 72 enhances manganese superoxide dismutase activity during myocardial ischemia-reperfusion injury, associated with mitochondrial protection and apoptosis reduction. Circulation, 106, I270-6.

SZABADOS, E., LITERATI-NAGY, P., FARKAS, B. & SUMEGI, B. 2000. BGP-15, a nicotinic amidoxime derivate protecting heart from ischemia reperfusion injury through modulation of poly(ADP-ribose) polymerase. Biochem Pharmacol, 59, 937-45.

TAKAHASHI, N., HARADA, M., HIROTA, Y., NOSE, E., AZHARY, J. M., KOIKE, H., KUNITOMI, C., YOSHINO, O., IZUMI, G., HIRATA, T., KOGA, K., WADA-HIRAIKE, O., CHANG, R. J., SHIMASAKI, S., FUJII, T. & OSUGA, Y. 2017. Activation of Endoplasmic Reticulum Stress in Granulosa Cells from Patients with Polycystic Ovary Syndrome Contributes to Ovarian Fibrosis. Sci Rep, 7, 10824.

TAN, J., TOWN, T., CRAWFORD, F., MORI, T., DELLEDONNE, A., CRESCENTINI, R., OBREGON, D., FLAVELL, R. A. & MULLAN, M. J. 2002. Role of CD40 ligand in amyloidosis in transgenic Alzheimer's mice. Nat Neurosci, 5, 1288-93.

TAN, J., TOWN, T., PARIS, D., MORI, T., SUO, Z., CRAWFORD, F., MATTSON, M. P., FLAVELL, R. A. & MULLAN, M. 1999. Microglial activation resulting from CD40-CD40L interaction after beta-amyloid stimulation. Science, 286, 2352-5.

TERWEL, D., MUYLLAERT, D., DEWACHTER, I., BORGHGRAEF, P., CROES, S., DEVIJVER, H. & VAN LEUVEN, F. 2008. Amyloid activates GSK-3beta to aggravate neuronal tauopathy in bigenic mice. Am J Pathol, 172, 786-98.

TERWEL, D., STEFFENSEN, K. R., VERGHESE, P. B., KUMMER, M. P., GUSTAFSSON, J., HOLTZMAN, D. M. & HENEKA, M. T. 2011. Critical role of astroglial apolipoprotein E and liver X receptor-α expression for microglial Aβ phagocytosis. J Neurosci, 31, 7049-59.

THOM, M., LIU, J. Y., THOMPSON, P., PHADKE, R., NARKIEWICZ, M., MARTINIAN, L., MARSDON, D., KOEPP, M., CABOCLO, L., CATARINO, C. B. & SISODIYA, S. M. 2011. Neurofibrillary tangle pathology and Braak staging in chronic epilepsy in relation to traumatic brain injury and hippocampal sclerosis: a post-mortem study. Brain, 134, 2969-81.

TOWNSEND, M., MEHTA, T. & SELKOE, D. J. 2007. Soluble Abeta inhibits specific signal transduction cascades common to the insulin receptor pathway. J Biol Chem, 282, 33305-12.

TURNER, P. R., O'CONNOR, K., TATE, W. P. & ABRAHAM, W. C. 2003. Roles of amyloid precursor protein and its fragments in regulating neural activity, plasticity and memory. Prog Neurobiol, 70, 1-32.

TURTURICI, G., SCONZO, G. & GERACI, F. 2011. Hsp70 and its molecular role in nervous system diseases. Biochem Res Int, 2011, 618127.

VIANA, R. J., STEER, C. J. & RODRIGUES, C. M. 2011. Amyloid-beta peptide-induced secretion of endoplasmic reticulum chaperone glycoprotein GRP94. J Alzheimers Dis, 27, 61-73.

VIZCAYCHIPI, M. P., XU, L., BARRETO, G. E., MA, D., MAZE, M. & GIFFARD, R. G. 2011. Heat shock protein 72 overexpression prevents early postoperative memory decline after orthopedic surgery under general anesthesia in mice. Anesthesiology, 114, 891-900.

VODOVOTZ, Y., LUCIA, M. S., FLANDERS, K. C., CHESLER, L., XIE, Q. W., SMITH, T. W., WEIDNER, J., MUMFORD, R., WEBBER, R., NATHAN, C., ROBERTS, A. B., LIPPA, C. F. & SPORN, M. B. 1996. Inducible nitric oxide synthase in tangle-bearing neurons of patients with Alzheimer's disease. J Exp Med, 184, 1425-33.

VON SCHULZE, A. T., DENG, F., MORRIS, J. K. & GEIGER, P. C. 2020. Heat therapy: possible benefits for cognitive function and the aging brain. J Appl Physiol (1985).

WAHRLE, S., DAS, P., NYBORG, A. C., MCLENDON, C., SHOJI, M., KAWARABAYASHI, T., YOUNKIN, L. H., YOUNKIN, S. G. & GOLDE, T. E. 2002. Cholesterol-dependent gamma-secretase activity in buoyant cholesterol-rich membrane microdomains. Neurobiol Dis, 9, 11-23.

WALLEN, E. S., BUETTNER, G. R. & MOSELEY, P. L. 1997. Oxidants differentially regulate the heat shock response. Int J Hyperthermia, 13, 517-24.

WANG, Y., MARTINEZ-VICENTE, M., KRUGER, U., KAUSHIK, S., WONG, E., MANDELKOW, E. M., CUERVO, A. M. & MANDELKOW, E. 2010. Synergy and antagonism of macroautophagy and chaperone-mediated autophagy in a cell model of pathological tau aggregation. Autophagy, 6, 182-3.

WANNAMETHEE, S. G., SHAPER, A. G., LENNON, L. & WHINCUP, P. H. 2007. Decreased muscle mass and increased central adiposity are independently related to mortality in older men. Am J Clin Nutr, 86, 1339-46.

WEITZEL, G., PILATUS, U. & RENSING, L. 1985. Similar dose response of heat shock protein synthesis and intracellular pH change in yeast. Exp Cell Res, 159, 252-6.

WELLEN, K. E. & HOTAMISLIGIL, G. S. 2005. Inflammation, stress, and diabetes. J Clin Invest, 115, 1111-9.

WESTERHEIDE, S. D., ANCKAR, J., STEVENS, S. M., JR., SISTONEN, L. & MORIMOTO, R. I. 2009. Stress-inducible regulation of heat shock factor 1 by the deacetylase SIRT1. Science, 323, 1063-6.

WESTWOOD, A. J., BEISER, A., DECARLI, C., HARRIS, T. B., CHEN, T. C., HE, X. M., ROUBENOFF, R., PIKULA, A., AU, R., BRAVERMAN, L. E., WOLF, P. A., VASAN, R. S. & SESHADRI, S. 2014. Insulin-like growth factor-1 and risk of Alzheimer dementia and brain atrophy. Neurology, 82, 1613-9.

WHILEY, L., SEN, A., HEATON, J., PROITSI, P., GARCÍA-GÓMEZ, D., LEUNG, R., SMITH, N., THAMBISETTY, M., KLOSZEWSKA, I., MECOCCI, P., SOININEN, H., TSOLAKI, M., VELLAS, B., LOVESTONE, S. & LEGIDO-QUIGLEY, C. 2014. Evidence of altered phosphatidylcholine metabolism in Alzheimer's disease. Neurobiol Aging, 35, 271-8.

WHITHAM, M., PARKER, B. L., FRIEDRICHSEN, M., HINGST, J. R., HJORTH, M., HUGHES, W. E., EGAN, C. L., CRON, L., WATT, K. I., KUCHEL, R. P., JAYASOORIAH, N., ESTEVEZ, E., PETZOLD, T., SUTER, C. M., GREGOREVIC, P., KIENS, B., RICHTER, E. A., JAMES, D. E., WOJTASZEWSKI, J. F. P. &

FEBBRAIO, M. A. 2018. Extracellular Vesicles Provide a Means for Tissue Crosstalk during Exercise. Cell Metab, 27, 237-251.e4.

WU, B. J., KINGSTON, R. E. & MORIMOTO, R. I. 1986. Human HSP70 promoter contains at least two distinct regulatory domains. Proc Natl Acad Sci U S A, 83, 629-33.

WU, L. L., RUSSELL, D. L., WONG, S. L., CHEN, M., TSAI, T. S., ST JOHN, J. C., NORMAN, R. J., FEBBRAIO, M. A., CARROLL, J. & ROBKER, R. L. 2015. Mitochondrial dysfunction in oocytes of obese mothers: transmission to offspring and reversal by pharmacological endoplasmic reticulum stress inhibitors. Development, 142, 681-91.

XU, L., XIONG, X., OUYANG, Y., BARRETO, G. & GIFFARD, R. 2011. Heat shock protein 72 (Hsp72) improves long term recovery after focal cerebral ischemia in mice. Neurosci Lett, 488, 279-82.

YAMAMOTO, N., IGBABVOA, U., SHIMADA, Y., OHNO-IWASHITA, Y., KOBAYASHI, M., WOOD, W. G., FUJITA, S. C. & YANAGISAWA, K. 2004. Accelerated Abeta aggregation in the presence of GM1-ganglioside-accumulated synaptosomes of aged apoE4-knock-in mouse brain. FEBS Lett, 569, 135-9.

YANAGISAWA, K. 2007. Role of gangliosides in Alzheimer's disease. Biochim Biophys Acta, 1768, 1943-51.

YEH, C. Y., VADHWANA, B., VERKHRATSKY, A. & RODRÍGUEZ, J. J. 2011. Early astrocytic atrophy in the entorhinal cortex of a triple transgenic animal model of Alzheimer's disease. ASN Neuro, 3, 271-9.

YOSHIIKE, Y., MINAI, R., MATSUO, Y., CHEN, Y. R., KIMURA, T. & TAKASHIMA, A. 2008. Amyloid oligomer conformation in a group of natively folded proteins. PLoS One, 3, e3235.

YUYAMA, K., SUN, H., SAKAI, S., MITSUTAKE, S., OKADA, M., TAHARA, H., FURUKAWA, J., FUJITANI, N., SHINOHARA, Y. & IGARASHI, Y. 2014. Decreased amyloid-β pathologies by intracerebral loading of glycosphingolipid-enriched exosomes in Alzheimer model mice. J Biol Chem, 289, 24488-98.

ZARROUK, A., DEBBABI, M., BEZINE, M., KARYM, E. M., BADREDDINE, A., ROUAUD, O., MOREAU, T., CHERKAOUI-MALKI, M., EL AYEB, M., NASSER, B., HAMMAMI, M. & LIZARD, G. 2018. Lipid Biomarkers in Alzheimer's Disease. Curr Alzheimer Res, 15, 303-312.

ZELIN, E. & FREEMAN, B. C. 2015. Lysine deacetylases regulate the heat shock response including the age-associated impairment of HSF1. J Mol Biol, 427, 1644-54.

ZHANG, B., GAITERI, C., BODEA, L. G., WANG, Z., MCELWEE, J., PODTELEZHNIKOV, A. A., ZHANG, C., XIE, T., TRAN, L., DOBRIN, R., FLUDER, E., CLURMAN, B., MELQUIST, S., NARAYANAN, M., SUVER, C., SHAH, H., MAHAJAN, M., GILLIS, T., MYSORE, J., MACDONALD, M. E., LAMB, J. R., BENNETT, D. A., MOLONY, C., STONE, D. J., GUDNASON, V., MYERS, A. J., SCHADT, E. E., NEUMANN, H., ZHU, J. & EMILSSON, V. 2013. Integrated systems approach identifies genetic nodes and networks in late-onset Alzheimer's disease. Cell, 153, 707-20.

ZHANG, B., RONG, R., LI, H., PENG, X., XIONG, L., WANG, Y., YU, X. & MAO, H. 2015. Heat shock protein 72 suppresses apoptosis by increasing the stability of X-linked inhibitor of apoptosis protein in renal ischemia/reperfusion injury. Mol Med Rep, 11, 1793-9.

ZHAO, W. Q., LACOR, P. N., CHEN, H., LAMBERT, M. P., QUON, M. J., KRAFFT, G. A. & KLEIN, W. L. 2009. Insulin receptor dysfunction impairs cellular clearance of neurotoxic oligomeric a{beta}. J Biol Chem, 284, 18742-53.

ZHAO, W. Q. & TOWNSEND, M. 2009. Insulin resistance and amyloidogenesis as common molecular foundation for type 2 diabetes and Alzheimer's disease. Biochim Biophys Acta, 1792, 482-96.

ZHAO, Y. & ZHAO, B. 2013. Oxidative stress and the pathogenesis of Alzheimer's disease. Oxid Med Cell Longev, 2013, 316523.

ZIYATDINOVA, S., GUREVICIUS, K., KUTCHIASHVILI, N., BOLKVADZE, T., NISSINEN, J., TANILA, H. & PITKÄNEN, A. 2011. Spontaneous epileptiform discharges in a mouse model of Alzheimer's disease are suppressed by antiepileptic drugs that block sodium channels. Epilepsy Res, 94, 75-85.